

From viruses to worms - regulation of macrophage activation in infectious disease

Sina Bohnacker

Vollständiger Abdruck der von der TUM School of Natural Sciences der Technischen
Universität München zur Erlangung des akademischen Grades einer

Doktorin der Naturwissenschaften (Dr. rer. nat.)

genehmigten Dissertation.

Vorsitz: Prof. Dr. Johannes Buchner

Prüfer*innen der Dissertation:

1. Prof. Dr. Matthias Feige
2. Prof. Dr. Julia Esser-von Bieren
3. Prof. Dr. Anne Krug

Die Dissertation wurde am 13.04.2023 bei der Technischen Universität München
eingereicht und durch die TUM School of Natural Sciences am 17.05.2023 angenommen.

*“You cannot get through a single day without having an impact on the world around you.
What you do makes a difference, and you have to decide
what kind of difference you want to make.”*

- Jane Goodall-

-To my husband, Mario -

Abstract

Macrophages possess immune regulatory functions that can be exploited by helminth parasites to evade the host immune system. Helminths can induce the production of anti-inflammatory mediators in macrophages to establish chronic infections. This thesis has provided new insights into the regulation of macrophage-mediated host defense and repair during helminth infections and during treatment with an immunomodulatory helminth molecule. In a mouse model of chronic intestinal helminth infection, we identified helminthic glutamate dehydrogenase (heGDH) as an indispensable factor for parasite chronicity by means of antibody-mediated neutralization or treatment with exogenous recombinant heGDH. Host macrophages efficiently internalize heGDH and represent key target cells of the enzyme *in vivo*. Mechanistically, the induction of PGE₂, as a primary immune regulatory mechanism of heGDH and of further immune regulatory factors (such as IL-12 family cytokines and IDO1) by heGDH requires the p300-mediated acetylation of histones. While we show the catalytic activity of heGDH to be dispensable for the p300-triggered induction of regulatory genes, an N-terminal handle-like structure, distinct from mammalian GDHs, may facilitate the interaction of heGDH with its targets. Furthermore, heGDH reprograms the macrophage metabolism, resulting in a phenotype with an increased glycolytic activity and the production of a specific amino acid and TCA metabolite profile, which enabled leukotriene suppression. Therefore, helminths employ a ubiquitous metabolic enzyme to epigenetically and metabolically target macrophages in order to evade host immunity.

Monocyte-derived macrophages (MDM) play a pivotal role in instigating the inflammatory response to severe acute respiratory syndrome coronavirus 2 (SARS-CoV-2), and they serve as a source for eicosanoids in airway inflammation. Investigation of transcriptional and eicosanoid reprogramming in MDM from convalescent COVID-19 patients demonstrated that individuals who experienced a mild course of COVID-19 retain a persistent transcriptional and metabolic imprint between 3-5 months after the infection. This imprint is characterized by an increase in the production of pro-inflammatory 5-lipoxygenase (5-LOX) metabolites and the downregulation of pro-resolving factors. Leukotriene synthesis is further enhanced by glucocorticoid treatment and remains elevated for 3-5 months but returned to baseline levels at 12 months post infection. MDM from convalescent SARS-CoV-2 infected individuals which are stimulated with either the SARS-CoV-2 spike protein or LPS, show an exaggerated prostanoid, type I interferon, and chemokine response. These results suggest an epigenetic reprogramming that leads to long-term modification of the innate immune compartment after SARS-CoV-2 infections.

Interleukins are an essential group of mediators that enable communication between the innate and adaptive immune system and play vital roles in regulating host immunity. One notable subset of cytokines is the interleukin 12 family, characterized by their heterodimeric nature and sharing of signaling receptors and cytokine subunits. Each IL-12 family member is a glycoprotein, although the precise impact of glycosylation on their biogenesis and function remained elusive. Identification of the specific glycosylation sites within human IL-12 family subunits that undergo modification upon secretion demonstrated that glycosylation is not necessary for the secretion of human IL-12 family cytokines, except for IL-35. Additionally, glycosylation has differing impacts on the functionality of IL-12 family cytokines, with IL-27 being most strongly affected. Taken together, this comprehensive analysis uncovers the impact of glycosylation on the biogenesis and function of IL-12 family cytokines, thereby laying the foundation for selectively modulating their secretion via targeted glycosylation modification.

Zusammenfassung

Makrophagen besitzen wichtige immunregulatorische Funktionen, die von Parasiten und deren Molekülen ausgenutzt werden können, um das Immunsystem des Wirts zu umgehen. Helminthen können die Produktion von entzündungshemmenden Mediatoren in Makrophagen induzieren, um somit chronische Infektionen zu etablieren. Im Rahmen dieser Arbeit konnten neue Erkenntnisse über die Regulation der Makrophagen-vermittelten Wirtsabwehr und Gewebsreparatur während unterschiedlicher Helmintheninfektionen gewonnen werden. Im Mausmodell für chronische intestinale Helmintheninfektionen wurde eine parasitäre Glutamat Dehydrogenase (GDH) als unverzichtbarer Faktor für die Immunevasion von Wurmparasiten identifiziert. Dies wurde zum Einen mittels Antikörper-vermittelter Neutralisierung und zum Anderen mittels Behandlung mit dem exogenen Protein bestätigt. Des Weiteren unterstrich die effektive Aufnahme der parasitären GDH durch Wirtsmakrophagen deren Bedeutsamkeit. Mechanistisch konnte gezeigt werden, dass die p300-vermittelte Acetylierung von Histonen eine entscheidende Rolle bei der Induktion von PGE₂ als primärer immunregulatorischer Mechanismus der parasitären GDH sowie weiterer immunregulatorischer Faktoren (wie Zytokine der IL-12-Familie und IDO1) spielt. Die katalytische Aktivität der parasitären GDH war für die p300-vermittelte Geninduktion jedoch nicht erforderlich. Unsere Daten weisen zudem daraufhin, dass eine N-terminale „schlüsselartige“ Struktur, welche sich von der GDH beim Menschen unterscheidet, die Möglichkeit bietet, mit Rezeptoren oder Bindungspartnern innerhalb der Makrophagen zu interagieren. Weiterhin wurde gezeigt, dass die parasitäre GDH - teilweise durch ihre katalytische Aktivität - zu einer Umprogrammierung des Makrophagen-Stoffwechsels führt, welche durch eine erhöhte glykolytische Aktivität und die Produktion spezifischer Aminosäuren und Krebszyklusintermediaten gekennzeichnet ist. Zusätzlich zur Umprogrammierung zeigte eines der induzierten Stoffwechselprodukte einen supprimierenden Effekt auf die Bildung pro-entzündlichen Leukotriene. Zusammenfassend nutzen Helminthen also ein ubiquitäres Stoffwechsellenzym, um Makrophagen epigenetisch und metabolisch so zu beeinflussen, dass eine reduzierte Immunantwort des Wirts und somit eine chronische Infektion induziert wird.

Makrophagen, die aus Monozyten differenzieren (MDM) spielen eine zentrale Rolle bei der Entstehung von Entzündungsreaktionen wie zum Beispiel während der Infektion mit SARS-CoV-2. Zudem dienen MDMs bei der Entzündung der Atemwege als signifikante Quelle für Eikosanoide. Mittels Analysen von Transkriptions- und Eikosanoidprofilen von MDMs

konnten wir zeigen, dass Personen, die einen milden Verlauf von COVID-19 hatten, auch 3 bis 5 Monate nach Beginn der Infektion eine anhaltende transkriptionelle und metabolische Prägung aufweisen. Diese Prägung war durch einen Anstieg der Produktion von entzündungsfördernden 5-Lipoxygenase Metaboliten und durch die Herunterregulierung von entzündungsauflösenden Faktoren gekennzeichnet. Eine Steroidbehandlung der MDMs *in vitro* führte zu einer weiteren Steigerung der Leukotrien-Synthese, welche für 3 bis 5 Monate erhöht blieb, jedoch 12 Monate nach der Infektion auf das Ausgangsniveau zurückkehrte. Wenn MDM von rekonvaleszenten SARS-CoV-2-Infizierten entweder mit dem SARS-CoV-2 Spike-Protein oder mit LPS stimuliert wurden, kam es zu übersteigerten Prostanoid-, Typ-I-Interferon- und Chemokin-Reaktionen. Zusammenfassend deuten diese Ergebnisse auf eine epigenetische Umprogrammierung des innate Immunsystems hin, welche nach einer COVID-19 Erkrankung zu langfristigen pro-entzündlichen Veränderungen führt.

Interleukine sind eine bedeutende Gruppe von Mediatoren, welche eine entscheidende Rolle bei der Regulation der Wirtsimmunität spielen, indem sie insbesondere die Kommunikation zwischen dem angeborenen und dem adaptiven Immunsystem ermöglichen. Eine bemerkenswerte Untergruppe von Zytokinen ist die Interleukin-12-Familie, welche durch ihre heterodimere Natur und die gemeinsame Nutzung von Signalrezeptoren und Zytokin-Untereinheiten gekennzeichnet ist. Zudem ist jedes bekannte Mitglied der IL-12-Familie ein Glykoprotein. Da die genauen Auswirkungen der Glykosylierung auf ihre Biogenese und Funktion noch nicht vollständig charakterisiert waren, wurden im Rahmen dieser Arbeit die spezifischen Glykosylierungsstellen in den Untereinheiten der menschlichen IL-12-Familie identifiziert und funktional charakterisiert. Es konnte gezeigt werden, dass die Glykosylierung für die Sekretion der Zytokine der IL-12-Familie mit Ausnahme von IL-35 nicht erforderlich ist. Darüber hinaus hat die Glykosylierung unterschiedliche Auswirkungen auf die Funktionalität der Zytokine, wobei IL-27 am stärksten von dieser posttranslationalen Modifikation betroffen ist. Insgesamt liefert diese umfassende Analyse eine Grundlage, um die Auswirkungen der Glykosylierung auf die Biogenese und Funktion einer zentralen Zytokinfamilie zu charakterisieren und damit therapeutisch nutzbar zu machen.

List of Publications and Conferences

1. Original Publications

This dissertation is based on the original publications listed below, which are referred in the text by their roman numbering.

- I *A helminth enzyme instigates immune evasion via a p300-prostaglandin axis in host macrophages*

Sina Bohnacker, Arie Geerlof, Fiona Henkel, Sandra Riemer, Franziska Hartung, André Mourão, Stefan Bohn, Ulrich F. Prodjinotho, Tarvi Teder, Jesper Z. Haeggström, Yannick Schreiber, Robert Gurke, Minhaz Ud-Dean, Francesca Alessandrini, Antonie Lechner, Agnieszka M. Kabat, Edward Pearce, Per-Johan Jakobsson, David Vöhringer, Matthias J Feige, Carsten B Schmidt-Weber, Clarissa Prazeres da Costa, Julia Esser-von Bieren

Planned submission to Cell Host and Microbe, 2023.

- II *Mild COVID-19 imprints a long-term inflammatory eicosanoid- and chemokine memory in monocyte-derived macrophages*

Sina Bohnacker*, Franziska Hartung*, Fiona D.R. Henkel*, Alessandro Quaranta, Johan Kolmert, Alina Priller, Minhaz Ud-Dean, Johanna Giglberger, Luisa M Kugler, Lisa Pechtold, Sarah Yazici, Antonie Lechner, Johanna Erber, Ulrike Protzer, Paul Lingor, Percy Knolle, Adam M Chaker, Carsten B Schmidt-Weber, Craig E. Wheelock, Julia Esser-von Bieren

Mucosal Immunology, 2022.

[10.1038/s41385-021-00482-8](https://doi.org/10.1038/s41385-021-00482-8)

- III *Influence of glycosylation on IL-12 family cytokine biogenesis and function*

Sina Bohnacker*, Karen Hildenbrand*, Isabel Aschenbrenner*, Stephanie I. Müller, Julia Esser-von Bieren, Matthias J. Feige

Molecular Immunology, 2020.

[10.1016/j.molimm.2020.07.015](https://doi.org/10.1016/j.molimm.2020.07.015)

*contributed equally

2. International Scientific Talks and Conference Papers

Parts of this dissertation have been presented at scientific conferences and have been published as a conference paper.

IV *A helminth glutamate dehydrogenase targets eicosanoid pathways to modulate type-2 immunity*

Sina Bohnacker, Fiona Henkel, Sandra Riemer, Franziska Hartung, Arie Geerlof, Andre Mourão, Antonie Lechner, Francesca Alessandrini, Agnieszka M. Kabat, Edward Pearce, Yannick Schreiber, Dominique Thomas, David Vöhringer, Matthias J. Feige, Carsten B. Schmidt-Weber, Julia Esser-von Bieren

Presented at:

EMBO | EMBL Symposium: Metabolism Meets Epigenetics (Digital)

November 17, 2021 to November 20, 2021

Poster presentation

EAACI: Immunology Winter School Digital 2022

January 27, 2022 to January 30, 2022

Oral presentation

ERS: Lung Science Conference 2022

January 27, 2022 to January 30, 2022

Lisbon, Portugal

Poster presentation

[10.1183/23120541.LSC-2022.20](https://doi.org/10.1183/23120541.LSC-2022.20)

Karolinska Institute: 8th European Workshop on Lipid Mediators

June 29, 2022 to July 01, 2022

Stockholm, Sweden

Oral presentation

Parasitic Helminths: New Perspectives in Biology and Infection

August 28, 2022 to September 02, 2022

Hydra, Greece

Oral presentation

3. Review Articles

This dissertation includes first author review articles listed below.

V *Macrophage regulation & function in helminth infection*

Antonie Lechner*, **Sina Bohnacker***, Julia Esser-von Bieren

Seminars in Immunology, 2021.

[10.1016/j.smim.2021.101526](https://doi.org/10.1016/j.smim.2021.101526)

VI *What Can Parasites Tell Us About the Pathogenesis and Treatment of Asthma and Allergic Diseases*

Sina Bohnacker*, Fabiana Troisi*, Marta De los Reyes Jiménez, Julia Esser-von Bieren.

Frontiers in Immunology, 2020.

[10.3389/fimmu.2020.02106](https://doi.org/10.3389/fimmu.2020.02106)

* contributed equally

4. Further Publications

The following publications are not discussed but compiled during the work for the dissertation.

VII *Human interleukin 12 alpha and EBI3 are cytokines with anti-inflammatory functions*

Karen Hildenbrand, **Sina Bohnacker**, Priyanka R. Menon, Anna Miesl, Fabien U. Prodjinotho, Patrick C. Strasser, Dragana A.M. Catic, Florian Rührnößl, Martin Haslbeck, Stephanie I. Müller, Clarissa Prazeres da Costa, Julia Esser-von Bieren and Matthias J. Feige

Under review in Science Advances, 2023.

VIII *Macrophages acquire a TNF-dependent inflammatory memory in allergic asthma*

Antonie Lechner, Fiona D R Henkel*, Franziska Hartung*, **Sina Bohnacker**, Francesca Alessandrini, Ekaterina O Gubernatorova, Marina S Drutskaya, Carlo Angioni, Yannick Schreiber, Pascal Haimerl, Yan Ge, Dominique Thomas, Agnieszka M Kabat, Edward J Pearce, Caspar Ohnmacht, Sergei A Nedospasov, Peter J Murray, Adam M Chaker, Carsten B Schmidt-Weber, Julia Esser-von Bieren

J Allergy Clin Immunol, 2021.

[10.1016/j.jaci.2021.11.026](https://doi.org/10.1016/j.jaci.2021.11.026)

IX *An anti-inflammatory eicosanoid switch mediates the suppression of type-2 inflammation by helminth larval products*

Marta De los Reyes Jiménez*, Antonie Lechner*, Francesca Alessandrini, **Sina Bohnacker**, Sonja Schindela, Aurélien Trompette, Pascal Haimerl, Dominique Thomas, Fiona D.R. Henkel, André Murão, Arie Geerlof, Clarissa Prazeres da Costa, Adam M. Chaker, Bernhard Brüne, Rolf Nüsing, Wolfgang A. Nockher, Matthias J. Feige, Martin Haslbeck, Caspar Ohnmacht, Benjamin J. Marsland, Nicola L. Harris, Carsten B. Schmidt-Weber, Julia Esser-von Bieren

Science Translational Medicine, 2020.

[10.1126/scitranslmed.aay0605](https://doi.org/10.1126/scitranslmed.aay0605)

X *The molecular basis of chaperone-mediated interleukin 23 assembly control*

Susanne Meier, **Sina Bohnacker**, Carolin J. Klose, Abraham Lopez, Christian A. Choe, Philipp W.N. Schmid, Nicolas Bloemeke, Florian Rührnößl, Martin Haslbeck, Julia Esser-von Bieren, Michael Sattler, Po-Ssu Huang, Matthias J. Feige

Nature Communications, 2019.

[10.1038/s41467-019-12006-x](https://doi.org/10.1038/s41467-019-12006-x)

* contributed equally

List of Abbreviations

α -KG	α -ketoglutarate
2-DG	2-deoxyglucose
5-LOX	5-lipoxygenase
AA	arachidonic acid
AAM	alternative activated macrophage
ACE2	angiotensin-converting enzyme 2
ACLY	ATP citrate lyase
AEP	asparagine endopeptidase
Akt	protein kinase B
ALR	absent in melanoma 2 (AIM2)-like receptors
APC	antigen presenting cell
Arg1	arginase 1
BALF	bronchoalveolar lavage fluid
BCG	bacillus Calmette–Guérin
BCR	b-cell receptor
BiP	binding immunoglobulin protein
BM	bone marrow
BMDM	bone-marrow derived macrophages
Breg	regulatory B cell
CARKL	carbohydrate kinase-like protein
CCR	chemokine receptor
cGAS	cyclic GMP-AMP synthase
CH25H	cholesterol 25-hydroxylase
CLR	c-type lectin receptor
CNX	calnexin
COVID-19	coronavirus disease 19
COX	cyclooxygenase
CRT	calreticulin
CYP	cytochrome P450
cysLT	cysteinyl leukotriene
DAMP	danger- associated molecular pattern
DC	dendritic cell
DC-SIGN	DC-specific intercellular adhesion molecule-3-grabbing non-integrin
DHA	docosahexaenoic acid
DXM	dexamethasone
E-protein	envelope protein
EBI3	Epstein-Barr virus induced gene 3
EDEM	ER degradation-enhancing alpha-mannosidase-like proteins
EET	epoxyeicosatrienoic acids
EPA	eicosapentaenoic acid
ER	endoplasmic reticulum
ERAD	ER-associated degradation
ERK	extracellular signal-regulated kinases
ERQC	ER-quality control
ES	excretory secretory
FAO	fatty acid oxidation
FLAP	5-LOX activating protein
FnIII	fibronectin III
FP	fluticasone propionate
GDH	glutamate dehydrogenase
GGT	γ -glutamyl transferase

List of Abbreviations

GI	gastrointestinal tract
Glc	glucosidase
GM-CSF	granulocyte-macrophage colony-stimulating factor
GPCR	g-protein coupled receptor
GSDMD	gasdermin D
HDAC	histone deacetylase
HDM	house dust mite
HETE	hydroxyeicosatetraenoic acids
HG	hydroxyglutarate
HIF	hypoxia-inducible factor
HLA	human leukocyte antigen
<i>Hpb</i>	<i>Heligmosomoides polygyrus bakeri</i>
HSCs	hematopoietic stem cell progenitors
IAV	influenza A virus
IFIT	interferon-induced proteins with tetratricopeptide repeats
IFN	interferon
Ig	immunoglobulin
IL	interleukin
ILC	innate lymphoid cell
iNOS	nitric oxide synthase; gene name: <i>nos2</i>
IRF	interferon regulatory factors
IRG	immune-responsive genes
ISG	interferon-stimulated genes
JAK	janus kinase
JNK	c-Jun N-terminal kinase
KDM5	lysine-specific demethylase 5A
KLF	kruppel-like factors
L-SIGN	liver/lymph node-specific intracellular adhesion molecules-non-integrin
LAMTOR1	proteins /late endosomal/ lysosomal adaptor, MAPK and MTOR activator 1
LGP2	probable ATP-dependent RNA helicase
LPS	lipopolysaccharide
CXCL	chemokine ligand
LT	leukotriene
LX	lipoxin
mAb	monoclonal antibody
MAPK	mitogen-activated protein kinase
MBD	membrane bound dipeptidase
MBP	major basic protein
MC	mast cell
MDA5	melanoma differentiation-associated protein 5
MGST2	microsomal glutathione S-transferase 2
MHC	major histocompatibility complex
MIF	macrophage migration inhibitory factor
MLN	mesenteric lymph node
MPO	myeloid peroxidase
MR	mannose receptor
MRC1	mannose receptor C-type1
mTORC	mechanistic target of rapamycin
MyD88	myeloid differentiation primary response 88
N-protein	nucleocapsid protein
NADPH	nicotinamide adenine dinucleotide phosphate
Nb	<i>Nippostrongylus brasiliensis</i>
NET	neutrophil extracellular trap
NF κ B	nuclear factor kappa-light-chain-enhancer of activated B-cells

List of Abbreviations

NK	natural killer cell
NLR	nucleotide-binding oligomerization domain (NOD)-like receptor
NLRP3	NLR family pyrin domain containing 3
NLS	nuclear localization sequence
NMU	neuromedin U
NO	nitric oxide
NSAIDs	non-steroidal anti-inflammatory drugs
OST	oligosaccharyltransferase
OXPPOS	oxidative phosphorylation
PAMP	pathogen- associated molecular pattern
PBMC	peripheral blood mononuclear cells
PDI	protein disulfide isomerase
PG	prostaglandin
PPAR	peroxisome proliferator-activated receptor
PPP	pentose phosphate pathway
PRR	pattern recognition receptor
PUFA	polyunsaturated fatty acid
RAG	recombination activating gene
RELM	resistin-like molecule
RLR	Retinoic acid-inducible gene I (RIG-I)-like receptors
ROS	reactive oxygen species
RSV	respiratory syncytial virus
S-protein	spike protein
SARS-CoV	severe acute respiratory syndrome coronavirus
SDH	succinate dehydrogenase
SEA	<i>Schistosoma mansoni</i> egg antigen
SI	small intestine
SOCS	suppressor of cytokine signaling
SPM	specialized proresolving mediator
SREBP	sterol regulatory element-binding protein
STAT	signal transducer and activator of transcription
STH	soil transmitted helminth
STING	stimulator of interferon genes
T-bet	T-box transcription factor TBX21
T _C	effector T-cell
TCA	tricarboxylic acid
TCR	T-cell receptor
TET	ten-eleven translocation (TET) methylcytosine dioxygenases
TGF	transforming growth factor
T _H	T helper cell
TLR	toll like receptor
TMPRSS2	transmembrane serine protease 2
Treg	regulatory T cell
TRIF	TIR-domain-containing adapter-inducing interferon- β
TSLP	thymic stromal lymphopietin
TVM	virtual memory T cell
TX	thromboxane
Tyk	tyrosine kinase
UGGT	UDP- glucose:glycoprotein glucosyltransferase
UPS	ubiquitin-proteasome system
VEGF	vascular endothelial growth factor
VSV	vesicular stomatitis virus
ZEB	zinc finger E-box-binding homeobox 1

Table of Contents

Abstract	I
Zusammenfassung.....	III
List of Publications and Conferences	V
List of Abbreviations.....	X
1 Introduction	1
1.1 Host immune response to infectious disease.....	1
1.1.1 Type 1 immunity- viral infections.....	1
1.1.2 The immune response to SARS-CoV-2 infection	6
1.1.3 Type 2 immunity- parasite infections.....	10
1.2 Macrophages as essential players during infectious disease	16
1.2.1 Monocyte, macrophage ontogeny and differentiation during infections.....	16
1.2.2 The metabolic signature of macrophages during infections	19
1.2.3 Metabolic and epigenetic reprogramming as a source for trained immunity	21
1.3 Helminths as modulators of type 2 immunity	25
1.3.1 Helminth-induced immune evasion by parasite-derived effector molecules	26
1.3.2 Protection from allergy and autoimmunity (“Hygiene hypothesis”)	35
1.3.3 Interplay between helminths and respiratory viral infections.....	36
1.4 Eicosanoids as key mediators during infection.....	38
1.4.1 The arachidonic acid metabolism.....	38
1.4.2 Role of eicosanoids during respiratory viral infections	41
1.4.3 Eicosanoid function during helminth infection	45
1.5 The IL-12 family as important cytokines of the host immunity	49
1.5.1 Functional diversity despite structural similarity	49
1.5.2 Impact of glycosylation on biogenesis and function of interleukins	52
2 Aims.....	54
3 Methods	56
4 Results	65
4.1 A helminth enzyme instigates immune evasion via a p300-prostaglandin axis in host macrophages.....	65
4.2 Mild COVID-19 imprints a long-term inflammatory eicosanoid- and chemokine memory in monocyte-derived macrophages	67

Table of Contents

4.3	Influence of glycosylation on IL-12 family cytokine biogenesis and function	69
5	Discussion	71
5.1	Parasitic GDHs: an evolutionary conserved enzyme for host immune evasion?	71
5.2	Macrophages as the primary target cells of helminths and heGDH	72
5.3	Epigenetic regulation of a type-2 suppressive macrophage phenotype by heGDH.....	74
5.4	<i>H. polygyrus</i> induced immune evasion by regulation of the AA pathway and T-cell subsets...	75
5.5	IL-4/-13 mediated type 2 immune response impairs PGE ₂ -driven immune evasion	77
5.6	How heGDH modulates the macrophages metabolism	78
5.7	Transient macrophage reprogramming after mild COVID-19 disease	80
5.8	Clinical implication for the treatment of acute or long COVID-19	82
5.9	Glycosylation deficiency and its impact on biogenesis and signaling of IL-12 family cytokines	84
5.10	Sugar moieties as important modifications for therapy and disease	85
6	Future perspectives	86
7	Acknowledgements	88
8	Bibliography.....	91
	Publications	147

1 Introduction

1.1 Host immune response to infectious disease

Despite the great medical progress in recent decades, infections still represent a major threat. Especially the last few years, in particular the pandemic triggered by "coronavirus disease 2019" (COVID-19), have again made it very clear to all of us what power pathogens can have. The statistics of the World Health Organization (WHO), aside from the current Corona pandemic, also show the relevance of **infectious diseases** caused by bacteria, viruses, and parasites worldwide. The top ten causes of death around the globe include several infectious diseases or infectious groups [1]. Therefore, it is important to understand what kind of disease the pathogen triggers, the mechanisms our immune system uses to fight the invader and at the same time, which mechanisms the pathogen exploits to evade the **host's immune response**. Based on this we can pay close attention to the risks of serious infections and develop new therapeutic approaches that help to prevent the detrimental consequences of infectious diseases.

1.1.1 Type 1 immunity- viral infections

Our body is constantly exposed to the external environment, and therefore, must be equipped to respond to and eliminate pathogens. Viral clearance and resolution of infection requires a complex, multi-faceted immune response, which is often referred as a "**Type 1 immune response**". It is initiated by epithelial cells and innate immune cells which subsequently activate the adaptive immune system. The ultimate goal of the immune response is to eliminate the infection and protect the host from future infections with the same (or similar) viruses.

Viral- (pathogen-) sensing via the innate immune system

Our body has evolved several defense mechanisms to protect us against viral infections. Among the first line of defense are the epithelial cells. They are critical in limiting virus spread and alerting the immune system to respond to the infection. The immune system responds to several kind of infections at forefront with the innate ("non-specific") response often associated with inflammation to block or inhibit initial infection, to protect cells from infection, or to eliminate virus-infected cells, and occur well before the onset of adaptive ("specific") immunity. The cellular innate immune system consisting of granulocytes, monocytes, macrophages, mast cells, dendritic cells (DCs), innate lymphoid cells (ILCs)

and natural killer (NK) cells reside at various anatomical barriers such as skin and mucous membranes to directly detect and target entering viruses. Despite mechanical or chemical barriers, including antimicrobial peptides, viruses can invade the body tissue. Epithelial cells as well as professional phagocytes like macrophages, but also DCs can sense pathogen-associated molecular patterns (PAMPs) including viral nucleic acids and viral membrane particles or danger-associated molecular patterns (DAMPs) of infiltrated or even dead cells through their cognate pattern recognition receptors (PRRs). PRRs that are important for pathogen recognition include membrane-bound Toll-like receptors (TLRs), cytoplasmic nucleotide oligomerization domain (NOD)-like receptors (NLRs), absent in melanoma 2 (AIM2)-like receptors (ALR), C-type lectin receptors (CLR), retinoic acid-inducible gene (RIG)-I-like receptors (RLRs), and other cytosolic sensors (Table 1). After recognition and signaling through these receptors, the host cells start to express different inflammatory mediators including cytokines, chemokines and lipids, induce cell death and clear infected cells by phagocytosis.

Table 1: Pattern recognition receptors and cytosolic sensors for pathogen recognition and initiation of host immune responses

Family	Receptor	Ligand	Location	Function	Ref.
TLR	TLR3	dsRNA	Endosomal	Signaling via MyD88 or TRIF followed by activation of NF κ B, MAPKs and IRFs to induce cytokine and interferon response	[2]
	TLR7/8	ssRNA	Endosomal		[3–6]
	TLR9	Hypomethylated CpG DNA	Endosomal		[7,8]
	TLR2/4	Virus coat proteins/bacteria	Plasma membrane		[9–12]
RLR	RIG-I/MDA5	dsRNA	Cytosolic	Initiate the release of inflammatory cytokines and type I interferons (IFNs)	[13–16]
	LGP2	regulating the function of RIG-I and MDA5	Cytosolic		[17]
CLR	MR/DC-SIGN/L-SIGN etc.	Glycosylated proteins	Plasma membrane	RAF1- and ERK – MAPKs and NF κ B signaling → inflammatory cytokine response	[18–21]
NLR	NLRP3	dsRNA	Cytosolic	Inflammasome activation	[22]
	NOD2	ssRNA	Cytosolic	Signaling via the MAPK and NF κ B pathway to induce cytokine responses	[23]
ALR	AIM2	dsDNA	Cytosolic and nuclear	Inflammasome activation	[24]
	IFI16	RNA/DNA			[25–28]
cGAS	cGAS	Microbial and cytosolic DNA	Cytosolic	Activation of STING pathway to induce proinflammatory cytokines and type I IFNs	[29]

Interferon response as a key pathway to limit viral infections

Interferons (IFNs) are a specialized group of cytokines mediating the host antiviral immune response. They can be divided in three different groups. Type I (encompassing IFN- α , - β , - ω , - ϵ , - κ , - τ and - δ) and type III (IFN- λ) IFNs are produced by most cell types and their secretion is triggered by the activation of PRRs, whereas type II IFNs (IFN- γ) are induced by other cytokines like IL-12 and the expression is restricted to T cells and NK cells [30,31] (Figure 1 and 2). Binding of type I, type II and type III IFNs to their respective receptors initiates a signaling cascade that results in the expression of interferon-stimulated genes (ISGs). Type I IFNs ligate the heterodimeric receptor IFNAR1/IFNAR2, which is expressed on all cells, while type II IFNs bind to IFNGR1/IFNGR2 and type III IFNs signal through the IL-10R2/IFNLR1 heterodimer [32]. Activation of these receptors triggers the phosphorylation of STAT1/2 by Janus kinase 1 (JAK1) and tyrosine kinase 2 (TYK2), the recruitment of IRF9, leading to the formation of the ISGF3 complex, which in turn translocates to the nucleus to activate the expression of ISGs [32,33] (Figure 2). ISGs are crucial in antiviral immunity by inhibiting viral entry or replication, inducing apoptosis, and recruiting other immune cells to the site of infection.

Activation of the adaptive immunity to viral infections

Additionally, to their direct antiviral activity, type I IFNs also play a role in initiating the adaptive immune response by the activation of DCs via upregulation of major histocompatibility complexes (MHC) and co-stimulatory molecules, while they can also directly act on CD4⁺ and CD8⁺ T cells, inducing T cell polarization to T_H1 or cytotoxic T cells [34] (Figure 1). Antigen presenting cells (APCs), including macrophages, DCs and B cells play a crucial role in activating naive T cells by presenting phagocytosed antigenic material on their surface within their MHC molecules to their specific T cell receptor (TCR) [35,36]. Their direct recognition of antigens within the MHCI or MHCII complexes and the expression of either CD4⁺ or CD8⁺ receptors initiate their differentiation into functionally distinct T cell subsets, including T helper cells (T_H; CD4⁺), cytotoxic T cells (T_C; CD8⁺), and T regulatory cells (Tregs; CD4⁺) [37,38]. Depending on the nature of the pathogen, helper T cells are functionally subdivided in T_H1, T_H2 or T_H17 cells [39,40]. Induction of signal transducer and activator of transcription (STAT)-4 followed by IL-12 signalling activates T-bet and results in T_H1 cell differentiation, characterized by IFN- γ secretion [41,42]. As mentioned earlier, T_H1 cells are crucial in removing intracellular pathogens such as viruses and become generated when DCs secrete IL-12 and IFN- γ cytokines, which in turn stimulates the secretion of their own cytokines (IFN- γ and TNF- β). The production of T_H1

cytokines leads to the recruitment and activation of phagocytic cells such as macrophages and neutrophils, induce B cell antibody switching as well as activates CD8⁺ T effector cell responses [43]. The activation of CD8⁺ cytotoxic T cells via MHC class I molecules results in the elimination of pathogens and infected host cells by releasing cytotoxins such as perforin and granzymes. Next to cytotoxic T cells, NK cells (as a part of the innate immune system) can directly target infected cells, without the necessity of the MHCI complex binding. This attribute of NK cells puts them in an offensive position even against intracellular pathogens that evade CD8⁺ cells by interfering with MHCI molecule expression [44,45] (Figure 1). After the viral infection has been efficiently contained by the various effector immune cells, it is important to prevent aberrant immune responses. Tregs are crucial mediators of immune homeostasis by their ability to dampen excessive immune responses. Foxp3 expressing Tregs are generated in the thymus or in the periphery and are characterized by the secretion of anti-inflammatory cytokines including IL-10, TGF- β and IL-35 [46].

The activation of CD4⁺ naïve T cells by antigens can also lead to migration from the T cell zone to germinal centers where they become T follicular helper cells (Tfh) upon the secretion of IL-6 and IL-21. Interaction of Tfh with follicular B cells triggers several processes such as isotype switching, somatic hypermutation, and rapid cellular division to seed germinal centers. B cells develop in the bone marrow and possess a unique B cell receptor consisting of a membrane bound Ig molecule and a signal transduction moiety that can efficiently bind to viral antigens [47]. Upon contact with the antigen, the B cell undergoes division to differentiate into two types: longlived plasma cells that produce high-affinity antibodies to directly neutralize the virus in the blood stream or germinal center-dependent memory B cells that react more rapidly to the same viral antigen upon secondary encounter [48] (Figure 1). Like for T cells, a small population of B cells also exhibit immunosuppressive functions and is referred to as regulatory B cells (Bregs). Together with Treg, Bregs dampen harmful immune responses and maintain tissue homeostasis via the production of inhibitory cytokines.

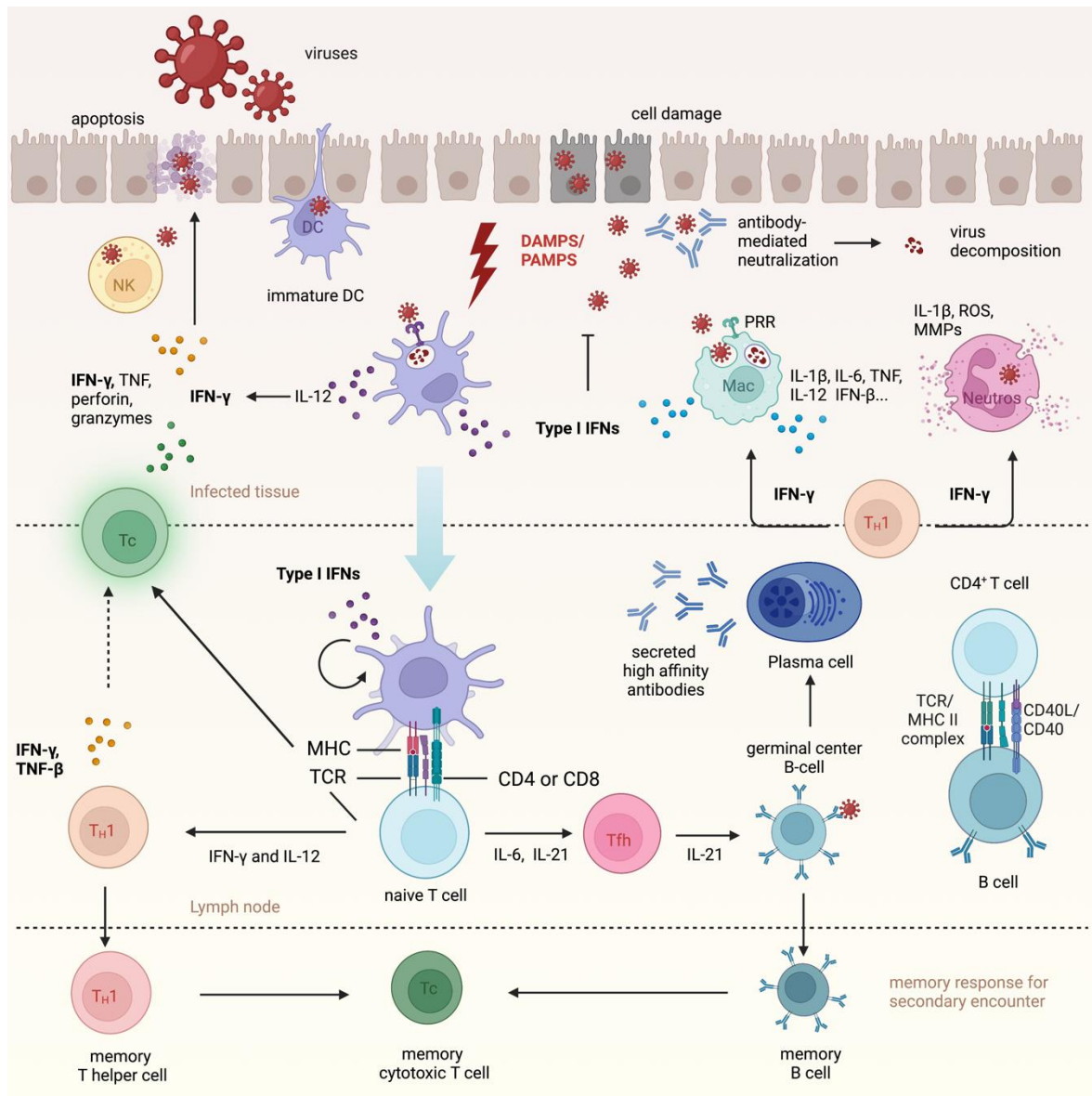


Figure 1: Type 1- (Host-) immune response to viral infections (created with Biorender.com)

1.1.2 The immune response to SARS-CoV-2 infection

In 2019, **SARS-CoV-2** emerged as a new pathogen that resulted in the COVID-19 pandemic, rapidly spreading throughout the world and leading to an ongoing public health crisis with over 750 million infections and 6.8 million deaths (WHO, March 2023). SARS-CoV-2 causes upper and lower respiratory tract infections that are often associated with fever, cough and loss of smell and taste. Most infections cause mild symptoms, and up to 20–40% of patients are asymptomatic. However, some patients experience severe disease and develop systemic inflammation, tissue damage, acute respiratory distress syndrome (ARDS), thromboembolic complications, cardiac injury and/or cytokine storm, which can be fatal [49–51]. Apart from the acute disease, SARS-CoV-2 infections can also lead to long-term sequelae after virus clearance, reaching from fatigue and headache, to airway dysfunction, including impaired pulmonary diffusion [52]. This pathological state is termed as „long-COVID“, with the persistence of more than 1 symptom for up to several weeks to months [52–54].

SARS-CoV-2 entry and the induction of an inflammatory response in macrophages

The main entry route occurs via binding of the SARS-CoV-2 Spike (S) protein to its principal cellular receptor, angiotensin-converting enzyme 2 (ACE2), while the host serine protease TMPRSS2 is important for proteolytic priming of the S-protein for receptor ligation and entry [55] (Figure 2). Apart from signaling through ACE2, SARS CoV-2 S-protein is highly glycosylated and can also be recognized by C-type lectin receptors like L-SIGN and DC-SIGN to induce inflammatory cytokine responses [56,57]. After the release of viral RNA; MDA5, LGP2 and RIG-I function as key regulators of antiviral type I IFN induction in epithelial cells and macrophages following infection with SARS-CoV-2 [58]. Increased evidence of further activation of the immune system by PRRs, especially TLRs has been shown, as TLR2 on macrophages is able to sense the envelope (E-) protein of SARS-CoV-2 to mount inflammatory responses [59]. The inflammatory response is dominated by the production and subsequent release of IFNs resulting in the induction of ISGs, with for example the production of Ly6E that can prevent SARS-CoV-2 entry and members of the IFIT family (IFIT1,-3 and -5) which inhibit viral replication [60,61]. In line, the SARS-CoV-2 E-protein triggered induction of TLR2 signaling concomitantly upregulates expression of *Nlrp3* and *Il1b* in macrophages [59]. In keeping with the TLR2 studies, human primary monocytes infected with SARS-CoV-2 show NLRP3-dependent caspase-1 and GSDMD cleavage and IL-1 β maturation [62,63]. NLRP3 leads to activation of caspase-1, the production and release of bioactive IL-1 β and IL-18 as well as cleavage of gasdermin

(GSDM) D, which forms pores in the plasma membrane to drive membrane rupture and pyroptotic cell death. Apart from the TLR2 induced expression of inflammasome genes, several PAMPs, including the viral RNA, ORF3a, the nucleocapsid (N)- and S-protein are implicated in NLRP3 inflammasome assembly and subsequent cytokine release [64–67]. Mechanistically, it has been proposed that SARS-CoV-2 infection causes an imbalance in intracellular potassium efflux to drive NLRP3 inflammasome activation and the release of IL-1 β and IL-18 [63] (Figure 2). However, even if the inflammasome drives protection against SARS-CoV-2 infection, increased levels of IL-1 β and IL-18 in plasma are correlating with disease severity and mortality in patients with COVID-19 [68,69].

Cytokine storms and cell death triggered by SARS-CoV-2

PRR signaling engaged by SARS-CoV-2 induces concurrent release of both IFNs and other pro-inflammatory cytokines [70]. Expression of numerous pro-inflammatory cytokines, chemokines and IFNs are elevated in patients with COVID-19, including that of IL-1 β , IL-18, IL-6, TNF, IL-12, IFN- β , IFN- γ , CCL2 and others [71] (Figure 2). These cytokines aid in clearing infections by the activation of immune cells, but also maintain cellular homeostasis and thus play a critical role in acute infections [72]. However, severe clinical outcomes are characterized by a slow decline in viral load as well as early and sustained release of pro-inflammatory cytokines during SARS-CoV-2 infection, contributing to cytokine storms [51]. In the context of COVID-19, the combination of TNF and IFN- γ leads to disease pathogenesis by signaling cooperatively in an STAT1 and IRF1 dependent manner to induce inflammatory cell death (PANoptosis) [73,74], suggesting that a positive feedback loop, in which cytokine secretion causes cell death results in more cytokine release, culminating in a cytokine storm that causes life-threatening damage to host tissues and organs. Overall, while cytokines are critical for the innate immune response and successful clearance of viral infections, their release must be controlled to prevent systemic cytokine storms and pathogenic inflammation during SARS-CoV-2 infection.

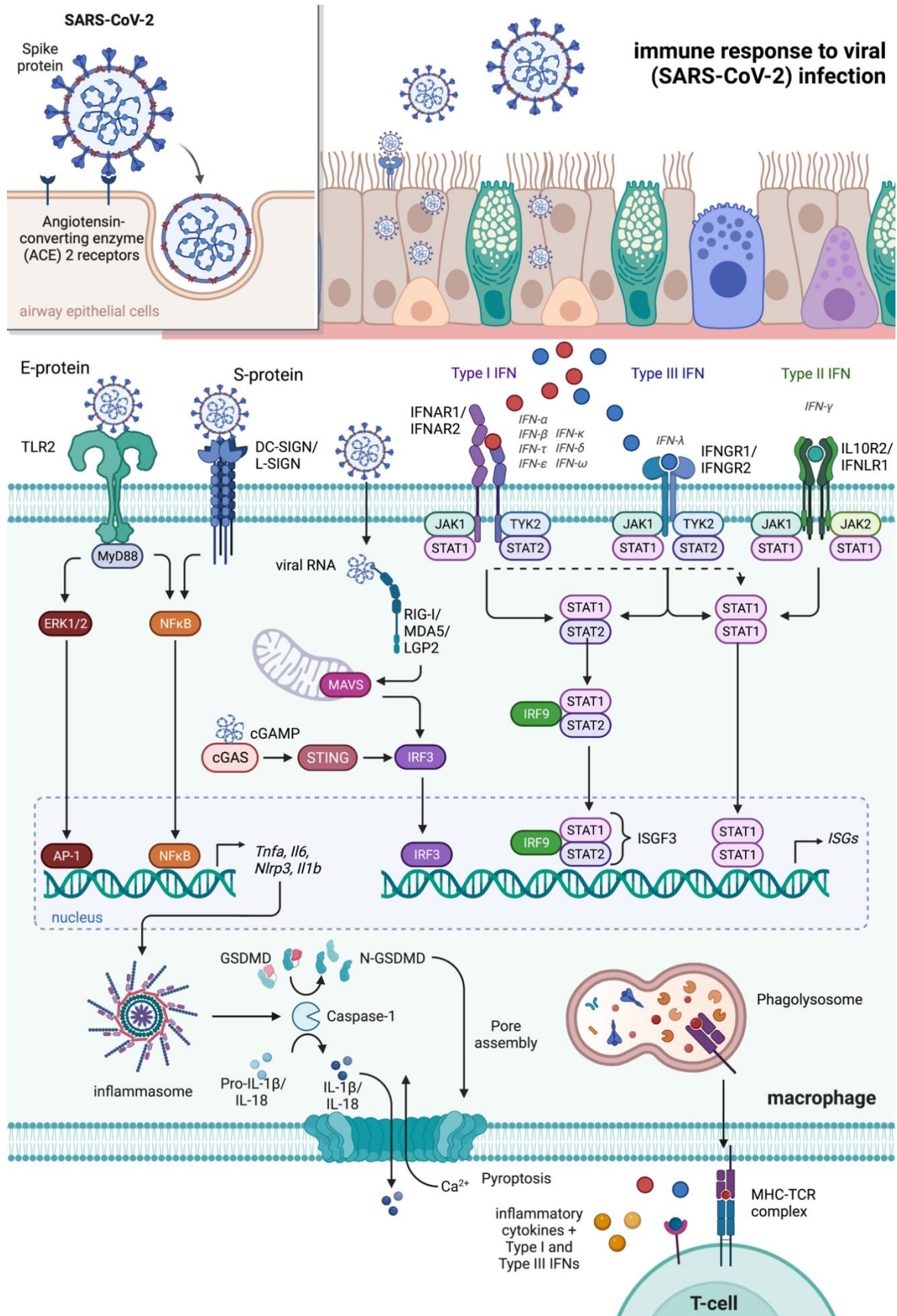


Figure 2: Crucial pathways/principles of the host immune response to SARS-CoV-2 (created with Biorender.com)

Cellular and humoral immune response to SARS-CoV-2

The magnitude of the initial viral load and the efficacy of the innate immune response, particularly that mediated by type I IFNs seem to be critical in setting the platform for both the subsequent adaptive response and the clinical outcome. Early development of a cytotoxic CD8⁺ T cell response, typically observed within 7 days of symptoms and peaking at 14 days, is correlated with effective viral clearance, mild disease and is in line with similar kinetics for humoral responses [75–77]. Effective viral control is associated with a T_H1 CD4⁺ phenotype, whereas a type 2 profile is often seen in those with severe disease [75,78]. High expression levels of effector molecules by CD8⁺ T cells in acute COVID-19 are associated with moderate illness [79]. Almost all viral proteins of SARS-CoV-2 can induce CD4⁺ and CD8⁺ T cell responses via the presentation on MHC molecules expressed by APCs [80] (Figure 2), whereas the S-protein induced T cell response is dominated by CD4⁺ T cells. Furthermore, S-protein can support antibody generation, with Tfh cells correlating with humoral immunity in the memory phase [81,82]. After the infection has been successfully warded off, a part of the defensive strategy is a long-term immune response for the future in the form of memory T cells. This is confirmed by the observation of SARS-CoV-2-specific memory T cell responses that are maintained in COVID-19 convalescent patients for up to 10 months post-symptom onset regardless of disease severity [83]. Also, long-lived CD8⁺ T memory responses, characterized by a CD45RA⁺ phenotype are identified after SARS-CoV-2 infection, suggesting that T cells play an important role in limiting the severity of reinfection [84].

Apart from cellular adaptive immune responses fulfilled by T cells, the humoral response against SARS-CoV-2 is similar to that against other coronavirus infections, involving the characteristic IgM and IgA production 5 days after the onset of symptoms and IgG production 14 days after the onset with specific neutralizing capacities for the S- or N-protein [85]. Particularly, secretory IgA can limit the transmission of SARS-CoV-2 through the airways in the first weeks to months post infection, whereas IgG is more stable than IgM and IgA antibodies over time [86]. However, a delayed humoral response and high titers of neutralizing antibodies reflect immunological imbalances that correlate with poor clinical outcomes [87–89]. Also the depletion of germinal centers in the spleen and lymph node, limiting B cell affinity maturation, isotype switching and production of mature antibodies, have been associated with increased mortality in COVID-19 patients [90,91], suggesting that an early onset of the adaptive immune response without aberrant activation is necessary for a protective host immune response against SARS-CoV-2 infection.

1.1.3 Type 2 immunity- parasite infections

Type 2 immunity is the host immune response that generates a protective immune response to multicellular **helminth parasites** and enables regenerative repair processes after tissue injury. In contrast, unnecessary type 2 immune activation in response to harmless environmental antigens, like allergens and venoms causes allergic reactions and tissue damage as well as chronic inflammatory diseases such as asthma and atopic dermatitis. Upon recognition of allergens or helminth infection, epithelial cells, stromal cells, glial cells, enteric neurons, tuft cells or DCs start to produce and release alarmins, including IL-25, IL-33, thymic stromal lymphopoietin (TSLP), neuropeptides (e.g. neuromedin U (NMU)) and bioactive lipid mediators (e.g. prostaglandin D₂, leukotrienes) [92–96] (Figure 3). Sentinel-derived alarmins and inflammatory mediators are involved in the recruitment and activation of further APCs as well as the expansion and/or differentiation of Gata3-expressing ILC2s and T_H2 cells [97–102] (Figure 3). Thus, these type 2 inducing cells act as sensory cells for the environment due to their proximity to the mucosal surface.

Alarmins as initiators of an effective type 2 immune response against helminths

Once secreted into the extracellular space by epithelial cells or DCs, IL-33 is processed by mast cell (MC)- and neutrophil-derived proteases, before binding to the IL-33R, termed ST2 on ILC2s, basophils, mast cells and T_H2 cells [103], thus enhancing type 2 cytokine responses and the expulsion of helminth parasites [104–106]. Similarly, IL-25 promotes worm expulsion and stimulates the differentiation of ILC2s, thereby promoting a potent type 2 cytokine response after helminth infection [107–110]. Tuft cell produced IL-25 can lead to increased production of IL-13 by ILC2s during helminth infection, which stimulates epithelial cell turn over and mucus production, resulting in worm clearance and tissue repair at the site of infection [94,111,112]. Like IL-25 and IL-33, epithelial derived TSLP promotes type 2 cytokine responses via regulation the polarization of T_H2 cells by suppressing IL-12 β production and surface expression of OX40L in DCs [113]. In addition to epithelial derived alarmins, neuron-derived signals play a pivotal role in regulating type 2 immune response during helminth infection. Specifically, NMU, which can be released by enteric cholinergic neurons upon activation via helminth-derived products, signals through its receptor, which is exclusively expressed by ILC2s and thereby promotes worm expulsion [114–116]. In a more recently published study, this is explained in an ILC2 and AREG-dependent manner [117]. Taken together, there is a complex relationship that exists between the mucosal epithelium and the nervous, endocrine, and immune system to initiate and regulate host-protective responses to helminth parasites.

ILC2s - first critical responders in type 2 immunity

Activated ILC2s and T_H2 cells secrete type 2 cytokines such as IL-4, -5, -9 and -13, which promote specific antihelminth responses including eosinophil recruitment, polarization of macrophages towards the alternative state and mucus production by goblet cells [118] (Figure 3). In line, in a more recent study, specific deletion of ILC2s uncovered the need for an appropriate eosinophil development, maturation, and recruitment and thus the requirement for orchestrating type 2 inflammation [119]. ILC2s have a non-redundant function in resistance to worm infections and in allergic lung inflammation [119]. Next to the more prominent type 2 cytokines (IL-4, -5 and -13), IL-9 enhances cytokine production and survival of ILC2s in an autocrine manner, leading to worm expulsion and tissue repair following helminth infection [120,121]. Furthermore, MHCII expressing ILC2s interact with antigen-specific T cells to promote autocrine IL-13 production and expulsion of parasites [122]. In line, ILC2-derived IL-13 licenses DCs to produce CCL17, which further potentiates the recruitment of T_H2 cells, suggesting that ILC2s are essential in the establishment of an adaptive immune response to helminth parasites [123].

Granulocytes, effective cells during helminth infection

Next to ILC2s, granulocytes, including eosinophils, neutrophils and basophils are important cell types during helminth infection (Figure 3). Eosinophils are recruited by eotaxin-1, which is regulated by ILC2s [124]. However, the central cytokine for eosinophil differentiation, extravasation from the bone marrow, survival and increased responsiveness towards eotaxin-1 is the type 2 cytokine, IL-5 [125]. Upon recruitment and activation, eosinophils mediate a rapid and potent response to diverse stimuli by releasing granules containing preformed cationic proteins, cytokines, chemokines, lipid mediators as well as growth factors like TGF β and VEGF [126]. Collectively, these soluble mediators activate anti-helminth mechanisms such as the secretion of mucus and the contraction of smooth muscle cells [125]. Furthermore, serum-activated eosinophils can interact with the parasite cuticle to directly release their granule content into the helminth or promote parasite clearance via the direct killing of larvae's after serum-activation *in vitro* [127–129]. In line, eosinophil deficiency can result in an increased worm burden which correlates with a diminished T_H2 cell infiltration and elevated *nos2* (iNOS) expression [130,131]. However, eosinophils are not essential for the type 2 immune response against all helminth parasites as e.g. eosinophil deficient mice infected with *Heligmosomoides polygyrus bakeri* (*H. polygyrus*) show similar worm burdens during primary and challenge infection [132].

Neutrophils accumulate during parasite infections, e.g. via the Ym-1 (a chitinase like protein (CLP)) dependent production of IL-17 from $\gamma\delta$ T cells or via CXCR2-mediated recruitment [133–135]. After recruitment and activation, neutrophil-derived IL-13 can induce alternatively activated macrophages (AAM) and thereby license macrophages to directly attach to and damage the parasitic larvae [133]. During a secondary infection, neutrophil trained macrophages as well as eosinophils surround the larvae, forming highly organized granulomas which are essential to confine the invading parasite and limit extensive host damage. Thus, neutrophils, macrophages and eosinophils cooperate to limit helminth survival. Furthermore, neutrophil extracellular DNA traps (NETs) are released and required for parasite killing [136,137]. Associated with NET formation is the facilitated and prolonged exposure of intracellular contents such as myeloperoxidase (MPO). In line, neutrophils and eosinophils require MPO and major basic protein (MBP) to kill helminth larvae *in vitro* and patients which were infected with the same parasite exhibit elevated serum levels of granular proteins [138,139], suggesting that NET formation is required for host defense against parasitic infections.

Although basophils constitute less than 1% of blood leukocytes under homeostatic conditions, peripheral basophilia is a hallmark of helminth infections. Similarly, as neutrophils and eosinophils, basophils are cytokine-producing granulocytes that contribute to type 2 responses via their secretion of IL-4, IL-6 and IL-13, as well as inflammatory lipid mediators including leukotrienes and prostaglandins that activate distinct components of anti-helminth immunity such as AAM macrophage polarization [140]. Furthermore, infiltrating basophils appear to be required for granuloma formation, contributing to acquired resistance [141]. However, it is also well known that basophils express the high-affinity IgE receptor Fc ϵ R1, which can bind antigen-specific IgE and become activated upon secondary exposure to antigens via Fc ϵ R1 cross-linking. Although IgE-mediated activation of basophils during primary infection is irrelevant for the expulsion of parasites, it is required for optimal T_H2 polarization and protective immunity after reinfection [142–144].

Mast cells (MCs) are tissue-resident granulocytes that, similar to basophils, are capable of contributing to anti-helminth immunity by crosslinking IgE and via the release of type 2 cytokines and effector molecules. Upon activation, MCs degranulate and release inflammatory mediators like histamine, eicosanoids, type 2 cytokines as well as the proteases mcpt1 and mcpt2 [145]. These effector molecules in turn induce the polarization of AAM macrophages, activate smooth muscle cell contraction, promote mucus production and increase the permeability of the intestinal epithelium leading to the expulsion of parasitic larvae [145,146]. Additionally, MCs might directly attack the parasites or prevent their

attachment to the epithelium by their release of mcpt2 and glycosaminoglycans [147–149]. Furthermore, MCs can also respond to signals released following helminth-induced epithelial cell damage such as ATP and activate ILC2s through their secretion of alarmins and PGD₂ [150–152]. In turn, ILC2s can promote MC survival and cytokine expression via the production of IL-9 [153,154] (Figure 3).

Macrophages as key effector cells during helminth infection

The importance of macrophages and their functions in resistance to parasites has been highlighted within the frame of this dissertation in the review “Macrophage regulation & function in helminth infection” (V) [155]. It is well appreciated that the strong type 2 cytokine response to helminths, characterized by the production of IL-4 and IL-13, results in the polarization of AAM or M2 macrophages, which are characterized by their expression of e.g. arg1, fizz1(retnla), ym1(chil3) and mrc1(cd206) [156,157] (Figure 3). Apart from IL-4 and IL-13 induced AAM polarization, macrophages are activated via helminth specific antibodies which can bind to FcεR (CD64) independently of IL-4Rα and STAT6 signaling, to directly trap parasitic larvae as well as drive the recruitment of myofibroblasts to granulomas, thus mediating tissue repair following helminth infection [158–160]. However, beyond type 2 cytokines and antibodies, ‘tissue-specific’ collectins, such as surfactant protein A (SP-A) and SP-D, the first component of the complement pathway C1q, as well as the phagocytosis of apoptotic cells can contribute to the activation of M2 macrophages following helminth infection [161–163]. Macrophages can further respond to chitin, which is an abundant biopolymer in eggs and cuticle of helminth parasites. Recognition of chitin drives an AAM phenotype that produces high levels of leukotriene B₄, thereby driving eosinophil recruitment, whereas the type 2 cytokine-mediated production of host-derived chitinases negatively regulates macrophage chemotaxis [164] (Figure 3). After activation, AAMs can directly act on helminth trapping and killing via the expression of their M2 polarization markers, such as Arginase 1 (Arg1), Chil3 and RELMα. For instance, a prime example is Arg1, which metabolically converts arginine into L-ornithine. In turn, L-ornithine and the polyamines spermidine, spermine and putrescine directly limit the motility of helminth larvae *in vitro* [158]. Furthermore, Arg1 activity contributes to parasite expulsion by increasing smooth muscle constriction [165], whereas further conversion of L-ornithine to proline and hydroxyproline promotes collagen-dependent tissue repair [166]. In keeping with these studies, Chil3 is implicated in the recruitment of eosinophils, which contributes to parasite killing in some helminth infections [167,168], while the activation of both RELMα and Chil3 correlates with tissue repair after infection with helminth parasites [169]. Indeed, compartmentalization of RELMα expressing macrophages specifically supports tissue

repair, extracellular matrix turnover and homeostasis, while providing protection during the infection with parasites in the lung [170]. Thus, in addition to priming macrophages for the direct trapping or damage of helminth larvae, the induction of a long-lived AAM phenotype provides mechanisms for reparative processes and thereby limit aberrant type 2 immunopathology.

The adaptive immune response to helminth infections: T- and B- cells

Downstream of the innate immune response to helminth infection, helminths potently induce the development of effector T_H2 cells via upregulating the transcription of type 2 cytokines in an STAT6 and GATA3 dependent manner. During helminth infection, naïve CD4⁺ T cells are primed via classical MHC class-II-mediated antigen presentation by DCs [101] (Figure 3). Primed T cells are activated to proliferate and differentiate to effector T_H2 cells, whereby IL-2 mediates initial T_H2 cell differentiation and IL-4 is required for expansion of antigen-specific T_H2 cells, which can in turn – in an autocrine feedback loop – produce IL-4 to further support T_H2 cell differentiation and expansion during helminth infection [171]. In the tissue, T_H2 cells orchestrate the activation and expansion of leukocytes primarily through the production of their cytokines, whereas IL-4 and IL-13 can also directly affect cell populations that express IL-4R but that are not derived from the bone marrow (BM), such as smooth-muscle cells, epithelial cells and myenteric neurons [172]. Activation of these non-hematopoietic cells increases smooth-muscle contractility, mucus production, and enhances fluids in the gut lumen, suggesting that T_H2 cell derived IL-4 and IL-13 can contribute to the ‘weep and sweep’ response that is characteristic of many intestinal helminth infections, in which increased luminal fluids (weep) and muscle contractility (sweep) are speculated to decrease adult worms and increase the likelihood of live parasite expulsion [173–175]. Apart from affecting weep and sweep reactions, IL-4 can mediate IgE or IgG1 class-switching in B cells, which in turn triggers mast cell and basophil degranulation. Although B cells do not provide complete protection or sterilizing immunity in some helminth infections, their various functions are arguably necessary to provide some level of type 2 anti-helminth immunity [176]. B cells are highly versatile due to their abilities to act as APCs and provide costimulatory signals, such as CD80/86, OX40L and ICOSL that are necessary for cell fate decisions of T_H2 cells during primary and secondary helminth infections [177–186]. In addition to directly promoting T_H2 cell polarization by priming naïve CD4⁺ T cells, B cells inhibit the capacity of DCs in producing T_H1-associated IL-12 and thus indirectly promote IL-4 associated T_H2 responses [187]. Furthermore, B cells generate follicles and reorganize follicular dendritic cells (FDCs) in an IL-4R α dependent manner to provide the optimal platform for the development of the protective immunity against helminth

parasites [188,189] (Figure 3). Next to promoting the differentiation of T_H2 cells, B cell derived antibodies mediate protection by activating eosinophils, macrophages, neutrophils, basophils and mast cells at the effector site (Figure 3). The roles of protective antibodies are more apparent during challenge infection, where antibodies are more specific, thereby triggering secretion of granulocyte-derived proteins which impairs migratory abilities of larvae to the tissue [190,191]. Apart from activating innate immune cells to directly or indirectly attack parasites, antibodies can impair the production of eggs and reduce the reproductive fitness of some worms [192,193], suggesting that B cells and antibodies can affect innate as well as adaptive immune cell responses to directly act on parasite development and invasion of tissues.

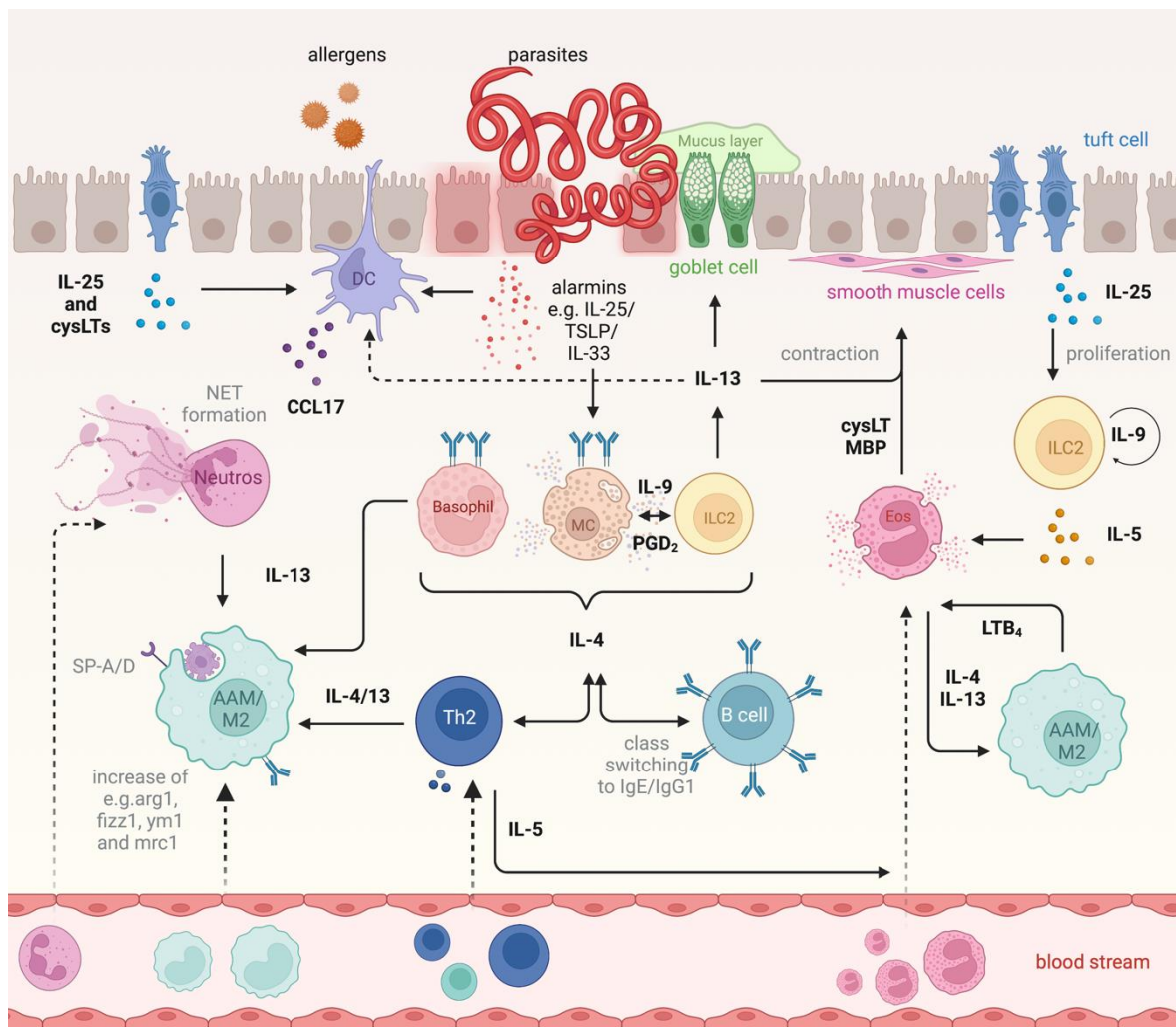


Figure 3: Principles of the host type 2 immunity to helminth infections (created with Biorender.com)

1.2 Macrophages as essential players during infectious disease

Macrophages (from Greek *μακρός* (*makrós*) = large, *φαγεῖν* (*phagein*) = to eat) , first described by Metchnikoff in the 19th century, are specialised cells involved in the detection, phagocytosis and destruction of infectious pathogens and other harmful organisms. In addition, they can also present antigens to T cells and initiate inflammation by releasing molecules, including cytokines, chemokines and bioactive lipid mediators to activate and recruit other immune cells (see section 1.1).

1.2.1 Monocyte, macrophage ontogeny and differentiation during infections

Ontologically, macrophages arise from macrophage precursors, which can be found in most tissues. However, there are also macrophage populations that can proliferate and maintain locally within the tissue independently of circulating precursors. For instance, macrophages within the epidermis, the central nervous system and the lung have the capacity to proliferate although they are terminally differentiated [194–197]. These macrophages, at least in mice, first develop on embryonic day 8 from the primitive ectoderm of the yolk sac and give rise to tissue-resident macrophages [198] (Figure 4). For instance, yolk-sac derived macrophages seed the embryonal lung on embryonal day 12.5, CD45⁺ cells expand on day 18.5 and finally fetal monocytes, but not fetal macrophages develop to alveolar macrophages during the first week of life [196]. Subsequently, the full development depends on a perinatal wave of epithelial derived GM-CSF, TGFβ as well as PPAR_γ, while maintenance needs persistent signaling of the first two [196,199,200].

Apart from fetal **macrophage development**, macrophages can arise during hematopoiesis (Figure 4). Definitive hematopoiesis begins in the fetal liver, which is first colonized by hematopoietic progenitor cells from the yolk sac and later from the haematogenous endothelium of the aorta gonadal mesonephros region of the embryo. Thereafter, the fetal liver is the source of definitive hematopoiesis, which generates circulating monocytes during embryogenesis. Coincident with postnatal bone formation, fetal liver hematopoiesis declines and is replaced by bone marrow hematopoiesis [198]. In the bone marrow, the predominant granulocyte-macrophage progenitor, under the influence of GATA2 and ZEB2, transitions to a monocyte-macrophage/dendritic cell precursor. From there, monocytes develop through the common monocyte precursor by expressing important transcription factors such as PU.1, IRF8, GATA2, and KLF4 [201]. After exit from the bone marrow, which depends on CCR2 in mice but is unclear in humans, monocytes comprise approximately 10% of circulating blood cells, whereas up to 90% of human blood monocytes exhibit the

classical monocyte surface marker combination HLAII⁺ CD14⁺ and CD16⁻, which corresponds to Ly6C^{hi} "proinflammatory" mouse monocytes. An intermediate subset (CD14⁺ CD16⁺ in humans or Ly6C^{int} in mice) appears to give rise to the nonclassical "patrolling" CD14^{lo} CD16⁺ monocytes, which in mice correspond to Ly6C^{lo} monocytes [201,202] (Figure 4). Classical monocytes can remain in the blood circulation for up to 72 hours before entering the respective organ to contribute to the predominant macrophage population or become intermediate or non-classical monocytes, which can again remain in the circulation for up to 7 days [201,203,204].

Although macrophages develop in several ways and show a divergent magnitude in their responsiveness to inflammatory cues in different tissues, they can polarize in a similar way (see also section 1.1). The simplified model of **macrophage polarization** includes the "classical" or "M1" phenotype, with activation upon lipopolysaccharide (LPS) or INF γ and the secretion of pro-inflammatory cytokines like IL-6, -12, -1 β , TNF, CXCL9, -10 and -11 as well as the production of reactive oxygen species (ROS) and nitric oxide (NO), whereas the "alternative activated" or "M2" phenotype is induced by IL-4 and IL-13 resulting in the secretion of IL-10 and in an advanced efferocytosis and tissue-reparative functions [205–211]. Thus, M1 macrophages are crucial for the host defense against bacteria and viruses, while M2 macrophages are characteristic for parasite infections or for the exposure to allergens (Figure 4). The picture of M1 and M2 describes the end of the polarization spectrum, because in between there are unlimited grades of polarization possibilities, which are depending on the current inflammatory trigger, the tissue and presence or absence of signaling molecules. For instance, M2 polarized macrophages include different subcategories ranging from M2a to M2c. M2a macrophages are important for tissue regeneration and show enhanced endocytic activity, which is identified by the IL-4 and IL-13 dependent surface expression of mannose receptor MRC1 (CD206) with the concomitant upregulation of Arg-1 and the production of proinflammatory cytokines and chemokines. In contrast, M2b macrophages are activated upon the stimulation with immune complexes and LPS, thus producing pro- as well as anti-inflammatory cytokines, including IL-1, IL-6, IL-10 and TNF α . M2c macrophages are activated by IL-10, TGF β and glucocorticoids, which in turn results in the production of IL-10 and TGF β , leading to the suppression of inflammatory responses [212]. Thus, macrophages are an ontogenetically diverse and functionally versatile cell type that can respond quickly to inflammatory cues, but at the same time repatriate homeostatic conditions.

Introduction

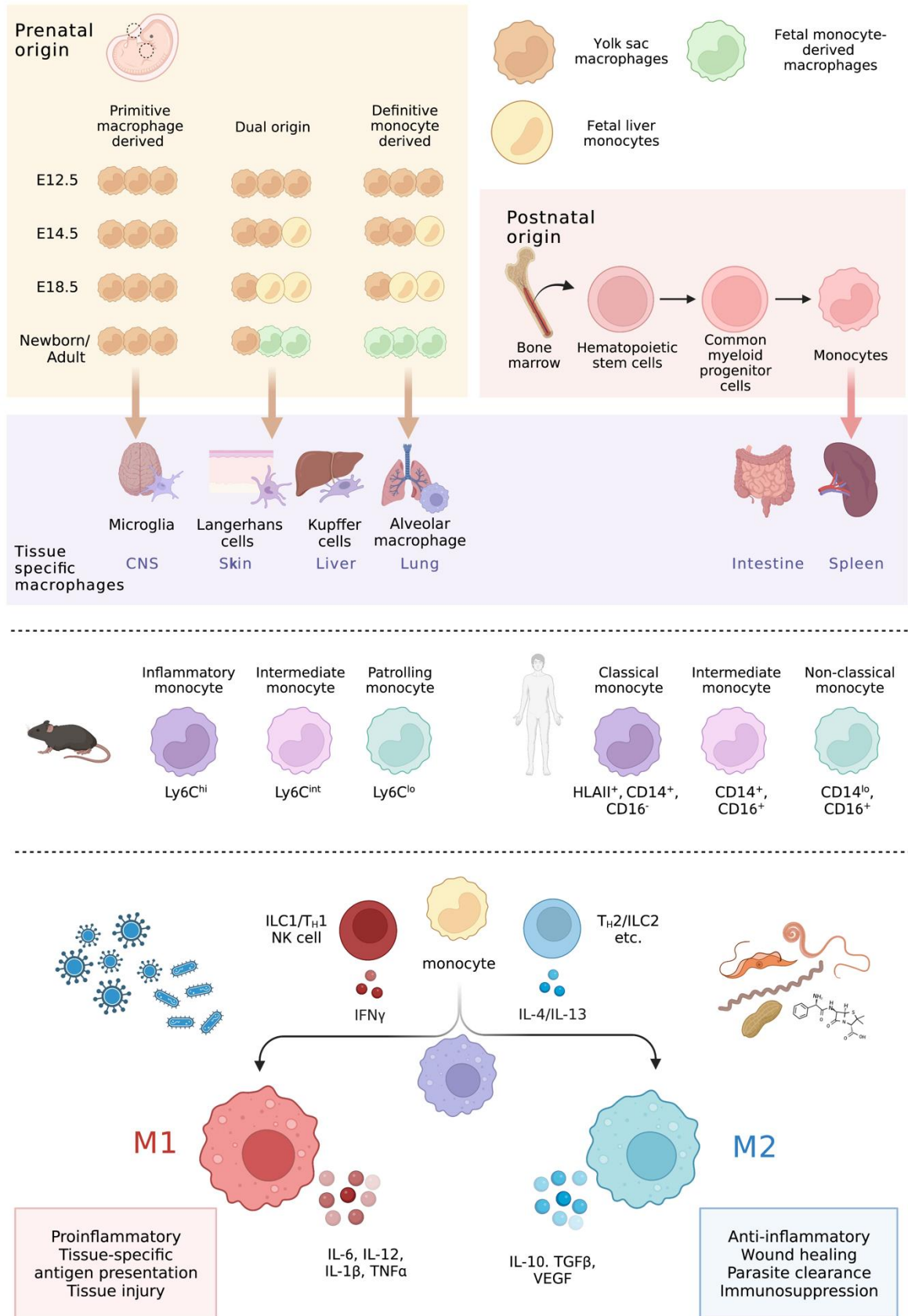


Figure 4: Ontogeny and differentiation of macrophage populations (created and adapted with BioRender.com)

1.2.2 The metabolic signature of macrophages during infections

Notably, **macrophages** must be plastic and coordinative and have to change their activation state to diverse facets of immune responses. Thus, macrophages can functionally adapt by reprogramming their **metabolism**. These metabolic changes are helpful to provide energy but also sustain changes in function and phenotype [213]. Five major pathways are used by most of cell types including macrophages to generate energy and to support the immune response to infections: glycolysis, the tricarboxylic acid (TCA) cycle, the pentose-phosphate pathway (PPP), fatty acid metabolism as well as the amino acid metabolism, which are all closely linked to each other. In most cells, energy supply is provided by the uptake of glucose. Once entering the cells through its transporters, glucose is metabolized through the glycolytic pathway (glycolysis). Along all these different steps, glycolysis can be exploited for the generation of amino acids or to provide intermediates for the PPP pathway, but its primary fate is to feed the TCA cycle with acetyl-CoA, which finally results in oxidative phosphorylation (OXPHOS) to generate energy in the form of ATP. Macrophages can respond to inflammatory cues with different pathways to meet their need. In case of classical, M1 activation, macrophages rely on increased glycolysis and the PPP, while mitochondrial OXPHOS is impaired. This rapid need of energy will allow them to sustain an inflammatory phenotype with increased phagocytosis, production of cytokines, chemokines, ROS as well as NO and thereby enhance bacterial or viral killing. On the other hand, alternative activation of macrophages is associated with the use of the TCA cycle, which is fueled by the fatty acid oxidation (FAO) and finally results in OXPHOS to generate energy. Generation of energy via OXPHOS promotes the glutamine metabolism as well as arginase activity, leading to the expression of M2 polarization markers with pro-reparative functions and the production of anti-inflammatory cytokines [214] (Figure 5).

Role of macrophage immunometabolism during viral infections in the lung

Similar to bacterial infections, macrophages adopt a more pro-inflammatory metabolic state during viral infections but with the concomitant increase in the interferon response. Even if macrophages are not the main producers of interferons, it is clear that they are able to control viral infections through the production of INFs with a dominant role for IFN- β [215]. Indeed, during VSV (Vesicular stomatitis virus) infection, glycolysis is increased through a type I IFN mediated pathway. Associated with increased glycolytic capacities, expression of glycolysis activator genes such as PFKFB3 promote viral phagocytosis and protects the mice during RSV infection [216]. In contrast, even if macrophages are highly glycolytic during SARS-CoV-2 infection, macrophages favor viral replication by increased ROS

production, which induces stabilization of hypoxia-inducible factor-1 α (HIF-1 α) and consequently promotes glycolysis (Figure 5). HIF-1 α -induced changes in monocyte metabolism by SARS-CoV-2 infection are associated with the direct inhibition of T cell response and reduced epithelial cell survival [217]. Thus, viruses can hijack host glycolysis (and metabolism in general) in an attempt to use these nutrients to sustain their replication and survival in the host as well as limit adaptive immunity [218,219]. Apart from affecting glycolysis, SARS-CoV-2 infection is linked to a reprogramming in lipid metabolism, where especially cholesterol is a point of entry into the cells [220]. In line, SARS-CoV-2 infected macrophages exhibit increased expression of several lipid synthesis modulators (including SREBP1/2, CD36, PPAR γ or DGAT-1) leading to the production of cholesterol and lipid droplets. In contrast to that, the host immune response to SARS-CoV-2 infection can limit viral infection by the induction of the interferon-inducible enzyme cholesterol 25-hydroxylase (CH25H), depleting cholesterol on the plasma membrane [221,222]. Thus, blockade of the cholesterol pathway can decrease both the viral replication and the inflammatory response induced by SARS-CoV-2 [223,224]. While little is known about the effect of virus infection on the PPP and TCA cycle in macrophages, the activation of macrophages by viral infections can affect the amino acid metabolism. Arginine is a critical metabolite for the replication of the virus and inhibition of Arg1 reduces viral replication and the ability to infect the host, however it might also be important in tissue repair after viral infection [225,226]. In contrast to arginine, viral infections enable macrophages to produce NO [227] (Figure 5). On the basis of this, some viruses like the Sendai virus try to restrain the production of NO as a mechanism to escape host immunity [228]. In fact, while beneficial at first, a sustained production of NO over time will lead to damage of host tissues and thereby to a decreased T_H1 response [227,229].

Macrophage metabolism during helminth infection

Although viral infections induce a more classical polarization of macrophages, and the glycolytic pathway is predominant, alternatively activated macrophages also manage to direct their metabolism towards glycolysis in an IL-4-dependent manner (Figure 5). In line, loss of the IL-4 induced signaling pathway consisting of AKT-mTORC2-IRF4 during helminth infection prevents AAM polarization and their ability to clear the infection [230]. Although glycolysis inhibition by the usage of the 2-Deoxyglucose (2-DG) can suppress AAM polarization by modulating the ATP levels and the JAK-STAT6 signaling, the application of this inhibitor also impacts cellular respiration [231]. In contrast to that, glucose depletion or galactose treatment without affecting OXPHOS does not affect AAM polarization [231]. Inhibition of other metabolic pathways during helminth infection, including

FAO, or the respiratory chain impacts several aspects of AAM polarization such as RELM α expression, while CD36 (scavenger receptor for fatty acid uptake) expression remains intact [231,232]. Apart from glycolysis, IL-4 activation can restrict the PPP in macrophages increasing the expression of the CARKL (Carbohydrate kinase-like) kinase that limits the production of sedoheptulose-7-phosphate, thus promoting an alternative activation [233] (Figure 5). A crucial regulator of AAM polarization is the protein LAMTOR1 (Late endosomal/lysosomal adaptor and MAPK and mTOR activator 1), which is necessary for the recruitment of mTORC1 to the lysosome in response to amino acid stimulation [234]. Importantly, macrophages deficient for LAMTOR1 or depleted in amino acids in the media are completely unable to express AAM polarization markers including Arg1, CD206 or RELM α , suggesting a crucial role for amino acids in the induction of AAM polarization [235]. The AAM effector molecule arginase 1 produces ornithine, which AAMs convert to hypusine used to post-transcriptionally modify a translation initiation factor, eIF5A. Polyamine-eIF5-hypusine regulates mitochondrial function and OXPHOS in AAMs and blockage of this pathway inhibits protective effects during helminth infection [236] (Figure 5). Thus, helminth infection can directly or indirectly induce metabolic programs that enable AAM activation and effector functions.

1.2.3 Metabolic and epigenetic reprogramming as a source for trained immunity

As mentioned, macrophage polarization induces a shift in metabolism. The increase in glycolysis during M1 polarization disrupts the TCA cycle at a point where isocitrate (aconitate) is converted into α -ketoglutarate (α -KG) [237]. This break influences the inflammatory output of macrophages by the accumulation of TCA intermediates. As a direct consequence, citrate accumulation results in the increased capacity to be converted to acetyl-CoA via ATP-citrate lyase (ACLY), thus leading to histone acetylation, which in turn facilitates polymerase binding and gene transcription [238,239]. Alternatively, citrate is exported via the citrate transporter and contributes to fatty acid or eicosanoid synthesis. Furthermore, accumulation of the TCA intermediate aconitate is metabolized via immune-responsive gene 1 (IRG1) to itaconate. In turn, itaconate is able to inhibit succinate dehydrogenase (SDH) which contributes to succinate accumulation, while at the same time showing anti-inflammatory functions with for instance the regulation of type I interferons during viral infection [240]. An increased succinate/ α -KG ratio contributes to HIF-1 α stabilization in the nucleus and thus to an increased IL-1 β production [241]. Stabilization of HIF-1 α is further promoted by the concomitant increase of ROS, formed via NADPH production in the PPP or directly in the mitochondria due to the TCA cycle disruption

[242,243] (Figure 5). In contrast to M1, AAMs have an intact TCA cycle and mainly meet their energy demand via fatty acid oxidation and oxidative phosphorylation. The rely on OXPHOS in AAMs could also be explained by the reciprocal ratio of α -KG to succinate due to increased glutaminolysis [244]. As already explained for histone acetylation by the increased production of acetyl-CoA, there is an intricate link between metabolic activity and epigenetic remodeling, where metabolites function as important cofactors for histone modifying enzymes [239,244,245]. For instance, α -KG and O_2 provide help for dioxygenases like the HIF-degrading prolyl hydroxylases or lysine demethylases such as KDM5 [246]. In contrast, 2-hydroxyglutarate which is a further downstream metabolite of α -KG inhibits histone demethylases and TET 5-methylcytosine hydroxylases [247,248]. A role in histone modification also during helminth infection has been described for Jmjd3, a H3K27 demethylase which is necessary for AAM polarization in an IRF4-dependent manner [249] (Figure 5). More general, AAM activation is regulated by IL-4 and STAT6 signaling, leading to repression of selective enhancers, diminished p300 histonacetyltransferase activity and increased histondeacetylase (HDAC) binding which further reduces the inflammatory response [250]. In contrast, an attribution for HDAC3 in the negative regulation of AAM polarization has been shown [251]. However, another study uncovered IL-4-triggered H3K27ac at enhancer regions of AAM genes (e.g. *arg1*) [252], suggesting a central role for H3K27 modification in AAM polarization and functions during helminth infections.

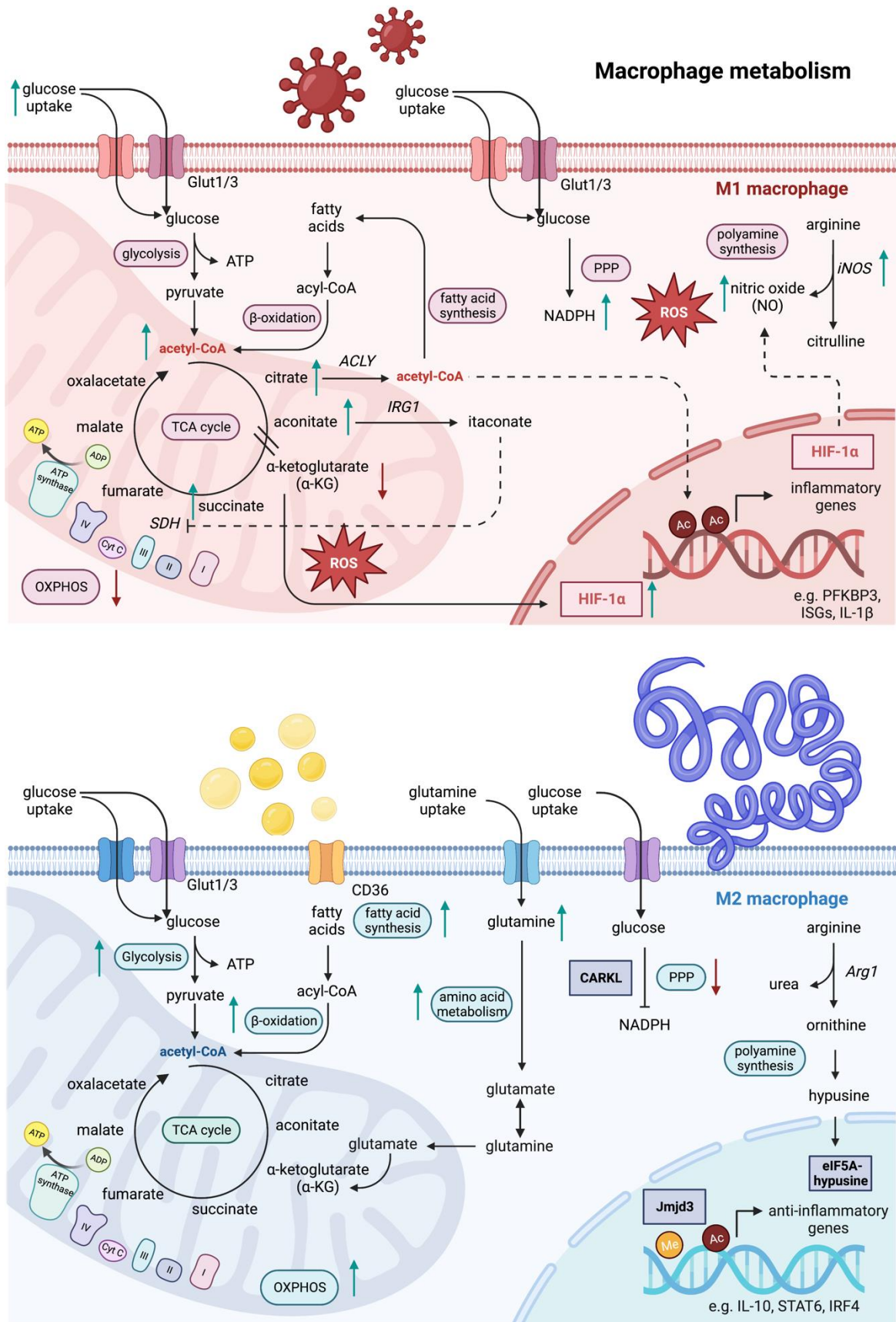





Figure 5: Epigenetic and metabolic reprogramming in infected macrophage populations (adapted and created with Biorender.com).

In addition to the acute regulation of macrophage activation, helminth infections can have anti-inflammatory long-term effects due to metabolic and epigenetic reprogramming in hematopoietic precursors which differentiate into hyporesponsive monocytes [253,254]. Indeed, the long-term reprogramming of monocytes and macrophages can result in lasting protection against infectious diseases without activating the adaptive immune system. Such unspecific immune memory, evident in macrophages and other innate immune cells is termed “**trained immunity**”. One of the first studies showed that monocytes “trained” with the polysaccharide β -glucan can induce protection against *Staphylococcus aureus* [255]. When subjected to a lethal dose of *Candida albicans* after “training” of monocytes with β -glucan, mice without an adaptive immune response were protected, which correlated with an increase in histone methylation (H3K4me3) and acetylation (H3K27ac) at promoter regions of glycolytic genes, enhanced glycolysis and inflammatory cytokine production [256,257]. To enable long-time memory in rather short-lived cells like monocytes, metabolic or epigenetic reprogramming has to take place at the progenitor level, which is termed “central trained immunity” [258]. Central trained immunity can for instance be provoked by vaccination with Bacillus Calmette–Guérin (BCG), enabling protection against tuberculosis. BCG can enter the bone marrow and impact methylation patterns in hematopoietic stem cells (HSCs), which are giving rise to bone marrow derived macrophages (BMDM) and CD14⁺ monocytes, showing increased antimycobacterial activity [259–261]. In contrast to enhanced innate immune responses, trained immunity can also lead to tolerance for instance by stimulation with LPS. LPS-induced hyporesponsiveness results from an increase in histone acetylation leading to an increased expression of IRG1 with the associated production of itaconate, whereas in sepsis, tolerogenic responses are dependent on cyclooxygenase activity [262,263]. Apart from central trained immunity, peripheral trained immunity is induced in local cells. Viral infections are able to induce a state of trained immunity in resident alveolar macrophages with the help of CD8⁺ T cells, enhancing antibacterial defense in the lung [264]. Taken together, epigenetic reprogramming of BM-derived, recruited and resident proliferating macrophages may result in diverse and persistent alterations of macrophage effector functions, particularly following chronic infections.

1.3 Helminths as modulators of type 2 immunity

Soil transmitted **helminths** (STHs), such as whipworms, roundworms, and hookworms, are among the most prevalent parasites in humans. Of note, around one billion people are still infected with one of those species worldwide (Table 2), primarily in tropical and subtropical regions where exposure to infective larvae is common [265]. Although infections by these pathogens are generally not fatal, they are associated with high rates of morbidity, with repeated infections that can lead to anemia, malnourishment, and impaired cognitive development. Once they have infected the host, adult STHs reside in their niches and often establish chronic infections, which can last for many years, with the presence of adult worms being well tolerated by the host immune cells at mucosal sites [265]. In this setting almost every facet of the immune system is modified or even recalibrated, with infected subjects displaying a state of immune hyporesponsiveness that can be considered as a form of immunologic tolerance.

Table 2: Helminth classification. This table includes all helminths mentioned in this thesis

Phylum	Order/Class	Host	Scientific name	
Flatworm (platyhelminths) 	Cestoda	Carnivores/ Rabbits	<i>Taenia pisiformis/ crassiceps</i>	
		Humans/ Pigs	<i>Taenia solium</i>	
	Trematoda	Rhabditida	Humans	<i>Onchocerca volvulus</i>
		Fish-eating mammals/ Humans		<i>Clonorchis sinensis</i>
			Wild ruminants/ Humans	<i>Fasciola hepatica</i>
		Wild mammals/ Humans	<i>Schistosoma japonicum/ mansoni</i>	
Trichocephalida		<i>Trichinella spiralis</i>		
Roundworm/ Whipworm (nematode)  	Ascaridida	Carnivores/ Humans	<i>Toxocara canis</i>	
		Humans/ Pigs	<i>Ascaris lumbricoides/ suum</i>	
	Rhabditida	Carnivores	<i>Ancylostoma caninum/ ceylanicum</i>	
		Carnivores/ (Humans)	<i>Dirofilaria immitis</i>	
			<i>Brugia malayi</i>	
		Humans	<i>Necator americanus</i>	
			<i>Strongyloides stercoralis</i>	
			<i>Acanthocheilonema viteae</i>	
			<i>Heligmosomoides polygyrus bakeri</i>	
		Rodents	<i>Litomosoides sigmodontis</i>	
	<i>Nippostrongylus brasiliensis</i>			
	<i>Strongyloides venezuelensis</i>			
Trichocephalida	Humans/ Pigs	<i>Trichuris suis</i>		

Several mouse models of parasitic infection have been used to study how the host's immune system responds to tissue-migrating parasites and how chronic infection leads to tolerance. The most commonly used parasites include *Nippostrongylus brasiliensis* and *Heligmosomoides polygyrus bakeri* (*Hpb*). *N. brasiliensis* goes through a life cycle that involves skin penetration, tissue migration to the lungs, colonization of the gut, and egg reproduction before being expelled by the host [266]. In contrast, the strictly enteric *H. polygyrus* is a chronic infection that persists for several months in the rodent host by establishing itself in the small intestine [266,267] (Figure 6).

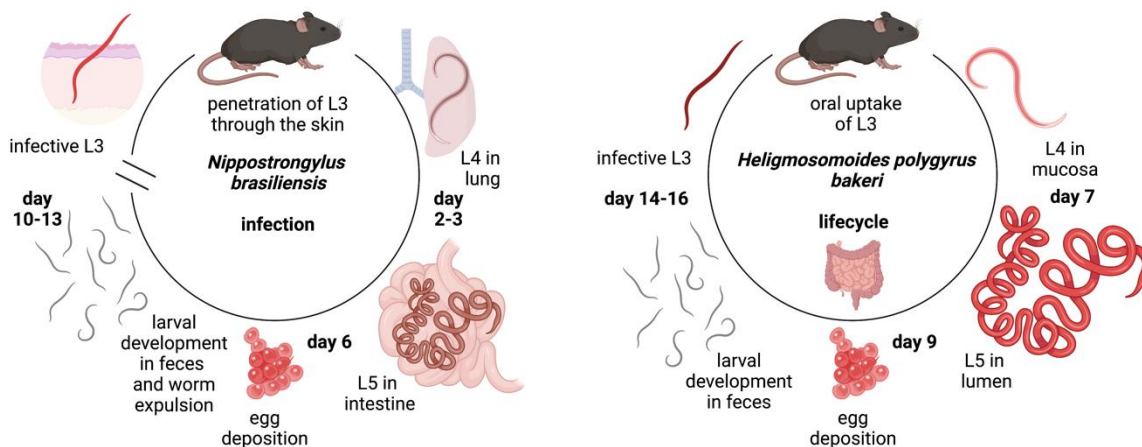


Figure 6: Model infection with *N. brasiliensis* or *H. polygyrus* (created with BioRender.com)

1.3.1 Helminth-induced immune evasion by parasite-derived effector molecules

To study the ways in which helminths influence the immune system, it is important to focus on the mechanisms involved in their removal from the body, as these are likely to be the main targets of modulation. Thus, it is becoming clear that parasites have evolved strategies to manipulate, undermine, or evade any aspect of the host immune response by a spectrum of immunomodulatory molecules that are now beginning to be defined. Recent advances in helminth genomics and proteomics have uncovered a wealth of such immunomodulatory products (Table 3).

Parasite-derived molecules neutralize factors form the first line of defense

After invading the body and activating epithelial cells by tissue injury, parasite infections result in the release of “alarmin” cytokines such as IL-33. The murine intestinal nematode *H. polygyrus* has evolved an alarmin release inhibitor (**HpARI**) within its excretory secretory (ES) products to suppress IL-33 release [268,269] (Figure 7). HpARI contains three domains, with the first binding to DNA, while the second and third domain are binding to

active IL-33. Attachment and tethering in the nucleus of necrotic cells impedes the interaction of the complex with the IL-33 receptor ST2. During *N. brasiliensis* infection, HpARI administration suppresses the host type 2 immune response, thus abrogating the expulsion of adult worms from the intestinal lumen. Crucially, HpARI prevents IL-33 release from human lung explants and blocks human IL-33 release in a transgenic mouse model [269]. Apart from binding of IL-33, *H. polygyrus* can interfere with the IL-33 pathway at multiple levels. The recently discovered Binds Alarmin Receptor and Inhibits (**HpBARI**) protein blocks the ST2 receptor in men and mice [270] (Figure 7). Another undefined *H. polygyrus* product further downregulates IL-33 production through induction of IL-1 β resulting in parasite chronicity, whereas the release of *H. polygyrus*-derived **exosomes** can suppress the transcription of ST2 [271–273] (Figure 7). Exosomes are small membrane-enclosed structures which can transport cargo such as microRNAs (miRNA), proteins or metabolites. Several other studies describe an involvement of helminth-derived extracellular vesicles in modulating host immunity and especially macrophage polarization. Delivery of *Fasciola hepatica*-derived miRNA, fhe-miR-125b downregulates classical activation of macrophages by inhibiting *traf* [274]. In line, macrophage classical activation is also suppressed by *Taenia pisiformis* exosomes, which deliver the miRNA let7-5p to inhibit macrophage *Cebpd* mRNA and thus reduce *il12* and *nos2* gene expression [275]. In contrast, although the mechanism is unclear, *Schistosoma japonicum*-derived exosomes could promote M1 polarization, whereas preventing of AAM polarization and reduction of IL-10 is triggered by *H. polygyrus*-shuttled exosomes, suggesting that it is beneficial for parasites to target the activation and polarization of macrophages [273,276] (Figure 7). Different stages of parasites lifecycle can require specific conditions in order to thrive in different tissue settings and efficiently evade host immunity.

Helminth-derived factors modulating the innate immune response by targeting macrophages and DCs

Macrophages adopt a dominant role during parasite infections, and they are producers of a broad repertoire of effector molecules which can be targeted by helminth parasites (see also section before). Based on this, a review on “Macrophage regulation and function in helminth infection” (V) is published as part of this dissertation.

A crucial point is the recognition of and reaction to pathogen molecules by PRRs on myeloid cells (see section 1.1). These reactions can be targeted by helminth molecules, with for instance the blockage of TLR ligand-induced DC and macrophage activation, interfering with receptors and their signaling, as well as antigen presentation and downstream effector

mechanisms. One of the earliest identified helminth molecules, **ES-62**, secreted from the filarial nematode *Acanthocheilonema viteae* carries immunomodulatory phosphorylcholine (PC) moieties, that induce sequestration of the MyD88 signaling protein, leading to suppression of TLR and IL-33 signaling [277–280]. A different mechanism is deployed by the immunomodulatory fatty acid binding protein **Fh12** (and its recombinant form, Fh15) from the liver fluke *F. hepatica*. Both proteins can induce alternative activation in human monocyte-derived macrophages (MDMs), in part by downregulating the coreceptor CD14, which leads to the suppression of the TLR4 signaling cascade (p38, ERK, JNK) and thus ultimately to diminished IL-12 and IL-1 β levels [281]. Furthermore, cysteine proteases from *F. hepatica* (**FhCL1**) and *Schistosoma mansoni* (**SmCB1**) directly suppress myeloid cell TLR signaling by the intracellular degradation of TLR3 and TLR4 [282]. In contrast, some helminth-derived molecules can actually stimulate the activity of TLRs or CTLs instead of inhibiting them. For instance, the phospholipid lysophosphatidylserine (**lyso-PS**), which is enriched in the tegument of *S. mansoni* adult worms [283] can act as a TLR2 agonist. On the basis of this, lyso-PS has the ability to foster DC maturation, which affects the activation of IL-10 producing Treg cells, ultimately leading to the suppression of effector T cell proliferation [284]. In contrast, the 66-amino acid mucin-like polypeptide from *F. hepatica* (**Fhmuc**) is not directly activating TLR4 signaling, but it enhances LPS-induced TLR4 activation of DCs, resulting in a T_H1 cell response [285,286].

When host myeloid cells are activated through one of their cognate PRRs, they initiate the proteolytic processing of exogenous antigens as well as start to express a large variety of stimulatory surface receptors and mediators. Helminths can counter regulate these processes with an arsenal of protein modulators, ranging from protease inhibitors to receptor ligands. Among the inhibitors, cystatins interfere with cysteine proteases involved in antigen processing, such as lysosomal cathepsins and asparaginyl endopeptidase (AEP). Several helminth-derived cystatins have been discovered, including CPI-2 from *Brugia malayi*, LsCystatin from *Litomosoides sigmodontis*, Onchocystatin from *Onchocerca volvulus*, AvCystatin from *A. viteae*, Nippocystatin from *N. brasiliensis* as well as cystatins from *S. japonicum*, *Ascaris lumbricoides*, *Trichinella spiralis* and the liver fluke *Clonorchis sinensis* [287–296]. The filarial cystatin, **CPI-2** from *B. malayi*, specifically inhibits AEP in human cells, thereby blocking antigen processing, while **LsCystatin** reduces nitric oxide- and antigen-specific proliferative responses [287,288]. Studies have also demonstrated that **Onchocystatin**, **AvCystatin**, and other helminth cystatins, possess broad immunomodulatory properties, such as the induction of IL-10 from human monocytes and macrophages, as well as downregulation of MHCII and CD86 [291–296]. The specific

physiological target of these cystatins *in vivo* has yet to be identified, but cystatin- induced upregulation of IL-10 in macrophages is mediated via MyD88 (TLR2 and TLR4) signaling [297]. This may suggest that TLR-signaling is likely involved in the cystatin-triggered induction of IL-10 producing macrophages, which on the one hand can inhibit inflammation and on the other hand drive helminth-induced immune evasion.

Apart from signaling through PRRs, helminths can modulate myeloid cells through the mimicry of host cytokines. Specifically, macrophage migration inhibitory factor (MIF) proteins, which are evolutionarily ancient and which can activate myeloid cells in mammals, have been found to have homologs in nematodes such as *B. malayi* and *T. spiralis* [298–300]. However, in helminth infection, endogenous MIF plays a protective role in reducing parasite burden through stimulation of both innate and adaptive immune cells in a STAT3-dependent manner [301,302]. Parasite-derived homologs mirror the activity of the host protein, inducing the release of interleukin-8 from monocytes. Additionally, **MIF** from *B. malayi* potentiate alternative activation of macrophages in synergy with IL-4 [303], suggesting that the mimicry does not always adopt the host cytokine function. Similarly, *F. hepatica* can secrete a protein termed helminth defense molecule, or **FhHDM-1**, which is a mimicry of the mammalian cathelicidin-like host defense peptide. FhHDM-1 binds LPS and thus prevents TLR4- dependent macrophage activation [304]. It can further be internalized by the endosomal pathway leading to degradation by cathepsin L which releases a short C-terminal peptide, which in turn prevents antigen processing by acidification and NLRP3 inflammasome inactivation [305,306]. Furthermore, FhHDM-1 influences macrophage metabolism towards the induction of glutaminolysis and the accumulation of α -ketoglutarate, resulting in the inhibition of inflammatory functions [307].

Apart from signaling pathways and antigen processing, helminth molecules, such as **Omega-1**, a glycoprotein released by *S. mansoni* eggs, and its homolog **CP1412** from *S. japonicum* can significantly impact myeloid cell protein expression. Omega-1 is a T2 ribonuclease that is recognized through the mannose receptor (MR) on DCs via binding to its glycan moiety, Lewis-X. After being taken up, Omega-1 causes the global degradation of RNA within the cell, thereby suppressing the activation and maturation of DCs, blocking the upregulation of CD86 and MHCII as well as the synthesis of IL-12 in response to CD40 ligation. This ultimately favors the induction of both T_H2 cells and regulatory T cells [308–313]. In contrast, Omega-1 acts on multiple PRRs, including the CTL receptor dectin-1 and TLR2, resulting in the secretion of the inflammasome-dependent IL-1 β in peritoneal macrophages [314]. Additionally, recent studies have highlighted the beneficial effects of helminth infection on host metabolism, which can be replicated by helminth products such

as *S. mansoni* egg antigen (SEA) or recombinant Omega-1. Injection of Omega-1 into obese mice improves insulin sensitivity through the release of IL-33 from white adipose tissue, which in turn induces ILC2 activation and M2 macrophage differentiation. The mechanism behind this effect is thought to involve the RNase activity of omega-1 and the ligation of the MR [224–228].

Another example of manipulation of myeloid cell signaling by helminth-derived molecules includes the abundant larval transcript (**ALT**) protein from *B. malayi*, where upon transfection in macrophages, ALT is found to induce upregulation of SOCS1, a potent inhibitor of IFN- γ signaling during inflammatory responses [320]. Apart from that, some helminth proteins contain a nuclear localization signal (NLS) for rapid translocation to the nucleus, including the *S. japonicum*-derived molecule **Sj16**, which induces IL-10 and inhibits DC maturation following nuclear translocation [321]. Thus, macrophages and DCs represent an attractive target for helminths and their immunomodulatory products, which often lead to upregulation of anti-inflammatory mediators and tolerized T cell responses (Figure 7).

Helminth-derived products defeat granulocyte function

Granulocytes, specifically eosinophils and neutrophils, have the ability to migrate towards the site of infection and eliminate pathogens through a range of mechanisms, including the release of toxic compounds, deprivation of essential nutrients, and alteration of the parasitic microenvironment (see section 1.1). In order to evade granulocyte-mediated host defense, parasites may secrete molecules that inhibit the recruitment and function of these effector cells, thus promoting their survival (Figure 7). For instance, hookworms, such as *Necator americanus* can secrete metalloproteinases which can specifically cleave eotaxin-1 (CCL1), but not IL-8, eotaxin-2 or LTB₄, thereby inhibiting the eotaxin-mediated recruitment and activation of eosinophils [322]. Neutrophils contribute to helminth damage and worm expulsion by promoting the development of AAMs [133]. Parasites have evolved different strategies to modulate neutrophil migration. Interestingly, *S. mansoni* eggs can secrete a chemokine binding protein (**SmCKBP**) that has the ability to bind and block IL-8, CCL2, CCL3, CCL5, and CX3CL1, which leads to the missing activation of chemokine receptors and finally to reduced neutrophil migration. In contrast, blocking of SmCKBP *in vivo* results in increased neutrophilia in *S. mansoni* egg-induced granulomas [323]. In concert with chemokines, the process of cell migration also involves engagement with integrins, such as CD11b/CD18, to enable extravasation. A protein found in *Ancylostoma caninum*, referred to as **NIF**, binds to this integrin in conjunction with fibrinogen, thus hindering the binding of

human neutrophils to vascular endothelial cells [324]. Lastly, a more recent study has uncovered a deoxyribonuclease (DNase II) to degrade NET formation and thus evade host immune response to the larval state [137].

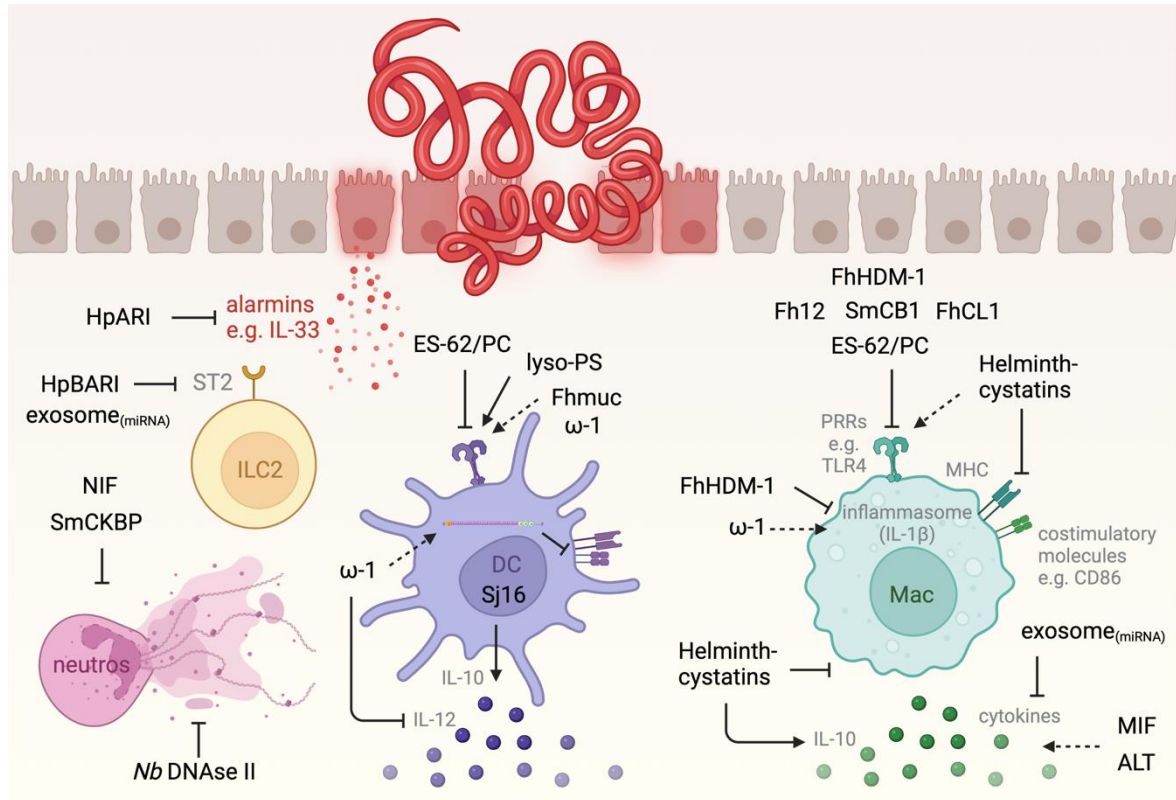


Figure 7: The early host immune response is modulated by helminth molecules (created with Biorender.com)

Adaptive immune response is targeted on multiple levels by helminth effector molecules

Manipulation of adaptive immune responses has the potential to elicit long-term effects in the host organism, such as the establishment of memory responses that recognize the parasite as a part of the host which leads to chronicity. Parasitic helminths possess a variety of mechanisms for suppressing effector responses and promoting the induction of regulatory responses, including regulatory T- and B-cells (Table 3).

A prime example of both homologous and de novo-generated immunomodulatory molecules from helminth parasites can be found in the parasite ligands of the TGF β receptor. The consequences of host TGF β signaling is largely immunosuppressive, resulting in the generation of inducible Treg cells, inhibition of DCs, macrophage, effector T cells and a shift towards the production of IgA antibodies [325]. Therefore, activation of the TGF β pathway would be beneficial for a parasite that seeks to evade the host's immune response. Indeed, several parasitic TGF β homologues have been identified. The *B. malayi*

TGH-2 protein signals through the TGF β R [326], while extracts from the parasite *L. sigmodontis* can bind the TGF β R in a manner that cannot be blocked by antibodies specific to TGF β [327]. In contrast, the *F. hepatica*-derived protein **FhTLM** can bind host receptors with lower affinity and its activity can be inhibited by anti-TGF β antibodies. Immunologically, FhTLM stimulates the production of IL-10 in macrophages, indicative for an immune-regulatory function [328]. Another striking example, which affects the TGF β pathway is derived from *H. polygyrus*. Studies have demonstrated that secreted products (HES) from this parasite activate the TGF β signaling pathway by phosphorylation of SMAD-2/3 to induce regulatory T cells *in vitro*, even in the presence of pro-inflammatory cytokines, and to a similar extent as TGF β itself [329]. More recently, the factor responsible for this activity is characterized as the unrelated protein called **TGM** (TGF β mimic), which is able to bind with high affinity to both TGF β receptor I and II [330]. While the TGF β pathway directly induces regulatory T cells, other helminth-derived molecules exploit indirect pathways to modulate host T cell responses. The secreted anti-inflammatory protein 2 (**AIP-2**) from *A. caninum* directly licenses DCs to promote the induction of Treg and IL-10 responses, and it is able to reduce the levels of inflammatory cytokines by altering DC function [331]. Similarly, **PAS-1** from *Ascaris suum* induces an expansion of CD25⁺ Treg cells, while it can induce CD8 $\gamma\delta$ TCR T cells [332]. Apart from inducing regulatory T cells, **AcK1** found in *A. caninum* and *Ancylostoma ceylanicum*, as well as **BmK1**, discovered in *B. malayi* are peptides that inhibit primarily the proliferation of memory T cells without affecting naive or central memory subsets by targeting the voltage-gated potassium (Kv) 1.3 channel [333].

Another relevant target for helminth parasites is the host B cell response, which is known to be crucial for parasite ejection [334]. Next to modulating TLR function on myeloid cells, **ES-62** is also able to uncouple the B-cell receptor (BCR) machinery, leading to unresponsiveness [335]. Ancylostoma secreted protein 2 from *N. americanus* (**Na-ASP-2**) can bind CD79A, a component of the BCR that leads to downregulation of mRNA expression of proteins involved in signaling and transendothelial migration [336]. Finally, **IPSE** from *S. mansoni* induces IL-10 producing B cells, while *S. mansoni*-derived **SM22.6** and **PIII** trigger the expansion of CD4⁺ Foxp3⁺ T cells [337,338], suggesting that the same parasite can affect T- and B-cell responses.

Thus, the adaptive response during helminth infection then determines effector cell responses and whether the outcome of infection is inflammation, resolution, parasite ejection, or tolerance. Taken together, the discovery of all these helminth molecules

Introduction

(Table 3) shows a potent modulation of the innate- as well as adaptive immune system often by their capacities to shift pro-inflammatory responses towards anti-inflammatory or regulatory mechanisms which allows the parasites to survive within the host. This has the potential both to transform our understanding of parasite adaptation to the host and to develop possible therapies for type 2 inflammatory diseases, such as asthma and allergy.

Table 3: Immune-regulatory molecules produced by helminths and their cellular mechanisms to drive evasion

Helminth molecule	Abb.	Species	Function and physiological consequences	Ref.
<i>Modulation of the early host immune response by helminth effector molecules</i>				
Alarmin release inhibitor	HpARI	<i>H. polygyrus</i>	Blocking of IL-33	[269]
Binds Alarmin Receptor and Inhibits	HpBARI	<i>H. polygyrus</i>	Blocking of ST2 receptor	[270]
Exosome	EV	<i>H. polygyrus</i>	Contains miRNAs that target epithelial cells and macrophages → loss of ST2	[272,273]
	EV	<i>F. hepatica</i>	Contains fhe-miR-125b miRNA that targets <i>Traf</i>	[274]
	EV	<i>T. pisiformis</i>	Contains let7-5p miRNA that targets <i>Cebpd</i> → reduction of <i>Il12</i> and <i>Nos2</i> gene expression	[275]
	EV	<i>S. japonicum</i>	Promote M1 differentiation	[276]
Excretory-secretory product 62	ES-62	<i>A. viteae</i>	Modulates myeloid cell responses by suppressing TLR signaling, uncoupling of BCR machinery from the MAPK Erk pathway	[277–280,335]
Fatty acid binding protein	Fh12/15	<i>F. hepatica</i>	Induction of AAMs; suppress LPS-induced activation via binding to CD14	[281]
Cathepsin L peptidases	FhCL1	<i>F. hepatica</i>	Degrades TLR3	[282]
Lyso-phosphatidyl-serine	Lyso-PS	<i>S. mansoni</i>	TLR2 agonist, induces DC maturation and activation of IL-10 producing T cells	[283,284]
Mucin-like polypeptide	Fhmuc	<i>F. hepatica</i>	Enhances LPS-induced TLR4 activation of DCs and T _H 1 cell induction	[285,286]
	CPI-2	<i>B. malayi</i>		[287]
	LSCystatin	<i>L. sigmodonti</i>		[288]
	Onchocystatin	<i>O. volvulus</i>		[289]
	AvCystatin	<i>A. vitae</i>		[291]
	Nippocystatin	<i>N. brasiliensis</i>	Induction of regulatory IL-10 producing macrophages	[296]
	rSjCystatin	<i>S. japonicum</i>		[292]
	rAi-CPI	<i>A. lumbricoides</i>	[293]	
	rCsStefin-1	<i>C. sinensis</i>	[294]	
	TsCstN	<i>T. spiralis</i>	[295]	

Introduction

Macrophage Migration Inhibitory Factor homolog-1	MIF-1	<i>B. malayi</i> ; <i>T. spiralis</i>	Induce IL-8 release from monocytes and AAM polarization in synergy with IL-4	[298–300,303]
Helminth defense molecule-1	FhHDM-1	<i>F. hepatica</i>	Can bind LPS which prevents TLR4 signaling and NLPR3 inflammasome activation via acidification	[304–307]
Omega-1	ω -1	<i>S. mansoni</i>	Ribonuclease degrades mRNA after uptake via MR, thus primes DCs for enhanced T _H 2 cell response; IL-1 β secretion from macrophages	[308–314]
	CP1412	<i>S. japonicum</i>		
Abundant Larval Transcript	ALT	<i>B. malayi</i>	Upregulation of SOCS1 which inhibits IFN- γ signaling	[320]
16 kDa polypeptide	Sj16	<i>S. japonicum</i>	Translocates to the nucleus and induces IL-10 production in DCs	[321]
Chemokine binding protein	SmCKBP	<i>S. mansoni</i>	Inhibits neutrophil recruitment and neutralize chemokine activity	[323]
Neutrophil inhibitory factor	NIF	<i>A. caninum</i>	Blocks neutrophil extravasation by binding to integrins	[324]
Deoxy-ribonuclease	DNAse II	<i>N. brasiliensis</i>	Degradation of NETs	[137]
<i>Modulation of the adaptive host immune response by helminth effector molecules</i>				
TGF- β homolog-2	TGH-2	<i>B. malayi</i>	Binds to TGF β R which leads to suppression of T effector cell responses	[326]
TGF-like molecule	FhTLM	<i>F. hepatica</i>	Binds to TGF β R and induces IL-10 production in macrophages	[328]
TGF- β mimic	TGM	<i>H. polygyrus</i>	Binds to TGF β R which leads to induction of Treg cells	[329,330]
anti-inflammatory protein 2	AIP-2	<i>N. americanus</i>	Treg cell induction	[331]
Protein of Ascaris suum-1	PAS-1	<i>A. suum</i>	Induction of IL-10 producing Treg cells and IFN- γ producing CD8 γ δ TCR T cells	[332]
Inhibitor of potassium channel	Bmk1	<i>B. malayi</i>	Suppress the proliferation of memory T cells	[333]
	AcK1	<i>A. caninum</i>		
Ancylostoma secreted protein-2	NaASP-2	<i>N. americanus</i>	Binding to CD79A on B cells, inhibiting BCR signaling	[336]
IL-4 inducing principle from <i>S. mansoni</i> eggs	IPSE	<i>S. mansoni</i>	Induces IL-10 in B cells and enhances their capacity to induce Treg cells	[337,338]

1.3.2 Protection from allergy and autoimmunity (“Hygiene hypothesis”)

An overview of the relationship between parasite infections, helminth-derived molecules and allergic diseases is discussed in the scope of this dissertation within the review: "What Can Parasites Tell Us About the Pathogenesis and Treatment of Asthma and Allergic Diseases" (VI) [339].

The health conditions in different countries around the globe show significant contrasts, with low-income countries experiencing high rates of parasite infections due to worse public health, housing and sanitation conditions, while developed societies see a rise in allergic and autoimmune disorders such as asthma, type 1 diabetes and inflammatory bowel disease (IBD) [340–343]. 15-30 % of the population in urban areas are affected by allergic diseases and asthma, whereas the prevalence of asthma and allergic disorders appears to be low in rural areas [341,344]. The “**hygiene hypothesis**” links the increased hygiene conditions as well as the use of antibiotics and vaccines in developed countries to an overreaction of the immune system to harmless substances including those from the environment or from our own body with the reduction in the exposure to microbes, such as parasites [345,346]. However, the protective role of parasite infections in type 2 inflammatory disorders, such as allergy could not be demonstrated in all studies. For instance, infection with *A. lumbricoides*, *Strongyloides stercoralis* or *Toxocara* parasites correlates with an increased asthma prevalence, sensitization to allergens, allergic airway inflammation and parasite-specific IgE titers [347–353]. In contrast, other epidemiological studies show that the presence of parasites, in particular *Schistosoma* species may help prevent these overreactions. Especially, the treatment of people with anti-helminthics increase the susceptibility for allergic reactions and the overall responsiveness [354–359]. Allergy-protective effects of helminths are related to the intensity and chronicity of the infection, parasite burden, as well as the lower amount of inflammatory type 2 cytokines and the increase of IL-10 [357,359–361], leading to the possibility that parasites can be used as treatment options for type 2 inflammatory disorders. However, little is known about the correct dose or duration of live parasite infection required for protective effects in humans. Safety concerns about detrimental effects of parasite infection limit clinical trials, and high immunological variation, e.g., due to different genetic background, age and immunological status of the patients, complicates the interpretation of data. Concerns regarding the safety and efficacy of helminth infections may be overcome by helminth-derived anti-inflammatory molecules as well as the identification and characterization of cellular and molecular targets within the host.

1.3.3 Interplay between helminths and respiratory viral infections

Since helminths share a long coevolutionary history with humans, and as already mentioned their eradication is thought to have caused changes to host physiology, metabolism, and immunity, helminths are major modulators of host susceptibility to other infectious diseases, such as viral infections. One of the earlier studies uncovered that a coinfection of mice with *A. suum* or *N. brasiliensis* and influenza virus results in adverse clinical outcomes. In comparison to mice infected with influenza virus alone, coinfection leads to an increased mortality [362,363], suggesting that a coinfection with helminths that traverse through the lungs and a simultaneous respiratory viral infection can be detrimental to the host (Figure 8). Thus, infection of the same tissue may exacerbate physical damage thereby compromising its integrity. However, the precise mechanisms by which these lung-dwelling helminths impact the pathogenesis of respiratory viruses and the timepoint of viral infection, i.e., during or after the lung-dwelling stage of helminth infection, need to be further investigated.

Conversely, enteric helminth infections appear to be protective against respiratory viral infections. Coinfection of mice with *H. polygyrus* and influenza virus (IAV) decreases the pulmonary consolidation and shows a tendency towards decreased viral titers [363,364]. Corroborating evidence that helminths limit lung immunopathology but at the same time support viral infections by mitigating the infiltration of immune cells came from a study showing that enteric helminth infection can reduce the activation and the trafficking of several immune cells types [365]. Coinfection with *T. spiralis* and IAV reduces the number of neutrophils, NK cells as well as T cells in the lung [366]. Theoretically, attenuated recruitment of immune cells could also prevent the accumulation of protective cells, such as CD8⁺ T cells in the lung, which ultimately leads to impairment of the host antiviral response. However, coinfection with *H. polygyrus* or *T. spiralis* results in only minor changes in viral load, suggesting that a few protective virus specific CD8⁺ T cells are sufficient for the clearance of influenza virus in the lung [366,367]. Although CD8⁺ T cells are not directly involved in anti-helminth immunity, helminth-induced type 2 cytokines can cause bystander activation of naïve CD8⁺ T cells. These activated CD44⁺CD8⁺ T cells resemble virtual memory T cells (TVM cells) that are implicated in protection against viral infections [368,369]. In line, *S. mansoni* infection induces TVM-like CD8⁺ T cells to boost antiviral T cell responses and protect mice against murine gamma herpesvirus (MHV)-68 infection [370]. Whether accumulation of TVM-like CD8⁺ T cells during other helminth infections, such as *H. polygyrus*, can contribute to the protective effects seen with influenza virus coinfection

remains elusive. Apart from inducing TVM cells, coinfection with *S. mansoni* protected mice against an influenza, paramyxovirus, pneumonia (PVM), and a model of human respiratory syncytial virus (RSV) infection by TNF α mediated goblet cell hyperplasia and mucus secretion [371] (Figure 8).

Type I IFN induction is another mechanism which helminths can use to protect against viral infections. Although helminths are generally not associated with the direct regulation of type I IFNs, *H. polygyrus* infection upregulates type I IFNs in the lung and protect mice against RSV. Interestingly, protective effects of *H. polygyrus* are not dependent on adaptive immunity (RAG1 $-/-$) or on type 2 cytokine signaling (IL-4R α $-/-$), while when mice lacking receptors for type I IFNs (IFNAR1 $-/-$), protective effects disappeared. However, germ-free mice did not recapitulate the beneficial effects of enteric helminth coinfection in preventing RSV disease [372], suggesting that enteric helminths may impact IFN signaling via changes in the composition of commensal bacteria [373,374]. Furthermore, type I IFN signaling in DCs can support T_H2 induction in response to SEA, while at the same time SEA-induced type I IFNs could induce regulatory B cells, which both could affect anti-viral immunity [375,376] (Figure 8). In addition to type 2 immune responses, helminths can induce an anti-inflammatory or regulatory response characterized by the induction of regulatory T cells that suppress inflammation via production of cytokines such as IL-10 and TGF β . For instance, the suppression on neutralizing antibodies to an influenza vaccine by infection with *L. sigmodontis* is associated with a systemic and sustained expansion of IL-10 producing Treg cells, even after clearance of the parasite [377].

Possible effects of helminth infection on the current pandemic caused by SARS-CoV-2 have been extensively discussed [378–381]. Unlike some respiratory viruses that are confined to the lungs, SARS-CoV-2 affects multiple organs including the GI tract [382]. Since the immune response and pathogenesis of SARS-CoV-2 is systemic, the outcome of coinfection is difficult to predict. However, a recent study showed that parasite-induced regulatory mechanisms are associated with decreased severity of COVID-19 in a cohort of African patients [383]. In line, a further study supports this concept and shows that a previous infection with lung migrating helminths can limit disease severity during SARS-CoV-2 infection by enhancing anti-viral CD8⁺ T cell responses in a macrophage-dependent manner [384]. Thus, enteric helminths may mediate host resistance to respiratory viral infections and disease pathogenesis by several potential mechanisms, but the timing of viral infection relative to the helminth life cycle and tissue compartmentalization must be considered.

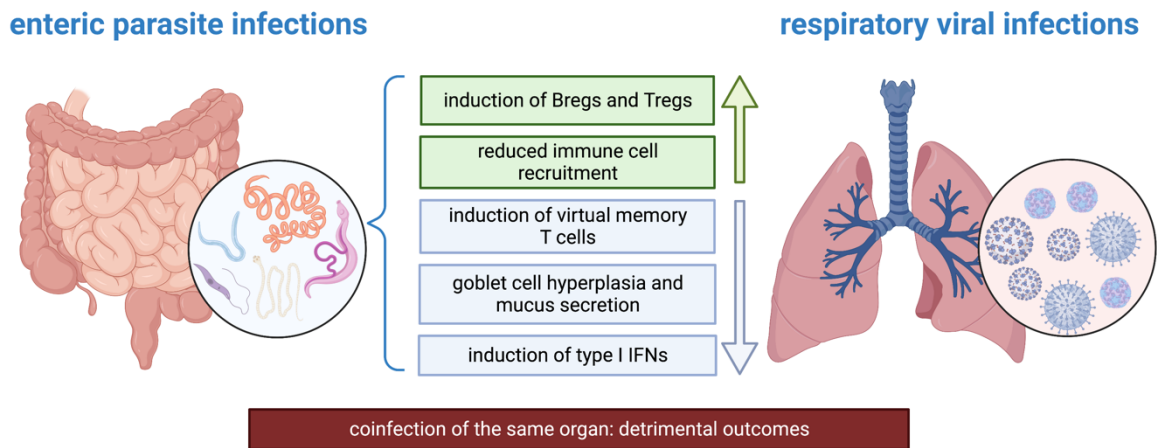


Figure 8: Helminths in their enteric phase can often protect against respiratory viruses (created with Biorender.com)

1.4 Eicosanoids as key mediators during infection

The immune system's response to infections involves a complex system of molecular signaling molecules which are rapidly coordinated, and which can often trigger opposing actions. Next to cytokines, a group of bioactive lipids can cover these requirements. **Eicosanoids** (from Greek εἴκοσι, "twenty") are a group of hydrophobic hormone-like substances derived primarily from the membrane-associated 20-carbon, ω -6 fatty acid, arachidonic acid (AA). Numerous enzymes can metabolize AA into four eicosanoid subfamilies with distinct biological functions: prostanoids, leukotrienes (LTs), hydroxyeicosatetraenoic acids (HETEs) and epoxyeicosatrienoic acids (EETs) (Figure 9).

1.4.1 The arachidonic acid metabolism

Starting point of eicosanoid biosynthesis is the cleavage of AA from membrane phospholipids by phospholipase A2, followed by metabolization into a variety of powerful eicosanoids [385,386]. The two most well-known pathways are the 5-lipoxygenase (5-LOX) pathway giving rise to the leukotrienes and the cyclooxygenase (COX) pathway resulting in the formation of prostanoids [387–389].

The 5-lipoxygenase (5-LOX) pathway

The 5-LOX and 5-LOX activating protein (FLAP) oxidize AA to 5-HETE or LTA_4 which can either be metabolized to LTB_4 , by the LTA_4 hydrolase or to LTC_4 by the glutathione transferase LTC_4 synthase [390,391]. LTC_4 belongs to the cysteinyl leukotrienes (cysLTs)

and can be further converted into LTD₄ by γ -glutamyl transferase (GGT) and to LTE₄ by the membrane-bound dipeptidase (MBD) [392,393]. LTs are predominantly produced by myeloid cells and can exert chemotactic functions on neutrophils, eosinophils and T cells (LTB₄), regulate immune cell activation and survival, vascular permeabilization, smooth muscle contraction and airway remodeling [388,394–398]. In addition to hematopoietic cells, tuft cells have been identified as a new source of cysLTs, contributing to host defense against helminth parasites or allergic airway inflammation [399,400]. Different cell types can form different LT metabolites. Murine neutrophils produce mainly LTB₄, while murine eosinophils produce higher levels of cysLTs [401]. In humans, eosinophils produce both LTB₄ as well as cysLTs [402,403]. However, platelets for example do not express the 5-LOX, but can convert neutrophil-secreted LTA₄ into cysLTs [404]. CysLTs can signal via their G-protein coupled receptors (GPCR) CysLTR1 and CysLTR2, whereas two new receptors for LTE₄ have been discovered more recently, including the GRP99/OXGR1 and P2Y₁₂ [405–408]. For LTB₄, two receptors (BLT1 and BLT2) with high- and low-affinity binding are described [409,410].

The cyclooxygenase (COX) pathway

In contrast to the leukotriene pathway, the cyclooxygenase pathway can convert AA to the pre-courser PGH₂. Two isoforms of the cyclooxygenase exist: the constitutively active COX-1, which is expressed in most cells and the COX-2, which is induced under inflammatory conditions [411,412]. The non-steroidal anti-inflammatory drugs (NSAIDs) such as aspirin, ibuprofen, indomethacin can non-specifically inhibit both COX-1 and COX-2 while the COXIBs such as celecoxib and valdecoxib are COX-2 specific inhibitors. Upon activation of the cyclooxygenase pathway, PGH₂ is quickly metabolized into the prostanoids: prostaglandin (PG)D₂, PGE₂, PGF_{2 α} , PGI₂ (also known as prostacyclin) and thromboxane A₂ (TXA₂) by their respective PG synthases [413–416]. TXA₂ is an unstable metabolite and therefore directly hydrolyzed to TXB₂. Immediately after synthesis, prostanoids are released from the cell and exert their effects, like the leukotrienes, through binding of GPCRs on the target cell. TXB₂ for example can induce vasoconstriction and platelet aggregation, whereas prostacyclin signaling prevents the formation of blood clots, induce vasodilation and promote leukocyte adhesion [417–419]. Thus, a delicate balance in the levels of PGI₂ and TXA₂ is very critical in the maintenance of proper vascular function. PGF_{2 α} as another prostanoids derives mainly from COX-1 in the female reproductive system, where it plays an important role in uterine contraction, ovulation and initiation of parturition [420,421]. Furthermore, it is involved in vascular biology, pain and acute

inflammation [422,423]. In contrast to that, PGD₂ exerts both pro- and anti-inflammatory properties depending on the receptor to which it binds. For instance, PGD₂ promotes viral-induced bronchiolitis via binding to DP2 receptor [424]. However, the more known function of DP2 signaling by allergic stimuli results in chemotaxis of eosinophils, neutrophil recruitment and the release of T_H2 cytokines [425–428]. On the other hand, PGD₂ exerts anti-inflammatory activity via DP1 signaling, resulting in the amelioration of lung inflammation [429,430]. Similarly, PGE₂ can have various effects depending on the binding to one of its four E-prostanoid receptors, EP1-4. PGE₂ is known to suppress T_H1 responses and shifts towards T_H2 responses resulting in an ineffective development of the antiviral immune response. Moreover, PGE₂ can modulate DC maturation and the balance of Treg cells to T_H17 responses, whereas it was found to affect the immune response to infections such as RSV and IAV enabling increased replication and viral dissemination [431–436]. Thus, depending on the EP receptor profiles of individual cell types and tissues, PGE₂ can have diverse effects with e.g. modulating the immune system by shifting T_H responses and thus affect the interplay between innate and adaptive immunity.

12-/15-lipoxygenase, lipoxins and specialized pro-resolving mediators (SPMs)

Additionally, 5-/12-/15-LOX can convert AA to 12-/15- HETEs or lipoxins (LXs) depending on the host species (e.g. human vs mice), cell type and enzyme isoforms [437]. Lipoxins are part of the specialized pro-resolving lipid mediators (SPM). Maresins and docosanoids (ω -3 fatty acids derivatives), formed from eicosapentaenoic acid (EPA), which leads to E-series resolvins or docosahexaenoic acid (DHA), resulting in D-series protectins, are primarily responsible for anti-inflammatory functions and the resolution of inflammation [438,439]. However, even it is known that macrophages form the enzymes needed to produce SPMs, only tiny amounts under non-physiological conditions are detectable. On the basis this, signaling and occurrence of SPMs challenge their role as endogenous mediators of the resolution of inflammation [440].

Cytochrome P450 metabolism of AA

Apart from the pathways described above, polyunsaturated fatty acids (PUFAs) can undergo auto-oxidation or can be metabolized by cytochrome P450 (CYP) enzymes, which convert AA to EETs and 20-HETE [441]. EETs are associated with anti-inflammatory effects by attenuating the cytokine-mediated activation of NF- κ B and the adherence of leukocytes to the blood vessel wall [442]. Inhibition of the soluble epoxide hydrolase, which further converts epoxides to their corresponding diols, is assessed as a new treatment option for

inflammation [443]. In contrast, 20-HETE can activate NF- κ B signaling and increase the expression of molecules and cytokines that promote inflammation [444].

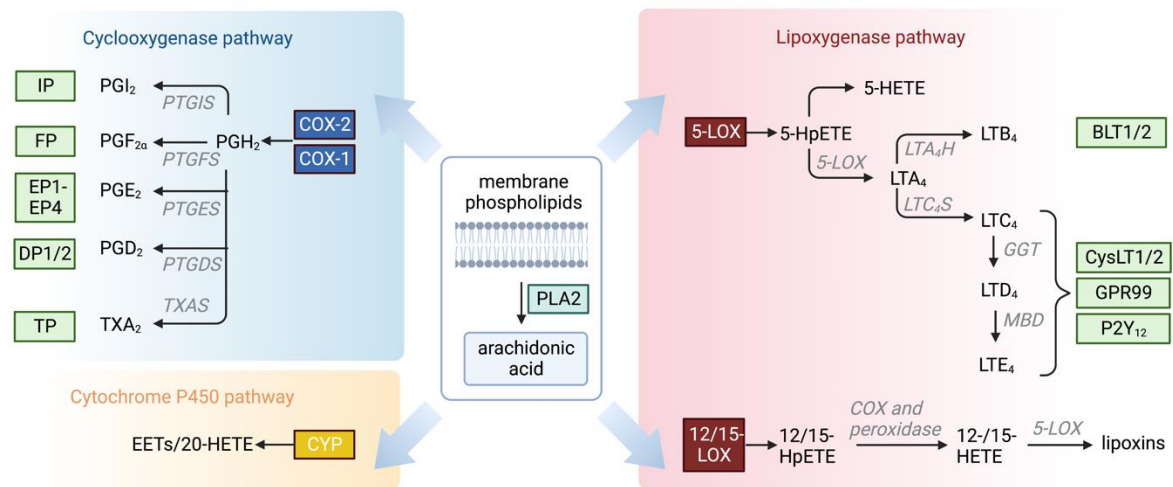


Figure 9: Eicosanoid biosynthesis pathway and receptor signaling (created with BioRender.com)

1.4.2 Role of eicosanoids during respiratory viral infections

Eicosanoids are immunomodulatory and thus also impact viral replication and the host's antiviral response. Apart from IAV and RSV infection, SARS-CoV-2 infection results in increased levels of ω -3 and ω -6 fatty acids and their derivatives in different body fluids, which is associated with increased numbers of infiltrating immune cells [445,446]. Thus, unmasking the eicosanoid storm that may occur in severe COVID-19 as well as other viral disease has made this pathway an attractive target for treatment of respiratory viral infections [447–449].

The cyclooxygenase pathway and the impact on respiratory viral infections

Genetic deletion or pharmacologic inhibition of COX-2 is associated with a decrease in the production of pro-inflammatory cytokines and pulmonary inflammation, thus improving mortality in mouse models of IAV infection [450–454]. However, mortality is higher in COX1 $-/-$ mice as well as in mice treated with a selective COX-1 inhibitor [450,451]. Of note, PGE₂ and PGD₂ are the most studied prostanoids during respiratory viral infection. Inhibition of PGE₂ production or genetic deletion of mPGES-1 improves antiviral immunity and survival of mice after IAV infection by permitting greater infiltration of myeloid cells into the lung. This is accompanied by an increased capacity for apoptosis and IFN- β production in macrophages, ultimately leading to the activation of adaptive immunity. PGE₂ suppresses

the innate and adaptive immune response to IAV infection in an EP2/EP4 and type I interferon-dependent manner [436]. In contrast, inhibition of mPGES-1 exhibits anti-viral effects by suppressing the induction of pro-inflammatory genes (TNF α , IL-8, CCL5, and CXCL10) in IAV-infected cells [455]. However, the accumulation of PGE₂ after IAV infection leads to the expression of IL-27, which in turn is responsible for the STAT1/2 mediated inhibition of viral replication. Furthermore, clinical analysis showed that IL-27 levels are significantly elevated in a cohort of patients infected with IAV and that circulating IL-27 correlated positively with PGE₂ levels [456]. Like IAV, RSV induces the release of PGE₂ *in vitro*, in animal models, and in lungs of infants with RSV bronchiolitis [431,457–459]. Treatment with COX inhibitors decreases the RSV replication *in vitro* and diminishes immunopathology *in vivo*, whereas it suppresses transcription and production of the proinflammatory cytokines, including IL-8 and RANTES (CCL5), leading to the suppression of IRF and NF- κ B [431]. As IAV and RSV hijack the PGE₂ pathway to suppress innate and adaptive immunity, a significant immunosuppressive or immune regulatory role of PGE₂ during SARS-CoV-2 infection is possible. Increased levels of PGE₂ were found and correlated positively with COVID-19 severity [460]. Moreover, an interaction between PTGES and nsp7, which is conserved among MERS-CoV, SARS-CoV, and SARS-CoV-2 has been described [461]. Compared to PGE₂, the role of PGD₂ production and signaling in COVID-19 has been characterized in more detail: Middle-aged mice lacking expression of DP1 or phospholipase A2 are protected from severe disease, whereas treatment with a DP1 antagonist protected the mice from lethal infection [462]. This could be due to the delayed migration of DCs to the lung and lymph nodes via downregulation of the chemokine CCR7, because the impact of DP1 signaling and delayed DC migration on adaptive immune responses appears to be age dependent [463,464]. Interestingly, DP1 inhibition enhances DC migration as well as T cell proliferation and increases survival in older mice after SARS-CoV and IAV infection [464]. Furthermore, PGD₂ also contributes to the pathogenesis of RSV bronchiolitis in a DP2-dependent manner resulting in an increased viral load and morbidity after IFN- λ downregulation [424]. This effect is recapitulated by treatment with a DP1 agonist, suggesting that the two receptors for PGD₂ have different roles in the regulation of antiviral responses. Even if Prostacyclin (PGI₂) has not been well studied in context of viral infection, one study showed that mice overexpressing PGIS in airway epithelial cells display lower viral titers after RSV infection. In contrast, mice lacking the IP exhibit higher viral titers, suggesting that PGI₂ may enhance the antiviral response and improve viral clearance [465]. In general, COX inhibition or deficiency seems to be associated with less exuberant inflammation and infection. Even if PGF_{2 α} and TXA₂ have not been investigated with respect to modulation of viral clearance or host response to viral

infection, the role of PGE₂ and PGD₂ as immunomodulatory mediators in balancing proinflammatory actions with suppressive effects on innate and adaptive immune function to evade host immune response have been extensively characterized (Table 4).

Respiratory viral infections and the lipoxygenase pathway

The products of the 5-LOX pathway include diverse roles on respiratory viral infections, with LTB₄ as the protective mediator, whereas cysLTs engage detrimental functions. LTB₄ exhibits antiviral activity in both *in vitro* and *in vivo* models of viral infections through various mechanisms, such as promoting the release of antimicrobial peptides [466–468] and activating the NOD2 pathway, which leads to an increase in the production of interferons [469]. LTB₄ administration in mice after infection with IAV reduces the viral load as well as lung pathology [467]. Additionally, LTB₄ promotes disease tolerance to IAV infection by the release of IFN- α , which further decreases the proliferation of inflammatory macrophages and reduces lung injury via signaling through BLT1 [470]. Furthermore, LTB₄ treatment triggers an enhanced antiviral response in primary human neutrophils by increasing myeloperoxidase (MPO) activity and α -defensin production, resulting in an improved virucidal activity against influenza virus, human coronavirus, and RSV [468]. Thus, the effects of LTB₄ on neutrophils are similar in both men and mice. In contrast, signaling of cysLTs through their CysLT1 receptor increases susceptibility of alveolar epithelial cells to influenza virus infection and treatment with a CysLT1 antagonist improves survival [471]. Furthermore, CysLT1 receptor antagonism decreases airway hyper-responsiveness in mice challenged with RSV [472] and also attenuates airway hyper-responsiveness, infiltration of inflammatory cells, and excessive mucus production upon reinfection [473]. An increase of 5-LOX products in the serum of severely infected COVID-19 patients is accompanied by an increase of 5-LOX expression in monocytes, macrophages, as well as, neutrophils [474]. In line, patients with COVID-19 who were hospitalized and received a leukotriene receptor antagonist showed lower risk of their condition worsening (as measured by an increase in the COVID-19 ordinal scale form day 1 to day 3 of hospitalization) compared to those who did not receive the treatment [475]. Thus, anti-viral immunity is regulated by the signaling of LTs, which can in general either have adverse or beneficial effects on the immune system's ability to fend off respiratory viruses (Table 4).

Table 4: Role of eicosanoids during IAV, RSV and SARS infection

Pathway	Mediator	infection	Function and physiological consequences	Ref.
COX	COX-2	IAV	↑ Mortality ↑ Pro-inflammatory cytokines and inflammation	[450–454]
	COX	RSV	↑ Immune pathology ↑ Replication ↑ IRF, NF-κB and pro-inflammatory cytokines	[431]
	PGE ₂	IAV	↑ Mortality and viral load ↑ Pro-inflammatory genes as well as IL-27 ↓ Infiltrating myeloid cells ↓ Apoptosis and IFN-β production via signaling through EP2/4 in macrophages ↓ CD4 ⁺ and CD8 ⁺ T cell activation	[436,455,456]
		SARS	↑ Disease severity	[460]
	PGD ₂	IAV/ SARS	Signaling via DP1 → ↑ disease severity DCs downregulate CCR7 → delayed migration to lymph nodes → ↓ T cell proliferation	[462–464]
		RSV	DP2- dependent downregulation of IFN-λ → ↑ viral load and morbidity	[424]
	PGI ₂	RSV	↓ Viral titer	[465]
LOX	LTB ₄	IAV/RSV/ SARS	↑ Antiviral activity ↑ Antimicrobial peptides ↑ Activation of NOD2 → ↑ interferons ↑ MPO activity, α-defensin production in neutrophils ↑ IFN-α release, ↓ inflammatory macrophages and ↓ Lung injury through signaling via BLT1 ↓ Viral load	[466–470]
			↓ Survival	
	cysLTs	IAV	↑ Susceptibility to infection via signaling through CysLTR1	[471]
RSV		↑ Airway hyperresponsiveness ↑ Inflammatory cells ↑ mucus production	[472,473]	

SPMs and their effect on SARS-CoV-2 infection

The role of cytochrome P450–derived eicosanoids in regulating the host response to viral infections has not been studied to date. However, the increase of CYP-derived lipid mediators correlates with the severity of SARS-CoV-2 infection [474]. In contrast to that, a higher ratio of EPA + DHA to total erythrocyte fatty acids, is linked to a lower risk of death in COVID-19 patients [476]. Based on this, omega-3 fatty acids EPA and DHA have been proposed as a potential additive treatment for COVID-19 [447]. In line, a pilot study with supplementing EPA + DHA and a case report of using icosapent ethyl in COVID-19 patients also indicates potential benefits with regard to survival rate and cardiovascular disease risk reduction [477,478].

1.4.3 Eicosanoid function during helminth infection

During helminth infection, the host immune response activates inflammatory cells and induces the secretion of lipid mediators to control the immune response, favour the expulsion of the parasite as well as initiate tissue repair. However, these organisms can develop survival strategies, including the regulation of lipid mediator pathways to evade the host immune response. Important roles for both, LOX and COX metabolites are identified in host defense against helminths. For instance, pharmacological inhibition of the COX pathway or genetic deletion of the 5-LOX pathway results in an altered type 2 cytokine level [479,480] during infection with *Strongyloides venezuelensis*, thus suggesting cross-regulation of cytokine and eicosanoid pathways during type 2 immunity [481].

Prostaglandins in regulating immune response during helminth infection

Similar to viral infections, PGE₂ is one of the most studied prostanoids during parasite infections. Thus, regulatory roles of macrophage-derived PGE₂ in helminths are discussed in one of our published review articles (V) [155]. In the context of helminth infection, an increase in the production of PGE₂ in monocytes and macrophages following the infection with *O. volvulus*, *H. polygyrus*, *Taenia solium*, *Taenia crassiceps* or *B.malayi* could be detected [482–486]. While one study reports no significant role of PGE₂ in the clearance of the lung-dwelling parasite *N.brasiliensis* [487], several others describe helminth-induced PGE₂ as a regulator of type 2 immune response both during helminth infection and in allergic airway inflammation [484,488–491]. However, few studies propose that PGE₂ exhibit pro-inflammatory functions in the regulation of type 2 inflammation by altering the balance of T_H1 versus T_H2, which allows for the emergence of type 2 immunity [492,493]. For instance, SEA from *S. mansoni*, which is well known to drive potent T_H2 responses, triggers DCs to produce PGE₂, which subsequently—in an autocrine manner—induces OX40 ligand (OX40L) expression to license these DCs to drive T_H2 responses [492]. Intestinal sections from mice exposed to a challenged infection with *H. polygyrus* show a PGE₂-triggered increase in mucosal permeability and secretory response, while the sodium-linked glucose absorption is reduced [174]. Thus, the pro- and anti-inflammatory function of helminth induced PGE₂ might be regulated by the binding to different receptors and the timing and stage of helminth infection. PGD₂, classically known as a driver of allergic airway promotes T_H2 cytokine production and recruitment of ILC2s during allergic inflammation and helminth infection [494–496]. However, recent findings could demonstrate that a PGD₂ and DP2 axis leads to suppressive effects during *N. brasiliensis* infection by acting on small intestinal epithelial cells with a decrease in worm clearance and goblet cell hyperplasia

[497]. Moreover, PGD₂ as well as other prostanoids, including PGF_{2α} and TXB₂ are upregulated in the acute phase of *N. brasiliensis* infected lungs [498]. In contrast to that, mice which are infected with *B. malayi* show a decrease in the secretion of PGD₂ from splenic macrophages, whereas monocyte-derived macrophages treated with a *H. polygyrus* L3 extract show an increase of prostanoids and thromboxanes [483,499]. In line, humans infected with *Dirofilaria immitis* have significantly higher TXA₂ levels in the serum, although it is not clear whether this is elicited by the helminth parasite or by the secondary infection with *Wolbachia bacteria* [500]. Furthermore, PGI₂ is discovered as the most abundant AAM-derived eicosanoid during *B. malayi* infection [486]. Together, these data propose a more dominant role for PGD₂ signaling during helminth infection, whereas the specific functions for PGF_{2α}, PGI₂ and thromboxanes remain elusive.

In addition to the ability of parasites to induce prostanoid secretion in host cells, helminths such as Schistosomes and *Onchocerca* spp. can produce prostaglandins themselves [501–505]. *S. mansoni* can produce lipid mediators including prostaglandins at various stages of its lifecycle [506,507]. For instance, PGD₂ production by schistosomes triggers proinflammatory effects in the host, including activation of eosinophils [502], whereas schistosome-derived PGE₂ induces the production of IL-10, thus promoting the migration and survival of the parasite [488,492,503,506]. In line, *Trichuris suis*, a whipworm, is able to produce PGE₂ that directly suppresses the production of cytokines in LPS-stimulated DCs [508]. In addition, other helminth parasites, such as microfilaria *B. malayi*, produce a lot of different prostanoids, which exert immunomodulatory roles such as the prevention of platelet aggregation [509,510]. The functions of COX-derived lipid mediators during parasite infections are summarized in Table 5.

The role of leukotrienes during helminth infection

Leukotrienes released from immune cells efficiently participate in protective immune responses during helminth infections. This for instance has been shown by the increase of LTB₄ and LTC₄ in a gut homogenate of rats challenged with *T. spiralis*, which is associated with the rapid expulsion of the parasite [511]. Rapid anti-helminth immunity is enabled by tuft-cell derived cysLTs that activate type 2 immunity [400]. In line, hematopoietic stem cells from granulomas of *S. mansoni*-infected mice exhibit an increased expression of 5-LOX as well as LTC₄S and a TGFβ- regulated cysLT production [512]. Furthermore, the usage of 5-LOX deficient mice confirmed a contribution of LTs to *S. mansoni*-induced inflammation, granuloma formation and tissue remodeling [513,514]. In contrast, an increase of LTB₄, but not LTC₄ in the lung and small intestine during infection with *S. venezuelensis* is associated

with a decrease in larval recovery in the lung or worm burden in the intestine [480]. The increase of LTB₄ concentrations is often associated with a recruitment of mast cells, eosinophils, macrophages and lymphocytes during helminth infection [515–517]. Based on this, LT inhibition or knock out of the 5-LOX pathway results in a greater parasite burden, in an increased production of IL-12 but also in a decreased number of eosinophils [480,518]. The clear impact on the recruitment of eosinophils and mast cells by LTs could be explained by the upregulation of Mac-1 with late changes in VLA-4 profiles on both peritoneal cavity and bronchoalveolar lavage fluids after *Toxocara canis* infection [518]. Thus, LTs might play an important role in eosinophilic inflammation during parasite infections by inducing leukocyte recruitment and modulating the expression of adhesion molecules. Apart from that, LTB₄ can enhance the ability of neutrophils and eosinophils to directly kill parasites in a complement-dependent manner [519]. The cytotoxicity of eosinophils against helminths has been associated with the expression of cellular receptors (high affinity IgE receptor, FcεRI), adhesion molecules, as well as the degranulation and release of cationic proteins [520]. An *in vitro* assay confirmed that IgE-coated schistosomula can induce eosinophil attachment under the concomitant release of LTC₄, ultimately leading to the death of the parasite [521]. In contrast to that, parasites, like *A. lumbricoides* and *A. suum* have evolved a potential survival strategy by targeting fatty acids including LTs with their ABA-1 protein [522–524]. Helminths, especially schistosomes and *F. hepatica* can produce LTs by themselves [503,525], which for example could help in entering the host [507,526]. This suggests that LT inhibition might influence liver remodeling and pathology after parasite infection. In the context of parasite infection, both host- and parasite derived lipid mediators dictate the outcomes of the host-pathogen interaction, including persistence versus expulsion of the parasite and the extent of collateral damage to the host (Table 5).

Table 5: Role of host- or parasite-derived eicosanoids during helminth infection

Pathway	Mediator	infection	Function and physiological consequences	Ref.
Host-derived COX	COX	<i>S. venezuelensis</i>	↑ Eosinophils and type 2 cytokines ↓ Larvae and worm burden	[479]
		<i>N. brasiliensis</i>	No clearance	[487]
	PGE ₂	<i>T. solium</i> /	↑ IL-10 and regulatory T cells by EP2/EP4 signaling	[484]
		<i>S. mansoni</i>	↑ IL-10 and IL-4 ↓ IFN-γ	[488]
		<i>H. polygyrus</i>	↑ Mucosal permeability ↓ Glucose absorption	[174]
PGD ₂	<i>N. brasiliensis</i>	Signaling via CRTH2 ↓ Worm clearance ↓ Goblet cell hyperplasia	[497]	
Parasite-derived COX	prostanoids	<i>B. malayi</i>	Produces a lot of different prostanoids, e.g., for the prevention of platelet aggregation	[509,510]
	PGE ₂	<i>S. mansoni</i>	↑ IL-10 ↑ Migration and survival	[488,492,502,506]
		<i>T. suis</i>	↓ Pro-inflammatory cytokines in DCs	[508]
	PGD ₂	<i>S. mansoni</i>	↑ Pro-inflammatory effects ↑ Eosinophils	[502]
Host-derived LOX	LTs	<i>T. canis</i>	↑ Mac-1 and changes in VLA-4	[518]
	LTs	<i>A. lumbricoides</i> / <i>A. suum</i>	Can bind LTs via ABA-1	[522–524]
		<i>T. spiralis</i>	↓ Rapid expulsion of parasites ↓ Larvae recovery and worm burden	[511]
	LTB ₄	<i>S. venezuelensis</i>	↓ IL-12 ↑ Eosinophils and L-5	[480]
		<i>T. canis</i> / <i>N. brasiliensis</i> / <i>F. hepatica</i>	↑ Recruitment of mast cells, eosinophils, macrophages, and lymphocytes	[515–517]
		<i>S. mansoni</i>	↑ Direct killing by eosinophils and neutrophils	[519,521]
	cysLTs	<i>T. spiralis</i> / <i>N. brasiliensis</i> / <i>H. polygyrus</i>	↑ Rapid expulsion of parasites	[400,511]
		<i>S. mansoni</i>	↑ Inflammation ↑ Granuloma formation ↑ Tissue remodeling	[512–514]
Parasite-derived LOX	LTs	<i>S. mansoni</i> / <i>F. hepatica</i>	↑ Entering the host	[503,507,525,526]

1.5 The IL-12 family as important cytokines of the host immunity

Interleukins are small secreted proteins which are crucial for the communication between various immune cell types and thus significant for the regulation of the immune system also during infectious disease. Next to their ability to connect the innate with the adaptive immune system they facilitate a wide variety of functions, including cell growth, differentiation, and activation in an auto- and paracrine manner. Based on structural similarities and receptor engagement more than 60 ILs are currently categorized into nine families [527]. One group among the large variety of cytokines is the **interleukin 12 family**.

1.5.1 Functional diversity despite structural similarity

The interleukin 12 family is hallmarked by its heterodimeric nature, intriguing cross-utilization of cytokine subunits and sharing of signaling receptors. Only five distinct subunits are required to form this cytokine family which consists of at least four members: IL-12, IL-23, IL-27 and IL-35. Each of these IL-12 family members is assembled by one α - (four-helical bundle) and one β -subunit (β -sheets that form fibronectin type III and Ig domains). On the basis of this, IL-12 consist of IL-12 α and IL-12 β , IL-23 α and IL-12 β give rise to IL-23, IL-27 α and EBI3 build IL-27 and IL-35 is formed by IL-12 α and EBI3 [528]. Interestingly, IL-12 and IL-23 are the only two that share the feature of an intermolecular disulfide bridge. However, this disulfide bridge is dispensable for secretion of the heterodimer, but it may stabilize the complex against dissociation once secreted [529]. The combinatorial complexity is not only restricted to the interleukins, but it also applies to the IL-12 heterodimeric family receptors, where five different receptor chains can form four different signaling complexes [530]. Despite structural similarities, the interleukin 12 family operates on opposing sides of the immunological balance reaching from pro- to anti-inflammatory functions. Upon binding of the corresponding IL, receptor subunits dimerize and induce Jak/STAT signaling. As mentioned previously (see section 1.1), IL-12 is a cytokine, secreted by APCs, that stimulates the pro-inflammatory functions of T cells and contributes to the induction of T_H1 cells and CD8⁺ T_C, which are essential for fighting viral infections [531]. On the other hand, IL-23, which is the most pro-inflammatory member of the IL-12 family, is responsible for the induction of T_H17 cells with the concomitant production of IL-17, which is in turn linked to inflammatory disorders and autoimmune diseases such as psoriasis [532,533]. In contrast to that, IL-27 is an immune-modulatory cytokine that promotes T_H1 and Treg cell differentiation, but suppresses pro-inflammatory T_H17 cells [534]. IL-35 is the only member of the family with solely immune-inhibitory functions including the suppression

of conventional T cells and their conversion into suppressive Treg cells [535]. The secretion of unpaired IL-12 family members adds an additional layer of immune-regulatory functions with for instance, the secretion of IL-12 β monomers or homodimers which act as antagonists in IL-12 and IL-23 signaling [536], while additionally promoting the migration of macrophages and DCs during respiratory infections [537,538]. Thus, the IL-12 family cytokines with their opposing immune functions play a pivotal role in balancing our immune system.

Biogenesis and cytokine assembly of the IL-12 family

Like other secreted mammalian proteins, IL-12 family cytokines are produced in the endoplasmic reticulum (ER), where they obtain their native structure and assemble into heterodimeric complexes before being transported further along the secretory pathway towards the cell surface for secretion. In contrast to the cytosol, the ER provides a perfect oxidative environment for protein folding and oligomeric assembly and it serves as calcium storage for proper chaperone function [539]. In order to ensure the accuracy of the maturation process, the exit from the ER is tightly regulated by a stringent endoplasmic reticulum quality control system (ERQC) which inhibits secretion of incompletely folded or misfolded proteins with potential detrimental effects to the cell and the organism [540]. Permanently misfolded proteins are destroyed by the ubiquitin-proteasome system (UPS) through a process called ER-associated degradation (ERAD) [541]. This process involves the recognition of terminally misfolded proteins in the ER, their retrotranslocation through the ER-membrane, and finally the degradation via the cytosolic UPS [542].

For the biogenesis of human IL-12 family cytokines, a clear picture of ER quality control has emerged: On the one hand, α subunits are incompletely structured in isolation, and thus hardly, if at all, secreted by themselves, whereas β subunits, which can also be secreted alone, induce structure formation in their respective α subunit and thus regulate trafficking and export of the heterodimeric cytokine [534,543–547]. Before forming secretion-competent heterodimers, isolated α -subunits are retained within the ER by cellular chaperone machineries such as BiP or protein disulfide isomerases (PDI). Cysteines which exist in all α -subunits can form non-native disulfide bonds or wrongly folded and assembled oligomers, which are targeted for degradation. The correct formation of at least one internal disulfide bridge in IL-12 α and IL-23 α is critical for correct folding and secretion with IL-12 β . In contrast to that, IL-27 α has only one cysteine and thus is not able to form intramolecular disulfide bridges, but it exposes hydrophobic residues which causes BiP binding, resulting

Introduction

in ER retention and degradation. However, once assembled with their respective β -subunits, chaperone binding sites are buried within the native structure, thus allowing for the release from the ER to fulfill their function [529,532,545,547–551].

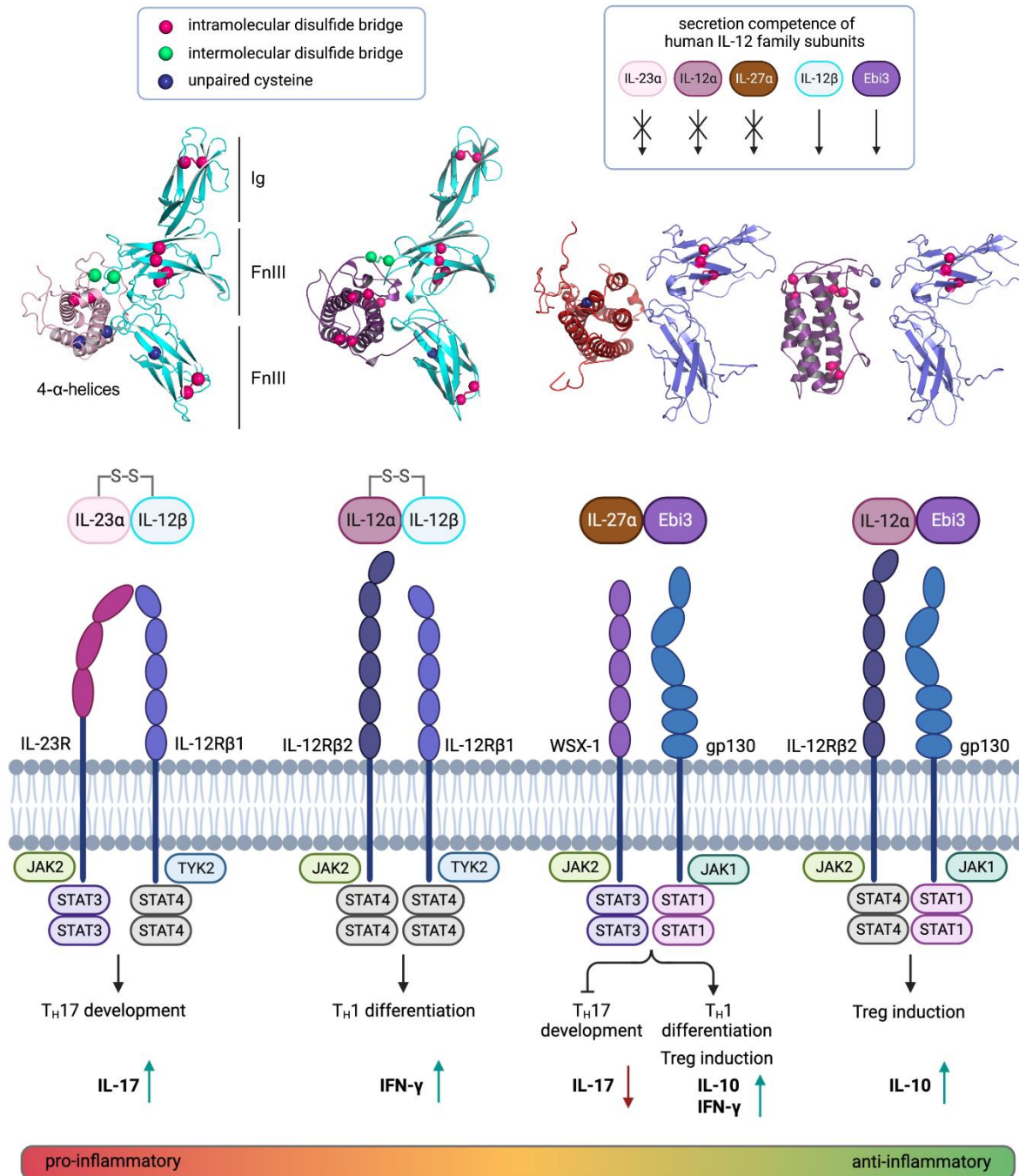


Figure 10: Secretion/ER quality principles and signaling of human IL-12 family cytokines (created with Pymol, Affinity Designer and Biorender.com)

1.5.2 Impact of glycosylation on biogenesis and function of interleukins

A further major chaperone family of the ER, that is crucial for ERQC, are the lectins. Lectins, like calnexin (CNX) and calreticulin (CRT) sense a proteins **glycosylation state** in order to assist folding by slowing down folding kinetics and preventing premature ER release [552–554]. Substrate proteins, also including IL-12 family members, get N-glycosylated at their NXS/T sequence, where X can be any amino acid residue except proline (Figure 11). The oligosaccharyltransferase (OST)- dependent transfer of $\text{Glc}_3\text{Man}_9\text{GlcNAc}_2$ units to the asparagine residue in the target protein sequence affect protein folding at an early state [555,556]. After the cleavage of two of the three glucose residues, the nascent glycoprotein is capable of interacting with CNX or CRT. Additionally, CNX, which is anchored to the ER membrane via its transmembrane domain, and CRT, a soluble protein, can recruit further folding factors such as PDI ERp57 to assist in folding of the target protein [557]. The final glucosidase cleavage releases the protein from the lectin cycle. If the protein remains misfolded, UDP- glucose:glycoprotein glucosyltransferase (UGGT) can reverse this process through glucosylation of the substrate, which allows for additional time for the protein to attain its proper folded conformation [558]. However, if excessive cycles are needed, ER mannosidase I and ER degradation-enhancing alpha-mannosidase-like proteins (EDEMs) remove mannose residues, thereby preventing re-entry into the CNX/CRT cycle and directing the protein towards degradation via ERAD and transfer to UPS [542,559]. Correctly folded proteins which have passed the CNX-CRT quality control cycle and are assembled with further subunits are transported via the ERGIC to the Golgi, where further post-translational modifications like O-linked glycosylations are possible [560] (Figure 11).

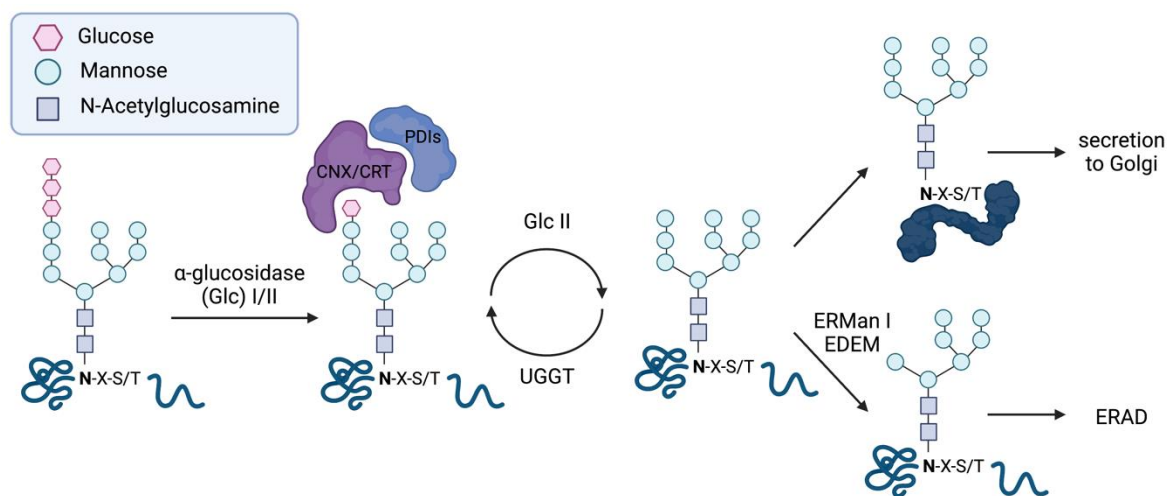


Figure 11: The calnexin/calreticulin cycle in ER quality control for glycoproteins (created with Biorender.com)

Carbohydrates can change physiological properties of interleukins or their receptors

Once secreted, hydrophilic **carbohydrates** of the sugar moiety can alter the biophysical properties of the polypeptide as well as their function as signaling molecules. For instance, extension of IL-2 with an extensively glycosylated hinge region amplifies the interleukin's half-life tremendously, enhancing the time of Treg induction, thereby leading to the reduction of autoimmune disease progression [561]. Different N-glycan structures can affect the lifetime individually, exemplified by the observation that 2,6-sialylated glycoforms of IL-6 are cleared faster than the corresponding IL-6 with terminal galactose. However, compared to the non-glycosylated form of IL-6, plasma clearance is delayed for almost all glycosylated IL-6 isoforms [562]. On the basis of this, glycosylation as a posttranslational modification can influence bioavailability by protecting against proteolysis [563], suggesting that N-glycosylation increases solubility and stability by reducing backbone flexibility or protecting proteins from proteolysis. However, protein engineering by adding complex N-glycans to interleukins can also lead to a reduced binding capacity to their receptors [564], thus making it necessary to probe the roles of N-glycans. Also naturally occurring glycosylation's or differentially glycosylated intermediates of the same interleukin can affect the function and the outcome of a disease. For instance, diabetes resistance encoded by *Idd3* correlates with the production of unglycosylated and multiple glycosylated IL-2 molecules, whereas diabetes susceptibility is associated with primarily single glycosylated species [565]. Furthermore, glycan chains can serve as molecular addresses, marking the intra- or extracellular destination and thus play an important role in protein trafficking [566,567]. In the case of administration of a glycoprotein as a therapy, this must be taken into account, because different glycostructures can have an impact on tissue distribution, as e.g. demonstrated for an antibody-IL-12 fusion protein [568].

In line with the N-glycan dependent increase in stability, N-linked glycosylation is also essential for the stability of cytokine receptors [569]. A study on the IL-11 receptor by using site-directed mutagenesis uncovered a role for N-glycosylation sites which differently control maturation, trafficking and proteolysis of the signal transducer [570]. Both studies, including the IL-6 as well as the IL-11 receptor suggested that N-glycosylation does not affect the signaling function, however glycosylation of the IL-1 receptor is required for optimal binding of IL-1 [571], suggesting that every aspect from maturation, solubility, stability, trafficking, proteolysis as well as biological function can be influenced by a protein's glycosylation state.

2 Aims

This thesis aims to address three different research objectives that focus in general on the regulation of the host immune response during infection and inflammation. The major overarching aim of the first two studies was to define how infectious diseases modulate macrophage activation and function. As a third aim, this thesis explored how the glycosylation status of host-derived immune mediators (interleukins) determines signaling and immune cell function.

The main goal of the first publication (I) was to understand how a glutamate dehydrogenase (GDH) derived from the parasite *H. polygyrus bakeri* (*Hpb*) can suppress host defense via modulation of macrophage effector functions. We therefore aimed to investigate the mechanism of immune evasion by assessing global changes in gene expression of helminthic GDH (heGDH)-treated macrophages as well as by characterizing effects of heGDH on the metabolism, epigenetic landscape, and effector functions of human macrophages *in vitro*. To further confirm results achieved in human macrophage cultures, effects on immune evasion of this parasitic enzyme were assessed during different murine models of parasite infections. As macrophages not only play pivotal roles during parasite infections, but they are also potent producers of eicosanoids (key mediators during type 2 inflammation), a particular interest was to study the roles of the arachidonic acid (AA) metabolic pathway in parasitic GDH-driven immune evasion.

Apart from their effector functions in type 2 immunity, monocytes and macrophages are also important inflammatory drivers during acute viral infections, such as during SARS-CoV-2 infection. However, how monocyte- and macrophage-derived inflammatory mediators persist after resolved respiratory viral infection with SARS-CoV-2 and how these cells react to a secondary trigger remained unanswered. Thus, we aimed to investigate in the second publication (II) if alterations in monocyte- and macrophage metabolism (AA-metabolism) as well as inflammatory cytokine production persists in convalescent COVID-19 patients and moreover if these inflammatory mediators are affected by treatment with glucocorticoids. Furthermore, to assess how monocyte-derived macrophages from these recovered patients react to a secondary inflammatory insult; gene expression, eicosanoid and cytokine/chemokine production was assessed after stimulation with SARS-CoV-2 spike protein or bacterial derived LPS.

The IL-12 family has a unique immunological role during infectious diseases and is increasingly relevant in immunotherapy. Despite its importance, the glycosylation pattern of this family of proteins, a key structural modification, remains largely undefined. The objective of the third part (III) of this thesis was to determine the common and unique principles of protein glycosylation for each member of the IL-12 family. A particular focus was set on cytokine assembly and secretion in order to determine if glycosylation is necessary for the formation of heterodimers and their subsequent secretion. Additionally, the functionality of glycosylation-deficient mutants was analyzed in relevant cell types to compare the impact of glycosylation of every single IL-12 family member.

3 Methods

Details about materials and manufacturers used for experimental procedures within this dissertation can be found in each “Materials and Methods” section of the individual publications. All methods, which are described in the publications but are not mentioned here, were performed without technical assistance from my side. A brief method description is appended below, while a more detailed version of all the methods can be found in the enclosed manuscripts, shown by the roman numbering in brackets.

3.1 Helminth infection and treatment with heGDH (I)

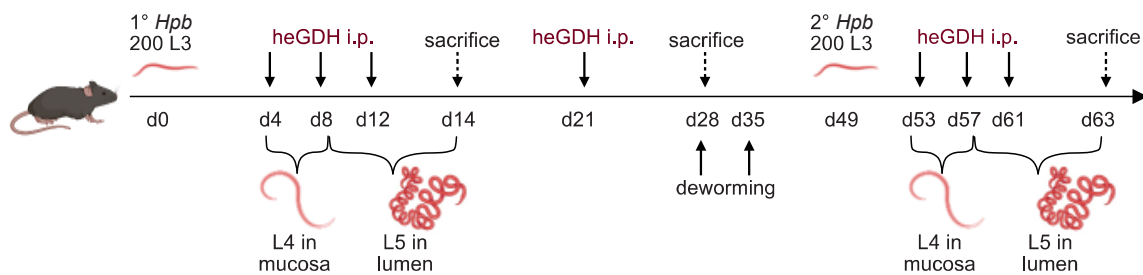


Figure 12: Infection with *Hpb* and further treatment with heGDH for different time points (created with Affinity Designer and Biorender.com)

All animal experiments were approved by the local authorities (Regierung von Oberbayern). Mice were infected with *Hpb* by oral gavage with 200 L3 stage larvae diluted in sterile PBS. Control animals received the same amount of PBS. Mice were sacrificed at the indicated time points (14 days post primary and secondary infection or 28 days post primary infection) (Figure 12). heGDH treatment was performed intraperitoneally at day 4, 8 and 12 for the 14-days primary infection experiment. When mice were sacrificed at 28 days post primary infection, mice were treated at days 4, 8 and 21. For secondary infection experiment, mice were infected with 200 *Hpb* larvae and two courses of antihelminthic were administered at days 28 and 35 p.i. Mice were re-infected with 200 larvae at day 49 and heGDH injection was performed at day 53, 57 and 61. In the absence of heGDH treatment, mice received PBS.

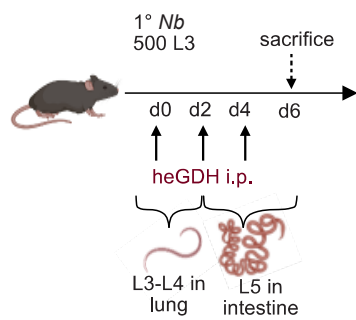


Figure 13: Infection with *Nb* and treatment with heGDH (created with Affinity Designer and Biorender.com)

For infection with *N. brasiliensis* (*Nb*), mice were infected s.c. with 500 infectious third-stage larvae (L3). Intranasal treatment with heGDH was performed at day 0, 2 and 4 (Figure 13). 6 days post infection, the airways of the mice were lavaged five times. Cell-free bronchoalveolar lavage fluid (BALF) was frozen immediately with or without equal volumes of methanol. Small intestine (SI) of *Hpb* or *Nb* infected mice was removed and opened to count adult worms at the luminal surface.

3.2 Blocking of heGDH using mAb treatment during infection with *Hpb* (I)

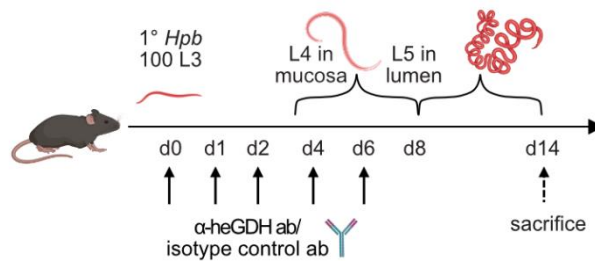


Figure 14: Infection with *Hpb* and further treatment with mAb against heGDH (created with Affinity Designer and Biorender.com)

For blocking experiments, α -heGDH monoclonal antibody (mAb) or isotype control antibody was administered intraperitoneally on day 0-2, 4 and 6 (Figure 14). Mice were sacrificed at day 14 post infection and adult worms in the SI were counted.

3.3 Histology of tissues (I, II)

For histology, the proximal 5 cm of the small intestine of *Nb*- or *Hpb*-infected mice was freed from mucus, extensively washed with cold PBS supplemented with double antibiotics, then rolled into “Swiss rolls”. Lung of *Nb* experiments and Swiss rolls of *Hpb*- an *Nb*-infected mice were placed in a tissue cassette and fixed in 3.7% formaldehyde before standard formalin-fixed, paraffin-embedded (FFPE) processing or in OCT medium for cryosections. For publication II, ALI cells were fixed in 4% formaldehyde and embedded in paraffin. Sections of all tissues were cut and stained with hematoxylin and eosin at the Histology Core Laboratory of the Dermatology Clinic (Klinikum Rechts der Isar). Images were recorded with the EVOS system. Linear means intercept (Lmi) was quantified as a score of *N. brasiliensis*-driven lung damage, as described previously [134].

3.4 BAL and peritoneal macrophage culture (I)

Peritoneal cells were obtained by peritoneal lavage with RPMI medium, whereas alveolar macrophages within the procedure of BALF. Total murine peritoneal cells as well as BAL cells were incubated at 37°C and 5% CO₂ for 4-5 hours, before rigorous washing with warm PBS and medium replenishment. Adherent macrophages were stimulated with calcium ionophore at 37°C and centrifuged at 4°C for harvest of supernatants for EIA and ELISA. Cells pellets were collected, lysed, and stored as described for MDM and BMDM.

3.5 Intestinal culture supernatants (I)

1-2 cm of the duodenal part of the SI from infected mice was incubated for 6 hours (*Nb*) or overnight (*Hpb*) in medium with double antibiotics at 37°C before supernatants were harvested and analyzed by LC-MS/MS.

3.6 Peripheral blood mononuclear cell (PBMC) isolation and culture (I-III)

All human experiments were approved by the local ethics committee at the Klinikum Rechts der Isar of the TUM. After written informed consent, blood from healthy human donors or SARS-CoV-2 seropositive patients was used for the isolation of PBMCs via density gradient centrifugation. Monocytes from the PBMC section were enriched via CD14 positive selection. CD14 negative PBMCs were frozen in FBS containing 10% DMSO. Thawed CD14 negative PBMCs were culture in RPMI and stimulated with the supernatants of transfected HEK293T cells expressing the IL-12 or IL-23 constructs for 24 and 72 hours, respectively. After harvesting, cells were washed once with PBS prior to lysis in RLT buffer supplemented with 1% β -mercaptoethanol (β -Me), while supernatants were frozen for cytokine analysis.

3.7 Cell culture of HEK 239T cells, transient transfection and de-glycosylation experiments (III)

Human embryonic kidney (HEK) 293T cells were cultured in Dulbecco's modified Eagle's medium (DMEM) supplemented with FBS and antibiotics at 37 °C and 5% CO₂. Transient transfections were carried out in poly D-lysine dishes using GeneCellin according to the manufacturer's protocol. A total DNA amount of 2 μ g (p35) or 4 μ g (p60) was used.

The α -subunit DNA was co-transfected with the β -subunit DNA or empty vector in a ratio of 1:2 for IL-23. For secretion and de-glycosylation experiments, cells were transfected for 8 hours and then supplemented with fresh medium for another 16 hours. To analyze secreted proteins, the medium was centrifuged and supplemented with 0.1 volumes of 500 mM Tris/HCl, pH 7.5, 1.5 M NaCl, complemented with protease inhibitor. Cells were lysed after washing twice with ice-cold PBS. Cell lysis was carried out in RIPA buffer on ice. Samples were de-glycosylated with PNGase F or a mix of O- Glycosidase and α 2-2,6,8 Neuraminidase according to the manufacturer's protocol.

3.8 Monocyte-derived (MDM) or bone-marrow derived (BMDM) macrophage culture (I, II)

CD14⁺ PBMCs were used to differentiate monocyte-derived macrophages (MDM). Alveolar-like MDM were cultured for 6-7 days in the presence of GM-CSF and TGF β . Bone marrow derived macrophages (BMDM) from bone marrow of wildtype C57BL/6 or EP2^{-/-} mice were isolated and cultured for 6 days in the presence of M-CSF. For both MDM and BMDM, exchange of medium and replenishment of cytokines on the third day was performed. After 6 days incubation, cells were harvested and stimulated. For publication II, MDMs (from post-COVID-19 and seronegative patients) were stimulated for 24 hours with LPS, SARS-CoV-2 spike protein, HDM extract, FP or dexamethasone (DXM). When indicated for publication I, cells were treated for 24 hours with heGDH, mutant heGDH^{K126A, D204N} or for 30 min, 3 hours, or 24 hours with AF488-fluorochrome labeled heGDH. To compare endotoxin dependent effects, MDM were stimulated with LPS. For p300 inhibitor studies, p300 inhibitor was added 1 hour prior to heGDH stimulation. MDM were harvested after 24 hours and BMDM after 6 hours stimulation with p300 inhibitor. For experiments with neutralizing antibodies, MDM were incubated with anti-human IL-12/IL-23 (p40) antibody, the respective isotype control antibody or anti-heGDH mAb before heGDH was added. Stimulation of M2 polarized MDM with heGDH was done after 48 hours pre-incubation with IL-4 and IL-13. Wildtype BMDM were incubated with anti-mouse IL-12 p40 or isotype control antibody. To test effects of p40, MDM were treated with recombinantly produced human IL-12 β for 24 hours. TCA-metabolite effects were assessed by stimulation of MDM with D-2-hydroxyglutarate (HG), L-2-HG, itaconate or α -KG. PUFA production was elicited by stimulating cells with ionophore for 10 min at 37°C during harvesting. Cells were not treated with ionophore when they were used for FACS analysis. Supernatants of cells were stored at -70°C in 50% MeOH for LC-MS/MS analysis or undiluted for cytokine analysis. Cell pellets were lysed in RLT buffer with 1% β -Me and stored at -70°C for RNA extraction. For western

blot analysis, cell pellets were lysed with RIPA buffer supplemented with complete protease inhibitor cocktail and phosphatase inhibitor cocktail and stored at -70°C.

3.9 Immunofluorescence (IF)- and immunohistochemistry (IHC) staining (I)

Tissue for immunofluorescence and immunohistochemistry staining of *Hpb*-infected intestine was first deparaffinized and rehydrated. To reduce the autofluorescence background, autofluorescence reducing reagent was used. Before both staining's, antigen retrieval by repeated boiling in sodium-citrate buffer was performed. Subsequent, tissue was permeabilized and blocked with BSA and donkey serum at room temperature. Tissues for immunohistochemistry staining were further blocked with a Avidin/Biotin Blocking Kit.

For immunofluorescence staining of MDM or BMDM, cells were seeded on glass-chamber slides and fixed for 15 minutes with 4% paraformaldehyde, followed by permeabilization with acetone. After the same blocking procedure, cells or tissue were incubated with primary antibodies overnight. Where indicated, blocking of anti-heGDH mAb with its antigen peptide was performed in ratio of 1:1 overnight at 4°C while rotating. Fluorescence conjugated secondary antibodies were used for detection of immunofluorescence staining. Before images were recorded, cells were mounted and stained with Fluoroshield containing DAPI. Detection and development of IHC staining's were performed by applying ABC Peroxidase Standard Staining and DAB Enhanced Liquid Substrate System. Before recording with the EVOS system, nuclear counterstain and mounting was done.

3.10 Chromatin immunoprecipitation (ChIP) (I)

For the ChIP with formaldehyde crosslinking, MDM were washed once with warm PBS and incubated for 30 min at 37°C and 5% CO₂ with accutase to detach the cells. ChIP protocol steps were performed as previously described [572], except fragmentation of the chromatin, which was carried out by using a focused-ultrasonicator for 15 min at 6°C with 140W peak power, 5% duty factor and 200 cycles/burst. Instead of agarose beads, ChIP grade protein A/G magnetic beads were added to the chromatin. Antibody mixture and incubation was done for 2 hours at 4°C while rotating. DNA purification was performed with MinElute PCR Purification Kit. Eluted DNA was either subjected to ChIP-seq or used for ChIP-qPCR experiments. Input chromatin DNA was prepared from 1/4 of chromatin amount used for ChIP.

3.11 ChIP quantitative real time-polymerase chain reaction (qRT-PCR) (I)

For all primer pairs, input chromatin DNA was used to generate standard curves and verify amplification efficiency between 90–100%. qPCR was performed on a ViiA7 Real-Time PCR System. Changes in enrichment at specific regions were normalized to 3 different positive control regions which did not show changes in histone modifications during stimulation with heGDH.

3.12 RNA isolation and qRT-PCR (I-III)

RNA was extracted using a spin-column kit and transcribed into cDNA using the HighCapacity cDNA Reverse Transcription kit according to the manufacturer's instructions or submitted for total RNA sequencing. FastStart Universal or PowerUp SYBR Green master mixes were used for 10 ng cDNA template and qPCR was performed on a ViiA7 Real-Time PCR or QuantStudio 5 System. All expression levels were normalized to house-keeping genes and relative gene expression was represented as $2^{-\Delta CT}$ ($\Delta CT = \Delta CT_{(gene)} - CT_{(housekeeper)}$). A list of primers is shown in every publication.

3.13 Flow-cytometry (FACS) (I, II)

Mesenteric lymph nodes (MLN) of *Hpb* infected mice were removed and transferred in RPMI medium on ice until further processing for FACS analysis. Cells of MLN were forced through a 70 μ m cell strainer using cold PBS to prepare a single cell suspension. T cell population were stained extracellularly. After 30 min fixation and permeabilization using a Fixation/Permeabilization kit, intracellular staining was performed. EP2^{-/-} BMDM as well as MDM were stained extracellularly. Live/dead aqua stain was used for all cells to exclude dead cells from the analysis. All samples were acquired in a BD LSRFortessa.

3.14 Metabolic flux analysis (seahorse assay) of MDM and BMDM (I)

MDM and BMDM were cultured on Seahorse Miniplates. On the day of the assay, medium was exchanged to the Seahorse XF RPMI medium, pH 7.4 supplemented with glucose, pyruvate and L-glutamine. Cell Mito Stress Test was performed according to the manufacturer's instructions with subsequent injections of oligomycin, FCCP (MDM: 1 μ M, BMDM: 5 μ M) and rotenone and antimycin A. After the assay was performed, cells were lysed in RIPA buffer and protein concentration was determined for normalization.

3.15 LDH cytotoxicity assay (I)

Cellular cytotoxicity of stimulation with the p300 inhibitor in MDM and BMDM was quantified using the LDH cytotoxicity assay kit, according to the manufacturer's instructions.

3.16 EIA and ELISAs (I-III)

The concentration of cysLTs and PGE₂ in culture supernatants was determined by using commercially available enzyme immunoassay (EIA) kits, according to the manufacturer's instructions. MDM and PBMC supernatants were analyzed for different chemokine and cytokine secretion. All ELISAs were used according to the manufacturer's instructions.

3.17 Westernblot (I, III)

The protein concentration was determined by the BCA method for MDM and BMDM lysates, which were diluted to equal concentrations between 12-20 µg. NuPAGE LDS Sample buffer and NuPAGE Sample Reducing Agent was added to total MDM/BMDM lysates and heated at 95 °C for 5 minutes. HEK supernatants from publication III were supplemented with 0.2 volumes of 5x Laemmli buffer containing β-Me. Samples were loaded on Bolt 4-12% Bis-Tris Plus gels (I) or 12% SDS-PAGE gels (III) and separated by electrophoresis. Proteins were transferred to a PVDF membrane either 1 hour at RT (I) or overnight at 4°C (III) with subsequent blocking in 5% nonfat dry milk in 1x TBS containing 0.05% Tween for several hours. Membranes were incubated overnight with primary antibodies, washed and incubated with the corresponding secondary horseradish peroxidase-conjugated antibody. Detection was performed using enhanced chemiluminescence and recorded with the ECL Chemocam Imager or Fusion Pulse 6 imager.

3.18 Expression and purification of heGDH (I)

The cloning, expression and purification of heGDH as previously published [483] was initiated by me, but further improved and optimized by the Protein Expression and Purification Facility at the Helmholtz Center Munich.

Briefly, heGDH expression constructs were transformed into *E. coli* strain BL21 (DE3) CC4 (overexpressing the (co-)chaperones GroEL, GroES, DnaK, DnaJ, GrpE and ClpB) and cultured overnight at 20°C containing auto-induction medium and antibiotics. Cells were

harvested by centrifugation after reaching saturation, resuspended in lysis buffer and lysed by sonication. The lysate was clarified by centrifugation and filtration. The supernatant was applied to a 5-ml HiTrap Chelating column. Bound proteins were eluted with a linear gradient from 50 to 300 mM imidazole. Fractions containing heGDH were pooled and dialyzed overnight at 4°C. Next, 5 mM ATP and 1 mM MgCl₂ were added, and the solution was incubated overnight at 4°C to detach bound chaperones. The solution was applied to a 5-ml HiTrap Chelating HP column. Fractions containing heGDH were pooled and dialyzed overnight at 4°C in the presence of His-tagged TEV protease. The cleaved off heGDH was further purified by affinity chromatography as described above and the flow-through and protein containing wash fractions were pooled and concentrated. Concentrated heGDH was subsequently subjected to size exclusion chromatography using a HiLoad 16/600 Superdex 200 column. The fractions containing heGDH were pooled and dialyzed overnight against PBS pH 7.4 at 4°C. Finally, the protein solution was concentrated to approx. 2 mg/ml and stored in aliquots at -70°C.

3.19 Fluorochrome labeling of heGDH (I)

HeGDH was labeled with an Atto 488 Protein Labeling Kit according to the manufacturer's instructions. Subsequently, the fluorochrome conjugated protein was purified with a PD-10 desalting column.

3.20 GDH activity assay (I)

GDH activity of purified recombinant heGDH or mutant heGDH was determined both in the direction of glutamate formation and utilization. Assays were carried out at 37 °C in an assay mixture containing phosphate buffer and 5 µg protein. The enzyme activity of heGDH was determined in the direction of glutamate utilization by the rate of production of NAD⁺/NADP⁺ or by the rate of utilization of NADH/NADPH in the direction of glutamate formation, measured spectrophotometrically at 340 nm. The optimum pH was determined in both directions with substrate concentrations of 0.5 mM α-ketoglutarate and 40 mM ammonia or 5 mM glutamate with the pH range 5.5-9.5. The optimum concentration of co-factors was determined by using NAD(P)⁺ concentrations from 0 to 3 mM with 4 mM glutamate or 0 to 0.8 mM NAD(P)H with 0.5 mM α-ketoglutarate and 10 mM ammonia. The K_m for glutamate was determined in reaction mixtures containing 0-15 mM glutamate and 3 mM NAD⁺ and the K_m for α-ketoglutarate with 0-1 mM α-ketoglutarate, 10 mM ammonia and 0.4 mM NADH. The K_m for ammonia was determined with 0-100 mM ammonia, 0.5 mM

α -ketoglutarate and 0.4 mM NADH. The inhibitory/stimulatory effects of GTP, bithionol and α -heGDH mAb on GDH activity were determined in the direction of both glutamate utilization and formation reaction with following concentrations: 3 mM NAD⁺, 0.4 mM NADH, 4 mM glutamate, 0.5 mM α -ketoglutarate and 10 mM ammonia.

3.21 iLite receptor activation assay (III)

For IL-12 and IL-23, a receptor activation assay was performed using IL-12 or IL-23 iLite[®] reporter cells, according to the supplier's instruction. The cells were stimulated with HEK293T supernatants containing 10 ng/ml secreted IL-12 or IL-23 constructs, previously quantified via immunoblotting by comparing immunoblot signals to those of recombinant IL-12 or IL-23 with known concentrations. The firefly and renilla luminescence signals were detected via the Dual-Glo Luciferase Assay System in a multimode microplate reader.

3.22 Data analysis and statistics (I-III)

Immunofluorescence stainings and western blots were analyzed by Fiji. Additionally, western blots were quantified by Fiji or Bio-1D software. Flow cytometry data was evaluated with the Flowjo v10 software. Seahorse assays were analyzed with the help of Seahorse Wave Desktop Software. Lmi quantification was done by Aperio eSlide Manager. Data of all publications were analyzed by GraphPad Prism software. For LC-MS/MS (lipid mediator) and ELISA (cytokines/ chemokines) data, missing values below the lower limit of detection were interpolated using $\frac{1}{4}$ of the minimum value for each metabolite. Statistical analysis of two group comparisons was performed using Mann-Whitney (unpaired), Wilcoxon test (paired) or t test depending on normal distribution. For comparison of more groups, RM one-way ANOVA, Friedmann test (paired) or Kruskal-Wallis test (unpaired) with Dunn correction was used with correction for multiple comparisons. $P < .05$ was considered statistically significant. Heat maps, except for RNA sequencing data, were generated by the Broad Institute's Morpheus software.

4 Results

4.1 A helminth enzyme instigates immune evasion via a p300-prostaglandin axis in host macrophages

Summary

We previously identified the glutamate dehydrogenase (GDH) within the larval extract of *H. polygyrus* as a major immune regulatory protein that is able to suppress HDM-induced allergic airway inflammation [483]. However, the exact mechanism of action as well as the role of helminthic GDH (heGDH) during helminth infection remained unknown.

Investigation of the necessity of GDH for *H. polygyrus* during the infection with *Hpb* was demonstrated by neutralizing heGDH with a specific mAb, which resulted in a lower worm burden. This key result confirmed that heGDH is a central factor involved in the *Hpb*-mediated suppression of type 2 immunity. To assess whether heGDH can affect macrophages, MDM as well as BMDM were treated with a fluorochrome-labeled version of heGDH to track cellular uptake. After confirming the uptake of heGDH into macrophages, we performed RNA sequencing, which revealed broad changes in transcriptional profiles with a strong induction of immune-regulatory genes including *IDO1*, *PTGES*, *PTGS2*, *IL12B* and *EBI3* in heGDH-treated MDMs compared to untreated or LPS stimulated cells. We further found PGE₂ synthetic enzymes (*PTGES*, *PTGS2*) as well as *IL12B* to be epigenetically controlled by the recruitment of the p300 histonacetyltransferase (HAT) using pharmacological inhibition and knock down of p300 during stimulation with heGDH. The increase of PGE₂-synthetic enzymes found by RNAseq was further confirmed by the quantification of oxylipins in MDMs following treatment with heGDH. In keeping with our previous work [483], heGDH reprogrammed macrophages to an immunomodulatory phenotype with the suppression of type-2 inducing leukotrienes and the induction of regulatory prostanoids and cytokines. Further investigation of the role of heGDH and the induction of prostanoids *in vivo* during infection with *Hpb* and treatment with heGDH confirmed the correlation between immune regulation by heGDH and the p300-mediated PGE₂ production in host macrophages. Thus, heGDH led to an increase in worm burdens, the suppression of AAM polarization in an EP2-dependent manner and a decrease in inflammatory T_H2 cells. Moreover, translation of mouse to human studies showed that the abundance of SEA-induced T_H2 cells as well as SEA-induced IL-4 production in human PBMC cultures was suppressed by heGDH treatment. In contrast, heGDH increased the

percentage of regulatory T cells in human PBMCs in the dependency on PGE₂ production by monocytes. However, the full and IL-4/IL-13 dependent development of a type 2 immune response overruled the heGDH driven immune evasion as shown during challenge infection with *Hpb* and primary infection with *N. brasiliensis*. Nevertheless, heGDH still induced prostanoid production in host macrophages and improved pulmonary tissue repair following infection with *Nb*.

The induction of the prostanoid pathway was dependent on structure elements provided by heGDH, as a catalytically inactive mutant of heGDH displayed an unaltered prostanoid inducing function. Structure determination by electron microscopy and X-ray crystallography revealed the N-terminal domain as the most different part compared to human GDH, suggesting that the p300-prostaglandin axis is mediated via N-terminal binding to potential interaction partners in macrophages. In contrast, the catalytic activity was necessary for suppression of LTs. This was partially mediated via downstream products of heGDH. L-2-HG, found at elevated levels in macrophages following heGDH stimulation, was shown to suppress cysLT production. Metabolic shifts induced by heGDH were not restricted to the eicosanoid pathway, but also affected glycolysis, TCA cycle and amino acid metabolism. The p300-dependent upregulation of the glycolysis activator gene *PFKFB3* resulted in an increased glycolysis, further confirming the prevention of M2 polarization by heGDH. Thus, heGDH was identified and characterized as an immunomodulatory candidate protein, mediating immune evasion by affecting macrophage metabolism and T cell function, particularly through induction of the p300-prostaglandin axis.

Contribution of the authors

Julia Esser-von Bieren, Sina Bohnacker, Clarissa Prazeres da Costa, Carsten B Schmidt-Weber and Matthias J. Feige conceptualized the study. Sina Bohnacker and Julia Esser-von Bieren wrote the manuscript. Sina Bohnacker, Fiona Henkel, and Franziska Hartung performed *in vivo* experiments with the help of Francesca Alessandrini and Antonie Lechner. Fiona Henkel, Yannick Schreiber and Robert Gurke measured oxylipins. Sina Bohnacker performed all cellular (MDM and BMDM) *in vitro* assays with the help of Sandra Riemer. Arie Geerlof produced heGDH. André Santos Dias Mourao and Stefan Bohn solved the structure of heGDH. Fabien Prodjinotho performed T_H2 cell and Treg assays. Agnieszka M. Kabat from Edward J. Pearce group performed targeted metabolomics. Tarvi Teder from Jesper Z. Haeggströms lab analyzed the LTC₄S activity. Per-Johan Jakobsson provided the PTGES inhibitor. David Vöhringer provided *Hpb* larvae. Sina Bohnacker visualized the data with the help of Minhaz Ud-Dean and Christiane Böckel from the Institute of Computational Biology, Helmholtz Center Munich.

4.2 Mild COVID-19 imprints a long-term inflammatory eicosanoid- and chemokine memory in monocyte-derived macrophages

Summary

After more than three years into the pandemic, it has become clear that the innate immune system and in particular monocytes and macrophages are crucially linked to the heterogeneity of the COVID-19 disease courses. However, even if the pandemic will be under control due to world-wide vaccination programs and other medical measures, the sequelae of long COVID-19 and its potential burden on long-term health requires further studies into the role of this immune cell type. Thus, we investigated the presence of long-term reprogramming of the monocyte/ macrophage compartment in response to SARS-CoV-2 infection in subjects with a mild disease course. Health care workers at TUM university hospital were retrospectively categorized as either SARS-CoV-2 seronegative or seropositive based on their SARS-CoV-2 IgG titer. The cohort consisted of 36 seronegative and 68 previously COVID-19 infected individuals. The majority of patients (74%) reported several symptoms, mainly fatigue, during the time of infection in spring 2020, with a small portion (16%) reporting persistent symptoms 3-5 months after the infection. Monocytes as well as monocyte derived macrophages (MDM) from subjects at 3-5 months post SARS-CoV-2 infection showed an increased *CCL2* level compared to cells from seronegative controls. This persistent inflammatory imprint despite mild disease was confirmed by multiple analyses, including RNAseq, qPCR, ELISA and LC-MS/MS. The results showed higher expression of inflammatory chemokines, such as *CCL2* and *CCL8* in MDM from previously infected individuals, particularly after restimulation with SARS-CoV-2 S-protein or treatment with LPS. Furthermore, S-protein challenge of MDM from convalescent COVID-19 patients resulted in induction of ISGs (e.g. *IFI27*, *IFITIM1/3*, *ISG20*, *OAS1/3*) and M2-associated genes, indicative for an inflammatory imprint in MDM 3-5 months after SARS-CoV-2 infection as well as for a “training” effect after restimulation with SARS-CoV-2 S-protein.

Furthermore, gene expression analysis of previously infected COVID-19 patients compared to healthy controls uncovered an increase in the expression of genes involved in fatty acid synthesis, including *FASN* and *CYB5R2*, while genes implicated in the synthesis of pro-resolving lipid mediators, such as *SEMA7A* were downregulated. In line, eicosanoid metabolic profiling in MDM from post-COVID-19 patients showed an increased synthesis of pro-inflammatory eicosanoid metabolites, dominated by the production of LTs when compared to MDM from seronegative patients. This effect was transient, because

exaggerated 5-LOX metabolites were back to baseline at 12 months post SARS-CoV-2 infection. In contrast to increased 5-LOX metabolites secreted by MDM from convalescent COVID-19 patients, MDM from previously infected patients challenged with S-protein showed a reduced LT profile, while prostanoids from the thromboxane pathway (TXB₂ and 12-HHTrE) were increased, suggesting a switch towards tissue reparative, vasoconstrictive, and immune-regulatory functions in MDM at 3-5 months after SARS-CoV-2 infection when cells were further challenged with spike protein.

Although RNAseq data revealed profound changes in chemokine gene expression of MDM from COVID19 patients, cytokine and chemokine production was not altered (also after subsequent stimulation with different inflammatory triggers) between MDM from seronegative or seropositive subjects 3-5 months after infection. As airway inflammation, including COVID-19 is commonly treated by glucocorticoids, steroid treatment with fluticasone propionate (FP) decreased the house-dust mite (HDM) induced production of inflammatory cytokines and prostanoids independently of patient status (seropositive or seronegative patients 3-5 months after SARS-CoV-2 infection). In contrast, usage of FP enhanced LT secretion in seronegative as well as seropositive patients 3-5 months after infection, indicative for a possible trade-off effect of glucocorticoid treatment during acute or long COVID-19 disease.

Contribution of the authors

Julia Esser-von Bieren, Craig E. Wheelock, Carsten B. Schmidt-Weber, Adam M. Chaker, Percy Knolle, Paul Lingor and Ulrike Protzer conceptualized the study. Sina Bohnacker, Franziska Hartung, Fiona Henkel and Julia Esser-von Bieren wrote the original manuscript. Alessandro Quaranta, Johan Kolmert and Craig E. Wheelock measured oxylipins. PBMC isolation of all donors was done by Sina Bohnacker, Franziska Hartung and Fiona Henkel. Sina Bohnacker performed all qPCR and ELISA experiments. Fiona Henkel analyzed LC-MS/MS measurements. Franziska Hartung analyzed RNA sequencing data sets. Sina Bohnacker, Franziska Hartung, Fiona Henkel, and Minhaz Ud-Dean visualized the data.

4.3 Influence of glycosylation on IL-12 family cytokine biogenesis and function

Summary

The IL-12 family of cytokines, consisting of heterodimeric glycoproteins, plays a crucial role in controlling T cell activity and orchestrating immune responses. However, the effect of glycosylation on the biogenesis and function of the various family members is still not fully understood. Thus, the overall glycosylation status of each subunit of the IL-12 family member was determined based on sequence analysis and specific glycosylation sites were identified by enzymatic removal of glycan moieties using PNGase F or O-glycosidase mix. The results showed that at least one subunit of every IL-12 family heterodimer, including IL-12 α , IL-12 β as well as EBI3 are N-glycosylated, whereas IL-27 α is the only subunit showing two specific O-glycosylation sites. Site-directed mutagenesis of all predicted glycosylated asparagine-sites to glutamine or O-glycosylated serine/threonine-sites to alanine confirmed glycosylation status of all IL-12 family members, except for IL-12 β . The presence of N-glycosylation sites in IL-12 β was analyzed, with predictions indicating N135 and N222 as potential sites. However, only N222 was experimentally confirmed. Further analysis of potential N-glycosylation sites below the threshold for prediction revealed that N125 and N303 were also present in IL-12 β to some extent. Mutation of all four “predicted” glycosylation sites confirmed the lack of glycans.

Glycosylation as an important post-translational modification is often coupled to ER folding and quality control processes which may impact IL-12 family cytokine secretion and function. Thus, we further assessed how glycosylation can affect heterodimerization, secretion and biological activity of IL-12 family members. Lack of glycosylation on IL-12 α as well as IL-12 β did not affect heterodimerization and secretion of IL-12 nor of IL-23. Although, completely deglycosylated IL-12 as well as IL-23 revealed a slight reduced receptor activation, both were found to be functionally active. IL-12, that completely lacks glycosylation at all was still able to induce gene expression of IFN- γ and unglycosylated IL-23 triggered IL-17 secretion in peripheral blood mononuclear cells (PBMCs). In contrast, glycosylation deficiency retained EBI3 in isolation. However, mutated as well as wild type EBI3 induced secretion of both IL-27 α as well as IL-27 α that lacks O-glycosylation sites with the concomitant secretion of itself, suggesting heterodimer formation of IL-27 even if both subunits lack their glycosylation sites. Furthermore, functional activity was tested by phosphorylation of STAT-1 in BL-2 cells, expressing IL-27R on their surface. Deglycosylated EBI3 affected biological activity, as the complex of wild-type IL-27 α with

non-glycosylated EBI3 as well as the overall deglycosylated IL-27 heterodimer induced significantly decreased STAT1 phosphorylation in comparison to wildtype IL-27, suggesting that glycosylation status of interleukins can affect cytokine signaling.

The secretion of IL-35, which shares the same β -subunit as IL-27, was significantly impacted by the absence of glycosylation. The mutation of either IL-12 α or EBI3, the two subunits of IL-35, was sufficient to almost block secretion of the other subunit completely. Additionally, co-expression of non-glycosylated IL-12 α as well as EBI3 prevented co-secretion into the medium. The reduction in secretion of wild-type EBI3 (which is secretion-competent on its own) by IL-12 α that lacks glycosylation sites suggests that heterodimerization still took place, leading to retention of the heterodimeric cytokine by ERQC. As no sufficient secretion of deglycosylated IL-35 was found, no biological activity was investigated.

Taken together, glycosylation can impact both secretion and biological function of IL-12 family cytokines to different extents with the most dominant role for IL-35 secretion and IL-27 signaling.

Contribution of the authors

Sina Bohnacker, Karen Hildenbrand, Isabel Aschenbrenner, Julia Esser-von Bieren and Matthias J. Feige wrote the manuscript. Sina Bohnacker performed cell culture and transient transfections as well as immunoblot experiments of IL-23. Cell culture, transient transfection and immunoblots of IL-12, IL-27 and IL-35 were performed by Isabel Aschenbrenner and Karen Hildenbrand. Activity and receptor signaling assays for IL-23 and IL-12 was done by Sina Bohnacker. BL2 assays and STAT western blots were performed by Isabel Aschenbrenner. IL-27 α experiments were performed by Stephanie I. Müller. Sina Bohnacker, Karen Hildenbrand, Isabel Aschenbrenner, Stephanie I. Müller, Julia Esser-von Bieren and Matthias J Feige analyzed the data.

5 Discussion

In this dissertation, the multifaceted and multilayered host immune response to different internal and external triggers was examined. First, light was shed on the mechanism of actions and roles of a parasite-derived protein as well as on long-term effects of SARS-CoV-2 infection and how both are able to reprogram macrophages. Second, this dissertation contributes to a better mechanistic and functional understanding of host-derived interleukin 12 family cytokines by delineating how the glycosylation status affects their biogenesis and function as signaling molecules.

5.1 Parasitic GDHs: an evolutionary conserved enzyme for host immune evasion?

Glutamate dehydrogenase (GDH) has been identified as the major immunoregulatory component of an anti-inflammatory homogenate prepared of L3 stage larvae of the helminth *H. polygyrus bakeri* (“*HpbE*”) [483], able to modulate the AA metabolism and increasing the release of the regulatory prostanoid PGE₂ and the anti-inflammatory cytokine IL-10. In a comparative analysis of excretory/secretory products (HES) from adult stages of *Hpb*, GDH activity is present only in L3 extract and has not been found in HES or homogenates of L4 or L5 [483,573]. This suggests that the protein profile varies depending on the stage of the parasite lifecycle. However, secretion profiles of L3 and L4 compared to L5 (HES) were not determined, warranting further proteomic analysis in order to reveal if GDH can exclusively be secreted by L3. Further evidence for a developmental regulation is shown by a GDH from *H. contortus*, which is localized to the cytoplasm of the parasite’s gut and both GDH mRNA and protein are expressed almost exclusively during the blood-feeding stage [574]. Differences in protein composition in different stages may explain the distinct reprogramming of e.g. AA metabolism observed for heGDH, and HES, as only HES failed to induce the release of prostanoids in macrophages [483]. However, the roles of heGDH (apart from its metabolic function) in the living helminth and the reason for its higher expression in the L3 stage is unclear. The environment of the L3, which is located in the intestinal tissue, may induce glutamate metabolism in the early stage of the larvae. It is well-established that the availability of amino acids in tissues has a significant impact on immune cell functions [575], and macrophage activation/polarization, in particular, depend on glutamine metabolism [214]. Therefore, the usage of glutamine/glutamate via GDH could potentially create a more favorable host environment, enabling larvae to survive and molt into adult stages.

Several studies have implicated glutamate dehydrogenase as an evolutionary conserved enzyme in regulating host immunity. Early vaccination studies uncovered a parasitic GDH as the dominant protein within the soluble extract against which anti-helminth immunity was developed [574]. Interestingly, GDH derived from the parasite *T. cruzi* was identified as the immunomodulatory compound responsible for the production of IL-10 and IL-6 in CD11b⁺ cells, contributing to B cell expansion [576]. A more recent study about epilepsy induced by the parasitic cestode *Taenia solium* uncovered a GDH in viable cysts that instructs tolerogenic monocytes to release IL-10 and PGE₂ ultimately leading to the induction of regulatory T cell responses in mice and humans [484]. In line with these studies, helminthic GDH (heGDH) treated macrophages also release high amounts of IL-10, IL-6 and PGE₂, highlighting GDH as an evolutionary conserved immune regulatory enzyme shared between different parasites. However, further work is required to characterize if GDHs from different parasites share structural similarities and whether they instruct the same mechanism to drive host immune evasion. The immune regulatory functions of parasitic GDHs suggest a therapeutic potential, e.g., as a vaccine antigen for inducing immunity against a broad range of helminth parasites.

5.2 Macrophages as the primary target cells of helminths and heGDH

Macrophages are versatile cells and play a pivotal role in anti-helminth immunity by mediating worm trapping, regulating the immune system, and repairing tissue injury caused by migrating larvae [158,160,577]. Thus, helminth parasites have evolved products that can target and influence macrophages and their effector functions, resulting in immunomodulatory reactions [155]. To affect immune-regulatory mechanisms and macrophage metabolism helminthic molecules engage receptors, trigger receptor-mediated endocytosis or are transferred into the cell via helminth-derived exosomes [273,578]. Upstream mechanisms underlying the induction of the COX pathway have been previously described for *S. mansoni* egg antigen (SEA), which binds to dectin-1 and dectin-2, resulting in the secretion of PGE₂ from DCs [492]. In line, some parts of *Hpb* larval extracts (*HpbE*) are able to drive dectin-1 and -2 mediated *PTGES* expression [483]. However, internalization of fluorescent-labeled heGDH or heGDH mediated *PTGES* expression was not affected by inhibiting or deleting dectin-1 or -2, suggesting that recombinant heGDH, possibly due to production in *E. coli*, carries no carbohydrate structures and thus has to use other internalization strategies to perform its immune-regulatory functions. Preliminary analyses revealed an enrichment of CD64 in heGDH treated cells, which was in line with proteomic analysis, identifying CD64 as a potential interaction partner of heGDH. Indeed,

colocalization of heGDH and Fc γ RI (CD64) was observed during helminth infection. In line, highly activated and organ specific monocyte-derived macrophages during helminth infection are strongly positive for CD64 [579] and play an important role in helminth trapping [159], suggesting that CD64 serves as the potential entry point targeted by heGDH to reprogram macrophages in the surrounding of the larvae. However, how heGDH interacts with CD64 on a structural basis [580] by e.g. providing a binding surface within its N-terminal handle-like structure remains to be defined.

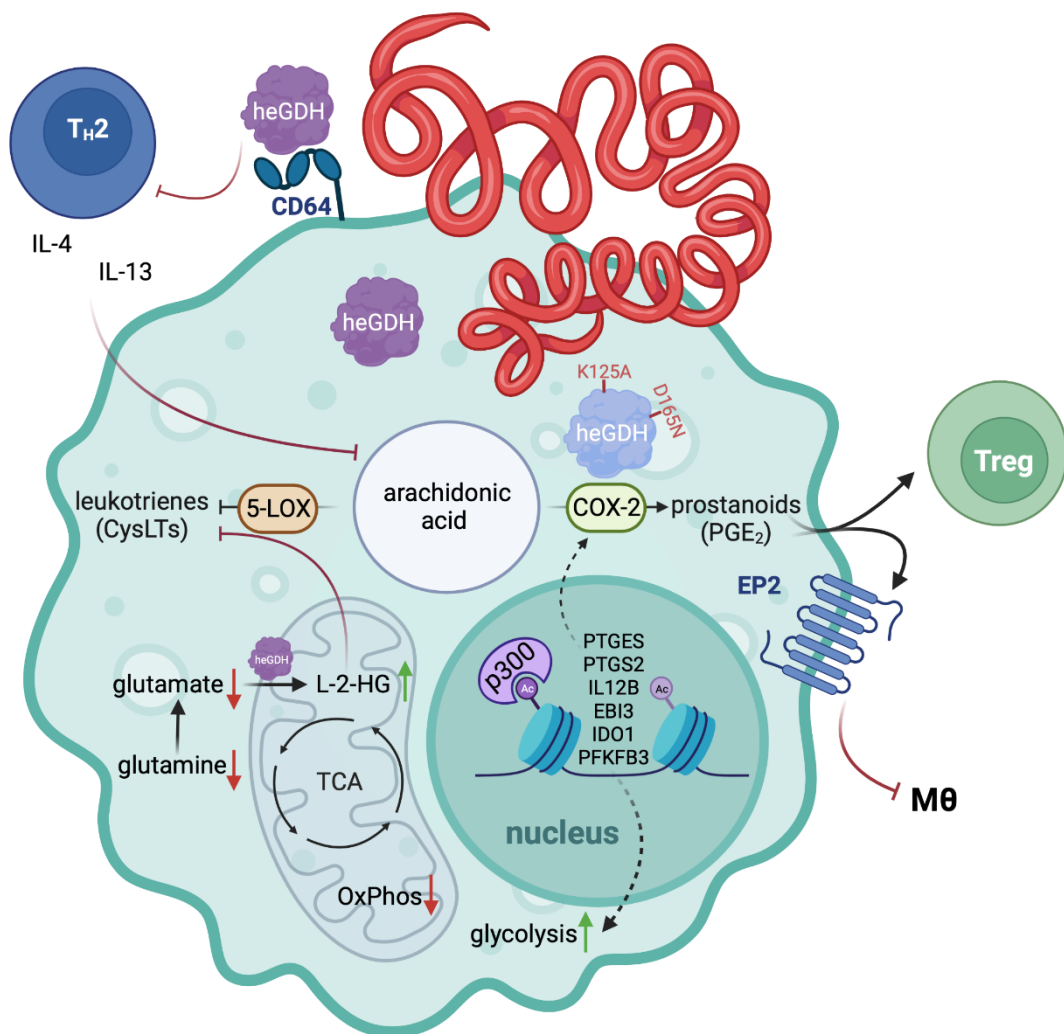


Figure 15: Schematic illustration of reprogrammed monocyte-derived macrophages after treatment with *H. polygyrus* glutamate dehydrogenase from publication I (created with BioRender.com)

5.3 Epigenetic regulation of a type-2 suppressive macrophage phenotype by heGDH

Helminth infections, such as with *F. hepatica* or *S. mansoni* can have significant impacts on hematopoiesis, potentially causing long-lasting effects through anti-inflammatory reprogramming that may extend to macrophage progenitors [253,581]. Helminth infection can also affect the resident macrophage populations, which have the ability to self-renew, especially in the context of type 2 immunity [582]. The specific epigenetic mechanisms and chromatin landscapes associated with helminth-induced regulatory macrophage reprogramming are not yet fully understood. However, IL-4-triggered H3K27ac modification has been observed at enhancer regions of AAM genes such as *Arg1* and *Mmp12* [252]. Another study identified HDAC3 as a negative regulator of alternative activation, indicating the importance of H3K27 modifications in macrophage polarization and functions during helminth infection [251]. Acetylation of H3K27 is a well-defined marker of enhancer activity which requires CBP/p300 histone acetyltransferase activity [583]. PGE₂ synthetic enzymes (COX-2 and mPGES-1) as well as IL-12 β are epigenetically controlled by HDAC-mediated recruitment of the p300 HAT [584–586]. In keeping with these studies, helminthic GDH was able to induce acetylation of H3K27 in an p300-dependent manner (Figure 15). But how CD64 receptor engagement induced p300 HAT activity needs to be investigated. In a study of adipose-derived stem cell and angiogenesis, C-reactive protein was found to bind to CD64, inducing ERK1/2 and Akt phosphorylation, which in turn activates HIF-1 α to enter the nucleus and bind together with p300 in the VEGF promoter, stimulating VEGF gene and protein expression [587]. Thus, this describes a potential link between CD64 receptor binding and the activation of a p300-dependent induction of immune-regulatory genes.

The site and duration of helminth infection also plays a role in macrophage reprogramming and its functional consequences [588]. Consequently, epigenetic reprogramming of BM-derived, recruited, and resident proliferating macrophages may result in diverse and often persistent alterations of macrophage effector functions, especially following chronic helminth infections. A first hint of myeloid reprogramming by helminths in humans as an immune evasion strategy is reported by previously infected *N. americanus* patients that developed a monocytosis and increased the expression of IL-10 in monocytes [589]. The reprogramming of peritoneal macrophages by the heGDH-induced and H3K27ac-dependent upregulation of PGE₂ remained at least for 3 days. It is currently unclear whether heGDH treatment induces long lasting epigenetic modifications in BM-derived monocytes/macrophages or their progenitors *in vivo* and how long the heGDH-mediated impact on e.g.

airway macrophages during HDM-induced allergic airway inflammation maintains [483]. It would thus be interesting to study if the anti-inflammatory phenotype of heGDH-treated macrophage is transient or whether it leads to sustained anti-inflammatory long-term activity. Such lasting anti-inflammatory effects would represent a major advantage with regards to a potential use of heGDH as a therapeutic strategy in type 2 inflammatory disorders. However, sustained anti-inflammatory remodeling of macrophages can endanger host immunity and make the host more susceptible to subsequent infections such as IAV e.g. via the sustained production of PGE₂ [436,455,456]. Analysis of PGE₂ induction in peritoneal macrophages 7 days after intraperitoneal treatment with heGDH revealed no persistent effect, suggesting that a more acute macrophage reprogramming is necessary to modulate host immune responses. In line, a less persistent macrophage reprogramming would also be beneficial as treatment for type 2 disorders in the lung, because medication could be paused in case of infection without lagging of immunosuppression.

5.4 *H. polygyrus* induced immune evasion by regulation of the AA pathway and T-cell subsets

Helminth parasites have evolved different mechanisms to modulate type 2 inflammation, including suppression of ILC2 activation, blocking IL-33 release, and induction of an immune-regulatory macrophage phenotype [268,291,590]. Eicosanoids are lipid mediators derived from arachidonic acid that play a significant role in anti-helminth (type 2) immunity [400,483]. Thus, heGDH-induced reprogramming of AA metabolism uncovered a potential evasion strategy used by the parasitic nematode *Heligmosomoides polygyrus bakeri* (*Hpb*) to suppress type 2 immune responses [483].

7 days post-infection, *Hpb* triggers the release of regulatory prostanoids (PGE₂ and 6-keto PGF_{1α}), which can modulate type 2 immune responses by inducing a regulatory macrophage polarization and limit type 2 cytokine production by ILC2s [483,491,591]. Furthermore, *Hpb* induces the production of COX metabolites including 12-HHT and TXB₂, which are involved in tissue repair and blood clotting [483,592,593]. In contrast, *Hpb* suppressed the release of pro-inflammatory mediators, including cysLTs and LTB₄, which induce T_H2 cell activation, vascular leakage, eosinophil recruitment, and mucus production by goblet cells [96,483,594]. A similar eicosanoid profile is observed during helminth infection with *B. malayi*, which decreased PGD₂ production, but increased PGI₂ and TXB₂ production in macrophages possibly to enable immune evasion [486,499]. The COX product PGE₂ is produced by multiple helminth parasites themselves and it is efficiently

induced by multiple helminth products in myeloid cells [483,484,492,508]. A more recent study shed light on parasitic GDH's as an possible evolutionary conserved enzyme - amongst different parasites- involved in PGE₂ and IL-10 upregulation in tolerogenic monocytes [484,595]. In line, heGDH induces prostanoids with a strong increase in PGE₂, but also IL-10, while it decreases the production of the 5-LOX products 5-HETE and the cysLTs (Figure 15). Moreover, the heGDH induced shift in the arachidonic acid metabolism towards an increased production of prostanoids, especially PGE₂, suppressed M2 polarization in an EP2-dependent manner *in vivo* and modulated human T cell function *in vitro*. In keeping with the study of *T. solium* GDH and in contrast to human GDH [484], the immune suppressive functions of heGDH relied on the suppression of a helminth-induced T_H2 response and on the capacity to induce Tregs partially in the dependence of PGE₂ production. Similarly, PGE₂ can regulate T_H1 and T_H17 responses by inhibiting IL-12 and IL-23 production in monocytes and macrophages, while inducing Tregs and IL-10 production [596–598].

The suppressive capacity of heGDH on T_H2 cells is observed after 28 days post *Hpb* infection, suggesting that the induction of regulatory macrophages by heGDH is particularly important at the beginning of infection, and that these reprogrammed macrophage populations can affect T cells at later time points of parasite infection. Induction of Tregs by heGDH could be verified in human PBMCs *in vitro* but was not studied in detailed during *Hpb* infection *in vivo*. As only mesenteric lymph nodes were assessed, it is unclear, whether heGDH can affect Treg induction locally in granulomas or the small intestinal lamina propria during *H. polygyrus* infection. Moreover, the conversion of naïve T cells into Tregs by e.g. PGE₂ binding to EP2/4 [484] needs to be further investigated. Treg induction by regulating tryptophan metabolism could play a further role, as heGDH is a strong *IDO1* inducer. *IDO1* activates regulatory T cells and blocks their conversion into T effector cells also during parasite infections [599,600]. Mechanistically, IKK α -induced *IDO* can inhibit T_H2 cell responses, while inducing the expression of Foxp3 in CD4⁺ T cells during allergy [601]. But, whether heGDH induced *IDO1* expression in macrophages contributes to Treg induction and T_H2 cell suppression remains elusive and requires further experimental work, e.g., in mice lacking *IDO1* in macrophages.

5.5 IL-4/-13 mediated type 2 immune response impairs PGE₂-driven immune evasion

Multiple studies have shown crucial roles for host-derived IL-4 and IL-13 in AAM-mediated anti-helminth immunity [133,602]. During infection with helminths that trigger a rapid innate type 2 immune response, e.g. the rat parasite *N. brasiliensis*, type 2 activated granulocytes [133,603] and innate lymphoid cells (ILC2s) [602] can drive early AAM activation, thus enabling rapid parasite control. Additionally, challenge infection with *H. polygyrus* triggers a type 2 immune response, which is dependent on T_H2 cells (IL-4 and IL-13), antibodies and Arginase-1 expressing macrophages [157,158]. Thus, it is necessary for the parasite to evade the mechanisms that trigger a rapid and innate host immune response. For instance, AIP-2 from *A. caninum* can suppress OVA- or HDM- induced airway inflammation by inducing regulatory T cells and suppressing T_H2/ILC2 cytokine production by reprogramming CD103⁺ DCs [331]. In keeping with these studies, heGDH is able to suppress SEA-induced IL-4 production in human PBMCs (Figure 15). These immune suppressive functions of heGDH on a helminth induced T_H2 response and its capacity to induce Tregs partially depended on PGE₂ production. PGE₂ can limit ILC2 and mast cell function in an EP2 dependent manner [604,605], but whether PGE₂ directly affects IL-4/IL-13 production remains less understood. In contrast, studies on the effect of IL-4 on PGE₂ secretion revealed that IL-4 can inhibit COX-2 expression and consequently prevents secretion of PGE₂ [606]. This is in line with the effects observed during heGDH treatment of macrophages which were previously treated with IL-4 and IL-13, suggesting that a full developed and IL-4/-13 driven T_H2 response can limit the immunosuppressive capacity of heGDH by restricting the production of PGE₂. This could explain why treatment with heGDH only caused a slight increase in worm burdens during infection with *N. brasiliensis* and challenge infection with *H. polygyrus*. The increased production of PGE₂ in isolated BAL macrophages or peritoneal macrophages from parasite infected mice could however be restored *ex vivo* due to the persistent epigenetic changes in macrophages in the absence of the type 2 cytokine environment. The timing of when PGE₂ upregulation occurs during helminth infection may be a critical factor. If PGE₂ is upregulated first, before IL-4 and IL-13 are produced, this may be sufficient to maintain immune evasion. However, if IL-4 and IL-13 secretion occurs at the same time, they may inhibit PGE₂ production and thus reduce the effect of heGDH-mediated immune evasion.

Additionally, PGE₂ actively participates in tissue repair responses [607,608]. During the early inflammatory phase of tissue repair, PGE₂ produced by macrophages and stromal cells can activate myofibroblasts, promoting wound contraction and wound closure in the skin and intestine [607,609–611]. The positive effects of PGE₂ are mostly dependent on the EP2 and EP4 receptors. In the subsequent proliferative phase, myofibroblasts can produce PGE₂, which induces a regulatory macrophage phenotype expressing high levels of IL-10 and Arg1, both of which have been implicated in preventing tissue damage and regulating pathological tissue remodeling in type 2 immunity [158,612,613]. Due to its regulatory effects on fibroblasts, PGE₂ also functions as an important negative regulator of pulmonary fibrosis and airway remodeling in asthma [614,615], suggesting a potential role for heGDH-induced PGE₂ during helminth-induced tissue damage. In line, *N. brasiliensis* induced tissue damage [616] is significantly improved after heGDH administration. However, it remains to be investigated whether the improvement in wound healing is due to heGDH-triggered PGE₂ production. Nevertheless, taken together, these investigations verify again that PGE₂ is an important factor in the heGDH mediated immune evasion. To strengthen the data and provide a more definitive proof of the role of PGE₂ in immune evasion and repair, a more detailed study assessing the effects of heGDH during the infection with helminths in mice lacking *PTGES* in myeloid cells is required.

5.6 How heGDH modulates the macrophages metabolism

The enzyme glutamate dehydrogenase (GDH) catalyzes the conversion of glutamate to α -ketoglutarate (α -KG) and vice versa, altering macrophage metabolism by affecting the immediate surroundings of the cell or the internal metabolite balance of the macrophage itself. An analysis of glutamine/glutamate consumption in GDH-treated macrophages showed a decrease in educts and an increase in the enzymatic reduced TCA intermediate 2-hydroxyglutarate (2-HG). 2-HG is a chiral molecule that can exist in either the D-enantiomer or the L-enantiomer. Although cancer-associated IDH1/2 mutants produce D-2-HG, biochemical studies have demonstrated that L-2-HG also functions as a potent inhibitor of α -KG-dependent enzymes [248,617]. Under conditions of oxygen limitation, mammalian cells selectively produce L-2-HG via enzymatic reduction of α -KG [618]. Helminthic GDH increased basal glycolysis and reduced OXPHOS in a p300-dependent fashion, thus contributing to 2-HG conversion [619]. In contrast, another helminth-derived product, FhHDM-1 switched macrophage metabolism to a dependence on OXPHOS fueled by fatty acids and supported by the induction of glutaminolysis. The catabolism of glutamine resulted in an accumulation of α -KG [307]. In general, the production of α -KG via

glutaminolysis is important for AAMs, including engagement of FAO and Jmjd3-dependent epigenetic reprogramming of M2 genes. This M2-promoting mechanism is further modulated by a high α -KG/succinate ratio, while a low ratio strengthens the proinflammatory phenotype in classically activated (M1) macrophages [244]. In heGDH-treated macrophages, no upregulation of succinate or α -KG could be measured, indicating a specific immune-regulatory macrophage population, rather than a strict M1 or M2-associated macrophage phenotype. Although α -KG and 2-HG are implicated in epigenetic regulation, e.g. by promoting DNA and histone methylation [244,247,618], metabolic reprogramming does not primarily rely on heGDH's catalytic activity. The potential link between epigenetic regulation and macrophage metabolism is based on the p300-dependent upregulation of *PFKFB3*, a positive regulator of glycolysis [216,620].

The production of eicosanoids can be regulated by several factors, including the availability of TCA cycle intermediates. For instance, citrate export via SLC25A1, the mitochondrial citrate carrier is required for regulating the levels of NO and prostaglandins by the production of acetyl-CoA and the subsequent production of TNF α or INF- γ [621]. Based on our RNA sequencing data, the citrate carrier expression in heGDH treated macrophages is unaltered. However, further investigation is necessary to determine whether citrate, which is significantly increased in heGDH treated macrophages, plays a role in the production of AA-metabolites. Succinate has been shown to activate the transcription factor HIF-1 α , which in turn upregulates PGE₂ and TXB₂ production [241,483,622,623]. Although *HpbE* demonstrates a HIF-1 α mediated upregulation of prostanoids, no significant increase in succinate nor a dependence on HIF-1 α in heGDH-treated macrophages could be observed. More recent studies also showed the involvement of succinate in cysLT regulation. Succinate is associated with increased generation of cysLTs during allergic reactions in mast cells via binding to its receptor [624], whereas in tuft cells, succinate alone is not able to change 5-LOX expression [400]. Further investigations on how downstream metabolites of heGDH affect eicosanoid production revealed that L-2-HG selectively reduced the production of cysLTs by affecting LTC₄S activity. However, the precise mechanism by which L-2-HG attenuates leukotriene synthesis in the intracellular milieu is presently not well understood.

5.7 Transient macrophage reprogramming after mild COVID-19 disease

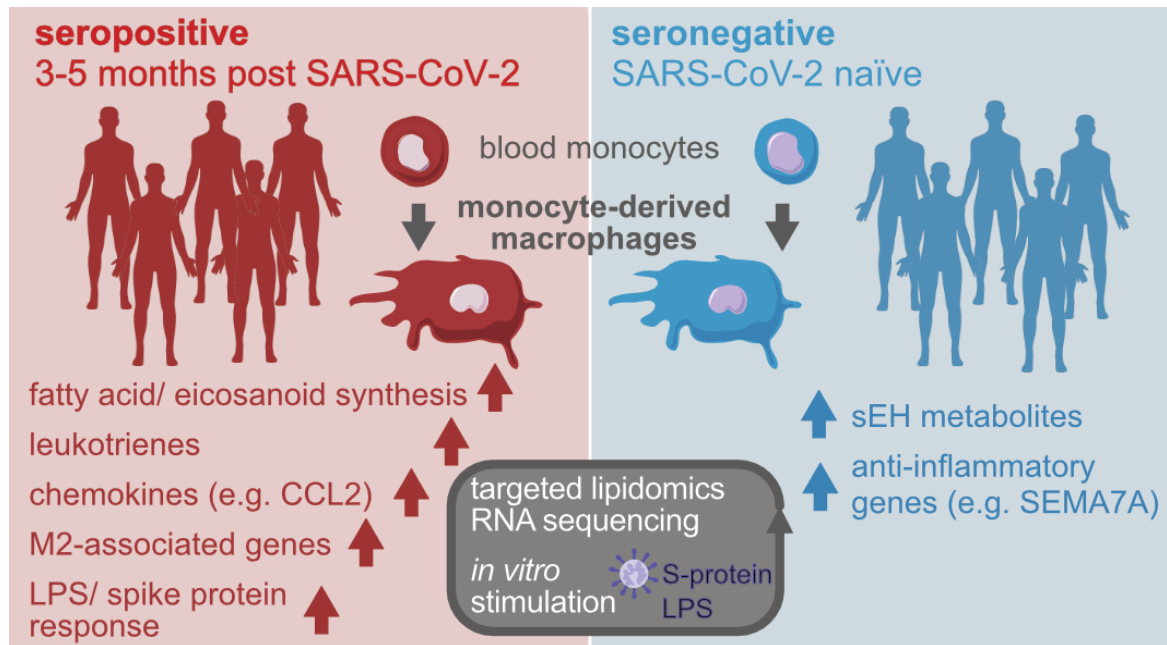


Figure 16: Schematic illustration of reprogrammed monocyte-derived macrophages after previous infection with SARS-CoV-2 from publication II [625].

The primary mode of entry for SARS-CoV-2 is through the recognition of its transmembrane S-glycoprotein by ACE2 and subsequent processing by TMPRSS2. However, MDM from previously infected COVID-19 patients expressed ACE2 and TMPRSS2 at levels that were significantly lower compared to those observed in airway epithelial cells - the primary target cells of SARS-CoV-2. Nonetheless, macrophages have been shown to respond to S-proteins of SARS-CoV-2 through innate sensing mechanisms, such as C-type lectins [56,57], which were found to be upregulated in post-COVID-19 MDMs. Additional evidence shows that macrophages can be further activated by TLRs. Macrophage TLR2 is capable of sensing the envelope (E-) protein of SARS-CoV-2 and initiating inflammatory responses, including the production and release of IFNs and the upregulation of *Nlrp3* and *Il1b* expression in macrophages [59]. In keeping with this study, but in contrast to the E- protein of SARS-CoV-2, S-protein stimulation of MDM previously infected with SARS-CoV-2 increased IL-1 β secretion. This can underlie a reprogrammed and persistent inflammasome activation [626]. However, whether C-type lectins or TLR2 are the main entry route used by SARS-CoV-2 or whether S-protein stimulation of previously infected MDM can increase IL-1 β in a TLR2 dependent manner remains elusive. A detailed characterization of SARS-CoV-2 infection routes by stimulating macrophages with S- or E- proteins of SARS-CoV-2, while lacking different PRRs would provide further insights.

Severe SARS-CoV-2 infections are known to cause hyper-inflammation in the lungs, primarily due to the action of monocyte-derived cells [627]. This hyper-inflammation is characterized by an overproduction of chemokines and cytokines, commonly known as the “cytokine storm” [50]. In our study, cytokine production was found to be similar in seronegative and seropositive MDM at 3-5 months after infection with SARS-CoV-2, potentially due to mild disease course or the time period between infection and analysis of cytokines/chemokines secreted by MDM from previously infected patients. However, apart from an aberrant cytokine and chemokine production, severely ill infected COVID-19 patients exhibit a dysregulated arachidonic acid metabolism [474]. In keeping with this study, distinct eicosanoid formation patterns were observed in MDM from patients with mild COVID-19, 3-5 months post infection, with an increased production of leukotrienes, predominantly LTB₄ and an increased production of prostanoid metabolites (12-HHTrE) (Figure 16). As LTB₄ is essential for resistance against respiratory viruses and participates in the production of interferons [468,469], this could be considered as a marker for an efficient anti-viral immune response in mildly infected COVID-19 patients. The increased production of LTB₄ by macrophages following SARS-CoV-2 infection could potentially result in a decreased susceptibility to subsequent infections with for instance IAV [470]. However, previous viral infections may also cause immune paralysis, leading to reduced macrophage phagocytic capacity [628,629]. Even if being produced at lower concentrations as compared to LTB₄ also cysLTs, including LTC₄ and LTD₄ were produced in larger amounts by MDM from seropositive COVID-19 patients, which may be important as cysLTs in contrast to LTB₄ often worsen lung pathology [474,475,630]. Nevertheless, COVID-19 patients displayed an increased production of lipid mediators several months after the infection. This suggests that SARS-CoV-2 infection could induce a form of innate immune training within the monocyte compartment. However, this effect was transient as eicosanoid levels returned to baseline 12 months after SARS-CoV-2 infection. Similarly, previous exposure to viruses such as influenza can also trigger macrophage training resulting in either an enhanced or a tolerized response. For instance, influenza virus infection can result in increased numbers of alveolar macrophages that provide protection against subsequent *S. pneumoniae* infection [631]. However, previous influenza infection could also be detrimental to subsequent bacterial infections [628]. The timing between viral and bacterial infections influences the severity of co-infection, and studies have shown differing results depending on whether bacterial infections occurred during acute viral infection or after complete resolution of infection. In our study, provocation of MDM from seropositive or seronegative patients with LPS or S-protein resulted in an exaggerated chemokine-, IFN- and prostanoid response with the concomitant reduced ability to stimulate T cell responses

or promote resolution of inflammation (Figure 16). These findings align with previous studies that found monocyte dysfunction and a pro-inflammatory profile for up to 12 weeks after SARS-CoV-2 infection [632,633], suggesting that a trained pro-inflammatory macrophage state persists long-term even after mild disease. However, how this training effect of SARS-CoV-2 on monocytes is mechanistically imprinted (e.g., via epigenetic reprogramming) remains elusive. Additionally, other SARS-CoV-2 variants that can impact monocyte-macrophage reprogramming as a long-term consequence of mild SARS-CoV-2 infection have not been covered in this publication. Therefore, further research on these aspects is needed to gain a better understanding of long-lasting cytokine/chemokine and eicosanoid abnormalities and their role in the disease, which may provide additional therapeutic options to prevent long-COVID.

5.8 Clinical implication for the treatment of acute or long COVID-19

Despite several approved vaccines, no specific treatment for acute SARS-CoV-2 infection or long-COVID-19 is currently available. Conflicting efficacy has been reported for common therapies such as viral RNA polymerase inhibitors and no long-term consequences of these treatments have been studied so far [634–636]. As discussed above, severe clinical outcomes are characterized by a sustained release of pro-inflammatory cytokines [51]. Anti-inflammatory corticosteroids such as dexamethasone have been effective in some studies, but may have negative consequences due to their immunosuppressive action in later phases of SARS-CoV-2 infection [635,637,638]. Furthermore, severely ill patients exhibit an altered eicosanoid metabolism with increased pro-inflammatory lipid mediators and pro-thrombotic metabolites [445,474]. Glucocorticoid treatment of MDM from post COVID-19 patients reduced pro-inflammatory cytokines, and pro-thrombotic metabolites like TXB₂, but further exaggerated leukotriene production. Furthermore, fluticasone propionate treatment reduced the formation of 12-HHTrE, implicated in wound healing [592] in MDM from convalescent COVID-19 patients. Thus, even after resolution of mild infection, application of glucocorticoids can have adverse effects with the possibility to aggravate lung pathology by increasing LTs [639]. In contrast, severely ill COVID-19 patients which received a leukotriene receptor antagonist showed lower risk of their condition worsening [475]. Thus, co-administration of a cysLTs receptor antagonist represents a further option to improve disease severity and may be recommended to alleviate long-term effects of SARS-CoV-2 infection [640,641].

Next to 5-LOX metabolites, the formation of SPMs in COVID-19 patients was found to be increased [642,643], and administering resolvins could improve thrombosis, which is a co-occurring pathology in SARS-CoV-2 infections [644]. Although it remains to be investigated how SPMs interact with pro-inflammatory lipid mediators and whether their levels are related to disease severity, reduced SPM formation is associated with obesity, a risk factor for severe COVID-19. This could partially explain the heightened susceptibility to COVID-19 in obese individuals [645]. Therefore, it has been suggested that a dietary intervention leading to increased plasma SPM concentration, such as fish oil supplementation, could be a potential additive therapy [646]. Several studies supplementing omega-3 fatty acids or fish oil are currently underway, and preliminary data suggest a lower death rate [476]. In general, the eicosanoid metabolism likely plays a critical role in COVID-19 pathology and should be evaluated in patient treatment.

However, the absence of a specific clinical diagnosis for long COVID made it challenging to establish good treatment options. Also, we could not establish a direct positive correlation between increased MDM leukotriene production and long-term symptoms. Indeed, surprisingly seropositive patients with a high production of 5-LOX metabolites showed less acute symptoms and a faster decline in SARS-CoV-2 serum IgG titers, suggestive of particularly mild disease. A further limitation of the study is that only mild COVID-19 cases that had resolved mostly at 12 months post-infection were investigated. Consequently, it is essential to conduct further studies on eicosanoid reprogramming in a cohort with well-defined long COVID symptoms. Such investigations would be crucial in determining the possible pathological significance of the observed inflammatory macrophage memory and provide a platform for developing additional therapeutic options for long-COVID.

5.9 Glycosylation deficiency and its impact on biogenesis and signaling of IL-12 family cytokines

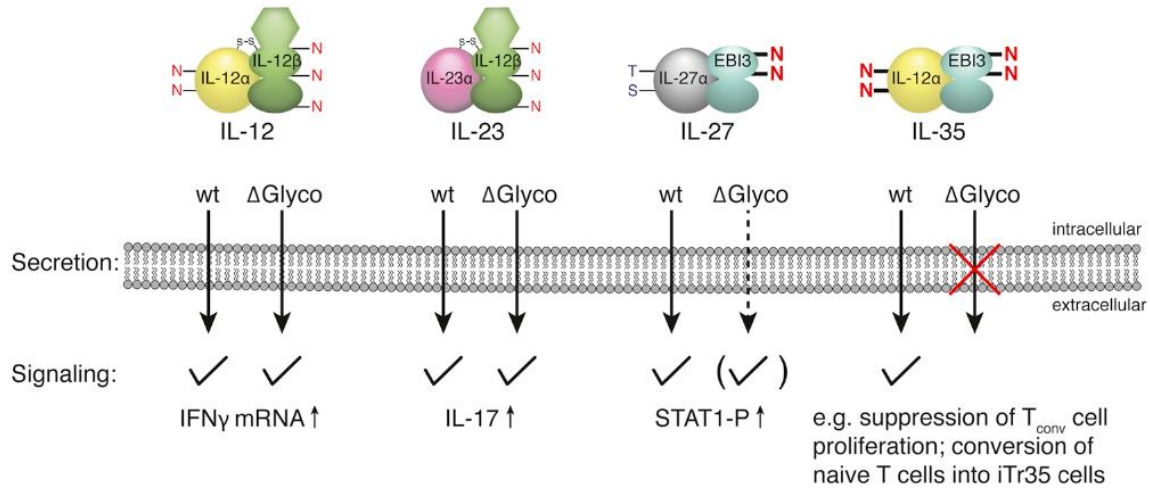


Figure 17: Schematic illustration of the impact of glycosylation on the human IL-12 family from publication III.

Despite N-linked glycosylation being a prevalent modification in the ER [647], previous studies have provided incomplete descriptions of glycosylation in IL-12 family cytokines [648–651]. Enzymatic treatment and mutagenesis-based analyses performed in the frame of this thesis identified new glycosylation sites within IL-12 family members (Figure 17). Interestingly, the impact of glycosylation on the biogenesis and signaling of the investigated cytokines was diverse, ranging from no effect for IL-12 and IL-23 to diminished secretion/function for IL-27 and complete cellular retention in the case of IL-35 (Figure 17). The lack of glycosylation impaired β -subunit secretion, such as with EBI3 that negatively affected secretion of IL-27 or abrogated secretion for IL-35. These findings suggest that the assembly-dependent folding and secretion of human α -subunits [534,546] plays a crucial role in these processes.

Despite its lack of N-glycans, IL-27 heterodimer can be secreted. Unglycosylated EBI3 is not able to pass ERQC, but when co-expressed with non-glycosylated IL-27 α , which relies on EBI3 for secretion, heterodimer secretion occurred. This underlies subunit interaction and mutually enhanced secretion, which is also described in an inter-species analysis where the pairing of two secretion-incompetent IL-27 subunits from different species resulted in induced secretion [652]. The IL-27 subunits appear to be (partially) folded even in the absence of glycosylation, exposing certain features that prevent them from passing ERQC. Over the four human IL-12 family cytokines investigated, IL-35 was found to rely the most on glycosylation for secretion. Thus, this might explain previous failures to reconstitute

IL-35 using a recombinant non-glycosylated IL-12 α subunit purified from bacteria [651]. In contrast to EBI3, non-glycosylated IL-12 β behaved similarly to its wild-type counterpart and still formed IL-12 and IL-23. Heterodimers containing IL-12 β are generally less affected by their extent of glycosylation than those containing EBI3, likely due to the presence of intermolecular disulfide bridges, which facilitate heterodimer secretion even without other stabilizing factors such as sugar moieties [529,653]. IL-12 and IL-23 retained their functionality with respect to IFN- γ or IL-17 induction in human lymphocytes, respectively, and exhibited receptor activation capabilities in reporter cell lines. However, impaired functionality for IL-27 when its β -subunit lacked N-glycosylation could be explained by its N-glycosylation site Asn105 which faces towards the N-terminal domain of gp130 [654], suggesting a supportive role of Asn105-linked glycosylation in EBI3 for proper signaling via its receptor.

5.10 Sugar moieties as important modifications for therapy and disease

IL-12 family cytokines are promising targets for therapeutics and biopharmaceuticals. However, glycosylation patterns can influence protein characteristics such as solubility, stability, and biodistribution. Although functionality was observed for non-glycosylated IL-12 family cytokines, their biological activity may vary depending on their glycosylation patterns. Thus, it is necessary to probe the role of N-glycans, as for instance, disease occurrence/progression can correlate with the production of differentially glycosylated cytokine species [565]. In contrast, modifying glycosylation patterns could open new opportunities for rationally modifying IL-12 family cytokine functionality with for instance extension of the proteins' half-life, differing receptor engagement or the targeted distribution within the tissue [561,562,568].

Interestingly, deleting glycosylation sites of EBI3 abolishes IL-35 formation but is compatible with the formation of functional IL-12 and IL-27, which share one subunit with IL-35. This finding is particularly relevant since a simple knockout of a single IL-12 family subunit generally affects more than one heterodimeric family member due to chain sharing promiscuity within the family. Therefore, mutating glycosylation sites may be a viable way to selectively delete IL-35 from an organism's cytokine repertoire, which could be of interest in immunosuppressive conditions, such as cancer forms that are difficult to treat [655,656]. Thus, targeting interleukin subunit glycosylation may represent a promising strategy for future immunotherapies [657].

6 Future perspectives

The identification of heGDH's immune evasion mechanism opens up new alleys of immunomodulatory therapy against airway inflammation or infectious diseases. Thus, heGDH could become a first-in-class immunomodulator, but further research on the protein's stability, toxicity and pharmacokinetics is necessary to bring this molecule into clinical testing. Additionally, the effect of GDH-mediated immunomodulation on immune responses towards infectious diseases needs to be characterized, especially if prolonged efficacy (by epigenetically reprogrammed macrophages) is present. Based on current literature, *H. polygyrus* has been shown to induce the upregulation of type I interferons (IFNs) within the lungs, which in turn protects the host against viral infections [372]. Furthermore, the analysis of heGDH gene expression has revealed a marked increase in the production of type I IFNs, which suggests a potential novel mechanism by which enteric helminth-derived molecules may confer resistance against respiratory viral infections. Type I IFNs have broad immune regulatory and -stimulatory functions that are only partially characterized in the context of type 2 immune responses [372,375]. The interferon- α/β receptor (IFNAR) is widely expressed on hematopoietic and non-hematopoietic cells and represents the prime receptor of type I IFNs. As heGDH induces multiple downstream targets of IFNAR signaling in human MDM one hypothesis would be that IFNAR mediates major immune regulatory effects of heGDH in type 2 immune settings. In addition, the administration of helminth-derived molecules, including heGDH, could bring significant benefits for the management of infectious diseases, including acute SARS-CoV-2 infection or long COVID-19, owing to their ability to promote the upregulation of type I IFNs and ameliorate the detrimental effects of leukotrienes uncovered in publication I and II. Understanding programs that determine and regulate macrophage eicosanoid profiles are powerful options to influence type 2 inflammation such as asthma and allergies, but also infectious diseases with aberrant eicosanoid production [474]. In particular, heGDH induces the arachidonic acid metabolite PGE₂, which enables an immunosuppressive environment for tissue repair and host immune evasion, e.g. by modulating IFN responses, thereby suppressing protective immunity against influenza infection [436,658]. Additionally, PGE₂ can regulate T_H1 and T_H17 responses by inhibiting IL-12 and IL-23 production in monocytes and macrophages, while inducing regulatory T cells and IL-10 production [484,596,597]. Interestingly, IFNAR signaling has analogous effects on IL-12, IL-23 and IL-10 production in DCs [659], suggesting that it may control maladaptive T_H1 and T_H17 responses during helminth infection.

Signaling by viral nucleic acids and subsequently by type I IFN is central to antiviral innate immunity. These signaling events are also likely to engage metabolic changes in immune and nonimmune cells to support antiviral defense. Thus, elevated IFN signaling is linked to the upregulation of glycolysis activator genes, including *PFKFB3*, which stimulates viral phagocytosis and confers protection against respiratory viral infections [216]. The upregulation of *PFKFB3* by heGDH is associated with a heightened glycolytic activity. As a result, the augmented production of IFNs in macrophages treated with heGDH may also enhance the p300-dependent *PFKFB3* expression, which in turn could potentially provide protection against viral infections. An additional aspect that has been considered is the modulation of adaptive immunity by helminths. While it has been demonstrated that helminths can reduce the severity of disease during SARS-CoV-2 infection by promoting macrophage-mediated anti-viral CD8⁺ T-cell responses [384], the CD8⁺ T-cell-mediated immune response to West Nile Virus (WNV) is suppressed by *Hpb* infection [660]. Therefore, it remains to be elucidated whether the administration of heGDH -maybe also via the production of IL-12 family cytokines- could have an impact on anti-viral T cell responses.

The interleukin-12 family functions on both sides of the immunological equilibrium, encompassing both pro- and anti-inflammatory roles. As we have observed a pronounced induction of secretion-competent β -subunits (IL-12 β and EBI3) by heGDH, it remains further to be investigated whether IL-12 family cytokines contribute to immune regulatory effects of heGDH. Indeed, IL-12 acts as a negative regulator of type 2 immune responses in allergic asthma [661,662] and helminth infection [663], while it promotes T_H1 immunity and IFN γ production particularly during chronic infection with intracellular pathogens [664,665]. Similarly, IL-35 and IL-27 antagonize type 2 immune responses and EBI3^{-/-} mice develop enhanced allergic airway inflammation [666,667], while both IL-12 β and EBI3 have been implicated in anti-viral immunity and the regulation of immunopathology in IAV infection [456,668,669]. Thus, IL12 β and EBI3 could mediate a heGDH-driven shift from type 2 to type 1 immunity with relevance to host defense and vaccine responses to e.g. respiratory infections.

Taken together, targeting the intricate crosstalk between type I IFNs (viral infections), eicosanoids and IL-12 family cytokines offers multifaceted opportunities for helminths to regulate host immunity in different settings of infection and inflammation.

7 Acknowledgements

Als aller Erstes möchte ich mich ganz herzlich bei meiner Betreuerin **Julia Esser-von Bieren** bedanken: Danke Julia, für deine exzellente fachliche Führung meines liebenden Promotionsprojekts (Go: Hpb!). Deine Motivation, Dein Input, Dein beeindruckendes Wissen und Deine Führung haben mich immer geleitet und unterstützt. Ich danke dir außerdem für das Entfalten meiner Unabhängigkeit. Der Freiraum, den du mir geboten hast, ist einfach unschlagbar. Des Weiteren danke ich dir für deine wertschätzende Art, durch welche ich nie die Motivation verloren habe. Durch meinen, aber auch Deinen Anspruch konnte ich über mich und meine Grenzen hinauswachsen. Das macht unglaublich viel aus und ich bin sehr froh, dass ich in Deiner Arbeitsgruppe promovieren durfte.

Ebenso möchte ich meinem offiziellen Doktorvater **Matthias Feige** danken. Zuerst einmal vielen Dank für die Möglichkeit der Masterarbeit und die Vermittlung meiner Promotionsstelle. Durch dich habe ich mich auch immer als Teil nicht nur einer Gruppe, sondern auch deiner Gruppe gesehen. Die vielen Kollaborationsprojekte, die ich in den letzten vier ein halb Jahren zusammen mit deiner Gruppe erarbeiten konnten, haben mich so viel Neues lernen lassen. Dein Anspruch hat mir ermöglicht über mich hinauszuwachsen. Ebenso haben deine kreativen Ideen zu meinem Promotionsprojekt es dazu gemacht was es heute ist! Daher vielen, vielen Dank an dich Matthias!

Ebenso ist es mir wichtig allen **kollaborierenden KollegInnen** zu danken, ohne welche die in dieser Dissertation veröffentlichten Publikationen nicht möglich gewesen wären. Ein besonderer Dank geht auch an meine Studentinnen **Emily Hensch**, **Lara Paulini** und **Sandra Riemer**, welche ich betreuen durfte und welche mich bei meinen Experimenten immer so tatkräftig unterstützt haben. Ein besonderer Dank geht auch an **Karen Hildenbrand** aus dem CPB Lab für die coole Zusammenarbeit am IL-35 und Glycoprojekt (hier auch ein großes Danke an **Isabel Aschenbrenner**). Mit dir kann ich einfach so viel lachen, lernen und mich über Dinge rund um Arbeit oder das Leben austauschen.

Des Weiteren danke ich dem ganzen ZAUM, und dem IAF für tolle Ideen während den „Progress Reports“, zahlreichen Blutspenden oder aber auch dem ein oder anderen Event, wie dem Brunchen oder dem Krapfen essen. Ein besonderer Dank gilt **Francesca Alessandrini**, **Johanna Grosch** und **Benjamin Schnautz** für das Helfen bei den Mausexperimente. Ohne euch hätte ich das nicht geschafft!

Als Nächstes möchte ich dem gesamten **EvB lab** *Danke* sagen!

Zuerst ein großes Dankeschön an **Fiona Henkel**. Es war mir wirklich ein innerliches Blumenpflücken mit dir zusammen zu arbeiten. Ich bin dir so dankbar, dass du mich vor allem am Anfang mit vielem im Labor vertraut gemacht hast, dich mit mir zusammen „unlösbaren“ Rechenaufgaben sowie ersten Parasiteninfektionen gestellt und Nächte der Mausexperimente durchstanden hast! Danke auch, dass du mich immer weitergebracht hast und für alle Diskussionen offen warst. Ich vermisse die Zeit mit dir.

Das nächste riesen Dankeschön widme ich **Franziska Hartung**. Ich bin sehr froh, dass du dich für unsere Gruppen entschieden hast, denn sonst hätte ich einen so großartigen, netten und hilfsbereiten Menschen wie dich nie kennen lernen dürfen. Ich danke dir vielmals für deine Unterstützung und Hilfe bei all meinen Projekten. Natürlich vor allem die Mausexperimente ;-). Ohne dich wäre ich nicht so weit gekommen! Ebenso Danke für die Konferenzen, Partynächte, Abendessen, Skitage und viel, viel mehr mit dir! Du hast die Zeit meines PhDs unvergesslich gemacht.

Vielen Dank auch an **Antonie Lechner**, **Sonja Schindela** und **Pascal Haimerl** für die tolle Aufnahme in die EvB Group, die Einführung ins Lab und die Liebe zu Parasiten und Allergien! Für die Unterstützung und technische Hilfe bei Experimenten, tollen Diskussionen während Mittagessen, unvergesslichen Dinner Partys bei Pascal zu Hause oder Gruppen Retreats. Ebenso ein Danke an unsere neuen Familienmitglieder **Benedikt Spitzlberger**, **Eya Ben Salah** und **Mirjana Drinic** für neuen Input und beim Sammeln vieler toller Momente auf dem Oktoberfest oder auf unsere Reise nach Stockholm!

Die Arbeit mit der gesamten EvB Gruppe hat mir einfach eine Menge Spaß bereitet. Ihr habt mir emotionalen Halt gegeben und ich konnte wunderbar mit Euch lachen. Daher würde ich die Reise meines PhDs mit keiner anderen Gruppe durchleben wollen. Ohne Euch hätte ich das nicht geschafft, deswegen *Danke!*

Zuletzt möchte ich mich bei meiner Familie bedanken. Vielen Dank **Mama** und **Papa** für die Unterstützung während meiner gesamten beruflichen Karriere, der fortlaufenden Bestärkung in meinem Weg und der Motivation bei vielen „Ups and Downs“. Tausend Dank! Mama, des Weiteren danke ich dir für die unzählbare Telefonate und das du immer an mich geglaubt hast. Du bist meine wahre „*Gia dinh*“. Ebenso vielen Dank an meinen Bruder **Dennis Stezelow + Familie** für die Entscheidung ich solle mein Studium an der TUM absolvieren und für die Unterstützung bei allen wichtigen Entscheidungen.

Das Beste kommt zum Schluss. Der größte Dank geht an meinen Ehemann, **Mario Bohnacker**, welchem ich auch diese Dissertation widme. Danke für das Teilen deines Lebens mit mir. Ich könnte mir niemand besseren an meiner Seite vorstellen. Deine unerlässliche Unterstützung beeindruckt mich jeden Tag aufs Neue. Ich danke dir, dass du sprichwörtlich mein Fels in der Brandung bist. Mich bei allen stressigen Momenten, den Höhen und Tiefen unterstützt und an mich glaubst. Danke fürs Zuhören, bei jeder einzelnen Präsentation, dem Korrekturlesen aller meiner Abschlussarbeiten und einfach für alles was du mir gibst. Danke das du in dieser Reise an meiner Seite warst und auf das noch viele weitere tolle und spannende Reisen kommen mögen! Du bist der *Beste*!

8 Bibliography

- [1] World Health Organization. The top 10 causes of death n.d. <https://www.who.int/news-room/fact-sheets/detail/the-top-10-causes-of-death>.
- [2] Alexopoulou L, Holt AC, Medzhitov R, Flavell RA. Recognition of double-stranded RNA and activation of NF- κ B by Toll-like receptor 3. *Nature* 2001;413:732–8. <https://doi.org/10.1038/35099560>.
- [3] Lund JM, Alexopoulou L, Sato A, Karow M, Adams NC, Gale NW, et al. Recognition of single-stranded RNA viruses by Toll-like receptor 7. *Proc Natl Acad Sci USA* 2004;101:5598–603. <https://doi.org/10.1073/pnas.0400937101>.
- [4] Bender AT, Tzvetkov E, Pereira A, Wu Y, Kasar S, Przetak MM, et al. TLR7 and TLR8 Differentially Activate the IRF and NF- κ B Pathways in Specific Cell Types to Promote Inflammation. *ImmunoHorizons* 2020;4:93–107. <https://doi.org/10.4049/immunohorizons.2000002>.
- [5] Pluta L, Yousefi B, Damania B, Khan AA. Endosomal TLR-8 Senses microRNA-1294 Resulting in the Production of NF κ B Dependent Cytokines. *Front Immunol* 2019;10:2860. <https://doi.org/10.3389/fimmu.2019.02860>.
- [6] Wang JP, Bowen GN, Padden C, Cerny A, Finberg RW, Newburger PE, et al. Toll-like receptor-mediated activation of neutrophils by influenza A virus. *Blood* 2008;112:2028–34. <https://doi.org/10.1182/blood-2008-01-132860>.
- [7] Hochrein H, Schlatter B, O’Keeffe M, Wagner C, Schmitz F, Schiemann M, et al. Herpes simplex virus type-1 induces IFN- α production via Toll-like receptor 9-dependent and -independent pathways. *Proc Natl Acad Sci USA* 2004;101:11416–21. <https://doi.org/10.1073/pnas.0403555101>.
- [8] Lund J, Sato A, Akira S, Medzhitov R, Iwasaki A. Toll-like Receptor 9-mediated Recognition of Herpes Simplex Virus-2 by Plasmacytoid Dendritic Cells. *Journal of Experimental Medicine* 2003;198:513–20. <https://doi.org/10.1084/jem.20030162>.
- [9] Szomolanyi-Tsuda E, Liang X, Welsh RM, Kurt-Jones EA, Finberg RW. Role for TLR2 in NK Cell-Mediated Control of Murine Cytomegalovirus In Vivo. *J Virol* 2006;80:4286–91. <https://doi.org/10.1128/JVI.80.9.4286-4291.2006>.
- [10] Barbalat R, Lau L, Locksley RM, Barton GM. Toll-like receptor 2 on inflammatory monocytes induces type I interferon in response to viral but not bacterial ligands. *Nat Immunol* 2009;10:1200–7. <https://doi.org/10.1038/ni.1792>.
- [11] Modhiran N, Watterson D, Muller DA, Panetta AK, Sester DP, Liu L, et al. Dengue virus NS1 protein activates cells via Toll-like receptor 4 and disrupts endothelial cell monolayer integrity. *Sci Transl Med* 2015;7:304ra142. <https://doi.org/10.1126/scitranslmed.aaa3863>.
- [12] Olejnik J, Forero A, Deflubé LR, Hume AJ, Manhart WA, Nishida A, et al. Ebolaviruses Associated with Differential Pathogenicity Induce Distinct Host Responses in Human Macrophages. *J Virol* 2017;91:e00179-17. <https://doi.org/10.1128/JVI.00179-17>.

- [13] Hornung V, Ellegast J, Kim S, Brzózka K, Jung A, Kato H, et al. 5'-Triphosphate RNA Is the Ligand for RIG-I. *Science* 2006;314:994–7. <https://doi.org/10.1126/science.1132505>.
- [14] Pichlmair A, Schulz O, Tan CP, Näslund TI, Liljeström P, Weber F, et al. RIG-I-Mediated Antiviral Responses to Single-Stranded RNA Bearing 5'-Phosphates. *Science* 2006;314:997–1001. <https://doi.org/10.1126/science.1132998>.
- [15] Kato H, Takeuchi O, Sato S, Yoneyama M, Yamamoto M, Matsui K, et al. Differential roles of MDA5 and RIG-I helicases in the recognition of RNA viruses. *Nature* 2006;441:101–5. <https://doi.org/10.1038/nature04734>.
- [16] Gitlin L, Barchet W, Gilfillan S, Cella M, Beutler B, Flavell RA, et al. Essential role of mda-5 in type I IFN responses to polyriboinosinic:polyribocytidylic acid and encephalomyocarditis picornavirus. *Proc Natl Acad Sci USA* 2006;103:8459–64. <https://doi.org/10.1073/pnas.0603082103>.
- [17] Satoh T, Kato H, Kumagai Y, Yoneyama M, Sato S, Matsushita K, et al. LGP2 is a positive regulator of RIG-I- and MDA5-mediated antiviral responses. *Proc Natl Acad Sci USA* 2010;107:1512–7. <https://doi.org/10.1073/pnas.0912986107>.
- [18] Bermejo-Jambrina M, Eder J, Helgers LC, Hertoghs N, Nijmeijer BM, Stunnenberg M, et al. C-Type Lectin Receptors in Antiviral Immunity and Viral Escape. *Front Immunol* 2018;9:590. <https://doi.org/10.3389/fimmu.2018.00590>.
- [19] Miller JL, deWet BJM, Martinez-Pomares L, Radcliffe CM, Dwek RA, Rudd PM, et al. The Mannose Receptor Mediates Dengue Virus Infection of Macrophages. *PLoS Pathog* 2008;4:e17. <https://doi.org/10.1371/journal.ppat.0040017>.
- [20] Lin G, Simmons G, Pöhlmann S, Baribaud F, Ni H, Leslie GJ, et al. Differential N-Linked Glycosylation of Human Immunodeficiency Virus and Ebola Virus Envelope Glycoproteins Modulates Interactions with DC-SIGN and DC-SIGNR. *J Virol* 2003;77:1337–46. <https://doi.org/10.1128/JVI.77.2.1337-1346.2003>.
- [21] Marzi A, Gramberg T, Simmons G, Möller P, Rennekamp AJ, Krumbiegel M, et al. DC-SIGN and DC-SIGNR Interact with the Glycoprotein of Marburg Virus and the S Protein of Severe Acute Respiratory Syndrome Coronavirus. *J Virol* 2004;78:12090–5. <https://doi.org/10.1128/JVI.78.21.12090-12095.2004>.
- [22] Franchi L, Eigenbrod T, Muñoz-Planillo R, Ozkurede U, Kim Y-G, Chakrabarti A, et al. Cytosolic Double-Stranded RNA Activates the NLRP3 Inflammasome via MAVS-Induced Membrane Permeabilization and K⁺ Efflux. *The Journal of Immunology* 2014;193:4214–22. <https://doi.org/10.4049/jimmunol.1400582>.
- [23] Sabbah A, Chang TH, Harnack R, Frohlich V, Tominaga K, Dube PH, et al. Activation of innate immune antiviral responses by Nod2. *Nat Immunol* 2009;10:1073–80. <https://doi.org/10.1038/ni.1782>.
- [24] Rathinam VAK, Jiang Z, Waggoner SN, Sharma S, Cole LE, Waggoner L, et al. The AIM2 inflammasome is essential for host defense against cytosolic bacteria and DNA viruses. *Nat Immunol* 2010;11:395–402. <https://doi.org/10.1038/ni.1864>.

- [25] Jiang Z, Wei F, Zhang Y, Wang T, Gao W, Yu S, et al. IFI16 directly senses viral RNA and enhances RIG-I transcription and activation to restrict influenza virus infection. *Nat Microbiol* 2021;6:932–45. <https://doi.org/10.1038/s41564-021-00907-x>.
- [26] Orzalli MH, Conwell SE, Berrios C, DeCaprio JA, Knipe DM. Nuclear interferon-inducible protein 16 promotes silencing of herpesviral and transfected DNA. *Proc Natl Acad Sci U S A* 2013;110:E4492-4501. <https://doi.org/10.1073/pnas.1316194110>.
- [27] Kerur N, Veettil MV, Sharma-Walia N, Bottero V, Sadagopan S, Otageri P, et al. IFI16 Acts as a Nuclear Pathogen Sensor to Induce the Inflammasome in Response to Kaposi Sarcoma-Associated Herpesvirus Infection. *Cell Host & Microbe* 2011;9:363–75. <https://doi.org/10.1016/j.chom.2011.04.008>.
- [28] Unterholzner L, Keating SE, Baran M, Horan KA, Jensen SB, Sharma S, et al. IFI16 is an innate immune sensor for intracellular DNA. *Nat Immunol* 2010;11:997–1004. <https://doi.org/10.1038/ni.1932>.
- [29] Wu J, Sun L, Chen X, Du F, Shi H, Chen C, et al. Cyclic GMP-AMP Is an Endogenous Second Messenger in Innate Immune Signaling by Cytosolic DNA. *Science* 2013;339:826–30. <https://doi.org/10.1126/science.1229963>.
- [30] Samuel CE. Antiviral Actions of Interferons. *Clin Microbiol Rev* 2001;14:778–809. <https://doi.org/10.1128/CMR.14.4.778-809.2001>.
- [31] Fensterl V, Sen GC. Interferons and viral infections. *BioFactors* 2009;35:14–20. <https://doi.org/10.1002/biof.6>.
- [32] Plataniias LC. Mechanisms of type-I- and type-II-interferon-mediated signalling. *Nat Rev Immunol* 2005;5:375–86. <https://doi.org/10.1038/nri1604>.
- [33] Schindler C, Shuai K, Prezioso VR, Darnell JE. Interferon-Dependent Tyrosine Phosphorylation of a Latent Cytoplasmic Transcription Factor. *Science* 1992;257:809–13. <https://doi.org/10.1126/science.1496401>.
- [34] Crouse J, Kalinke U, Oxenius A. Regulation of antiviral T cell responses by type I interferons. *Nat Rev Immunol* 2015;15:231–42. <https://doi.org/10.1038/nri3806>.
- [35] Banchereau J, Steinman RM. Dendritic cells and the control of immunity. *Nature* 1998;392:245–52. <https://doi.org/10.1038/32588>.
- [36] Chan CW, Crafton E, Fan H-N, Flook J, Yoshimura K, Skarica M, et al. Interferon-producing killer dendritic cells provide a link between innate and adaptive immunity. *Nat Med* 2006;12:207–13. <https://doi.org/10.1038/nm1352>.
- [37] Doyle C, Strominger JL. Interaction between CD4 and class II MHC molecules mediates cell adhesion. *Nature* 1987;330:256–9. <https://doi.org/10.1038/330256a0>.
- [38] König R, Huang L-Y, Germain RN. MHC class II interaction with CD4 mediated by a region analogous to the MHC class I binding site for CD8. *Nature* 1992;356:796–8. <https://doi.org/10.1038/356796a0>.
- [39] Mosmann TR, Cherwinski H, Bond MW, Giedlin MA, Coffman RL. Two types of murine helper T cell clone. I. Definition according to profiles of lymphokine activities and secreted proteins. *J Immunol* 1986;136:2348–57.

- [40] Harrington LE, Hatton RD, Mangan PR, Turner H, Murphy TL, Murphy KM, et al. Interleukin 17–producing CD4+ effector T cells develop via a lineage distinct from the T helper type 1 and 2 lineages. *Nat Immunol* 2005;6:1123–32. <https://doi.org/10.1038/ni1254>.
- [41] Usui T, Preiss JC, Kanno Y, Yao ZJ, Bream JH, O’Shea JJ, et al. T-bet regulates Th1 responses through essential effects on GATA-3 function rather than on IFNG gene acetylation and transcription. *Journal of Experimental Medicine* 2006;203:755–66. <https://doi.org/10.1084/jem.20052165>.
- [42] Thieu VT, Yu Q, Chang H-C, Yeh N, Nguyen ET, Sehra S, et al. Signal Transducer and Activator of Transcription 4 Is Required for the Transcription Factor T-bet to Promote T Helper 1 Cell-Fate Determination. *Immunity* 2008;29:679–90. <https://doi.org/10.1016/j.immuni.2008.08.017>.
- [43] Romagnani S. Type 1 T helper and type 2 T helper cells: Functions, regulation and role in protection and disease. *Int J Clin Lab Res* 1992;21:152–8. <https://doi.org/10.1007/BF02591635>.
- [44] Sun JC, Lanier LL. NK cell development, homeostasis and function: parallels with CD8+ T cells. *Nat Rev Immunol* 2011;11:645–57. <https://doi.org/10.1038/nri3044>.
- [45] Jonjić S, Babić M, Polić B, Krmpotić A. Immune evasion of natural killer cells by viruses. *Current Opinion in Immunology* 2008;20:30–8. <https://doi.org/10.1016/j.coi.2007.11.002>.
- [46] Veiga-Parga T, Sehrawat S, Rouse BT. Role of regulatory T cells during virus infection. *Immunol Rev* 2013;255:182–96. <https://doi.org/10.1111/imr.12085>.
- [47] Lam JH, Smith FL, Baumgarth N. B Cell Activation and Response Regulation During Viral Infections. *Viral Immunology* 2020;33:294–306. <https://doi.org/10.1089/vim.2019.0207>.
- [48] Crotty S. A brief history of T cell help to B cells. *Nat Rev Immunol* 2015;15:185–9. <https://doi.org/10.1038/nri3803>.
- [49] Zhou P, Yang X-L, Wang X-G, Hu B, Zhang L, Zhang W, et al. A pneumonia outbreak associated with a new coronavirus of probable bat origin. *Nature* 2020;579:270–3. <https://doi.org/10.1038/s41586-020-2012-7>.
- [50] Huang C, Wang Y, Li X, Ren L, Zhao J, Hu Y, et al. Clinical features of patients infected with 2019 novel coronavirus in Wuhan, China. *The Lancet* 2020;395:497–506. [https://doi.org/10.1016/S0140-6736\(20\)30183-5](https://doi.org/10.1016/S0140-6736(20)30183-5).
- [51] Karki R, Kanneganti T-D. The ‘cytokine storm’: molecular mechanisms and therapeutic prospects. *Trends in Immunology* 2021;42:681–705. <https://doi.org/10.1016/j.it.2021.06.001>.
- [52] Huang C, Huang L, Wang Y, Li X, Ren L, Gu X, et al. 6-month consequences of COVID-19 in patients discharged from hospital: a cohort study. *The Lancet* 2021;397:220–32. [https://doi.org/10.1016/S0140-6736\(20\)32656-8](https://doi.org/10.1016/S0140-6736(20)32656-8).

- [53] Logue JK, Franko NM, McCulloch DJ, McDonald D, Magedson A, Wolf CR, et al. Sequelae in Adults at 6 Months After COVID-19 Infection. *JAMA Netw Open* 2021;4:e210830. <https://doi.org/10.1001/jamanetworkopen.2021.0830>.
- [54] Carfi A, Bernabei R, Landi F, for the Gemelli Against COVID-19 Post-Acute Care Study Group. Persistent Symptoms in Patients After Acute COVID-19. *JAMA* 2020;324:603. <https://doi.org/10.1001/jama.2020.12603>.
- [55] Hoffmann M, Kleine-Weber H, Schroeder S, Krüger N, Herrler T, Erichsen S, et al. SARS-CoV-2 Cell Entry Depends on ACE2 and TMPRSS2 and Is Blocked by a Clinically Proven Protease Inhibitor. *Cell* 2020;181:271-280.e8. <https://doi.org/10.1016/j.cell.2020.02.052>.
- [56] Lu Q, Liu J, Zhao S, Gomez Castro MF, Laurent-Rolle M, Dong J, et al. SARS-CoV-2 exacerbates proinflammatory responses in myeloid cells through C-type lectin receptors and Tweety family member 2. *Immunity* 2021;54:1304-1319.e9. <https://doi.org/10.1016/j.immuni.2021.05.006>.
- [57] Amraei R, Yin W, Napoleon MA, Suder EL, Berrigan J, Zhao Q, et al. CD209L/L-SIGN and CD209/DC-SIGN Act as Receptors for SARS-CoV-2. *ACS Cent Sci* 2021;7:1156–65. <https://doi.org/10.1021/acscentsci.0c01537>.
- [58] Yin X, Riva L, Pu Y, Martin-Sancho L, Kanamune J, Yamamoto Y, et al. MDA5 Governs the Innate Immune Response to SARS-CoV-2 in Lung Epithelial Cells. *Cell Reports* 2021;34:108628. <https://doi.org/10.1016/j.celrep.2020.108628>.
- [59] Zheng M, Karki R, Williams EP, Yang D, Fitzpatrick E, Vogel P, et al. TLR2 senses the SARS-CoV-2 envelope protein to produce inflammatory cytokines. *Nat Immunol* 2021;22:829–38. <https://doi.org/10.1038/s41590-021-00937-x>.
- [60] Pfaender S, Mar KB, Michailidis E, Kratzel A, Boys IN, V'kovski P, et al. LY6E impairs coronavirus fusion and confers immune control of viral disease. *Nat Microbiol* 2020;5:1330–9. <https://doi.org/10.1038/s41564-020-0769-y>.
- [61] Martin-Sancho L, Lewinski MK, Pache L, Stoneham CA, Yin X, Becker ME, et al. Functional landscape of SARS-CoV-2 cellular restriction. *Molecular Cell* 2021;81:2656-2668.e8. <https://doi.org/10.1016/j.molcel.2021.04.008>.
- [62] Rodrigues TS, de Sá KSG, Ishimoto AY, Becerra A, Oliveira S, Almeida L, et al. Inflammasomes are activated in response to SARS-CoV-2 infection and are associated with COVID-19 severity in patients. *Journal of Experimental Medicine* 2021;218:e20201707. <https://doi.org/10.1084/jem.20201707>.
- [63] Ferreira AC, Soares VC, de Azevedo-Quintanilha IG, Dias S da SG, Fintelman-Rodrigues N, Sacramento CQ, et al. SARS-CoV-2 engages inflammasome and pyroptosis in human primary monocytes. *Cell Death Discov* 2021;7:43. <https://doi.org/10.1038/s41420-021-00428-w>.
- [64] Campbell GR, To RK, Hanna J, Spector SA. SARS-CoV-2, SARS-CoV-1, and HIV-1 derived ssRNA sequences activate the NLRP3 inflammasome in human macrophages through a non-classical pathway. *IScience* 2021;24:102295. <https://doi.org/10.1016/j.isci.2021.102295>.

- [65] Xu H, Chitre SA, Akinyemi IA, Loeb JC, Lednicky JA, McIntosh MT, et al. SARS-CoV-2 viroporin triggers the NLRP3 inflammatory pathway. *Microbiology*; 2020. <https://doi.org/10.1101/2020.10.27.357731>.
- [66] Pan P, Shen M, Yu Z, Ge W, Chen K, Tian M, et al. SARS-CoV-2 N protein promotes NLRP3 inflammasome activation to induce hyperinflammation. *Nat Commun* 2021;12:4664. <https://doi.org/10.1038/s41467-021-25015-6>.
- [67] Theobald SJ, Simonis A, Georgomanolis T, Kreer C, Zehner M, Einfeld HS, et al. Long-lived macrophage reprogramming drives spike protein-mediated inflammasome activation in COVID-19. *EMBO Mol Med* 2021;13. <https://doi.org/10.15252/emmm.202114150>.
- [68] Qin C, Zhou L, Hu Z, Zhang S, Yang S, Tao Y, et al. Dysregulation of Immune Response in Patients With Coronavirus 2019 (COVID-19) in Wuhan, China. *Clinical Infectious Diseases* 2020;71:762–8. <https://doi.org/10.1093/cid/ciaa248>.
- [69] Laing AG, Lorenc A, del Molino del Barrio I, Das A, Fish M, Monin L, et al. A dynamic COVID-19 immune signature includes associations with poor prognosis. *Nat Med* 2020;26:1623–35. <https://doi.org/10.1038/s41591-020-1038-6>.
- [70] Schultze JL, Aschenbrenner AC. COVID-19 and the human innate immune system. *Cell* 2021;184:1671–92. <https://doi.org/10.1016/j.cell.2021.02.029>.
- [71] Winkler ES, Bailey AL, Kafai NM, Nair S, McCune BT, Yu J, et al. SARS-CoV-2 infection of human ACE2-transgenic mice causes severe lung inflammation and impaired function. *Nat Immunol* 2020;21:1327–35. <https://doi.org/10.1038/s41590-020-0778-2>.
- [72] Zhang Q, Bastard P, Liu Z, Le Pen J, Moncada-Velez M, Chen J, et al. Inborn errors of type I IFN immunity in patients with life-threatening COVID-19. *Science* 2020;370:eabd4570. <https://doi.org/10.1126/science.abd4570>.
- [73] Karki R, Sharma BR, Tuladhar S, Williams EP, Zalduondo L, Samir P, et al. Synergism of TNF- α and IFN- γ Triggers Inflammatory Cell Death, Tissue Damage, and Mortality in SARS-CoV-2 Infection and Cytokine Shock Syndromes. *Cell* 2021;184:149-168.e17. <https://doi.org/10.1016/j.cell.2020.11.025>.
- [74] Zhang F, Mears JR, Shakib L, Beynor JI, Shanaj S, Korsunsky I, et al. IFN- γ and TNF- α drive a CXCL10+ CCL2+ macrophage phenotype expanded in severe COVID-19 lungs and inflammatory diseases with tissue inflammation. *Genome Med* 2021;13:64. <https://doi.org/10.1186/s13073-021-00881-3>.
- [75] Notarbartolo S, Ranzani V, Bandera A, Gruarin P, Bevilacqua V, Putignano AR, et al. Integrated longitudinal immunophenotypic, transcriptional, and repertoire analyses delineate immune responses in patients with COVID-19. *Sci Immunol* 2021;6:eabg5021. <https://doi.org/10.1126/sciimmunol.abg5021>.
- [76] Lucas C, Klein J, Sundaram ME, Liu F, Wong P, Silva J, et al. Delayed production of neutralizing antibodies correlates with fatal COVID-19. *Nat Med* 2021;27:1178–86. <https://doi.org/10.1038/s41591-021-01355-0>.
- [77] Bergamaschi L, Mescia F, Turner L, Hanson AL, Kotagiri P, Dunmore BJ, et al. Longitudinal analysis reveals that delayed bystander CD8+ T cell activation and early

- immune pathology distinguish severe COVID-19 from mild disease. *Immunity* 2021;54:1257-1275.e8. <https://doi.org/10.1016/j.immuni.2021.05.010>.
- [78] Graham MB, Braciale VL, Braciale TJ. Influenza virus-specific CD4+ T helper type 2 T lymphocytes do not promote recovery from experimental virus infection. *Journal of Experimental Medicine* 1994;180:1273–82. <https://doi.org/10.1084/jem.180.4.1273>.
- [79] Su Y, Chen D, Yuan D, Lausted C, Choi J, Dai CL, et al. Multi-Omics Resolves a Sharp Disease-State Shift between Mild and Moderate COVID-19. *Cell* 2020;183:1479-1495.e20. <https://doi.org/10.1016/j.cell.2020.10.037>.
- [80] Tarke A, Sidney J, Kidd CK, Dan JM, Ramirez SI, Yu ED, et al. Comprehensive analysis of T cell immunodominance and immunoprevalence of SARS-CoV-2 epitopes in COVID-19 cases. *Cell Reports Medicine* 2021;2:100204. <https://doi.org/10.1016/j.xcrm.2021.100204>.
- [81] Juno JA, Tan H-X, Lee WS, Reynaldi A, Kelly HG, Wragg K, et al. Humoral and circulating follicular helper T cell responses in recovered patients with COVID-19. *Nat Med* 2020;26:1428–34. <https://doi.org/10.1038/s41591-020-0995-0>.
- [82] Boppana S, Qin K, Files JK, Russell RM, Stoltz R, Bibollet-Ruche F, et al. SARS-CoV-2-specific circulating T follicular helper cells correlate with neutralizing antibodies and increase during early convalescence. *PLoS Pathog* 2021;17:e1009761. <https://doi.org/10.1371/journal.ppat.1009761>.
- [83] Jung JH, Rha M-S, Sa M, Choi HK, Jeon JH, Seok H, et al. SARS-CoV-2-specific T cell memory is sustained in COVID-19 convalescent patients for 10 months with successful development of stem cell-like memory T cells. *Nat Commun* 2021;12:4043. <https://doi.org/10.1038/s41467-021-24377-1>.
- [84] Adamo S, Michler J, Zurbuchen Y, Cervia C, Taeschler P, Raeber ME, et al. Signature of long-lived memory CD8+ T cells in acute SARS-CoV-2 infection. *Nature* 2022;602:148–55. <https://doi.org/10.1038/s41586-021-04280-x>.
- [85] Qi H, Liu B, Wang X, Zhang L. The humoral response and antibodies against SARS-CoV-2 infection. *Nat Immunol* 2022;23:1008–20. <https://doi.org/10.1038/s41590-022-01248-5>.
- [86] Wajnberg A, Amanat F, Firpo A, Altman DR, Bailey MJ, Mansour M, et al. Robust neutralizing antibodies to SARS-CoV-2 infection persist for months. *Science* 2020;370:1227–30. <https://doi.org/10.1126/science.abd7728>.
- [87] Zervou FN, Louie P, Stachel A, Zacharioudakis IM, Ortiz-Mendez Y, Thomas K, et al. SARS-CoV-2 antibodies: IgA correlates with severity of disease in early COVID-19 infection. *Journal of Medical Virology* 2021;93:5409–15. <https://doi.org/10.1002/jmv.27058>.
- [88] Yan X, Chen G, Jin Z, Zhang Z, Zhang B, He J, et al. Anti-SARS-CoV-2 IgG levels in relation to disease severity of COVID-19. *Journal of Medical Virology* 2022;94:380–3. <https://doi.org/10.1002/jmv.27274>.
- [89] Hansen CB, Jarlhelt I, Pérez-Alós L, Hummelshøj Landsy L, Loftager M, Rosbjerg A, et al. SARS-CoV-2 Antibody Responses Are Correlated to Disease Severity in

- COVID-19 Convalescent Individuals. *The Journal of Immunology* 2021;206:109–17. <https://doi.org/10.4049/jimmunol.2000898>.
- [90] Kaneko N, Kuo H-H, Boucau J, Farmer JR, Allard-Chamard H, Mahajan VS, et al. Loss of Bcl-6-Expressing T Follicular Helper Cells and Germinal Centers in COVID-19. *Cell* 2020;183:143-157.e13. <https://doi.org/10.1016/j.cell.2020.08.025>.
- [91] Zohar T, Loos C, Fischinger S, Atyeo C, Wang C, Slein MD, et al. Compromised Humoral Functional Evolution Tracks with SARS-CoV-2 Mortality. *Cell* 2020;183:1508-1519.e12. <https://doi.org/10.1016/j.cell.2020.10.052>.
- [92] Hammad H, Lambrecht BN. Barrier Epithelial Cells and the Control of Type 2 Immunity. *Immunity* 2015;43:29–40. <https://doi.org/10.1016/j.immuni.2015.07.007>.
- [93] Dahlgren MW, Jones SW, Cautivo KM, Dubinin A, Ortiz-Carpena JF, Farhat S, et al. Adventitial Stromal Cells Define Group 2 Innate Lymphoid Cell Tissue Niches. *Immunity* 2019;50:707-722.e6. <https://doi.org/10.1016/j.immuni.2019.02.002>.
- [94] von Moltke J, Ji M, Liang H-E, Locksley RM. Tuft-cell-derived IL-25 regulates an intestinal ILC2–epithelial response circuit. *Nature* 2016;529:221–5. <https://doi.org/10.1038/nature16161>.
- [95] Hung L-Y, Tanaka Y, Herbine K, Pastore C, Singh B, Ferguson A, et al. Cellular context of IL-33 expression dictates impact on anti-helminth immunity. *Sci Immunol* 2020;5:eabc6259. <https://doi.org/10.1126/sciimmunol.abc6259>.
- [96] Barrett NA, Rahman OM, Fernandez JM, Parsons MW, Xing W, Austen KF, et al. Dectin-2 mediates Th2 immunity through the generation of cysteinyl leukotrienes. *Journal of Experimental Medicine* 2011;208:593–604. <https://doi.org/10.1084/jem.20100793>.
- [97] Walker JA, McKenzie ANJ. TH2 cell development and function. *Nat Rev Immunol* 2018;18:121–33. <https://doi.org/10.1038/nri.2017.118>.
- [98] Doherty TA, Khorram N, Lund S, Mehta AK, Croft M, Broide DH. Lung type 2 innate lymphoid cells express cysteinyl leukotriene receptor 1, which regulates TH2 cytokine production. *Journal of Allergy and Clinical Immunology* 2013;132:205–13. <https://doi.org/10.1016/j.jaci.2013.03.048>.
- [99] Fort MM, Cheung J, Yen D, Li J, Zurawski SM, Lo S, et al. IL-25 Induces IL-4, IL-5, and IL-13 and Th2-Associated Pathologies In Vivo. *Immunity* 2001;15:985–95. [https://doi.org/10.1016/S1074-7613\(01\)00243-6](https://doi.org/10.1016/S1074-7613(01)00243-6).
- [100] Schmitz J, Owyang A, Oldham E, Song Y, Murphy E, McClanahan TK, et al. IL-33, an Interleukin-1-like Cytokine that Signals via the IL-1 Receptor-Related Protein ST2 and Induces T Helper Type 2-Associated Cytokines. *Immunity* 2005;23:479–90. <https://doi.org/10.1016/j.immuni.2005.09.015>.
- [101] Phythian-Adams AT, Cook PC, Lundie RJ, Jones LH, Smith KA, Barr TA, et al. CD11c depletion severely disrupts Th2 induction and development in vivo. *Journal of Experimental Medicine* 2010;207:2089–96. <https://doi.org/10.1084/jem.20100734>.
- [102] von Moltke J, O’Leary CE, Barrett NA, Kanaoka Y, Austen KF, Locksley RM. Leukotrienes provide an NFAT-dependent signal that synergizes with IL-33 to

- activate ILC2s. *Journal of Experimental Medicine* 2017;214:27–37. <https://doi.org/10.1084/jem.20161274>.
- [103] Lefrançois E, Duval A, Mirey E, Roga S, Espinosa E, Cayrol C, et al. Central domain of IL-33 is cleaved by mast cell proteases for potent activation of group-2 innate lymphoid cells. *Proc Natl Acad Sci USA* 2014;111:15502–7. <https://doi.org/10.1073/pnas.1410700111>.
- [104] Hung L-Y, Lewkowich IP, Dawson LA, Downey J, Yang Y, Smith DE, et al. IL-33 drives biphasic IL-13 production for noncanonical Type 2 immunity against hookworms. *Proc Natl Acad Sci USA* 2013;110:282–7. <https://doi.org/10.1073/pnas.1206587110>.
- [105] Townsend MJ, Fallon PG, Matthews DJ, Jolin HE, McKenzie ANJ. T1/St2-Deficient Mice Demonstrate the Importance of T1/St2 in Developing Primary T Helper Cell Type 2 Responses. *Journal of Experimental Medicine* 2000;191:1069–76. <https://doi.org/10.1084/jem.191.6.1069>.
- [106] Yasuda K, Muto T, Kawagoe T, Matsumoto M, Sasaki Y, Matsushita K, et al. Contribution of IL-33-activated type II innate lymphoid cells to pulmonary eosinophilia in intestinal nematode-infected mice. *Proc Natl Acad Sci USA* 2012;109:3451–6. <https://doi.org/10.1073/pnas.1201042109>.
- [107] Fallon PG, Ballantyne SJ, Mangan NE, Barlow JL, Dasvarma A, Hewett DR, et al. Identification of an interleukin (IL)-25-dependent cell population that provides IL-4, IL-5, and IL-13 at the onset of helminth expulsion. *Journal of Experimental Medicine* 2006;203:1105–16. <https://doi.org/10.1084/jem.20051615>.
- [108] Angkasekwinai P, Srimanote P, Wang Y-H, Pootong A, Sakolvaree Y, Pattanapanyasat K, et al. Interleukin-25 (IL-25) Promotes Efficient Protective Immunity against *Trichinella spiralis* Infection by Enhancing the Antigen-Specific IL-9 Response. *Infect Immun* 2013;81:3731–41. <https://doi.org/10.1128/IAI.00646-13>.
- [109] Huang Y, Guo L, Qiu J, Chen X, Hu-Li J, Siebenlist U, et al. IL-25-responsive, lineage-negative KLRG1hi cells are multipotential ‘inflammatory’ type 2 innate lymphoid cells. *Nat Immunol* 2015;16:161–9. <https://doi.org/10.1038/ni.3078>.
- [110] Huang Y, Mao K, Chen X, Sun M, Kawabe T, Li W, et al. S1P-dependent interorgan trafficking of group 2 innate lymphoid cells supports host defense. *Science* 2018;359:114–9. <https://doi.org/10.1126/science.aam5809>.
- [111] Howitt MR, Lavoie S, Michaud M, Blum AM, Tran SV, Weinstock JV, et al. Tuft cells, taste-chemosensory cells, orchestrate parasite type 2 immunity in the gut. *Science* 2016;351:1329–33. <https://doi.org/10.1126/science.aaf1648>.
- [112] Gerbe F, Sidot E, Smyth DJ, Ohmoto M, Matsumoto I, Dardalhon V, et al. Intestinal epithelial tuft cells initiate type 2 mucosal immunity to helminth parasites. *Nature* 2016;529:226–30. <https://doi.org/10.1038/nature16527>.
- [113] Massacand JC, Stettler RC, Meier R, Humphreys NE, Grecis RK, Marsland BJ, et al. Helminth products bypass the need for TSLP in Th2 immune responses by directly modulating dendritic cell function. *Proceedings of the National Academy of Sciences* 2009;106:13968–73. <https://doi.org/10.1073/pnas.0906367106>.

- [114] Klose CSN, Mahlaköiv T, Moeller JB, Rankin LC, Flamar A-L, Kabata H, et al. The neuropeptide neuromedin U stimulates innate lymphoid cells and type 2 inflammation. *Nature* 2017;549:282–6. <https://doi.org/10.1038/nature23676>.
- [115] Cardoso V, Chesné J, Ribeiro H, García-Cassani B, Carvalho T, Bouchery T, et al. Neuronal regulation of type 2 innate lymphoid cells via neuromedin U. *Nature* 2017;549:277–81. <https://doi.org/10.1038/nature23469>.
- [116] Wallrapp A, Riesenfeld SJ, Burkett PR, Abdulnour R-EE, Nyman J, Dionne D, et al. The neuropeptide NMU amplifies ILC2-driven allergic lung inflammation. *Nature* 2017;549:351–6. <https://doi.org/10.1038/nature24029>.
- [117] Tsou AM, Yano H, Parkhurst CN, Mahlaköiv T, Chu C, Zhang W, et al. Neuropeptide regulation of non-redundant ILC2 responses at barrier surfaces. *Nature* 2022;611:787–93. <https://doi.org/10.1038/s41586-022-05297-6>.
- [118] Klose CSN, Artis D. Innate lymphoid cells as regulators of immunity, inflammation and tissue homeostasis. *Nat Immunol* 2016;17:765–74. <https://doi.org/10.1038/ni.3489>.
- [119] Jarick KJ, Topczewska PM, Jakob MO, Yano H, Arifuzzaman M, Gao X, et al. Non-redundant functions of group 2 innate lymphoid cells. *Nature* 2022;611:794–800. <https://doi.org/10.1038/s41586-022-05395-5>.
- [120] Turner J-E, Morrison PJ, Wilhelm C, Wilson M, Ahlfors H, Renauld J-C, et al. IL-9-mediated survival of type 2 innate lymphoid cells promotes damage control in helminth-induced lung inflammation. *Journal of Experimental Medicine* 2013;210:2951–65. <https://doi.org/10.1084/jem.20130071>.
- [121] Mohapatra A, Van Dyken SJ, Schneider C, Nussbaum JC, Liang H-E, Locksley RM. Group 2 innate lymphoid cells utilize the IRF4-IL-9 module to coordinate epithelial cell maintenance of lung homeostasis. *Mucosal Immunology* 2016;9:275–86. <https://doi.org/10.1038/mi.2015.59>.
- [122] Oliphant CJ, Hwang YY, Walker JA, Salimi M, Wong SH, Brewer JM, et al. MHCII-Mediated Dialog between Group 2 Innate Lymphoid Cells and CD4+ T Cells Potentiates Type 2 Immunity and Promotes Parasitic Helminth Expulsion. *Immunity* 2014;41:283–95. <https://doi.org/10.1016/j.immuni.2014.06.016>.
- [123] Halim TYF, Hwang YY, Scanlon ST, Zaghoulani H, Garbi N, Fallon PG, et al. Group 2 innate lymphoid cells license dendritic cells to potentiate memory TH2 cell responses. *Nat Immunol* 2016;17:57–64. <https://doi.org/10.1038/ni.3294>.
- [124] Nussbaum JC, Van Dyken SJ, von Moltke J, Cheng LE, Mohapatra A, Molofsky AB, et al. Type 2 innate lymphoid cells control eosinophil homeostasis. *Nature* 2013;502:245–8. <https://doi.org/10.1038/nature12526>.
- [125] Huang L, Appleton JA. Eosinophils in Helminth Infection: Defenders and Dupes. *Trends in Parasitology* 2016;32:798–807. <https://doi.org/10.1016/j.pt.2016.05.004>.
- [126] Weller PF, Spencer LA. Functions of tissue-resident eosinophils. *Nat Rev Immunol* 2017;17:746–60. <https://doi.org/10.1038/nri.2017.95>.

- [127] Scepek S, Moqbel R, Lindau M. Compound exocytosis and cumulative degranulation by eosinophils and their role in parasite killing. *Parasitology Today* 1994;10:276–8. [https://doi.org/10.1016/0169-4758\(94\)90146-5](https://doi.org/10.1016/0169-4758(94)90146-5).
- [128] Masure D, Wang T, Vlaminck J, Claerhoudt S, Chiers K, Van den Broeck W, et al. The Intestinal Expulsion of the Roundworm *Ascaris suum* Is Associated with Eosinophils, Intra-Epithelial T Cells and Decreased Intestinal Transit Time. *PLoS Negl Trop Dis* 2013;7:e2588. <https://doi.org/10.1371/journal.pntd.0002588>.
- [129] Masure D, Vlaminck J, Wang T, Chiers K, Van den Broeck W, Vercruysse J, et al. A Role for Eosinophils in the Intestinal Immunity against Infective *Ascaris suum* Larvae. *PLoS Negl Trop Dis* 2013;7:e2138. <https://doi.org/10.1371/journal.pntd.0002138>.
- [130] Fabre V, Beiting DP, Bliss SK, Gebreselassie NG, Gagliardo LF, Lee NA, et al. Eosinophil Deficiency Compromises Parasite Survival in Chronic Nematode Infection. *The Journal of Immunology* 2009;182:1577–83. <https://doi.org/10.4049/jimmunol.182.3.1577>.
- [131] Gebreselassie NG, Moorhead AR, Fabre V, Gagliardo LF, Lee NA, Lee JJ, et al. Eosinophils Preserve Parasitic Nematode Larvae by Regulating Local Immunity. *The Journal of Immunology* 2012;188:417–25. <https://doi.org/10.4049/jimmunol.1101980>.
- [132] Strandmark J, Steinfeld S, Berek C, Kühl AA, Rausch S, Hartmann S. Eosinophils are required to suppress Th2 responses in Peyer's patches during intestinal infection by nematodes. *Mucosal Immunology* 2017;10:661–72. <https://doi.org/10.1038/mi.2016.93>.
- [133] Chen F, Wu W, Millman A, Craft JF, Chen E, Patel N, et al. Neutrophils prime a long-lived effector macrophage phenotype that mediates accelerated helminth expulsion. *Nat Immunol* 2014;15:938–46. <https://doi.org/10.1038/ni.2984>.
- [134] Sutherland TE, Logan N, Rückerl D, Humbles AA, Allan SM, Papayannopoulos V, et al. Chitinase-like proteins promote IL-17-mediated neutrophilia in a tradeoff between nematode killing and host damage. *Nat Immunol* 2014;15:1116–25. <https://doi.org/10.1038/ni.3023>.
- [135] O'Connell AE, Redding KM, Hess JA, Lok JB, Nolan TJ, Abraham D. Soluble extract from the nematode *Strongyloides stercoralis* induces CXCR2 dependent/IL-17 independent neutrophil recruitment. *Microbes and Infection* 2011;13:536–44. <https://doi.org/10.1016/j.micinf.2011.01.016>.
- [136] Bonne-Année S, Kerepesi LA, Hess JA, Wesolowski J, Paumet F, Lok JB, et al. Extracellular traps are associated with human and mouse neutrophil and macrophage mediated killing of larval *Strongyloides stercoralis*. *Microbes and Infection* 2014;16:502–11. <https://doi.org/10.1016/j.micinf.2014.02.012>.
- [137] Bouchery T, Moyat M, Sotillo J, Silverstein S, Volpe B, Coakley G, et al. Hookworms Evade Host Immunity by Secreting a Deoxyribonuclease to Degrade Neutrophil Extracellular Traps. *Cell Host & Microbe* 2020;27:277–289.e6. <https://doi.org/10.1016/j.chom.2020.01.011>.
- [138] O'Connell AE, Hess JA, Santiago GA, Nolan TJ, Lok JB, Lee JJ, et al. Major Basic Protein from Eosinophils and Myeloperoxidase from Neutrophils Are Required for

- Protective Immunity to *Strongyloides stercoralis* in Mice. *Infect Immun* 2011;79:2770–8. <https://doi.org/10.1128/IAI.00931-10>.
- [139] Rajamanickam A, Munisankar S, Bhootra Y, Dolla CK, Nutman TB, Babu S. Elevated Systemic Levels of Eosinophil, Neutrophil, and Mast Cell Granular Proteins in *Strongyloides Stercoralis* Infection that Diminish following Treatment. *Front Immunol* 2018;9:207. <https://doi.org/10.3389/fimmu.2018.00207>.
- [140] Siracusa MC, Comeau MR, Artis D. New insights into basophil biology: initiators, regulators, and effectors of type 2 inflammation: Insights into basophil biology. *Annals of the New York Academy of Sciences* 2011;1217:166–77. <https://doi.org/10.1111/j.1749-6632.2010.05918.x>.
- [141] Anyan WK, Seki T, Kumagai T, Obata-Ninomiya K, Furushima-Shimogawara R, Kwansa-Bentum B, et al. Basophil depletion downregulates *Schistosoma mansoni* egg-induced granuloma formation. *Parasitology International* 2013;62:508–13. <https://doi.org/10.1016/j.parint.2013.07.003>.
- [142] Schwartz C, Turqueti-Neves A, Hartmann S, Yu P, Nimmerjahn F, Voehringer D. Basophil-mediated protection against gastrointestinal helminths requires IgE-induced cytokine secretion. *Proc Natl Acad Sci USA* 2014;111. <https://doi.org/10.1073/pnas.1412663111>.
- [143] Sullivan BM, Liang H-E, Bando JK, Wu D, Cheng LE, McKerrow JK, et al. Genetic analysis of basophil function in vivo. *Nat Immunol* 2011;12:527–35. <https://doi.org/10.1038/ni.2036>.
- [144] Ohnmacht C, Schwartz C, Panzer M, Schiedewitz I, Naumann R, Voehringer D. Basophils Orchestrate Chronic Allergic Dermatitis and Protective Immunity against Helminths. *Immunity* 2010;33:364–74. <https://doi.org/10.1016/j.immuni.2010.08.011>.
- [145] Voehringer D. Protective and pathological roles of mast cells and basophils. *Nat Rev Immunol* 2013;13:362–75. <https://doi.org/10.1038/nri3427>.
- [146] Vukman KV, Lalor R, Aldridge A, O'Neill SM. Mast cells: new therapeutic target in helminth immune modulation. *Parasite Immunol* 2016;38:45–52. <https://doi.org/10.1111/pim.12295>.
- [147] McKEAN PG, Pritchard DI. The action of a mast cell protease on the cuticular collagens of *Necator americanus*. *Parasite Immunol* 1989;11:293–7. <https://doi.org/10.1111/j.1365-3024.1989.tb00667.x>.
- [148] Maruyama H, Yabu Y, Yoshida A, Nawa Y, Ohta N. A Role of Mast Cell Glycosaminoglycans for the Immunological Expulsion of Intestinal Nematode, *Strongyloides venezuelensis*. *The Journal of Immunology* 2000;164:3749–54. <https://doi.org/10.4049/jimmunol.164.7.3749>.
- [149] Onah DN, Nawa Y. Mucosal mast cell-derived chondroitin sulphate levels in and worm expulsion from FcRgamma-knockout mice following oral challenge with *Strongyloides venezuelensis*. *J Vet Sci* 2004;5:221–6.
- [150] Lewis RA, Soter NA, Diamond PT, Austen KF, Oates JA, Roberts LJ. Prostaglandin D2 generation after activation of rat and human mast cells with anti-IgE. *The Journal of Immunology* 1982;129:1627–31. <https://doi.org/10.4049/jimmunol.129.4.1627>.

- [151] Shimokawa C, Kanaya T, Hachisuka M, Ishiwata K, Hisaeda H, Kurashima Y, et al. Mast Cells Are Crucial for Induction of Group 2 Innate Lymphoid Cells and Clearance of Helminth Infections. *Immunity* 2017;46:863-874.e4. <https://doi.org/10.1016/j.immuni.2017.04.017>.
- [152] Hepworth MR, Daniłowicz-Luebert E, Rausch S, Metz M, Klotz C, Maurer M, et al. Mast cells orchestrate type 2 immunity to helminths through regulation of tissue-derived cytokines. *Proc Natl Acad Sci USA* 2012;109:6644–9. <https://doi.org/10.1073/pnas.1112268109>.
- [153] Licona-Limón P, Henao-Mejia J, Temann AU, Gagliani N, Licona-Limón I, Ishigame H, et al. Th9 Cells Drive Host Immunity against Gastrointestinal Worm Infection. *Immunity* 2013;39:744–57. <https://doi.org/10.1016/j.immuni.2013.07.020>.
- [154] Noelle RJ, Nowak EC. Cellular sources and immune functions of interleukin-9. *Nat Rev Immunol* 2010;10:683–7. <https://doi.org/10.1038/nri2848>.
- [155] Lechner A, Bohnacker S, Esser-von Bieren J. Macrophage regulation & function in helminth infection. *Seminars in Immunology* 2021;53:101526. <https://doi.org/10.1016/j.smim.2021.101526>.
- [156] Reece JJ, Siracusa MC, Scott AL. Innate Immune Responses to Lung-Stage Helminth Infection Induce Alternatively Activated Alveolar Macrophages. *Infect Immun* 2006;74:4970–81. <https://doi.org/10.1128/IAI.00687-06>.
- [157] Anthony RM, Urban JF, Alem F, Hamed HA, Rozo CT, Boucher J-L, et al. Memory TH2 cells induce alternatively activated macrophages to mediate protection against nematode parasites. *Nat Med* 2006;12:955–60. <https://doi.org/10.1038/nm1451>.
- [158] Esser-von Bieren J, Mosconi I, Guet R, Piersgilli A, Volpe B, Chen F, et al. Antibodies Trap Tissue Migrating Helminth Larvae and Prevent Tissue Damage by Driving IL-4R α -Independent Alternative Differentiation of Macrophages. *PLoS Pathog* 2013;9. <https://doi.org/10.1371/journal.ppat.1003771>.
- [159] Esser-von Bieren J, Volpe B, Kulagin M, Sutherland DB, Guet R, Seitz A, et al. Antibody-mediated trapping of helminth larvae requires CD11b and Fc γ receptor I. *J Immunol* 2015;194:1154–63. <https://doi.org/10.4049/jimmunol.1401645>.
- [160] Esser-von Bieren J, Volpe B, Sutherland DB, Bürgi J, Verbeek JS, Marsland BJ, et al. Immune Antibodies and Helminth Products Drive CXCR2-Dependent Macrophage-Myofibroblast Crosstalk to Promote Intestinal Repair. *PLoS Pathog* 2015;11:e1004778. <https://doi.org/10.1371/journal.ppat.1004778>.
- [161] Minutti CM, Jackson-Jones LH, García-Fojeda B, Knipper JA, Sutherland TE, Logan N, et al. Local amplifiers of IL-4R α -mediated macrophage activation promote repair in lung and liver. *Science* 2017;356:1076–80. <https://doi.org/10.1126/science.aaj2067>.
- [162] Thawer S, Auret J, Schnoeller C, Chetty A, Smith K, Darby M, et al. Surfactant Protein-D Is Essential for Immunity to Helminth Infection. *PLoS Pathog* 2016;12:e1005461. <https://doi.org/10.1371/journal.ppat.1005461>.

- [163] Bosurgi L, Cao YG, Cabeza-Cabrerizo M, Tucci A, Hughes LD, Kong Y, et al. Macrophage function in tissue repair and remodeling requires IL-4 or IL-13 with apoptotic cells. *Science* 2017;356:1072–6. <https://doi.org/10.1126/science.aai8132>.
- [164] Reese TA, Liang H-E, Tager AM, Luster AD, Van Rooijen N, Voehringer D, et al. Chitin induces accumulation in tissue of innate immune cells associated with allergy. *Nature* 2007;447:92–6. <https://doi.org/10.1038/nature05746>.
- [165] Zhao A, Urban JF, Anthony RM, Sun R, Stiltz J, van Rooijen N, et al. Th2 Cytokine-Induced Alterations in Intestinal Smooth Muscle Function Depend on Alternatively Activated Macrophages. *Gastroenterology* 2008;135:217-225.e1. <https://doi.org/10.1053/j.gastro.2008.03.077>.
- [166] Minutti CM, Knipper JA, Allen JE, Zaiss DMW. Tissue-specific contribution of macrophages to wound healing. *Seminars in Cell & Developmental Biology* 2017;61:3–11. <https://doi.org/10.1016/j.semcd.2016.08.006>.
- [167] Owhashi M, Arita H, Hayai N. Identification of a Novel Eosinophil Chemotactic Cytokine (ECF-L) as a Chitinase Family Protein. *Journal of Biological Chemistry* 2000;275:1279–86. <https://doi.org/10.1074/jbc.275.2.1279>.
- [168] Turner JD, Pionnier N, Furlong-Silva J, Sjoberg H, Cross S, Halliday A, et al. Interleukin-4 activated macrophages mediate immunity to filarial helminth infection by sustaining CCR3-dependent eosinophilia. *PLoS Pathog* 2018;14:e1006949. <https://doi.org/10.1371/journal.ppat.1006949>.
- [169] Faz-López B, Mayoral-Reyes H, Hernández-Pando R, Martínez-Labat P, McKay DM, Medina-Andrade I, et al. A Dual Role for Macrophages in Modulating Lung Tissue Damage/Repair during L2 *Toxocara canis* Infection. *Pathogens* 2019;8:280. <https://doi.org/10.3390/pathogens8040280>.
- [170] Krljanac B, Schubart C, Naumann R, Wirtz S, Culemann S, Krönke G, et al. RELM α -expressing macrophages protect against fatal lung damage and reduce parasite burden during helminth infection. *Sci Immunol* 2019;4:eaau3814. <https://doi.org/10.1126/sciimmunol.aau3814>.
- [171] Liu Z, Liu Q, Hamed H, Anthony RM, Foster A, Finkelman FD, et al. IL-2 and Autocrine IL-4 Drive the In Vivo Development of Antigen-Specific Th2 T Cells Elicited by Nematode Parasites. *The Journal of Immunology* 2005;174:2242–9. <https://doi.org/10.4049/jimmunol.174.4.2242>.
- [172] Finkelman FD, Shea-Donohue T, Morris SC, Gildea L, Strait R, Madden KB, et al. Interleukin-4- and interleukin-13-mediated host protection against intestinal nematode parasites. *Immunol Rev* 2004;201:139–55. <https://doi.org/10.1111/j.0105-2896.2004.00192.x>.
- [173] Madden KB, Yeung KA, Zhao A, Gause WC, Finkelman FD, Katona IM, et al. Enteric nematodes induce stereotypic STAT6-dependent alterations in intestinal epithelial cell function. *J Immunol* 2004;172:5616–21. <https://doi.org/10.4049/jimmunol.172.9.5616>.
- [174] Shea-Donohue T, Sullivan C, Finkelman FD, Madden KB, Morris SC, Goldhill J, et al. The Role of IL-4 in *Heligmosomoides polygyrus* -Induced Alterations in Murine

- Intestinal Epithelial Cell Function. *The Journal of Immunology* 2001;167:2234–9. <https://doi.org/10.4049/jimmunol.167.4.2234>.
- [175] Madden KB, Whitman L, Sullivan C, Gause WC, Urban JF, Katona IM, et al. Role of STAT6 and mast cells in IL-4- and IL-13-induced alterations in murine intestinal epithelial cell function. *J Immunol* 2002;169:4417–22. <https://doi.org/10.4049/jimmunol.169.8.4417>.
- [176] Zaini A, Good-Jacobson KL, Zaph C. Context-dependent roles of B cells during intestinal helminth infection. *PLoS Negl Trop Dis* 2021;15:e0009340. <https://doi.org/10.1371/journal.pntd.0009340>.
- [177] Bradley LM, Harbertson J, Biederman E, Zhang Y, Bradley SM, Linton P-J. Availability of antigen-presenting cells can determine the extent of CD4 effector expansion and priming for secretion of Th2 cytokines in vivo. *Eur J Immunol* 2002;32:2338–46. [https://doi.org/10.1002/1521-4141\(200208\)32:8<2338::AID-IMMU2338>3.0.CO;2-R](https://doi.org/10.1002/1521-4141(200208)32:8<2338::AID-IMMU2338>3.0.CO;2-R).
- [178] Wojciechowski W, Harris DP, Sprague F, Mousseau B, Makris M, Kusser K, et al. Cytokine-producing effector B cells regulate type 2 immunity to *H. polygyrus*. *Immunity* 2009;30:421–33. <https://doi.org/10.1016/j.immuni.2009.01.006>.
- [179] Horsnell WGC, Darby MG, Hoving JC, Nieuwenhuizen N, McSorley HJ, Ndlovu H, et al. IL-4R α -associated antigen processing by B cells promotes immunity in *Nippostrongylus brasiliensis* infection. *PLoS Pathog* 2013;9:e1003662. <https://doi.org/10.1371/journal.ppat.1003662>.
- [180] Liu Q, Liu Z, Roza CT, Hamed HA, Alem F, Urban JF, et al. The role of B cells in the development of CD4 effector T cells during a polarized Th2 immune response. *J Immunol* 2007;179:3821–30. <https://doi.org/10.4049/jimmunol.179.6.3821>.
- [181] Schweitzer AN, Sharpe AH. Studies Using Antigen-Presenting Cells Lacking Expression of Both B7-1 (CD80) and B7-2 (CD86) Show Distinct Requirements for B7 Molecules During Priming Versus Restimulation of Th2 But Not Th1 Cytokine Production. *The Journal of Immunology* 1998;161:2762–71. <https://doi.org/10.4049/jimmunol.161.6.2762>.
- [182] Linton P-J, Bautista B, Biederman E, Bradley ES, Harbertson J, Kondrack RM, et al. Costimulation via OX40L expressed by B cells is sufficient to determine the extent of primary CD4 cell expansion and Th2 cytokine secretion in vivo. *J Exp Med* 2003;197:875–83. <https://doi.org/10.1084/jem.20021290>.
- [183] Ekkens MJ, Liu Z, Liu Q, Whitmire J, Xiao S, Foster A, et al. The role of OX40 ligand interactions in the development of the Th2 response to the gastrointestinal nematode parasite *Heligmosomoides polygyrus*. *J Immunol* 2003;170:384–93. <https://doi.org/10.4049/jimmunol.170.1.384>.
- [184] Lane P. Role of OX40 signals in coordinating CD4 T cell selection, migration, and cytokine differentiation in T helper (Th)1 and Th2 cells. *J Exp Med* 2000;191:201–6. <https://doi.org/10.1084/jem.191.2.201>.
- [185] Coyle AJ, Gutierrez-Ramos J-C. The role of ICOS and other costimulatory molecules in allergy and asthma. *Springer Semin Immunopathol* 2004;25:349–59. <https://doi.org/10.1007/s00281-003-0154-y>.

- [186] Van DV, Bauer L, Kroczeck RA, Hutloff A. ICOS Costimulation Differentially Affects T Cells in Secondary Lymphoid Organs and Inflamed Tissues. *Am J Respir Cell Mol Biol* 2018;59:437–47. <https://doi.org/10.1165/rcmb.2017-0309OC>.
- [187] Moulin V, Andris F, Thielemans K, Maliszewski C, Urbain J, Moser M. B lymphocytes regulate dendritic cell (DC) function in vivo: increased interleukin 12 production by DCs from B cell-deficient mice results in T helper cell type 1 deviation. *J Exp Med* 2000;192:475–82. <https://doi.org/10.1084/jem.192.4.475>.
- [188] Dubey LK, Lebon L, Mosconi I, Yang C-Y, Scandella E, Ludewig B, et al. Lymphotoxin-Dependent B Cell-FRC Crosstalk Promotes De Novo Follicle Formation and Antibody Production following Intestinal Helminth Infection. *Cell Rep* 2016;15:1527–41. <https://doi.org/10.1016/j.celrep.2016.04.023>.
- [189] Dubey LK, Ludewig B, Luther SA, Harris NL. IL-4R α -Expressing B Cells Are Required for CXCL13 Production by Fibroblastic Reticular Cells. *Cell Rep* 2019;27:2442-2458.e5. <https://doi.org/10.1016/j.celrep.2019.04.079>.
- [190] Knott ML, Matthaehi KI, Giacomini PR, Wang H, Foster PS, Dent LA. Impaired resistance in early secondary *Nippostrongylus brasiliensis* infections in mice with defective eosinophilopoiesis. *Int J Parasitol* 2007;37:1367–78. <https://doi.org/10.1016/j.ijpara.2007.04.006>.
- [191] Huang L, Gebreselassie NG, Gagliardo LF, Ruyechan MC, Luber KL, Lee NA, et al. Eosinophils mediate protective immunity against secondary nematode infection. *J Immunol* 2015;194:283–90. <https://doi.org/10.4049/jimmunol.1402219>.
- [192] McCoy KD, Stoel M, Stettler R, Merky P, Fink K, Senn BM, et al. Polyclonal and specific antibodies mediate protective immunity against enteric helminth infection. *Cell Host Microbe* 2008;4:362–73. <https://doi.org/10.1016/j.chom.2008.08.014>.
- [193] Hewitson JP, Filbey KJ, Esser-von Bieren J, Camberis M, Schwartz C, Murray J, et al. Concerted activity of IgG1 antibodies and IL-4/IL-25-dependent effector cells trap helminth larvae in the tissues following vaccination with defined secreted antigens, providing sterile immunity to challenge infection. *PLoS Pathog* 2015;11:e1004676. <https://doi.org/10.1371/journal.ppat.1004676>.
- [194] Merad M, Manz MG, Karsunky H, Wagers A, Peters W, Charo I, et al. Langerhans cells renew in the skin throughout life under steady-state conditions. *Nat Immunol* 2002;3:1135–41. <https://doi.org/10.1038/ni852>.
- [195] Ajami B, Bennett JL, Krieger C, Tetzlaff W, Rossi FMV. Local self-renewal can sustain CNS microglia maintenance and function throughout adult life. *Nat Neurosci* 2007;10:1538–43. <https://doi.org/10.1038/nn2014>.
- [196] Guillemins M, De Kleer I, Henri S, Post S, Vanhoutte L, De Prijck S, et al. Alveolar macrophages develop from fetal monocytes that differentiate into long-lived cells in the first week of life via GM-CSF. *Journal of Experimental Medicine* 2013;210:1977–92. <https://doi.org/10.1084/jem.20131199>.
- [197] Yona S, Kim K-W, Wolf Y, Mildner A, Varol D, Breker M, et al. Fate Mapping Reveals Origins and Dynamics of Monocytes and Tissue Macrophages under Homeostasis. *Immunity* 2013;38:79–91. <https://doi.org/10.1016/j.immuni.2012.12.001>.

- [198] Wynn TA, Chawla A, Pollard JW. Macrophage biology in development, homeostasis and disease. *Nature* 2013;496:445–55. <https://doi.org/10.1038/nature12034>.
- [199] Schneider C, Nobs SP, Kurrer M, Rehrauer H, Thiele C, Kopf M. Induction of the nuclear receptor PPAR- γ by the cytokine GM-CSF is critical for the differentiation of fetal monocytes into alveolar macrophages. *Nat Immunol* 2014;15:1026–37. <https://doi.org/10.1038/ni.3005>.
- [200] Yu X, Buttgereit A, Lelios I, Utz SG, Cansever D, Becher B, et al. The Cytokine TGF- β Promotes the Development and Homeostasis of Alveolar Macrophages. *Immunity* 2017;47:903-912.e4. <https://doi.org/10.1016/j.immuni.2017.10.007>.
- [201] Guilliams M, Mildner A, Yona S. Developmental and Functional Heterogeneity of Monocytes. *Immunity* 2018;49:595–613. <https://doi.org/10.1016/j.immuni.2018.10.005>.
- [202] Mildner A, Schönheit J, Giladi A, David E, Lara-Astiaso D, Lorenzo-Vivas E, et al. Genomic Characterization of Murine Monocytes Reveals C/EBP β Transcription Factor Dependence of Ly6C⁺ Cells. *Immunity* 2017;46:849-862.e7. <https://doi.org/10.1016/j.immuni.2017.04.018>.
- [203] Yang J, Zhang L, Yu C, Yang X-F, Wang H. Monocyte and macrophage differentiation: circulation inflammatory monocyte as biomarker for inflammatory diseases. *Biomark Res* 2014;2:1. <https://doi.org/10.1186/2050-7771-2-1>.
- [204] Patel AA, Zhang Y, Fullerton JN, Boelen L, Rongvaux A, Maini AA, et al. The fate and lifespan of human monocyte subsets in steady state and systemic inflammation. *Journal of Experimental Medicine* 2017;214:1913–23. <https://doi.org/10.1084/jem.20170355>.
- [205] Ehrh S, Schnappinger D, Bekiranov S, Drenkow J, Shi S, Gingeras TR, et al. Reprogramming of the Macrophage Transcriptome in Response to Interferon- γ and Mycobacterium tuberculosis. *Journal of Experimental Medicine* 2001;194:1123–40. <https://doi.org/10.1084/jem.194.8.1123>.
- [206] Verreck FAW, de Boer T, Langenberg DML, van der Zanden L, Ottenhoff THM. Phenotypic and functional profiling of human proinflammatory type-1 and anti-inflammatory type-2 macrophages in response to microbial antigens and IFN- γ - and CD40L-mediated costimulation. *Journal of Leukocyte Biology* 2006;79:285–93. <https://doi.org/10.1189/jlb.0105015>.
- [207] Herbst S, Schaible UE, Schneider BE. Interferon Gamma Activated Macrophages Kill Mycobacteria by Nitric Oxide Induced Apoptosis. *PLoS ONE* 2011;6:e19105. <https://doi.org/10.1371/journal.pone.0019105>.
- [208] Martinez FO, Gordon S, Locati M, Mantovani A. Transcriptional Profiling of the Human Monocyte-to-Macrophage Differentiation and Polarization: New Molecules and Patterns of Gene Expression. *The Journal of Immunology* 2006;177:7303–11. <https://doi.org/10.4049/jimmunol.177.10.7303>.
- [209] Saradna A, Do DC, Kumar S, Fu Q-L, Gao P. Macrophage polarization and allergic asthma. *Translational Research* 2018;191:1–14. <https://doi.org/10.1016/j.trsl.2017.09.002>.

- [210] Stein M, Keshav S, Harris N, Gordon S. Interleukin 4 potently enhances murine macrophage mannose receptor activity: a marker of alternative immunologic macrophage activation. *Journal of Experimental Medicine* 1992;176:287–92. <https://doi.org/10.1084/jem.176.1.287>.
- [211] Doyle AG, Herbein G, Montaner LJ, Minty AJ, Caput D, Ferrara P, et al. Interleukin-13 alters the activation state of murine macrophages in vitro: Comparison with interleukin-4 and interferon- γ . *Eur J Immunol* 1994;24:1441–5. <https://doi.org/10.1002/eji.1830240630>.
- [212] Rószter T. Understanding the Mysterious M2 Macrophage through Activation Markers and Effector Mechanisms. *Mediators of Inflammation* 2015;2015:1–16. <https://doi.org/10.1155/2015/816460>.
- [213] Gauthier T, Chen W. Modulation of Macrophage Immunometabolism: A New Approach to Fight Infections. *Front Immunol* 2022;13:780839. <https://doi.org/10.3389/fimmu.2022.780839>.
- [214] Mills EL, O'Neill LA. Reprogramming mitochondrial metabolism in macrophages as an anti-inflammatory signal: HIGHLIGHTS. *Eur J Immunol* 2016;46:13–21. <https://doi.org/10.1002/eji.201445427>.
- [215] Högner K, Wolff T, Pleschka S, Plog S, Gruber AD, Kalinke U, et al. Macrophage-expressed IFN- β Contributes to Apoptotic Alveolar Epithelial Cell Injury in Severe Influenza Virus Pneumonia. *PLoS Pathog* 2013;9:e1003188. <https://doi.org/10.1371/journal.ppat.1003188>.
- [216] Jiang H, Shi H, Sun M, Wang Y, Meng Q, Guo P, et al. PFKFB3-Driven Macrophage Glycolytic Metabolism Is a Crucial Component of Innate Antiviral Defense. *The Journal of Immunology* 2016;197:2880–90. <https://doi.org/10.4049/jimmunol.1600474>.
- [217] Codo AC, Davanzo GG, Monteiro L de B, de Souza GF, Muraro SP, Virgilio-da-Silva JV, et al. Elevated Glucose Levels Favor SARS-CoV-2 Infection and Monocyte Response through a HIF-1 α /Glycolysis-Dependent Axis. *Cell Metabolism* 2020;32:437-446.e5. <https://doi.org/10.1016/j.cmet.2020.07.007>.
- [218] Mayer KA, Stöckl J, Zlabinger GJ, Gualdoni GA. Hijacking the Supplies: Metabolism as a Novel Facet of Virus-Host Interaction. *Front Immunol* 2019;10:1533. <https://doi.org/10.3389/fimmu.2019.01533>.
- [219] Thaker SK, Ch'ng J, Christofk HR. Viral hijacking of cellular metabolism. *BMC Biol* 2019;17:59. <https://doi.org/10.1186/s12915-019-0678-9>.
- [220] Li X, Zhu W, Fan M, Zhang J, Peng Y, Huang F, et al. Dependence of SARS-CoV-2 infection on cholesterol-rich lipid raft and endosomal acidification. *Computational and Structural Biotechnology Journal* 2021;19:1933–43. <https://doi.org/10.1016/j.csbj.2021.04.001>.
- [221] Zang R, Case JB, Yutuc E, Ma X, Shen S, Gomez Castro MF, et al. Cholesterol 25-hydroxylase suppresses SARS-CoV-2 replication by blocking membrane fusion. *Proc Natl Acad Sci USA* 2020;117:32105–13. <https://doi.org/10.1073/pnas.2012197117>.

- [222] Wang S, Li W, Hui H, Tiwari SK, Zhang Q, Croker BA, et al. Cholesterol 25-Hydroxylase inhibits SARS-CoV-2 and other coronaviruses by depleting membrane cholesterol. *EMBO J* 2020;39. <https://doi.org/10.15252/embj.2020106057>.
- [223] Dias SSG, Soares VC, Ferreira AC, Sacramento CQ, Fintelman-Rodrigues N, Temerozo JR, et al. Lipid droplets fuel SARS-CoV-2 replication and production of inflammatory mediators. *PLoS Pathog* 2020;16:e1009127. <https://doi.org/10.1371/journal.ppat.1009127>.
- [224] Lee W, Ahn JH, Park HH, Kim HN, Kim H, Yoo Y, et al. COVID-19-activated SREBP2 disturbs cholesterol biosynthesis and leads to cytokine storm. *Sig Transduct Target Ther* 2020;5:186. <https://doi.org/10.1038/s41392-020-00292-7>.
- [225] Sanchez MD, Ochoa AC, Foster TP. Development and evaluation of a host-targeted antiviral that abrogates herpes simplex virus replication through modulation of arginine-associated metabolic pathways. *Antiviral Research* 2016;132:13–25. <https://doi.org/10.1016/j.antiviral.2016.05.009>.
- [226] Burrack KS, Morrison TE. The Role of Myeloid Cell Activation and Arginine Metabolism in the Pathogenesis of Virus-Induced Diseases. *Front Immunol* 2014;5. <https://doi.org/10.3389/fimmu.2014.00428>.
- [227] Akaike T, Maeda H. Nitric oxide and virus infection: NO and virus infection. *Immunology* 2000;101:300–8. <https://doi.org/10.1046/j.1365-2567.2000.00142.x>.
- [228] Odkhuu E, Komatsu T, Koide N, Naiki Y, Takeuchi K, Tanaka Y, et al. Sendai virus C protein limits NO production in infected RAW264.7 macrophages. *Innate Immun* 2018;24:430–8. <https://doi.org/10.1177/1753425918796619>.
- [229] Perrone LA, Belser JA, Wadford DA, Katz JM, Tumpey TM. Inducible Nitric Oxide Contributes to Viral Pathogenesis Following Highly Pathogenic Influenza Virus Infection in Mice. *The Journal of Infectious Diseases* 2013;207:1576–84. <https://doi.org/10.1093/infdis/jit062>.
- [230] Huang SC-C, Smith AM, Everts B, Colonna M, Pearce EL, Schilling JD, et al. Metabolic Reprogramming Mediated by the mTORC2-IRF4 Signaling Axis Is Essential for Macrophage Alternative Activation. *Immunity* 2016;45:817–30. <https://doi.org/10.1016/j.immuni.2016.09.016>.
- [231] Wang F, Zhang S, Vuckovic I, Jeon R, Lerman A, Folmes CD, et al. Glycolytic Stimulation Is Not a Requirement for M2 Macrophage Differentiation. *Cell Metabolism* 2018;28:463-475.e4. <https://doi.org/10.1016/j.cmet.2018.08.012>.
- [232] Huang SC-C, Everts B, Ivanova Y, O'Sullivan D, Nascimento M, Smith AM, et al. Cell-intrinsic lysosomal lipolysis is essential for alternative activation of macrophages. *Nat Immunol* 2014;15:846–55. <https://doi.org/10.1038/ni.2956>.
- [233] Haschemi A, Kosma P, Gille L, Evans CR, Burant CF, Starkl P, et al. The Sedoheptulose Kinase CARKL Directs Macrophage Polarization through Control of Glucose Metabolism. *Cell Metabolism* 2012;15:813–26. <https://doi.org/10.1016/j.cmet.2012.04.023>.
- [234] Sancak Y, Bar-Peled L, Zoncu R, Markhard AL, Nada S, Sabatini DM. Regulator-Rag Complex Targets mTORC1 to the Lysosomal Surface and Is Necessary for Its

- Activation by Amino Acids. *Cell* 2010;141:290–303. <https://doi.org/10.1016/j.cell.2010.02.024>.
- [235] Kimura T, Nada S, Takegahara N, Okuno T, Nojima S, Kang S, et al. Polarization of M2 macrophages requires Lamtor1 that integrates cytokine and amino-acid signals. *Nat Commun* 2016;7:13130. <https://doi.org/10.1038/ncomms13130>.
- [236] Puleston DJ, Buck MD, Klein Geltink RI, Kyle RL, Caputa G, O’Sullivan D, et al. Polyamines and eIF5A Hypusination Modulate Mitochondrial Respiration and Macrophage Activation. *Cell Metabolism* 2019;30:352–363.e8. <https://doi.org/10.1016/j.cmet.2019.05.003>.
- [237] Jha AK, Huang SC-C, Sergushichev A, Lampropoulou V, Ivanova Y, Loginicheva E, et al. Network Integration of Parallel Metabolic and Transcriptional Data Reveals Metabolic Modules that Regulate Macrophage Polarization. *Immunity* 2015;42:419–30. <https://doi.org/10.1016/j.immuni.2015.02.005>.
- [238] Wellen KE, Hatzivassiliou G, Sachdeva UM, Bui TV, Cross JR, Thompson CB. ATP-Citrate Lyase Links Cellular Metabolism to Histone Acetylation. *Science* 2009;324:1076–80. <https://doi.org/10.1126/science.1164097>.
- [239] Lauterbach MA, Hanke JE, Serefidou M, Mangan MSJ, Kolbe C-C, Hess T, et al. Toll-like Receptor Signaling Rewires Macrophage Metabolism and Promotes Histone Acetylation via ATP-Citrate Lyase. *Immunity* 2019;51:997–1011.e7. <https://doi.org/10.1016/j.immuni.2019.11.009>.
- [240] O’Neill LAJ, Artyomov MN. Itaconate: the poster child of metabolic reprogramming in macrophage function. *Nat Rev Immunol* 2019;19:273–81. <https://doi.org/10.1038/s41577-019-0128-5>.
- [241] Tannahill GM, Curtis AM, Adamik J, Palsson-McDermott EM, McGettrick AF, Goel G, et al. Succinate is an inflammatory signal that induces IL-1 β through HIF-1 α . *Nature* 2013;496:238–42. <https://doi.org/10.1038/nature11986>.
- [242] Cameron AM, Castoldi A, Sanin DE, Flachsmann LJ, Field CS, Puleston DanielJ, et al. Inflammatory macrophage dependence on NAD⁺ salvage is a consequence of reactive oxygen species-mediated DNA damage. *Nat Immunol* 2019;20:420–32. <https://doi.org/10.1038/s41590-019-0336-y>.
- [243] West AP, Brodsky IE, Rahner C, Woo DK, Erdjument-Bromage H, Tempst P, et al. TLR signalling augments macrophage bactericidal activity through mitochondrial ROS. *Nature* 2011;472:476–80. <https://doi.org/10.1038/nature09973>.
- [244] Liu P-S, Wang H, Li X, Chao T, Teav T, Christen S, et al. α -ketoglutarate orchestrates macrophage activation through metabolic and epigenetic reprogramming. *Nat Immunol* 2017;18:985–94. <https://doi.org/10.1038/ni.3796>.
- [245] Phan AT, Goldrath AW, Glass CK. Metabolic and Epigenetic Coordination of T Cell and Macrophage Immunity. *Immunity* 2017;46:714–29. <https://doi.org/10.1016/j.immuni.2017.04.016>.
- [246] Islam MdS, Leissing TM, Chowdhury R, Hopkinson RJ, Schofield CJ. 2-Oxoglutarate-Dependent Oxygenases. *Annu Rev Biochem* 2018;87:585–620. <https://doi.org/10.1146/annurev-biochem-061516-044724>.

- [247] Janke R, Iavarone AT, Rine J. Oncometabolite D-2-Hydroxyglutarate enhances gene silencing through inhibition of specific H3K36 histone demethylases. *ELife* 2017;6:e22451. <https://doi.org/10.7554/eLife.22451>.
- [248] Chowdhury R, Yeoh KK, Tian Y, Hillringhaus L, Bagg EA, Rose NR, et al. The oncometabolite 2-hydroxyglutarate inhibits histone lysine demethylases. *EMBO Rep* 2011;12:463–9. <https://doi.org/10.1038/embor.2011.43>.
- [249] Satoh T, Takeuchi O, Vandenbon A, Yasuda K, Tanaka Y, Kumagai Y, et al. The Jmjd3-Irf4 axis regulates M2 macrophage polarization and host responses against helminth infection. *Nat Immunol* 2010;11:936–44. <https://doi.org/10.1038/ni.1920>.
- [250] Czimmerer Z, Daniel B, Horvath A, Ruckerl D, Nagy G, Kiss M, et al. The Transcription Factor STAT6 Mediates Direct Repression of Inflammatory Enhancers and Limits Activation of Alternatively Polarized Macrophages. *Immunity* 2018;48:75–90.e6. <https://doi.org/10.1016/j.immuni.2017.12.010>.
- [251] Mullican SE, Gaddis CA, Alenghat T, Nair MG, Giacomini PR, Everett LJ, et al. Histone deacetylase 3 is an epigenomic brake in macrophage alternative activation. *Genes Dev* 2011;25:2480–8. <https://doi.org/10.1101/gad.175950.111>.
- [252] Hoeksema MA, Shen Z, Holtman IR, Zheng A, Spann NJ, Cobo I, et al. Mechanisms underlying divergent responses of genetically distinct macrophages to IL-4. *Sci Adv* 2021;7:eabf9808. <https://doi.org/10.1126/sciadv.abf9808>.
- [253] Cunningham KT, Finlay CM, Mills KHG. Helminth Imprinting of Hematopoietic Stem Cells Sustains Anti-Inflammatory Trained Innate Immunity That Attenuates Autoimmune Disease. *Jl* 2021;ji2001225. <https://doi.org/10.4049/jimmunol.2001225>.
- [254] Cortes-Selva D, Elvington AF, Ready A, Rajwa B, Pearce EJ, Randolph GJ, et al. *Schistosoma mansoni* Infection-Induced Transcriptional Changes in Hepatic Macrophage Metabolism Correlate With an Athero-Protective Phenotype. *Front Immunol* 2018;9:2580. <https://doi.org/10.3389/fimmu.2018.02580>.
- [255] Di Luzio NR, Williams DL. Protective effect of glucan against systemic *Staphylococcus aureus* septicemia in normal and leukemic mice. *Infect Immun* 1978;20:804–10. <https://doi.org/10.1128/iai.20.3.804-810.1978>.
- [256] Quintin J, Saeed S, Martens JHA, Giamarellos-Bourboulis EJ, Ifrim DC, Logie C, et al. *Candida albicans* Infection Affords Protection against Reinfection via Functional Reprogramming of Monocytes. *Cell Host & Microbe* 2012;12:223–32. <https://doi.org/10.1016/j.chom.2012.06.006>.
- [257] Cheng S-C, Quintin J, Cramer RA, Shepardson KM, Saeed S, Kumar V, et al. mTOR- and HIF-1 α -mediated aerobic glycolysis as metabolic basis for trained immunity. *Science* 2014;345:1250684. <https://doi.org/10.1126/science.1250684>.
- [258] Netea MG, Domínguez-Andrés J, Barreiro LB, Chavakis T, Divangahi M, Fuchs E, et al. Defining trained immunity and its role in health and disease. *Nat Rev Immunol* 2020;20:375–88. <https://doi.org/10.1038/s41577-020-0285-6>.
- [259] Verma D, Parasa VR, Raffetseder J, Martis M, Mehta RB, Netea M, et al. Anti-mycobacterial activity correlates with altered DNA methylation pattern in immune

- cells from BCG-vaccinated subjects. *Sci Rep* 2017;7:12305. <https://doi.org/10.1038/s41598-017-12110-2>.
- [260] Kaufmann E, Sanz J, Dunn JL, Khan N, Mendonça LE, Pacis A, et al. BCG Educates Hematopoietic Stem Cells to Generate Protective Innate Immunity against Tuberculosis. *Cell* 2018;172:176-190.e19. <https://doi.org/10.1016/j.cell.2017.12.031>.
- [261] Cirovic B, de Bree LCJ, Groh L, Blok BA, Chan J, van der Velden WJFM, et al. BCG Vaccination in Humans Elicits Trained Immunity via the Hematopoietic Progenitor Compartment. *Cell Host & Microbe* 2020;28:322-334.e5. <https://doi.org/10.1016/j.chom.2020.05.014>.
- [262] Domínguez-Andrés J, Novakovic B, Li Y, Scicluna BP, Gresnigt MS, Arts RJW, et al. The Itaconate Pathway Is a Central Regulatory Node Linking Innate Immune Tolerance and Trained Immunity. *Cell Metabolism* 2019;29:211-220.e5. <https://doi.org/10.1016/j.cmet.2018.09.003>.
- [263] Leijte GP, Kiers D, van der Heijden W, Jansen A, Gerretsen J, Boerrigter V, et al. Treatment With Acetylsalicylic Acid Reverses Endotoxin Tolerance in Humans In Vivo: A Randomized Placebo-Controlled Study. *Critical Care Medicine* 2019;47:508–16. <https://doi.org/10.1097/CCM.00000000000003630>.
- [264] Yao Y, Jeyanathan M, Haddadi S, Barra NG, Vaseghi-Shanjani M, Damjanovic D, et al. Induction of Autonomous Memory Alveolar Macrophages Requires T Cell Help and Is Critical to Trained Immunity. *Cell* 2018;175:1634-1650.e17. <https://doi.org/10.1016/j.cell.2018.09.042>.
- [265] Loukas A, Maizels RM, Hotez PJ. The yin and yang of human soil-transmitted helminth infections. *International Journal for Parasitology* 2021;51:1243–53. <https://doi.org/10.1016/j.ijpara.2021.11.001>.
- [266] Camberis M, Le Gros G, Urban J. Animal Model of *Nippostrongylus brasiliensis* and *Heligmosomoides polygyrus*. In: Coligan JE, Bierer BE, Margulies DH, Shevach EM, Strober W, editors. *Current Protocols in Immunology*, Hoboken, NJ, USA: John Wiley & Sons, Inc.; 2003, p. im1912s55. <https://doi.org/10.1002/0471142735.im1912s55>.
- [267] Reynolds LA, Filbey KJ, Maizels RM. Immunity to the model intestinal helminth parasite *Heligmosomoides polygyrus*. *Semin Immunopathol* 2012;34:829–46. <https://doi.org/10.1007/s00281-012-0347-3>.
- [268] McSorley HJ, Blair NF, Smith KA, McKenzie ANJ, Maizels RM. Blockade of IL-33 release and suppression of type 2 innate lymphoid cell responses by helminth secreted products in airway allergy. *Mucosal Immunology* 2014;7:1068–78. <https://doi.org/10.1038/mi.2013.123>.
- [269] Osbourn M, Soares DC, Vacca F, Cohen ES, Scott IC, Gregory WF, et al. HpARI Protein Secreted by a Helminth Parasite Suppresses Interleukin-33. *Immunity* 2017;47:739-751.e5. <https://doi.org/10.1016/j.immuni.2017.09.015>.
- [270] Vacca F, Chauché C, Jamwal A, Hinchy EC, Heieis G, Webster H, et al. A helminth-derived suppressor of ST2 blocks allergic responses. *ELife* 2020;9:e54017. <https://doi.org/10.7554/eLife.54017>.

- [271] Zaiss MM, Maslowski KM, Mosconi I, Guenat N, Marsland BJ, Harris NL. IL-1 β suppresses innate IL-25 and IL-33 production and maintains helminth chronicity. *PLoS Pathog* 2013;9:e1003531. <https://doi.org/10.1371/journal.ppat.1003531>.
- [272] Buck AH, Coakley G, Simbari F, McSorley HJ, Quintana JF, Le Bihan T, et al. Exosomes secreted by nematode parasites transfer small RNAs to mammalian cells and modulate innate immunity. *Nat Commun* 2014;5:5488. <https://doi.org/10.1038/ncomms6488>.
- [273] Coakley G, McCaskill JL, Borger JG, Simbari F, Robertson E, Millar M, et al. Extracellular Vesicles from a Helminth Parasite Suppress Macrophage Activation and Constitute an Effective Vaccine for Protective Immunity. *Cell Reports* 2017;19:1545–57. <https://doi.org/10.1016/j.celrep.2017.05.001>.
- [274] Tran N, Ricafrente A, To J, Lund M, Marques TM, Gama-Carvalho M, et al. *Fasciola hepatica* hijacks host macrophage miRNA machinery to modulate early innate immune responses. *Sci Rep* 2021;11:6712. <https://doi.org/10.1038/s41598-021-86125-1>.
- [275] Wang L, Liu T, Chen G, Li Y, Zhang S, Mao L, et al. Exosomal microRNA let-7-5p from *Taenia pisiformis* Cysticercus Prompted Macrophage to M2 Polarization through Inhibiting the Expression of C/EBP δ . *Microorganisms* 2021;9:1403. <https://doi.org/10.3390/microorganisms9071403>.
- [276] Wang L, Li Z, Shen J, Liu Z, Liang J, Wu X, et al. Exosome-like vesicles derived by *Schistosoma japonicum* adult worms mediates M1 type immune- activity of macrophage. *Parasitol Res* 2015;114:1865–73. <https://doi.org/10.1007/s00436-015-4373-7>.
- [277] Ball DH, Al-Riyami L, Harnett W, Harnett MM. IL-33/ST2 signalling and crosstalk with Fc ϵ RI and TLR4 is targeted by the parasitic worm product, ES-62. *Sci Rep* 2018;8:4497. <https://doi.org/10.1038/s41598-018-22716-9>.
- [278] Pineda MA, Lumb F, Harnett MM, Harnett W. ES-62, a therapeutic anti-inflammatory agent evolved by the filarial nematode *Acanthocheilonema viteae*. *Molecular and Biochemical Parasitology* 2014;194:1–8. <https://doi.org/10.1016/j.molbiopara.2014.03.003>.
- [279] Goodridge HS, McGUINNESS S, Houston KM, Egan CA, Al-Riyami L, Alcocer MJC, et al. Phosphorylcholine mimics the effects of ES-62 on macrophages and dendritic cells. *Parasite Immunol* 2007;29:127–37. <https://doi.org/10.1111/j.1365-3024.2006.00926.x>.
- [280] Goodridge HS, Wilson EH, Harnett W, Campbell CC, Harnett MM, Liew FY. Modulation of Macrophage Cytokine Production by ES-62, a Secreted Product of the Filarial Nematode *Acanthocheilonema viteae*. *J Immunol* 2001;167:940–5. <https://doi.org/10.4049/jimmunol.167.2.940>.
- [281] Ramos-Benítez MJ, Ruiz-Jiménez C, Aguayo V, Espino AM. Recombinant *Fasciola hepatica* fatty acid binding protein suppresses toll-like receptor stimulation in response to multiple bacterial ligands. *Sci Rep* 2017;7:5455. <https://doi.org/10.1038/s41598-017-05735-w>.

- [282] Donnelly S, O'Neill SM, Stack CM, Robinson MW, Turnbull L, Whitchurch C, et al. Helminth Cysteine Proteases Inhibit TRIF-dependent Activation of Macrophages via Degradation of TLR3. *Journal of Biological Chemistry* 2010;285:3383–92. <https://doi.org/10.1074/jbc.M109.060368>.
- [283] Retra K, deWalick S, Schmitz M, Yazdanbakhsh M, Tielens AGM, Brouwers JFHM, et al. The tegumental surface membranes of *Schistosoma mansoni* are enriched in parasite-specific phospholipid species. *International Journal for Parasitology* 2015;45:629–36. <https://doi.org/10.1016/j.ijpara.2015.03.011>.
- [284] van der Kleij D, Latz E, Brouwers JFHM, Kruize YCM, Schmitz M, Kurt-Jones EA, et al. A Novel Host-Parasite Lipid Cross-talk. *Journal of Biological Chemistry* 2002;277:48122–9. <https://doi.org/10.1074/jbc.M206941200>.
- [285] Noya V, Brossard N, Berasaín P, Rodríguez E, Chiale C, Mazal D, et al. A mucin-like peptide from *Fasciola hepatica* induces parasite-specific Th1-type cell immunity. *Parasitol Res* 2016;115:1053–63. <https://doi.org/10.1007/s00436-015-4834-z>.
- [286] Noya V, Brossard N, Rodríguez E, Dergan-Dylon LS, Carmona C, Rabinovich GA, et al. A mucin-like peptide from *Fasciola hepatica* instructs dendritic cells with parasite specific Th1-polarizing activity. *Sci Rep* 2017;7:40615. <https://doi.org/10.1038/srep40615>.
- [287] Manoury B, Gregory WF, Maizels RM, Watts C. Bm-CPI-2, a cystatin homolog secreted by the filarial parasite *Brugia malayi*, inhibits class II MHC-restricted antigen processing. *Current Biology* 2001;11:447–51. [https://doi.org/10.1016/S0960-9822\(01\)00118-X](https://doi.org/10.1016/S0960-9822(01)00118-X).
- [288] Pfaff AW, Schulz-Key H, Soboslay PT, Taylor DW, MacLennan K, Hoffmann WH. *Litomosoides sigmodontis* cystatin acts as an immunomodulator during experimental filariasis. *International Journal for Parasitology* 2002;8.
- [289] Schönemeyer A, Lucius R, Sonnenburg B, Brattig N, Sabat R, Schilling K, et al. Modulation of Human T Cell Responses and Macrophage Functions by Onchocystatin, a Secreted Protein of the Filarial Nematode *Onchocerca volvulus*. *J Immunol* 2001;167:3207–15. <https://doi.org/10.4049/jimmunol.167.6.3207>.
- [290] Daniłowicz-Luebert E, Steinfeld S, Kühl AA, Drozdenko G, Lucius R, Worm M, et al. A nematode immunomodulator suppresses grass pollen-specific allergic responses by controlling excessive Th2 inflammation. *International Journal for Parasitology* 2013;43:201–10. <https://doi.org/10.1016/j.ijpara.2012.10.014>.
- [291] Ziegler T, Rausch S, Steinfeld S, Klotz C, Hepworth MR, Kühl AA, et al. A Novel Regulatory Macrophage Induced by a Helminth Molecule Instructs IL-10 in CD4⁺ T Cells and Protects against Mucosal Inflammation. *J Immunol* 2015;194:1555–64. <https://doi.org/10.4049/jimmunol.1401217>.
- [292] Wang S, Xie Y, Yang X, Wang X, Yan K, Zhong Z, et al. Therapeutic potential of recombinant cystatin from *Schistosoma japonicum* in TNBS-induced experimental colitis of mice. *Parasites Vectors* 2016;9:6. <https://doi.org/10.1186/s13071-015-1288-1>.
- [293] Coronado S, Barrios L, Zakzuk J, Regino R, Ahumada V, Franco L, et al. A recombinant cystatin from *Ascaris lumbricoides* attenuates inflammation of DSS-

- induced colitis. *Parasite Immunol* 2017;39:e12425. <https://doi.org/10.1111/pim.12425>.
- [294] Jang SW, Cho MK, Park MK, Kang SA, Na B-K, Ahn SC, et al. Parasitic Helminth Cystatin Inhibits DSS-Induced Intestinal Inflammation Via IL-10 + F4/80 + Macrophage Recruitment. *Korean J Parasitol* 2011;49:245. <https://doi.org/10.3347/kjp.2011.49.3.245>.
- [295] Kobpornchai P, Flynn RJ, Reamtong O, Rittisoonthorn N, Kosoltanapiwat N, Boonnak K, et al. A novel cystatin derived from *Trichinella spiralis* suppresses macrophage-mediated inflammatory responses. *PLoS Negl Trop Dis* 2020;14:e0008192. <https://doi.org/10.1371/journal.pntd.0008192>.
- [296] Dainichi T, Maekawa Y, Ishii K, Zhang T, Nashed BF, Sakai T, et al. Nippocystatin, a Cysteine Protease Inhibitor from *Nippostrongylus brasiliensis*, Inhibits Antigen Processing and Modulates Antigen-Specific Immune Response. *Infect Immun* 2001;69:7380–6. <https://doi.org/10.1128/IAI.69.12.7380-7386.2001>.
- [297] Sanin DE, Prendergast CT, Mountford AP. IL-10 Production in Macrophages Is Regulated by a TLR-Driven CREB-Mediated Mechanism That Is Linked to Genes Involved in Cell Metabolism. *The Journal of Immunology* 2015;195:1218–32. <https://doi.org/10.4049/jimmunol.1500146>.
- [298] Vermeire JJ, Cho Y, Lolis E, Bucala R, Cappello M. Orthologs of macrophage migration inhibitory factor from parasitic nematodes. *Trends in Parasitology* 2008;24:355–63. <https://doi.org/10.1016/j.pt.2008.04.007>.
- [299] Zang X, Taylor P, Wang JM, Meyer DJ, Scott AL, Walkinshaw MD, et al. Homologues of Human Macrophage Migration Inhibitory Factor from a Parasitic Nematode: GENE CLONING, PROTEIN ACTIVITY, AND CRYSTAL STRUCTURE. *J Biol Chem* 2002;277:44261–7. <https://doi.org/10.1074/jbc.M204655200>.
- [300] Tan THP, Edgerton SAV, Kumari R, McALISTER MSB, Rowe SM, Nagl S, et al. Macrophage migration inhibitory factor of the parasitic nematode *Trichinella spiralis*. *Biochemical Journal* 2001;357:373–83. <https://doi.org/10.1042/bj3570373>.
- [301] Stavitsky AB, Metz C, Liu S, Xianli J, Bucala R. Blockade of macrophage migration inhibitory factor (MIF) in *Schistosoma japonicum*-infected mice results in an increased adult worm burden and reduced fecundity. *Parasite Immunol* 2003;25:369–74. <https://doi.org/10.1046/j.1365-3024.2003.00641.x>.
- [302] Filbey KJ, Varyani F, Harcus Y, Hewitson JP, Smyth DJ, McSorley HJ, et al. Macrophage Migration Inhibitory Factor (MIF) Is Essential for Type 2 Effector Cell Immunity to an Intestinal Helminth Parasite. *Front Immunol* 2019;10:2375. <https://doi.org/10.3389/fimmu.2019.02375>.
- [303] Prieto-Lafuente L, Gregory WF, Allen JE, Maizels RM. MIF homologues from a filarial nematode parasite synergize with IL-4 to induce alternative activation of host macrophages. *Journal of Leukocyte Biology* 2009;85:844–54. <https://doi.org/10.1189/jlb.0808459>.
- [304] Robinson MW, Donnelly S, Hutchinson AT, To J, Taylor NL, Norton RS, et al. A Family of Helminth Molecules that Modulate Innate Cell Responses via Molecular Mimicry of Host Antimicrobial Peptides. *PLoS Pathogens* 2011;7.

- [305] Robinson MW, Alvarado R, To J, Hutchinson AT, Dowdell SN, Lund M, et al. A helminth cathelicidin-like protein suppresses antigen processing and presentation in macrophages *via* inhibition of lysosomal vATPase. *FASEB j* 2012;26:4614–27. <https://doi.org/10.1096/fj.12-213876>.
- [306] Alvarado R, To J, Lund ME, Pinar A, Mansell A, Robinson MW, et al. The immune modulatory peptide FhHDM-1 secreted by the helminth *Fasciola hepatica* prevents NLRP3 inflammasome activation by inhibiting endolysosomal acidification in macrophages. *FASEB J* 2017;31:85–95. <https://doi.org/10.1096/fj.201500093R>.
- [307] Quinteros SL, von Krusenstiern E, Snyder NW, Tanaka A, O'Brien B, Donnelly S. The helminth derived peptide FhHDM-1 redirects macrophage metabolism towards glutaminolysis to regulate the pro-inflammatory response. *Front Immunol* 2023;14:1018076. <https://doi.org/10.3389/fimmu.2023.1018076>.
- [308] Everts B, Perona-Wright G, Smits HH, Hokke CH, van der Ham AJ, Fitzsimmons CM, et al. Omega-1, a glycoprotein secreted by *Schistosoma mansoni* eggs, drives Th2 responses. *Journal of Experimental Medicine* 2009;206:1673–80. <https://doi.org/10.1084/jem.20082460>.
- [309] Everts B, Hussaarts L, Driessen NN, Meevissen MHJ, Schramm G, van der Ham AJ, et al. Schistosome-derived omega-1 drives Th2 polarization by suppressing protein synthesis following internalization by the mannose receptor. *Journal of Experimental Medicine* 2012;209:1753–67. <https://doi.org/10.1084/jem.20111381>.
- [310] Steinfelder S, Andersen JF, Cannons JL, Feng CG, Joshi M, Dwyer D, et al. The major component in schistosome eggs responsible for conditioning dendritic cells for Th2 polarization is a T2 ribonuclease (omega-1). *Journal of Experimental Medicine* 2009;206:1681–90. <https://doi.org/10.1084/jem.20082462>.
- [311] Wilbers RHP, Westerhof LB, van Noort K, Obieglo K, Driessen NN, Everts B, et al. Production and glyco-engineering of immunomodulatory helminth glycoproteins in plants. *Sci Rep* 2017;7:45910. <https://doi.org/10.1038/srep45910>.
- [312] Ke X-D, Shen S, Song L-J, Yu C-X, Kikuchi M, Hirayama K, et al. Characterization of *Schistosoma japonicum* CP1412 protein as a novel member of the ribonuclease T2 molecule family with immune regulatory function. *Parasites Vectors* 2017;10:89. <https://doi.org/10.1186/s13071-016-1962-y>.
- [313] Zaccone P, Burton OT, Gibbs SE, Miller N, Jones FM, Schramm G, et al. The *S. mansoni* glycoprotein ω -1 induces Foxp3 expression in NOD mouse CD4⁺ T cells. *Eur J Immunol* 2011;41:2709–18. <https://doi.org/10.1002/eji.201141429>.
- [314] Ferguson BJ, Newland SA, Gibbs SE, Turlomousis P, Fernandes dos Santos P, Patel MN, et al. The *Schistosoma mansoni* T2 ribonuclease omega-1 modulates inflammasome-dependent IL-1 β secretion in macrophages. *International Journal for Parasitology* 2015;45:809–13. <https://doi.org/10.1016/j.ijpara.2015.08.005>.
- [315] Crowe J, Lumb FE, Harnett MM, Harnett W. Parasite excretory-secretory products and their effects on metabolic syndrome. *Parasite Immunol* 2017;39:e12410. <https://doi.org/10.1111/pim.12410>.

- [316] Wiria AE, Sartono E, Supali T, Yazdanbakhsh M. Helminth Infections, Type-2 Immune Response, and Metabolic Syndrome. *PLoS Pathog* 2014;10:e1004140. <https://doi.org/10.1371/journal.ppat.1004140>.
- [317] Husaarts L, García-Tardón N, Beek L, Heemskerk MM, Haerberlein S, Zon GC, et al. Chronic helminth infection and helminth-derived egg antigens promote adipose tissue M2 macrophages and improve insulin sensitivity in obese mice. *FASEB j* 2015;29:3027–39. <https://doi.org/10.1096/fj.14-266239>.
- [318] Wolfs IMJ, Stöger JL, Goossens P, Pöttgens C, Gijbels MJJ, Wijnands E, et al. Reprogramming macrophages to an anti-inflammatory phenotype by helminth antigens reduces murine atherosclerosis. *FASEB j* 2014;28:288–99. <https://doi.org/10.1096/fj.13-235911>.
- [319] Hams E, Bermingham R, Wurlod FA, Hogan AE, O'Shea D, Preston RJ, et al. The helminth T2 RNase ω 1 promotes metabolic homeostasis in an IL-33- and group 2 innate lymphoid cell-dependent mechanism. *FASEB j* 2016;30:824–35. <https://doi.org/10.1096/fj.15-277822>.
- [320] Gomez-Escobar N, Bennett C, Prieto-Lafuente L, Aebischer T, Blackburn CC, Maizels RM. Heterologous expression of the filarial nematode alt gene products reveals their potential to inhibit immune function. *BMC Biol* 2005;3:8. <https://doi.org/10.1186/1741-7007-3-8>.
- [321] Sun X, Yang F, Shen J, Liu Z, Liang J, Zheng H, et al. Recombinant Sj16 from *Schistosoma japonicum* contains a functional N-terminal nuclear localization signal necessary for nuclear translocation in dendritic cells and interleukin-10 production. *Parasitol Res* 2016;115:4559–71. <https://doi.org/10.1007/s00436-016-5247-3>.
- [322] Culley FJ, Brown A, Conroy DM, Sabroe I, Pritchard DI, Williams TJ. Eotaxin Is Specifically Cleaved by Hookworm Metalloproteases Preventing Its Action In Vitro and In Vivo. *The Journal of Immunology* 2000;165:6447–53. <https://doi.org/10.4049/jimmunol.165.11.6447>.
- [323] Smith P, Fallon RE, Mangan NE, Walsh CM, Saraiva M, Sayers JR, et al. *Schistosoma mansoni* secretes a chemokine binding protein with antiinflammatory activity. *Journal of Experimental Medicine* 2005;202:1319–25. <https://doi.org/10.1084/jem.20050955>.
- [324] Moyle M, Foster DL, McGrath DE, Brown SM, Laroche Y, De Meutter J, et al. A hookworm glycoprotein that inhibits neutrophil function is a ligand of the integrin CD11b/CD18. *J Biol Chem* 1994;269:10008–15.
- [325] Chen W, ten Dijke P. Immunoregulation by members of the TGF β superfamily. *Nat Rev Immunol* 2016;16:723–40. <https://doi.org/10.1038/nri.2016.112>.
- [326] Gomez-Escobar N, Gregory WF, Maizels RM. Identification of *tgh-2*, a Filarial Nematode Homolog of *Caenorhabditis elegans daf-7* and Human Transforming Growth Factor β , Expressed in Microfilarial and Adult Stages of *Brugia malayi*. *Infect Immun* 2000;68:6402–10. <https://doi.org/10.1128/IAI.68.11.6402-6410.2000>.
- [327] Hartmann W, Schramm C, Breloer M. *Litomosoides sigmodontis* induces TGF- β receptor responsive, IL-10-producing T cells that suppress bystander T-cell

- proliferation in mice: Immunomodulation. *Eur J Immunol* 2015;45:2568–81. <https://doi.org/10.1002/eji.201545503>.
- [328] Sulaiman AA, Zolnierczyk K, Japa O, Owen JP, Maddison BC, Emes RD, et al. A Trematode Parasite Derived Growth Factor Binds and Exerts Influences on Host Immune Functions via Host Cytokine Receptor Complexes. *PLoS Pathog* 2016;12:e1005991. <https://doi.org/10.1371/journal.ppat.1005991>.
- [329] Grainger JR, Smith KA, Hewitson JP, McSorley HJ, Harcus Y, Filbey KJ, et al. Helminth secretions induce de novo T cell Foxp3 expression and regulatory function through the TGF- β pathway. *J Exp Med* 2010;207:2331–41. <https://doi.org/10.1084/jem.20101074>.
- [330] Johnston CJC, Smyth DJ, Kodali RB, White MPJ, Harcus Y, Filbey KJ, et al. A structurally distinct TGF- β mimic from an intestinal helminth parasite potently induces regulatory T cells. *Nat Commun* 2017;8:1741. <https://doi.org/10.1038/s41467-017-01886-6>.
- [331] Navarro S, Pickering DA, Ferreira IB, Jones L, Ryan S, Troy S, et al. Hookworm recombinant protein promotes regulatory T cell responses that suppress experimental asthma. *Sci Transl Med* 2016;8:362ra143. <https://doi.org/10.1126/scitranslmed.aaf8807>.
- [332] De Araújo CAA, Perini A, Martins MA, Macedo MS, Macedo-Soares MF. PAS-1, an *Ascaris suum* Protein, Modulates Allergic Airway Inflammation via CD8+ $\gamma\delta$ TCR+ and CD4+ CD25+ FoxP3+ T Cells: PAS-1 Suppresses Allergic Responses via TREG Cells. *Scandinavian Journal of Immunology* 2010;72:491–503. <https://doi.org/10.1111/j.1365-3083.2010.02465.x>.
- [333] Chhabra S, Chang SC, Nguyen HM, Huq R, Tanner MR, Londono LM, et al. Kv1.3 channel-blocking immunomodulatory peptides from parasitic worms: implications for autoimmune diseases. *FASEB j* 2014;28:3952–64. <https://doi.org/10.1096/fj.14-251967>.
- [334] Harris N, Gause WC. To B or not to B: B cells and the Th2-type immune response to helminths. *Trends in Immunology* 2011;32:80–8. <https://doi.org/10.1016/j.it.2010.11.005>.
- [335] Deehan MR, Harnett W, Harnett MM. A Filarial Nematode-Secreted Phosphorylcholine-Containing Glycoprotein Uncouples the B Cell Antigen Receptor from Extracellular Signal-Regulated Kinase-Mitogen-Activated Protein Kinase by Promoting the Surface Ig-Mediated Recruitment of Src Homology 2 Domain-Containing Tyrosine Phosphatase-1 and Pac-1 Mitogen-Activated Kinase-Phosphatase. *The Journal of Immunology* 2001;166:7462–8. <https://doi.org/10.4049/jimmunol.166.12.7462>.
- [336] Tribolet L, Cantacessi C, Pickering DA, Navarro S, Doolan DL, Trieu A, et al. Probing of a Human Proteome Microarray With a Recombinant Pathogen Protein Reveals a Novel Mechanism by Which Hookworms Suppress B-Cell Receptor Signaling. *J Infect Dis* 2015;211:416–25. <https://doi.org/10.1093/infdis/jiu451>.
- [337] Haeberlein S, Obieglo K, Ozir-Fazalalikhani A, Chayé MAM, Veninga H, van der Vlugt LEPM, et al. Schistosome egg antigens, including the glycoprotein IPSE/alpha-1,

- trigger the development of regulatory B cells. *PLoS Pathog* 2017;13:e1006539. <https://doi.org/10.1371/journal.ppat.1006539>.
- [338] Cardoso LS, Oliveira SC, Góes AM, Oliveira RR, Pacífico LG, Marinho FV, et al. Schistosoma mansoni antigens modulate the allergic response in a murine model of ovalbumin-induced airway inflammation: S. mansoni antigens modulate allergy. *Clinical & Experimental Immunology* 2010;160:266–74. <https://doi.org/10.1111/j.1365-2249.2009.04084.x>.
- [339] Bohnacker S, Troisi F, de los Reyes Jiménez M, Esser-von Bieren J. What Can Parasites Tell Us About the Pathogenesis and Treatment of Asthma and Allergic Diseases. *Front Immunol* 2020;11:2106. <https://doi.org/10.3389/fimmu.2020.02106>.
- [340] Maizels RM. Parasitic helminth infections and the control of human allergic and autoimmune disorders. *Clin Microbiol Infect* 2016;22:481–6. <https://doi.org/10.1016/j.cmi.2016.04.024>.
- [341] Asher MI, Montefort S, Björkstén B, Lai CK, Strachan DP, Weiland SK, et al. Worldwide time trends in the prevalence of symptoms of asthma, allergic rhinoconjunctivitis, and eczema in childhood: ISAAC Phases One and Three repeat multicountry cross-sectional surveys. *The Lancet* 2006;368:733–43. [https://doi.org/10.1016/S0140-6736\(06\)69283-0](https://doi.org/10.1016/S0140-6736(06)69283-0).
- [342] Gale EAM. The Rise of Childhood Type 1 Diabetes in the 20th Century. *Diabetes* 2002;51:3353–61. <https://doi.org/10.2337/diabetes.51.12.3353>.
- [343] Economou M, Pappas G. New global map of Crohn's disease: Genetic, environmental, and socioeconomic correlations: *Inflammatory Bowel Diseases* 2008;14:709–20. <https://doi.org/10.1002/ibd.20352>.
- [344] Braman SS. The Global Burden of Asthma. *Chest* 2006;130:4S-12S. https://doi.org/10.1378/chest.130.1_suppl.4S.
- [345] Nicolaou N, Siddique N, Custovic A. Allergic disease in urban and rural populations: increasing prevalence with increasing urbanization. *Allergy* 2005;60:1357–60. <https://doi.org/10.1111/j.1398-9995.2005.00961.x>.
- [346] von Mutius E. Asthma and Allergies in Rural Areas of Europe. *Proceedings of the American Thoracic Society* 2007;4:212–6. <https://doi.org/10.1513/pats.200701-028AW>.
- [347] Palmer LJ, Celedón JC, Weiss ST, Wang B, Fang Z, Xu X. *Ascaris lumbricoides* infection is associated with increased risk of childhood asthma and atopy in rural China. *Am J Respir Crit Care Med* 2002;165:1489–93. <https://doi.org/10.1164/rccm.2107020>.
- [348] Dold S, Heinrich J, Wichmann HE, Wjst M. *Ascaris*-specific IgE and allergic sensitization in a cohort of school children in the former East Germany. *J Allergy Clin Immunol* 1998;102:414–20. [https://doi.org/10.1016/s0091-6749\(98\)70129-0](https://doi.org/10.1016/s0091-6749(98)70129-0).
- [349] Obihara CC, Beyers N, Gie RP, Hoekstra MO, Fincham JE, Marais BJ, et al. Respiratory atopic disease, *Ascaris*-immunoglobulin E and tuberculin testing in urban South African children. *Clin Exp Allergy* 2006;36:640–8. <https://doi.org/10.1111/j.1365-2222.2006.02479.x>.

- [350] Joubert JR, van Schalkwyk DJ, Turner KJ. *Ascaris lumbricoides* and the human immunogenic response: enhanced IgE-mediated reactivity to common inhaled allergens. *S Afr Med J* 1980;57:409–12.
- [351] Altintop L, Cakar B, Hokelek M, Bektas A, Yildiz L, Karaoglanoglu M. *Strongyloides stercoralis* hyperinfection in a patient with rheumatoid arthritis and bronchial asthma: a case report. *Ann Clin Microbiol Antimicrob* 2010;9:27. <https://doi.org/10.1186/1476-0711-9-27>.
- [352] Dunlap NE, Shin MS, Polt SS, Ho KJ. Strongyloidiasis manifested as asthma. *South Med J* 1984;77:77–8. <https://doi.org/10.1097/00007611-198401000-00021>.
- [353] Buijs J, Borsboom G, Renting M, Hilgersom WJ, van Wieringen JC, Jansen G, et al. Relationship between allergic manifestations and *Toxocara* seropositivity: a cross-sectional study among elementary school children. *Eur Respir J* 1997;10:1467–75. <https://doi.org/10.1183/09031936.97.10071467>.
- [354] Lynch NR, Hagel I, Perez M, Di Prisco MC, Lopez R, Alvarez N. Effect of anthelmintic treatment on the allergic reactivity of children in a tropical slum. *J Allergy Clin Immunol* 1993;92:404–11. [https://doi.org/10.1016/0091-6749\(93\)90119-z](https://doi.org/10.1016/0091-6749(93)90119-z).
- [355] van den Biggelaar AHJ, Rodrigues LC, van Ree R, van der Zee JS, Hoeksma-Kruize YCM, Souverijn JHM, et al. Long-term treatment of intestinal helminths increases mite skin-test reactivity in Gabonese schoolchildren. *J Infect Dis* 2004;189:892–900. <https://doi.org/10.1086/381767>.
- [356] Borkow G, Leng Q, Weisman Z, Stein M, Galai N, Kalinkovich A, et al. Chronic immune activation associated with intestinal helminth infections results in impaired signal transduction and anergy. *J Clin Invest* 2000;106:1053–60.
- [357] Stein M, Greenberg Z, Boaz M, Handzel ZT, Meshesha MK, Bentwich Z. The Role of Helminth Infection and Environment in the Development of Allergy: A Prospective Study of Newly-Arrived Ethiopian Immigrants in Israel. *PLoS Negl Trop Dis* 2016;10:e0004208. <https://doi.org/10.1371/journal.pntd.0004208>.
- [358] van den Biggelaar AH, van Ree R, Rodrigues LC, Lell B, Deelder AM, Kremsner PG, et al. Decreased atopy in children infected with *Schistosoma haematobium*: a role for parasite-induced interleukin-10. *Lancet* 2000;356:1723–7. [https://doi.org/10.1016/S0140-6736\(00\)03206-2](https://doi.org/10.1016/S0140-6736(00)03206-2).
- [359] Araujo MIA, Hoppe B, Medeiros M, Alcântara L, Almeida MC, Schriefer A, et al. Impaired T helper 2 response to aeroallergen in helminth-infected patients with asthma. *J Infect Dis* 2004;190:1797–803. <https://doi.org/10.1086/425017>.
- [360] Scrivener S, Yemaneberhan H, Zebenigus M, Tilahun D, Girma S, Ali S, et al. Independent effects of intestinal parasite infection and domestic allergen exposure on risk of wheeze in Ethiopia: a nested case-control study. *Lancet* 2001;358:1493–9. [https://doi.org/10.1016/S0140-6736\(01\)06579-5](https://doi.org/10.1016/S0140-6736(01)06579-5).
- [361] Smits HH, Hammad H, van Nimwegen M, Soullie T, Willart MA, Lievers E, et al. Protective effect of *Schistosoma mansoni* infection on allergic airway inflammation depends on the intensity and chronicity of infection. *J Allergy Clin Immunol* 2007;120:932–40. <https://doi.org/10.1016/j.jaci.2007.06.009>.

- [362] Nayak DP, Kelley GW. Synergistic Effect of *Ascaris* Migration and Influenza Infection in Mice. *The Journal of Parasitology* 1965;51:297. <https://doi.org/10.2307/3276103>.
- [363] Wescott RB, Todd AC. Interaction of *Nippostrongylus brasiliensis* and Influenza Virus in Mice. I. Influence of the Nematode on the Virus. *The Journal of Parasitology* 1966;52:242. <https://doi.org/10.2307/3276478>.
- [364] Chowaniec W, Wescott RB, Congdon LL. Interaction of *Nematospiroides dubius* and influenza virus in mice. *Experimental Parasitology* 1972;32:33–44. [https://doi.org/10.1016/0014-4894\(72\)90007-0](https://doi.org/10.1016/0014-4894(72)90007-0).
- [365] King IL, Mohrs K, Meli AP, Downey J, Lanthier P, Tzelepis F, et al. Intestinal helminth infection impacts the systemic distribution and function of the naive lymphocyte pool. *Mucosal Immunology* 2017;10:1160–8. <https://doi.org/10.1038/mi.2016.127>.
- [366] Furze RC, Hussell T, Selkirk ME. Amelioration of Influenza-Induced Pathology in Mice by Coinfection with *Trichinella spiralis*. *Infect Immun* 2006;74:1924–32. <https://doi.org/10.1128/IAI.74.3.1924-1932.2006>.
- [367] Osborne LC, Monticelli LA, Nice TJ, Sutherland TE, Siracusa MC, Hepworth MR, et al. Virus-helminth coinfection reveals a microbiota-independent mechanism of immunomodulation. *Science* 2014;345:578–82. <https://doi.org/10.1126/science.1256942>.
- [368] Lanzer KG, Cookenham T, Reiley WW, Blackman MA. Virtual memory cells make a major contribution to the response of aged influenza-naïve mice to influenza virus infection. *Immun Ageing* 2018;15:17. <https://doi.org/10.1186/s12979-018-0122-y>.
- [369] Quinn KM, Hussain T. Bystanders or real players: virtual memory T cells keep chronic infections in check. *Cell Mol Immunol* 2020;17:797–8. <https://doi.org/10.1038/s41423-020-0469-9>.
- [370] Rolot M, Dougall AM, Chetty A, Javaux J, Chen T, Xiao X, et al. Helminth-induced IL-4 expands bystander memory CD8+ T cells for early control of viral infection. *Nat Commun* 2018;9:4516. <https://doi.org/10.1038/s41467-018-06978-5>.
- [371] Scheer S, Krempl C, Kallfass C, Frey S, Jakob T, Mouahid G, et al. *S. mansoni* Bolsters Anti-Viral Immunity in the Murine Respiratory Tract. *PLoS ONE* 2014;9:e112469. <https://doi.org/10.1371/journal.pone.0112469>.
- [372] McFarlane AJ, McSorley HJ, Davidson DJ, Fitch PM, Errington C, Mackenzie KJ, et al. Enteric helminth-induced type I interferon signaling protects against pulmonary virus infection through interaction with the microbiota. *Journal of Allergy and Clinical Immunology* 2017;140:1068-1078.e6. <https://doi.org/10.1016/j.jaci.2017.01.016>.
- [373] Stefan KL, Kim MV, Iwasaki A, Kasper DL. Commensal Microbiota Modulation of Natural Resistance to Virus Infection. *Cell* 2020;183:1312-1324.e10. <https://doi.org/10.1016/j.cell.2020.10.047>.
- [374] Abt MC, Osborne LC, Monticelli LA, Doering TA, Alenghat T, Sonnenberg GF, et al. Commensal Bacteria Calibrate the Activation Threshold of Innate Antiviral Immunity. *Immunity* 2012;37:158–70. <https://doi.org/10.1016/j.immuni.2012.04.011>.

- [375] Webb LM, Lundie RJ, Borger JG, Brown SL, Connor LM, Cartwright AN, et al. Type I interferon is required for T helper (Th) 2 induction by dendritic cells. *EMBO J* 2017;36:2404–18. <https://doi.org/10.15252/embj.201695345>.
- [376] Obieglo K, Costain A, Webb LM, Ozir-Fazalalikhani A, Brown SL, MacDonald AS, et al. Type I interferons provide additive signals for murine regulatory B cell induction by *Schistosoma mansoni* eggs. *Eur J Immunol* 2019;49:1226–34. <https://doi.org/10.1002/eji.201847858>.
- [377] Hartmann W, Brunn M-L, Stetter N, Gagliani N, Muscate F, Stanelle-Bertram S, et al. Helminth Infections Suppress the Efficacy of Vaccination against Seasonal Influenza. *Cell Reports* 2019;29:2243-2256.e4. <https://doi.org/10.1016/j.celrep.2019.10.051>.
- [378] Cepon-Robins TJ, Gildner TE. Old friends meet a new foe. *Evolution, Medicine, and Public Health* 2020;2020:234–48. <https://doi.org/10.1093/emph/eoaa037>.
- [379] Siles-Lucas M, González-Miguel J, Geller R, Sanjuan R, Pérez-Arévalo J, Martínez-Moreno Á. Potential Influence of Helminth Molecules on COVID-19 Pathology. *Trends in Parasitology* 2021;37:11–4. <https://doi.org/10.1016/j.pt.2020.10.002>.
- [380] Bradbury RS, Piedrafita D, Greenhill A, Mahanty S. Will helminth co-infection modulate COVID-19 severity in endemic regions? *Nat Rev Immunol* 2020;20:342–342. <https://doi.org/10.1038/s41577-020-0330-5>.
- [381] Paniz-Mondolfi AE, Ramírez JD, Delgado-Noguera LA, Rodriguez-Morales AJ, Sordillo EM. COVID-19 and helminth infection: Beyond the Th1/Th2 paradigm. *PLoS Negl Trop Dis* 2021;15:e0009402. <https://doi.org/10.1371/journal.pntd.0009402>.
- [382] Lamers MM, Beumer J, van der Vaart J, Knoop K, Puschhof J, Breugem TI, et al. SARS-CoV-2 productively infects human gut enterocytes. *Science* 2020;369:50–4. <https://doi.org/10.1126/science.abc1669>.
- [383] Wolday D, Gebrecherkos T, Arefaine ZG, Kiros YK, Gebreegzabher A, Tasew G, et al. Effect of co-infection with intestinal parasites on COVID-19 severity: A prospective observational cohort study. *EClinicalMedicine* 2021;39:101054. <https://doi.org/10.1016/j.eclinm.2021.101054>.
- [384] Hilligan KL, Oyesola OO, Namasivayam S, Howard N, Clancy CS, Oland SD, et al. Helminth exposure protects against murine SARS-CoV-2 infection through macrophage dependent T cell activation. *BioRxiv* 2022:2022.11.09.515832. <https://doi.org/10.1101/2022.11.09.515832>.
- [385] Glaser KB, Asmis R, Dennis EA. Bacterial lipopolysaccharide priming of P388D1 macrophage-like cells for enhanced arachidonic acid metabolism. Platelet-activating factor receptor activation and regulation of phospholipase A2. *Journal of Biological Chemistry* 1990;265:8658–64. [https://doi.org/10.1016/S0021-9258\(19\)38938-0](https://doi.org/10.1016/S0021-9258(19)38938-0).
- [386] Mouchlis VD, Dennis EA. Phospholipase A2 catalysis and lipid mediator lipidomics. *Biochimica et Biophysica Acta (BBA) - Molecular and Cell Biology of Lipids* 2019;1864:766–71. <https://doi.org/10.1016/j.bbalip.2018.08.010>.
- [387] Samuelsson B, Hammarström S. Leukotrienes: A Novel Group of Biologically Active Compounds. *Vitamins & Hormones*, vol. 39, Elsevier; 1982, p. 1–30. [https://doi.org/10.1016/S0083-6729\(08\)61134-6](https://doi.org/10.1016/S0083-6729(08)61134-6).

- [388] Samuelsson B. Leukotrienes: Mediators of Immediate Hypersensitivity Reactions and Inflammation. *Science* 1983;220:568–75. <https://doi.org/10.1126/science.6301011>.
- [389] Vane JR, Moncada S. Polyunsaturated fatty acids as precursors of prostaglandins. *Acta Cardiol Suppl* 1979:21–37.
- [390] Maycock AL, Anderson MS, DeSousa DM, Kuehl FA. Leukotriene A4: preparation and enzymatic conversion in a cell-free system to leukotriene B4. *Journal of Biological Chemistry* 1982;257:13911–4. [https://doi.org/10.1016/S0021-9258\(19\)45318-0](https://doi.org/10.1016/S0021-9258(19)45318-0).
- [391] Jakschik BA, Harper T, Murphy RC. Leukotriene C4 and D4 formation by particulate enzymes. *Journal of Biological Chemistry* 1982;257:5346–9. [https://doi.org/10.1016/S0021-9258\(19\)83782-1](https://doi.org/10.1016/S0021-9258(19)83782-1).
- [392] Anderson ME, Allison RD, Meister A. Interconversion of leukotrienes catalyzed by purified gamma-glutamyl transpeptidase: concomitant formation of leukotriene D4 and gamma-glutamyl amino acids. *Proc Natl Acad Sci USA* 1982;79:1088–91. <https://doi.org/10.1073/pnas.79.4.1088>.
- [393] Lee CW, Lewis RA, Corey EJ, Austen KF. Conversion of leukotriene D4 to leukotriene E4 by a dipeptidase released from the specific granule of human polymorphonuclear leucocytes. *Immunology* 1983;48:27–35.
- [394] Goodarzi K, Goodarzi M, Tager AM, Luster AD, von Andrian UH. Leukotriene B4 and BLT1 control cytotoxic effector T cell recruitment to inflamed tissues. *Nat Immunol* 2003;4:965–73. <https://doi.org/10.1038/ni972>.
- [395] Oliveira SHP, Canetti C, Ribeiro RA, Cunha FQ. Neutrophil Migration Induced by IL-1 β Depends upon LTB4 Released by Macrophages and upon TNF- α and IL-1 β Released by Mast Cells. *Inflammation* 2008;31:36–46. <https://doi.org/10.1007/s10753-007-9047-x>.
- [396] Salimi M, Stöger L, Liu W, Go S, Pavord I, Klenerman P, et al. Cysteinyl leukotriene E4 activates human group 2 innate lymphoid cells and enhances the effect of prostaglandin D2 and epithelial cytokines. *Journal of Allergy and Clinical Immunology* 2017;140:1090-1100.e11. <https://doi.org/10.1016/j.jaci.2016.12.958>.
- [397] Weiss JW, Drazen JM, Coles N, McFadden ER, Weller PF, Corey EJ, et al. Bronchoconstrictor Effects of Leukotriene C in Humans. *Science* 1982;216:196–8. <https://doi.org/10.1126/science.7063880>.
- [398] Panettieri RA, Tan EML, Ciocca V, Luttmann MA, Leonard TB, Hay DWP. Effects of LTD₄ on Human Airway Smooth Muscle Cell Proliferation, Matrix Expression, and Contraction *In Vitro*: Differential Sensitivity to Cysteinyl Leukotriene Receptor Antagonists. *Am J Respir Cell Mol Biol* 1998;19:453–61. <https://doi.org/10.1165/ajrcmb.19.3.2999>.
- [399] Ualiyeva S, Hallen N, Kanaoka Y, Ledderose C, Matsumoto I, Junger WG, et al. Airway brush cells generate cysteinyl leukotrienes through the ATP sensor P2Y2. *Sci Immunol* 2020;5:eaax7224. <https://doi.org/10.1126/sciimmunol.aax7224>.

- [400] McGinty JW, Ting H-A, Billipp TE, Nadsombati MS, Khan DM, Barrett NA, et al. Tuft-Cell-Derived Leukotrienes Drive Rapid Anti-helminth Immunity in the Small Intestine but Are Dispensable for Anti-protist Immunity. *Immunity* 2020;S1074761320300765. <https://doi.org/10.1016/j.immuni.2020.02.005>.
- [401] Weller PF, Lee CW, Foster DW, Corey EJ, Austen KF, Lewis RA. Generation and metabolism of 5-lipoxygenase pathway leukotrienes by human eosinophils: predominant production of leukotriene C4. *Proc Natl Acad Sci USA* 1983;80:7626–30. <https://doi.org/10.1073/pnas.80.24.7626>.
- [402] Archambault A-S, Brassard J, Bernatchez É, Martin C, Di Marzo V, Laviolette M, et al. Human and Mouse Eosinophils Differ in Their Ability to Biosynthesize Eicosanoids, Docosanoids, the Endocannabinoid 2-Arachidonoyl-glycerol and Its Congeners. *Cells* 2022;11:141. <https://doi.org/10.3390/cells11010141>.
- [403] Sun J, Dahlén B, Agerberth B, Haeggström JZ. The antimicrobial peptide LL-37 induces synthesis and release of cysteinyl leukotrienes from human eosinophils--implications for asthma. *Allergy* 2013;68:304–11. <https://doi.org/10.1111/all.12087>.
- [404] Maclouf JA, Murphy RC. Transcellular metabolism of neutrophil-derived leukotriene A4 by human platelets. A potential cellular source of leukotriene C4. *J Biol Chem* 1988;263:174–81.
- [405] Lynch KR, O'Neill GP, Liu Q, Im D-S, Sawyer N, Metters KM, et al. Characterization of the human cysteinyl leukotriene CysLT1 receptor. *Nature* 1999;399:789–93. <https://doi.org/10.1038/21658>.
- [406] Heise CE, O'Dowd BF, Figueroa DJ, Sawyer N, Nguyen T, Im D-S, et al. Characterization of the Human Cysteinyl Leukotriene 2 Receptor. *Journal of Biological Chemistry* 2000;275:30531–6. <https://doi.org/10.1074/jbc.M003490200>.
- [407] Bankova LG, Lai J, Yoshimoto E, Boyce JA, Austen KF, Kanaoka Y, et al. Leukotriene E₄ elicits respiratory epithelial cell mucin release through the G-protein-coupled receptor, GPR99. *Proc Natl Acad Sci USA* 2016;113:6242–7. <https://doi.org/10.1073/pnas.1605957113>.
- [408] Paruchuri S, Tashimo H, Feng C, Maekawa A, Xing W, Jiang Y, et al. Leukotriene E4-induced pulmonary inflammation is mediated by the P2Y12 receptor. *Journal of Experimental Medicine* 2009;206:2543–55. <https://doi.org/10.1084/jem.20091240>.
- [409] Yokomizo T, Izumi T, Chang K, Takuwa Y, Shimizu T. A G-protein-coupled receptor for leukotriene B4 that mediates chemotaxis. *Nature* 1997;387:620–4. <https://doi.org/10.1038/42506>.
- [410] Yokomizo T, Kato K, Terawaki K, Izumi T, Shimizu T. A Second Leukotriene B4 Receptor, Blt2. *Journal of Experimental Medicine* 2000;192:421–32. <https://doi.org/10.1084/jem.192.3.421>.
- [411] Naraba H, Murakami M, Matsumoto H, Shimbara S, Ueno A, Kudo I, et al. Segregated Coupling of Phospholipases A2, Cyclooxygenases, and Terminal Prostanoid Synthases in Different Phases of Prostanoid Biosynthesis in Rat Peritoneal Macrophages. *The Journal of Immunology* 1998;160:2974–82. <https://doi.org/10.4049/jimmunol.160.6.2974>.

- [412] Smith WL, Langenbach R. Why there are two cyclooxygenase isozymes. *J Clin Invest* 2001;107:1491–5. <https://doi.org/10.1172/JCI13271>.
- [413] Jakobsson P-J, Thorén S, Morgenstern R, Samuelsson B. Identification of human prostaglandin E synthase: A microsomal, glutathione-dependent, inducible enzyme, constituting a potential novel drug target. *Proc Natl Acad Sci USA* 1999;96:7220–5. <https://doi.org/10.1073/pnas.96.13.7220>.
- [414] Hecker M, Haurand M, Ullrich V, Diczfalusy U, Hammarström S. Products, kinetics, and substrate specificity of homogeneous thromboxane synthase from human platelets: Development of a novel enzyme assay. *Archives of Biochemistry and Biophysics* 1987;254:124–35. [https://doi.org/10.1016/0003-9861\(87\)90088-9](https://doi.org/10.1016/0003-9861(87)90088-9).
- [415] Christ-Hazelhof E, Nugteren DH. Purification and characterisation of prostaglandin endoperoxide D-isomerase, a cytoplasmic, glutathione-requiring enzyme. *Biochimica et Biophysica Acta (BBA) - Lipids and Lipid Metabolism* 1979;572:43–51. [https://doi.org/10.1016/0005-2760\(79\)90198-X](https://doi.org/10.1016/0005-2760(79)90198-X).
- [416] Moncada S, Gryglewski R, Bunting S, Vane JR. An enzyme isolated from arteries transforms prostaglandin endoperoxides to an unstable substance that inhibits platelet aggregation. *Nature* 1976;263:663–5. <https://doi.org/10.1038/263663a0>.
- [417] Charo IF, Feinman RD, Detwiler TC, Smith JB, Ingerman CM, Silver MJ. Prostaglandin endoperoxides and thromboxane A₂ can induce platelet aggregation in the absence of secretion. *Nature* 1977;269:66–9. <https://doi.org/10.1038/269066a0>.
- [418] Yusuf MZ, Raslan Z, Atkinson L, Aburima A, Thomas SG, Naseem KM, et al. Prostacyclin reverses platelet stress fibre formation causing platelet aggregate instability. *Sci Rep* 2017;7:5582. <https://doi.org/10.1038/s41598-017-05817-9>.
- [419] Cheng Y, Austin SC, Rocca B, Koller BH, Coffman TM, Grosser T, et al. Role of Prostacyclin in the Cardiovascular Response to Thromboxane A₂. *Science* 2002;296:539–41. <https://doi.org/10.1126/science.1068711>.
- [420] Sugimoto Y, Yamasaki A, Segi E, Tsuboi K, Aze Y, Nishimura T, et al. Failure of Parturition in Mice Lacking the Prostaglandin F Receptor. *Science* 1997;277:681–3. <https://doi.org/10.1126/science.277.5326.681>.
- [421] Saito O, Guan Y, Qi Z, Davis LS, Kömhoff M, Sugimoto Y, et al. Expression of the prostaglandin F receptor (FP) gene along the mouse genitourinary tract. *American Journal of Physiology-Renal Physiology* 2003;284:F1164–70. <https://doi.org/10.1152/ajprenal.00441.2002>.
- [422] Nakahata K, Kinoshita H, Tokinaga Y, Ishida Y, Kimoto Y, Dojo M, et al. Vasodilation Mediated by Inward Rectifier K⁺ Channels in Cerebral Microvessels of Hypertensive and Normotensive Rats. *Anesthesia & Analgesia* 2006;102:571–6. <https://doi.org/10.1213/01.ane.0000194303.00844.5e>.
- [423] Kunori S, Matsumura S, Mabuchi T, Tatsumi S, Sugimoto Y, Minami T, et al. Involvement of prostaglandin F_{2α} receptor in ATP-induced mechanical allodynia. *Neuroscience* 2009;163:362–71. <https://doi.org/10.1016/j.neuroscience.2009.05.069>.

- [424] Werder RB, Lynch JP, Simpson JC, Zhang V, Hodge NH, Poh M, et al. PGD₂/DP₂ receptor activation promotes severe viral bronchiolitis by suppressing IFN- λ production. *Sci Transl Med* 2018;10:eaao0052. <https://doi.org/10.1126/scitranslmed.aao0052>.
- [425] Monneret G, Li H, Vasilescu J, Rokach J, Powell WS. 15-Deoxy- Δ 12,14,12,14-prostaglandins D₂ and J₂ Are Potent Activators of Human Eosinophils. *The Journal of Immunology* 2002;168:3563–9. <https://doi.org/10.4049/jimmunol.168.7.3563>.
- [426] Xue L, Barrow A, Fleming VM, Hunter MG, Ogg G, Klenerman P, et al. Leukotriene E₄ Activates Human Th₂ Cells for Exaggerated Proinflammatory Cytokine Production in Response to Prostaglandin D₂. *The Journal of Immunology* 2012;188:694–702. <https://doi.org/10.4049/jimmunol.1102474>.
- [427] Matsuoka T, Hirata M, Tanaka H, Takahashi Y, Murata T, Kabashima K, et al. Prostaglandin D₂ as a Mediator of Allergic Asthma. *Science* 2000;287:2013–7. <https://doi.org/10.1126/science.287.5460.2013>.
- [428] Jandl K, Stacher E, Bálint Z, Sturm EM, Maric J, Peinhaupt M, et al. Activated prostaglandin D₂ receptors on macrophages enhance neutrophil recruitment into the lung. *Journal of Allergy and Clinical Immunology* 2016;137:833–43. <https://doi.org/10.1016/j.jaci.2015.11.012>.
- [429] Murata T, Aritake K, Tsubosaka Y, Maruyama T, Nakagawa T, Hori M, et al. Anti-inflammatory role of PGD₂ in acute lung inflammation and therapeutic application of its signal enhancement. *Proc Natl Acad Sci USA* 2013;110:5205–10. <https://doi.org/10.1073/pnas.1218091110>.
- [430] Hammad H, Kool M, Soullié T, Narumiya S, Trottein F, Hoogsteden HC, et al. Activation of the D₁ prostanoid 1 receptor suppresses asthma by modulation of lung dendritic cell function and induction of regulatory T cells. *Journal of Experimental Medicine* 2007;204:357–67. <https://doi.org/10.1084/jem.20061196>.
- [431] Liu T, Zaman W, Kaphalia BS, Ansari GAS, Garofalo RP, Casola A. RSV-induced prostaglandin E₂ production occurs via cPLA₂ activation: Role in viral replication. *Virology* 2005;343:12–24. <https://doi.org/10.1016/j.virol.2005.08.012>.
- [432] Khayrullina T, Yen J-H, Jing H, Ganea D. In Vitro Differentiation of Dendritic Cells in the Presence of Prostaglandin E₂ Alters the IL-12/IL-23 Balance and Promotes Differentiation of Th₁₇ Cells. *The Journal of Immunology* 2008;181:721–35. <https://doi.org/10.4049/jimmunol.181.1.721>.
- [433] Chen H, Qin J, Wei P, Zhang J, Li Q, Fu L, et al. Effects of leukotriene B₄ and prostaglandin E₂ on the differentiation of murine Foxp₃⁺ T regulatory cells and Th₁₇ cells. *Prostaglandins, Leukotrienes and Essential Fatty Acids* 2009;80:195–200. <https://doi.org/10.1016/j.plefa.2009.01.006>.
- [434] Yao C, Sakata D, Esaki Y, Li Y, Matsuoka T, Kuroiwa K, et al. Prostaglandin E₂–EP₄ signaling promotes immune inflammation through TH₁ cell differentiation and TH₁₇ cell expansion. *Nat Med* 2009;15:633–40. <https://doi.org/10.1038/nm.1968>.
- [435] Yao C, Hirata T, Soontrapa K, Ma X, Takemori H, Narumiya S. Prostaglandin E₂ promotes Th₁ differentiation via synergistic amplification of IL-12 signalling by cAMP and PI3-kinase. *Nat Commun* 2013;4:1685. <https://doi.org/10.1038/ncomms2684>.

- [436] Coulombe F, Jaworska J, Verway M, Tzelepis F, Massoud A, Gillard J, et al. Targeted Prostaglandin E2 Inhibition Enhances Antiviral Immunity through Induction of Type I Interferon and Apoptosis in Macrophages. *Immunity* 2014;40:554–68. <https://doi.org/10.1016/j.immuni.2014.02.013>.
- [437] Serhan CN. Lipoxin biosynthesis and its impact in inflammatory and vascular events. *Biochimica et Biophysica Acta (BBA) - Lipids and Lipid Metabolism* 1994;1212:1–25. [https://doi.org/10.1016/0005-2760\(94\)90185-6](https://doi.org/10.1016/0005-2760(94)90185-6).
- [438] Serhan CN, Hong S, Gronert K, Colgan SP, Devchand PR, Mirick G, et al. Resolvins. *Journal of Experimental Medicine* 2002;196:1025–37. <https://doi.org/10.1084/jem.20020760>.
- [439] Serhan CN, Yang R, Martinod K, Kasuga K, Pillai PS, Porter TF, et al. Maresins: novel macrophage mediators with potent antiinflammatory and proresolving actions. *Journal of Experimental Medicine* 2009;206:15–23. <https://doi.org/10.1084/jem.20081880>.
- [440] Schebb NH, Kühn H, Kahnt AS, Rund KM, O'Donnell VB, Flamand N, et al. Formation, Signaling and Occurrence of Specialized Pro-Resolving Lipid Mediators—What is the Evidence so far? *Front Pharmacol* 2022;13:838782. <https://doi.org/10.3389/fphar.2022.838782>.
- [441] Spector AA. Arachidonic acid cytochrome P450 epoxygenase pathway. *Journal of Lipid Research* 2009;50:S52–6. <https://doi.org/10.1194/jlr.R800038-JLR200>.
- [442] Node K, Huo Y, Ruan X, Yang B, Spiecker M, Ley K, et al. Anti-inflammatory Properties of Cytochrome P450 Epoxygenase-Derived Eicosanoids. *Science* 1999;285:1276–9. <https://doi.org/10.1126/science.285.5431.1276>.
- [443] Schmelzer KR, Kubala L, Newman JW, Kim I-H, Eiserich JP, Hammock BD. Soluble epoxide hydrolase is a therapeutic target for acute inflammation. *Proc Natl Acad Sci USA* 2005;102:9772–7. <https://doi.org/10.1073/pnas.0503279102>.
- [444] Ishizuka T, Cheng J, Singh H, Vitto MD, Manthati VL, Falck JR, et al. 20-Hydroxyeicosatetraenoic Acid Stimulates Nuclear Factor- κ B Activation and the Production of Inflammatory Cytokines in Human Endothelial Cells. *J Pharmacol Exp Ther* 2008;324:103–10. <https://doi.org/10.1124/jpet.107.130336>.
- [445] Archambault A, Zaid Y, Rakotoarivelo V, Turcotte C, Doré É, Dubuc I, et al. High levels of eicosanoids and docosanoids in the lungs of intubated COVID-19 patients. *The FASEB Journal* 2021;35. <https://doi.org/10.1096/fj.202100540R>.
- [446] Zaid Y, Doré É, Dubuc I, Archambault A-S, Flamand O, Laviolette M, et al. Chemokines and eicosanoids fuel the hyperinflammation within the lungs of patients with severe COVID-19. *Journal of Allergy and Clinical Immunology* 2021;148:368-380.e3. <https://doi.org/10.1016/j.jaci.2021.05.032>.
- [447] Hammock BD, Wang W, Gilligan MM, Panigrahy D. Eicosanoids. *The American Journal of Pathology* 2020;190:1782–8. <https://doi.org/10.1016/j.ajpath.2020.06.010>.
- [448] Funk CD, Ardakani A. A Novel Strategy to Mitigate the Hyperinflammatory Response to COVID-19 by Targeting Leukotrienes. *Front Pharmacol* 2020;11:1214. <https://doi.org/10.3389/fphar.2020.01214>.

- [449] Hoxha M. What about COVID-19 and arachidonic acid pathway? *Eur J Clin Pharmacol* 2020;76:1501–4. <https://doi.org/10.1007/s00228-020-02941-w>.
- [450] Carey MA, Bradbury JA, Seubert JM, Langenbach R, Zeldin DC, Germolec DR. Contrasting Effects of Cyclooxygenase-1 (COX-1) and COX-2 Deficiency on the Host Response to Influenza A Viral Infection. *The Journal of Immunology* 2005;175:6878–84. <https://doi.org/10.4049/jimmunol.175.10.6878>.
- [451] Carey MA, Bradbury JA, Reboloso YD, Graves JP, Zeldin DC, Germolec DR. Pharmacologic Inhibition of COX-1 and COX-2 in Influenza A Viral Infection in Mice. *PLoS ONE* 2010;5:e11610. <https://doi.org/10.1371/journal.pone.0011610>.
- [452] Lauder SN, Taylor PR, Clark SR, Evans RL, Hindley JP, Smart K, et al. Paracetamol reduces influenza-induced immunopathology in a mouse model of infection without compromising virus clearance or the generation of protective immunity. *Thorax* 2011;66:368–74. <https://doi.org/10.1136/thx.2010.150318>.
- [453] Li C, Li C, Zhang AJX, To KKW, Lee ACY, Zhu H, et al. Avian Influenza A H7N9 Virus Induces Severe Pneumonia in Mice without Prior Adaptation and Responds to a Combination of Zanamivir and COX-2 Inhibitor. *PLoS ONE* 2014;9:e107966. <https://doi.org/10.1371/journal.pone.0107966>.
- [454] Zheng B-J, Chan K-W, Lin Y-P, Zhao G-Y, Chan C, Zhang H-J, et al. Delayed antiviral plus immunomodulator treatment still reduces mortality in mice infected by high inoculum of influenza A/H5N1 virus. *Proc Natl Acad Sci USA* 2008;105:8091–6. <https://doi.org/10.1073/pnas.0711942105>.
- [455] Park JH, Park EB, Lee JY, Min J-Y. Identification of novel membrane-associated prostaglandin E synthase-1 (mPGES-1) inhibitors with anti-influenza activities in vitro. *Biochemical and Biophysical Research Communications* 2016;469:848–55. <https://doi.org/10.1016/j.bbrc.2015.11.129>.
- [456] Liu L, Cao Z, Chen J, Li R, Cao Y, Zhu C, et al. Influenza A Virus Induces Interleukin-27 through Cyclooxygenase-2 and Protein Kinase A Signaling. *Journal of Biological Chemistry* 2012;287:11899–910. <https://doi.org/10.1074/jbc.M111.308064>.
- [457] Richardson JY, Ottolini MG, Pletneva L, Boukhvalova M, Zhang S, Vogel SN, et al. Respiratory Syncytial Virus (RSV) Infection Induces Cyclooxygenase 2: A Potential Target for RSV Therapy. *The Journal of Immunology* 2005;174:4356–64. <https://doi.org/10.4049/jimmunol.174.7.4356>.
- [458] Radi ZA, Meyerholz DK, Ackermann MR. Pulmonary Cyclooxygenase-1 (COX-1) and COX-2 Cellular Expression and Distribution After Respiratory Syncytial Virus and Parainfluenza Virus Infection. *Viral Immunology* 2010;23:43–8. <https://doi.org/10.1089/vim.2009.0042>.
- [459] Sznajder Y, Westcott JY, Wenzel SE, Mazer B, Tucci M, Joseph Toledano B. Airway eicosanoids in acute severe respiratory syncytial virus bronchiolitis. *The Journal of Pediatrics* 2004;145:115–8. <https://doi.org/10.1016/j.jpeds.2004.03.049>.
- [460] Ricke-Hoch M, Stelling E, Lasswitz L, Gunesch AP, Kasten M, Zapatero-Belinchón FJ, et al. Impaired immune response mediated by prostaglandin E2 promotes severe COVID-19 disease. *PLoS ONE* 2021;16:e0255335. <https://doi.org/10.1371/journal.pone.0255335>.

- [461] Gordon DE, Hiatt J, Bouhaddou M, Rezelj VV, Ulferts S, Braberg H, et al. Comparative host-coronavirus protein interaction networks reveal pan-viral disease mechanisms 2020.
- [462] Wong L-YR, Zheng J, Wilhelmsen K, Li K, Ortiz ME, Schnicker NJ, et al. Eicosanoid signaling blockade protects middle-aged mice from severe COVID-19. *Nature* 2022. <https://doi.org/10.1038/s41586-022-04630-3>.
- [463] Tumala B, Phelps KR, Zhang S, Bhattacharya S, Shornick LP. Prostaglandin D₂ Levels Regulate CD103⁺ Conventional Dendritic Cell Activation in Neonates During Respiratory Viral Infection. *Viral Immunology* 2018;31:658–67. <https://doi.org/10.1089/vim.2018.0090>.
- [464] Zhao J, Zhao J, Legge K, Perlman S. Age-related increases in PGD₂ expression impair respiratory DC migration, resulting in diminished T cell responses upon respiratory virus infection in mice. *J Clin Invest* 2011;121:4921–30. <https://doi.org/10.1172/JCI59777>.
- [465] Hashimoto K, Graham BS, Geraci MW, FitzGerald GA, Egan K, Zhou W, et al. Signaling through the Prostaglandin I₂ Receptor IP Protects against Respiratory Syncytial Virus-Induced Illness. *J Virol* 2004;78:10303–9. <https://doi.org/10.1128/JVI.78.19.10303-10309.2004>.
- [466] Flamand L, Tremblay MJ, Borgeat P. Leukotriene B₄ Triggers the In Vitro and In Vivo Release of Potent Antimicrobial Agents. *The Journal of Immunology* 2007;178:8036–45. <https://doi.org/10.4049/jimmunol.178.12.8036>.
- [467] Gaudreault É, Gosselin J. Leukotriene B₄ Induces Release of Antimicrobial Peptides in Lungs of Virally Infected Mice. *The Journal of Immunology* 2008;180:6211–21. <https://doi.org/10.4049/jimmunol.180.9.6211>.
- [468] Widgren H, Andersson M, Borgeat P, Flamand L, Johnston S, Greiff L. LTB₄ increases nasal neutrophil activity and conditions neutrophils to exert antiviral effects. *Respiratory Medicine* 2011;105:997–1006. <https://doi.org/10.1016/j.rmed.2010.12.021>.
- [469] Le Bel M, Gosselin J. Leukotriene B₄ Enhances NOD2-Dependent Innate Response against Influenza Virus Infection. *PLoS ONE* 2015;10:e0139856. <https://doi.org/10.1371/journal.pone.0139856>.
- [470] Pernet E, Downey J, Vinh DC, Powell WS, Divangahi M. Leukotriene B₄–type I interferon axis regulates macrophage-mediated disease tolerance to influenza infection. *Nat Microbiol* 2019;4:1389–400. <https://doi.org/10.1038/s41564-019-0444-3>.
- [471] Cardani A, Boulton A, Kim TS, Braciale TJ. Alveolar Macrophages Prevent Lethal Influenza Pneumonia By Inhibiting Infection Of Type-1 Alveolar Epithelial Cells. *PLoS Pathog* 2017;13:e1006140. <https://doi.org/10.1371/journal.ppat.1006140>.
- [472] Fullmer JJ, Khan AM, Elidemir O, Chiappetta C, Stark JM, Colasurdo GN. Role of cysteinyl leukotrienes in airway inflammation and responsiveness following RSV infection in BALB/c mice. *Pediatr Allergy Immunol* 2005;16:593–601. <https://doi.org/10.1111/j.1399-3038.2005.00248.x>.

- [473] Han J, Jia Y, Takeda K, Shiraishi Y, Okamoto M, Dakhama A, et al. Montelukast during Primary Infection Prevents Airway Hyperresponsiveness and Inflammation after Reinfection with Respiratory Syncytial Virus. *Am J Respir Crit Care Med* 2010;182:455–63. <https://doi.org/10.1164/rccm.200912-1811OC>.
- [474] Schwarz B, Sharma L, Roberts L, Peng X, Bermejo S, Leighton I, et al. Cutting Edge: Severe SARS-CoV-2 Infection in Humans Is Defined by a Shift in the Serum Lipidome, Resulting in Dysregulation of Eicosanoid Immune Mediators. *The Journal of Immunology* 2021;206:329–34. <https://doi.org/10.4049/jimmunol.2001025>.
- [475] Khan AR, Misdary C, Yegya-Raman N, Kim S, Narayanan N, Siddiqui S, et al. Montelukast in hospitalized patients diagnosed with COVID-19. *Journal of Asthma* 2022;59:780–6. <https://doi.org/10.1080/02770903.2021.1881967>.
- [476] Asher A, Tintle NL, Myers M, Lockshon L, Bacareza H, Harris WS. Blood omega-3 fatty acids and death from COVID-19: A pilot study. *Prostaglandins, Leukotrienes and Essential Fatty Acids* 2021;166:102250. <https://doi.org/10.1016/j.plefa.2021.102250>.
- [477] Doaei S, Gholami S, Rastgoo S, Gholamalizadeh M, Bourbour F, Bagheri SE, et al. The effect of omega-3 fatty acid supplementation on clinical and biochemical parameters of critically ill patients with COVID-19: a randomized clinical trial. *J Transl Med* 2021;19:128. <https://doi.org/10.1186/s12967-021-02795-5>.
- [478] Berger AA, Sherburne R, Urits I, Patel H, Eskander J. Icosapent Ethyl – A Successful Treatment for Symptomatic COVID-19 Infection. *Cureus* 2020. <https://doi.org/10.7759/cureus.10211>.
- [479] Machado ER, Carlos D, Lourenço EV, Souza GEP, Sorgi CA, Silva ÉV, et al. Cyclooxygenase-derived mediators regulate the immunological control of *Strongyloides venezuelensis* infection. *FEMS Immunol Med Microbiol* 2010;59:18–32. <https://doi.org/10.1111/j.1574-695X.2010.00656.x>.
- [480] Machado ER, Ueta MT, Lourenço EV, Anibal FF, Sorgi CA, Soares EG, et al. Leukotrienes Play a Role in the Control of Parasite Burden in Murine Strongyloidiasis. *The Journal of Immunology* 2005;175:3892–9. <https://doi.org/10.4049/jimmunol.175.6.3892>.
- [481] Esser-von Bieren J. Immune-regulation and -functions of eicosanoid lipid mediators. *Biological Chemistry* 2017;398:1177–91. <https://doi.org/10.1515/hsz-2017-0146>.
- [482] Brattig NW, Schwohl A, Hoerauf A, Büttner DW. Identification of the lipid mediator prostaglandin E2 in tissue immune cells of humans infected with the filaria *Onchocerca volvulus*. *Acta Tropica* 2009;112:231–5. <https://doi.org/10.1016/j.actatropica.2009.07.018>.
- [483] de los Reyes Jiménez M, Lechner A, Alessandrini F, Bohnacker S, Schindela S, Trompette A, et al. An anti-inflammatory eicosanoid switch mediates the suppression of type-2 inflammation by helminth larval products. *Sci Transl Med* 2020;12:eaay0605. <https://doi.org/10.1126/scitranslmed.aay0605>.
- [484] Prodjinotho UF, Gres V, Henkel F, Lacorcía M, Dandl R, Haslbeck M, et al. Helminthic dehydrogenase drives PGE₂ and IL-10 production in monocytes to potentiate Treg induction. *EMBO Reports* 2022. <https://doi.org/10.15252/embr.202154096>.

- [485] Rodríguez-Sosa M, Satoskar AR, Calderón R, Gomez-Garcia L, Saavedra R, Bojalil R, et al. Chronic Helminth Infection Induces Alternatively Activated Macrophages Expressing High Levels of CCR5 with Low Interleukin-12 Production and Th2-Biasing Ability. *Infect Immun* 2002;70:3656–64. <https://doi.org/10.1128/IAI.70.7.3656-3664.2002>.
- [486] Thomas GD, Rückerl D, Maskrey BH, Whitfield PD, Blaxter ML, Allen JE. The biology of nematode- and IL4R α -dependent murine macrophage polarization in vivo as defined by RNA-Seq and targeted lipidomics. *Blood* 2012;120:e93–104. <https://doi.org/10.1182/blood-2012-07-442640>.
- [487] Conder GA, Mayberry LF, Bristol JR, Castro GA, Lee BL, Kratzer DD, et al. Effects of PGE1 or PGE2 and/or acetazolamide on expulsion of from rats. *Prostaglandins* 1987;34:817–27. [https://doi.org/10.1016/0090-6980\(87\)90063-3](https://doi.org/10.1016/0090-6980(87)90063-3).
- [488] Ramaswamy K, Kumar P, He Y-X. A Role for Parasite-Induced PGE2 in IL-10-Mediated Host Immunoregulation by Skin Stage Schistosomula of *Schistosoma mansoni*. *The Journal of Immunology* 2000;165:4567–74. <https://doi.org/10.4049/jimmunol.165.8.4567>.
- [489] Sturm EM, Schratl P, Schuligoi R, Konya V, Sturm GJ, Lippe ITh, et al. Prostaglandin E2 Inhibits Eosinophil Trafficking through E-Prostanoid 2 Receptors. *The Journal of Immunology* 2008;181:7273–83. <https://doi.org/10.4049/jimmunol.181.10.7273>.
- [490] Kay LJ, Yeo WW, Peachell PT. Prostaglandin E₂ activates EP₂ receptors to inhibit human lung mast cell degranulation: Mast cell EP₂ receptors. *British Journal of Pharmacology* 2006;147:707–13. <https://doi.org/10.1038/sj.bjp.0706664>.
- [491] Maric J, Ravindran A, Mazzurana L, Björklund ÅK, Van Acker A, Rao A, et al. Prostaglandin E₂ suppresses human group 2 innate lymphoid cell function. *Journal of Allergy and Clinical Immunology* 2018;141:1761-1773.e6. <https://doi.org/10.1016/j.jaci.2017.09.050>.
- [492] Kaiser MMM, Ritter M, del Fresno C, Jónasdóttir HS, van der Ham AJ, Pelgrom LR, et al. Dectin-1/2–induced autocrine PGE2 signaling licenses dendritic cells to prime Th2 responses. *PLoS Biol* 2018;16:e2005504. <https://doi.org/10.1371/journal.pbio.2005504>.
- [493] Church RJ, Jania LA, Koller BH. Prostaglandin E2 Produced by the Lung Augments the Effector Phase of Allergic Inflammation. *The Journal of Immunology* 2012;188:4093–102. <https://doi.org/10.4049/jimmunol.1101873>.
- [494] Fajt ML, Gelhaus SL, Freeman B, Uvalle CE, Trudeau JB, Holguin F, et al. Prostaglandin D2 pathway upregulation: Relation to asthma severity, control, and TH2 inflammation. *Journal of Allergy and Clinical Immunology* 2013;131:1504-1512.e12. <https://doi.org/10.1016/j.jaci.2013.01.035>.
- [495] Tait Wojno ED, Monticelli LA, Tran SV, Alenghat T, Osborne LC, Thome JJ, et al. The prostaglandin D2 receptor CRTH2 regulates accumulation of group 2 innate lymphoid cells in the inflamed lung. *Mucosal Immunology* 2015;8:1313–23. <https://doi.org/10.1038/mi.2015.21>.

- [496] Oyesola OO, Duque C, Huang LC, Larson EM, Früh SP, Webb LM, et al. The Prostaglandin D₂ Receptor CRTH2 Promotes IL-33–Induced ILC2 Accumulation in the Lung. *J Immunol* 2020;204:1001–11. <https://doi.org/10.4049/jimmunol.1900745>.
- [497] Oyesola OO, Shanahan MT, Kanke M, Mooney BM, Webb LM, Smita S, et al. PGD2 and CRTH2 counteract Type 2 cytokine–elicited intestinal epithelial responses during helminth infection. *Journal of Experimental Medicine* 2021;218:e20202178. <https://doi.org/10.1084/jem.20202178>.
- [498] Henkel FDR, Friedl A, Haid M, Thomas D, Bouchery T, Haimerl P, et al. House dust mite drives pro-inflammatory eicosanoid reprogramming and macrophage effector functions. *Allergy* 2018;all.13700. <https://doi.org/10.1111/all.13700>.
- [499] Sharma A, Sharma P, Ganga L, Satoeya N, Mishra S, Vishwakarma AL, et al. Infective Larvae of *Brugia malayi* Induce Polarization of Host Macrophages that Helps in Immune Evasion. *Front Immunol* 2018;9:194. <https://doi.org/10.3389/fimmu.2018.00194>.
- [500] Morchón R, López-Belmonte J, Rodríguez-Barbero A, Simón F. High Levels of Serum Thromboxane B2 Are Generated during Human Pulmonary *Dirofilariasis*. *Clin Vaccine Immunol* 2006;13:1175–6. <https://doi.org/10.1128/CVI.00197-06>.
- [501] Angeli V, Faveeuw C, Roye O, Fontaine J, Teissier E, Capron A, et al. Role of the Parasite-Derived Prostaglandin D2 in the Inhibition of Epidermal Langerhans Cell Migration during *Schistosomiasis* Infection. *Journal of Experimental Medicine* 2001;193:1135–48. <https://doi.org/10.1084/jem.193.10.1135>.
- [502] Magalhães KG, Luna-Gomes T, Mesquita-Santos F, Corrêa R, Assunção LS, Atella GC, et al. Schistosomal Lipids Activate Human Eosinophils via Toll-Like Receptor 2 and PGD2 Receptors: 15-LO Role in Cytokine Secretion. *Front Immunol* 2019;9:3161. <https://doi.org/10.3389/fimmu.2018.03161>.
- [503] Salafsky B, Fusco AC. *Schistosoma mansoni*: A comparison of secreted vs nonsecreted eicosanoids in developing schistosomulae and adults. *Experimental Parasitology* 1987;64:361–7. [https://doi.org/10.1016/0014-4894\(87\)90048-8](https://doi.org/10.1016/0014-4894(87)90048-8).
- [504] Sommer A, Rickert R, Fischer P, Steinhart H, Walter RD, Liebau E. A Dominant Role for Extracellular Glutathione S -Transferase from *Onchocerca volvulus* Is the Production of Prostaglandin D₂. *Infect Immun* 2003;71:3603–6. <https://doi.org/10.1128/IAI.71.6.3603-3606.2003>.
- [505] Brattig NW, Schwohl A, Rickert R, Büttner DW. The filarial parasite *Onchocerca volvulus* generates the lipid mediator prostaglandin E2. *Microbes and Infection* 2006;8:873–9. <https://doi.org/10.1016/j.micinf.2005.10.014>.
- [506] Giera M, Kaiser MMM, Derks RJE, Steenvoorden E, Kruize YCM, Hokke CH, et al. The *Schistosoma mansoni* lipidome: Leads for immunomodulation. *Analytica Chimica Acta* 2018;1037:107–18. <https://doi.org/10.1016/j.aca.2017.11.058>.
- [507] Fusco AC, Salafsky B, Kevin MB. *Schistosoma mansoni*: Eicosanoid production by cercariae. *Experimental Parasitology* 1985;59:44–50. [https://doi.org/10.1016/0014-4894\(85\)90055-4](https://doi.org/10.1016/0014-4894(85)90055-4).

- [508] Laan LC, Williams AR, Stavenhagen K, Giera M, Kooij G, Vlasakov I, et al. The whipworm (*Trichuris suis*) secretes prostaglandin E2 to suppress proinflammatory properties in human dendritic cells. *FASEB j* 2017;31:719–31. <https://doi.org/10.1096/fj.201600841R>.
- [509] Weller PF, Liu LX, Buhlmann JE. Release of Prostaglandin E2 by Microfilariae of *Wuchereria bancrofti* and *Brugia malayi*. *The American Journal of Tropical Medicine and Hygiene* 1992;46:520–3. <https://doi.org/10.4269/ajtmh.1992.46.520>.
- [510] Liu LX, Weller PF. Intravascular filarial parasites inhibit platelet aggregation. Role of parasite-derived prostanoids. *J Clin Invest* 1992;89:1113–20. <https://doi.org/10.1172/JCI115691>.
- [511] Moqbel R, Wakelin D, MacDonald AJ, King SJ, Grecis RK, Kay AB. Release of leukotrienes during rapid expulsion of *Trichinella spiralis* from immune rats. *Immunology* 1987;60:425–30.
- [512] Paiva LA, Maya-Monteiro CM, Bandeira-Melo C, Silva PMR, El-Cheikh MC, Teodoro AJ, et al. Interplay of cysteinyl leukotrienes and TGF- β in the activation of hepatic stellate cells from *Schistosoma mansoni* granulomas. *Biochimica et Biophysica Acta (BBA) - Molecular and Cell Biology of Lipids* 2010;1801:1341–8. <https://doi.org/10.1016/j.bbalip.2010.08.014>.
- [513] Secor WE, Powell MR, Morgan J, Wynn TA, Funk CD. Mice deficient for 5-lipoxygenase, but not leukocyte-type 12-lipoxygenase, display altered immune responses during infection with *Schistosoma mansoni*. *Prostaglandins & Other Lipid Mediators* 1998;56:291–304. [https://doi.org/10.1016/S0090-6980\(98\)00059-8](https://doi.org/10.1016/S0090-6980(98)00059-8).
- [514] Toffoli da Silva G, Espíndola MS, Fontanari C, Rosada RS, Faccioli LH, Ramos SG, et al. 5-lipoxygenase pathway is essential for the control of granuloma extension induced by *Schistosoma mansoni* eggs in lung. *Experimental Parasitology* 2016;167:124–9. <https://doi.org/10.1016/j.exppara.2016.06.001>.
- [515] Carlos D, Machado ER, De Paula L, Sá-Nunes A, Sorgi CA, Jamur MC, et al. Evidence for eosinophil recruitment, leukotriene B4 production and mast cell hyperplasia following *Toxocara canis* infection in rats. *Braz J Med Biol Res* 2011;44:319–26. <https://doi.org/10.1590/S0100-879X2011000400008>.
- [516] Perdue MH, Ramage JK, Burget D, Marshall J, Masson S. Intestinal mucosal injury is associated with mast cell activation and leukotriene generation during *Nippostrongylus*-induced inflammation in the rat. *Digest Dis Sci* 1989;34:724–31. <https://doi.org/10.1007/BF01540344>.
- [517] Zafra R, Buffoni L, Martínez-Moreno A, Pérez-Écija A, Martínez-Moreno FJ, Pérez J. A Study of the Liver of Goats Immunized with a Synthetic Peptide of the Sm14 Antigen and Challenged with *Fasciola hepatica*. *Journal of Comparative Pathology* 2008;139:169–76. <https://doi.org/10.1016/j.jcpa.2008.06.004>.
- [518] Anibal FF, Rogerio AP, Malheiro A, Machado ER, Martins-Filho OA, Andrade MC, et al. Impact of MK886 on Eosinophil Counts and Phenotypic Features in Toxocariasis. *Scand J Immunol* 2007;65:344–52. <https://doi.org/10.1111/j.1365-3083.2007.01911.x>.

- [519] Moqbel R, Sass-Kuhn SP, Goetzl EJ, Kay AB. Enhancement of neutrophil- and eosinophil-mediated complement-dependent killing of schistosomula of *Schistosoma mansoni* in vitro by leukotriene B₄. *Clin Exp Immunol* 1983;52:519–27.
- [520] Nutten S, Trottein F, Gounni AS, Papin J-P, Capron A, Capron M. From allergy to schistosomes: role of Fc receptors and adhesion molecules in eosinophil effector function. *Mem Inst Oswaldo Cruz* 1997;92:9–14. <https://doi.org/10.1590/S0074-02761997000800003>.
- [521] Moqbel R, Macdonald AJ, Cromwell O, Kay AB. Release of leukotriene C₄ (LTC₄) from human eosinophils following adherence to IgE- and IgG-coated schistosomula of *Schistosoma mansoni*. *Immunology* 1990;69:435–42.
- [522] Kennedy MW, Qureshi F. Stage-specific secreted antigens of the parasitic larval stages of the nematode *Ascaris*. *Immunology* 1986;58:515–22.
- [523] Kennedy MW, Qureshi F, Haswell-Elkins M, Elkins DB. Homology and heterology between the secreted antigens of the parasitic larval stages of *Ascaris lumbricoides* and *Ascaris suum*. *Clin Exp Immunol* 1987;67:20–30.
- [524] Xia Y, Spence HJ, Moore J, Heaney N, McDERMOTT L, Cooper A, et al. The ABA-1 allergen of *Ascaris lumbricoides*: sequence polymorphism, stage and tissue-specific expression, lipid binding function, and protein biophysical properties. *Parasitology* 2000;120:211–24. <https://doi.org/10.1017/S0031182099005363>.
- [525] Ali SF, Joachim A, Dausgchies A. Eicosanoid production by adult *Fasciola hepatica* and plasma eicosanoid patterns during fasciolosis in sheep. *International Journal for Parasitology* 1999;29:743–8. [https://doi.org/10.1016/S0020-7519\(99\)00020-X](https://doi.org/10.1016/S0020-7519(99)00020-X).
- [526] Fusco AC, Salafsky B, Whitely K, Yohe S. *Schistosoma mansoni*: pH dependence of cercarial eicosanoid production, penetration, and transformation. *Experimental Parasitology* 1987;64:139–46. [https://doi.org/10.1016/0014-4894\(87\)90137-8](https://doi.org/10.1016/0014-4894(87)90137-8).
- [527] Akdis M, Aab A, Altunbulakli C, Azkur K, Costa RA, Cramer R, et al. Interleukins (from IL-1 to IL-38), interferons, transforming growth factor β , and TNF- α : Receptors, functions, and roles in diseases. *Journal of Allergy and Clinical Immunology* 2016;138:984–1010. <https://doi.org/10.1016/j.jaci.2016.06.033>.
- [528] Vignali DAA, Kuchroo VK. IL-12 family cytokines: immunological playmakers. *Nat Immunol* 2012;13:722–8. <https://doi.org/10.1038/ni.2366>.
- [529] Yoon C, Johnston SC, Tang J, Stahl M, Tobin JF, Somers WS. Charged residues dominate a unique interlocking topography in the heterodimeric cytokine interleukin-12. *The EMBO Journal* 2000;19:3530–41. <https://doi.org/10.1093/emboj/19.14.3530>.
- [530] Tait Wojno ED, Hunter CA, Stumhofer JS. The Immunobiology of the Interleukin-12 Family: Room for Discovery. *Immunity* 2019;50:851–70. <https://doi.org/10.1016/j.immuni.2019.03.011>.
- [531] Trinchieri G, Wysocka M, D'Andrea A, Rengaraju M, Aste-Amezaga M, Kubin M, et al. Natural killer cell stimulatory factor (NKSF) or interleukin-12 is a key regulator of immune response and inflammation. *Progress in Growth Factor Research* 1992;4:355–68. [https://doi.org/10.1016/0955-2235\(92\)90016-B](https://doi.org/10.1016/0955-2235(92)90016-B).

- [532] Oppmann B, Lesley R, Blom B, Timans JC, Xu Y, Hunte B, et al. Novel p19 Protein Engages IL-12p40 to Form a Cytokine, IL-23, with Biological Activities Similar as Well as Distinct from IL-12. *Immunity* 2000;13:715–25. [https://doi.org/10.1016/S1074-7613\(00\)00070-4](https://doi.org/10.1016/S1074-7613(00)00070-4).
- [533] Tang C, Chen S, Qian H, Huang W. Interleukin-23: as a drug target for autoimmune inflammatory diseases. *Immunology* 2012;135:112–24. <https://doi.org/10.1111/j.1365-2567.2011.03522.x>.
- [534] Pflanz S, Timans JC, Cheung J, Rosales R, Kanzler H, Gilbert J, et al. IL-27, a Heterodimeric Cytokine Composed of EBI3 and p28 Protein, Induces Proliferation of Naive CD4+ T Cells. *Immunity* 2002;16:779–90. [https://doi.org/10.1016/S1074-7613\(02\)00324-2](https://doi.org/10.1016/S1074-7613(02)00324-2).
- [535] Collison LW, Workman CJ, Kuo TT, Boyd K, Wang Y, Vignali KM, et al. The inhibitory cytokine IL-35 contributes to regulatory T-cell function. *Nature* 2007;450:566–9. <https://doi.org/10.1038/nature06306>.
- [536] Shimozato O, Ugai S, Chiyo M, Takenobu H, Nagakawa H, Wada A, et al. The secreted form of the p40 subunit of interleukin (IL)-12 inhibits IL-23 functions and abrogates IL-23-mediated antitumour effects. *Immunology* 2006;117:22–8. <https://doi.org/10.1111/j.1365-2567.2005.02257.x>.
- [537] Gunsten S, Mikols CL, Grayson MH, Schwendener RA, Agapov E, Tidwell RM, et al. IL-12 p80-dependent macrophage recruitment primes the host for increased survival following a lethal respiratory viral infection. *Immunology* 2009;126:500–13. <https://doi.org/10.1111/j.1365-2567.2008.02923.x>.
- [538] Khader SA, Partida-Sanchez S, Bell G, Jelley-Gibbs DM, Swain S, Pearl JE, et al. Interleukin 12p40 is required for dendritic cell migration and T cell priming after Mycobacterium tuberculosis infection. *Journal of Experimental Medicine* 2006;203:1805–15. <https://doi.org/10.1084/jem.20052545>.
- [539] Meldolesi J, Pozzan T. The endoplasmic reticulum Ca²⁺ store: a view from the lumen. *Trends in Biochemical Sciences* 1998;23:10–4. [https://doi.org/10.1016/S0968-0004\(97\)01143-2](https://doi.org/10.1016/S0968-0004(97)01143-2).
- [540] Kopito RR. ER Quality Control: The Cytoplasmic Connection. *Cell* 1997;88:427–30. [https://doi.org/10.1016/S0092-8674\(00\)81881-4](https://doi.org/10.1016/S0092-8674(00)81881-4).
- [541] Werner ED, Brodsky JL, McCracken AA. Proteasome-dependent endoplasmic reticulum-associated protein degradation: An unconventional route to a familiar fate. *Proc Natl Acad Sci USA* 1996;93:13797–801. <https://doi.org/10.1073/pnas.93.24.13797>.
- [542] Vembar SS, Brodsky JL. One step at a time: endoplasmic reticulum-associated degradation. *Nat Rev Mol Cell Biol* 2008;9:944–57. <https://doi.org/10.1038/nrm2546>.
- [543] Gubler U, Chua AO, Schoenhaut DS, Dwyer CM, McComas W, Motyka R, et al. Coexpression of two distinct genes is required to generate secreted bioactive cytotoxic lymphocyte maturation factor. *Proc Natl Acad Sci USA* 1991;88:4143–7. <https://doi.org/10.1073/pnas.88.10.4143>.

- [544] Jalah R, Rosati M, Ganneru B, Pilkington GR, Valentin A, Kulkarni V, et al. The p40 Subunit of Interleukin (IL)-12 Promotes Stabilization and Export of the p35 Subunit. *Journal of Biological Chemistry* 2013;288:6763–76. <https://doi.org/10.1074/jbc.M112.436675>.
- [545] Reitberger S, Haimerl P, Aschenbrenner I, Esser-von Bieren J, Feige MJ. Assembly-induced folding regulates interleukin 12 biogenesis and secretion. *J Biol Chem* 2017;292:8073–81. <https://doi.org/10.1074/jbc.M117.782284>.
- [546] Devergne O, Birkenbach M, Kieff E. Epstein–Barr virus-induced gene 3 and the p35 subunit of interleukin 12 form a novel heterodimeric hematopoietin. *Proc Natl Acad Sci USA* 1997;94:12041–6. <https://doi.org/10.1073/pnas.94.22.12041>.
- [547] Müller SI, Friedl A, Aschenbrenner I, Esser-von Bieren J, Zacharias M, Devergne O, et al. A folding switch regulates interleukin 27 biogenesis and secretion of its α -subunit as a cytokine. *Proc Natl Acad Sci USA* 2019;116:1585–90. <https://doi.org/10.1073/pnas.1816698116>.
- [548] Alloza I, Baxter A, Chen Q, Matthiesen R, Vandebroek K. Celecoxib Inhibits Interleukin-12 $\alpha\beta$ and β_2 Folding and Secretion by a Novel COX2-Independent Mechanism Involving Chaperones of the Endoplasmic Reticulum. *Mol Pharmacol* 2006;69:1579–87. <https://doi.org/10.1124/mol.105.020669>.
- [549] Mideksa YG, Fottner M, Braus S, Weiß CAM, Nguyen T, Meier S, et al. Site-Specific Protein Labeling with Fluorophores as a Tool To Monitor Protein Turnover. *ChemBioChem* 2020;21:1861–7. <https://doi.org/10.1002/cbic.201900651>.
- [550] McLaughlin M, Alloza I, Quoc HP, Scott CJ, Hirabayashi Y, Vandebroek K. Inhibition of Secretion of Interleukin (IL)-12/IL-23 Family Cytokines by 4-Trifluoromethyl-celecoxib Is Coupled to Degradation via the Endoplasmic Reticulum Stress Protein HERP. *Journal of Biological Chemistry* 2010;285:6960–9. <https://doi.org/10.1074/jbc.M109.056614>.
- [551] Meier S, Bohnacker S, Klose CJ, Lopez A, Choe CA, Schmid PWN, et al. The molecular basis of chaperone-mediated interleukin 23 assembly control. *Nat Commun* 2019;10:4121. <https://doi.org/10.1038/s41467-019-12006-x>.
- [552] Parodi AJ. Role of N-oligosaccharide endoplasmic reticulum processing reactions in glycoprotein folding and degradation. *Biochem J* 2000;348 Pt 1:1–13.
- [553] Tannous A, Pisoni GB, Hebert DN, Molinari M. N-linked sugar-regulated protein folding and quality control in the ER. *Seminars in Cell & Developmental Biology* 2015;41:79–89. <https://doi.org/10.1016/j.semcdb.2014.12.001>.
- [554] Hammond C, Braakman I, Helenius A. Role of N-linked oligosaccharide recognition, glucose trimming, and calnexin in glycoprotein folding and quality control. *Proc Natl Acad Sci USA* 1994;91:913–7. <https://doi.org/10.1073/pnas.91.3.913>.
- [555] Aebi M, Bernasconi R, Clerc S, Molinari M. N-glycan structures: recognition and processing in the ER. *Trends in Biochemical Sciences* 2010;35:74–82. <https://doi.org/10.1016/j.tibs.2009.10.001>.

- [556] Nilsson IM, von Heijne G. Determination of the distance between the oligosaccharyltransferase active site and the endoplasmic reticulum membrane. *J Biol Chem* 1993;268:5798–801.
- [557] Ellgaard L, Frickel E-M. Calnexin, Calreticulin, and ERp57: Teammates in Glycoprotein Folding. *CBB* 2003;39:223–48. <https://doi.org/10.1385/CBB:39:3:223>.
- [558] Lamriben L, Graham JB, Adams BM, Hebert DN. *N*-Glycan-based ER Molecular Chaperone and Protein Quality Control System: The Calnexin Binding Cycle: The Calnexin Binding Cycle. *Traffic* 2016;17:308–26. <https://doi.org/10.1111/tra.12358>.
- [559] Guerriero CJ, Brodsky JL. The Delicate Balance Between Secreted Protein Folding and Endoplasmic Reticulum-Associated Degradation in Human Physiology. *Physiological Reviews* 2012;92:537–76. <https://doi.org/10.1152/physrev.00027.2011>.
- [560] Potelle S, Klein A, Foulquier F. Golgi post-translational modifications and associated diseases. *J Inher Metab Dis* 2015;38:741–51. <https://doi.org/10.1007/s10545-015-9851-7>.
- [561] Ottolenghi A, Bolel P, Sarkar R, Greenshpan Y, Iraqi M, Ghosh S, et al. Life-extended glycosylated IL-2 promotes Treg induction and suppression of autoimmunity. *Sci Rep* 2021;11:7676. <https://doi.org/10.1038/s41598-021-87102-4>.
- [562] Reif A, Lam K, Weidler S, Lott M, Boos I, Lokau J, et al. Natural Glycoforms of Human Interleukin 6 Show Atypical Plasma Clearance. *Angew Chem Int Ed* 2021;60:13380–7. <https://doi.org/10.1002/anie.202101496>.
- [563] Vandooren J, Pereira RVS, Ugarte-Berzal E, Rybakin V, Noppen S, Stas MR, et al. Internal Disulfide Bonding and Glycosylation of Interleukin-7 Protect Against Proteolytic Inactivation by Neutrophil Metalloproteinases and Serine Proteases. *Front Immunol* 2021;12:701739. <https://doi.org/10.3389/fimmu.2021.701739>.
- [564] Li H, Zhang J, An C, Dong S. Probing *N*-Glycan Functions in Human Interleukin-17A Based on Chemically Synthesized Homogeneous Glycoforms. *J Am Chem Soc* 2021;143:2846–56. <https://doi.org/10.1021/jacs.0c12448>.
- [565] Podolin PL, Wilusz MB, Cubbon RM, Pajvani U, Lord CJ, Todd JA, et al. DIFFERENTIAL GLYCOSYLATION OF INTERLEUKIN 2, THE MOLECULAR BASIS FOR THE NOD Idd3 TYPE 1 DIABETES GENE? *Cytokine* 2000;12:477–82. <https://doi.org/10.1006/cyto.1999.0609>.
- [566] Hebert DN, Molinari M. Flagging and docking: dual roles for N-glycans in protein quality control and cellular proteostasis. *Trends in Biochemical Sciences* 2012;37:404–10. <https://doi.org/10.1016/j.tibs.2012.07.005>.
- [567] Shental-Bechor D, Levy Y. Effect of glycosylation on protein folding: A close look at thermodynamic stabilization. *Proc Natl Acad Sci USA* 2008;105:8256–61. <https://doi.org/10.1073/pnas.0801340105>.
- [568] Bootz F, Venetz D, Ziffels B, Neri D. Different tissue distribution properties for glycosylation variants of fusion proteins containing the p40 subunit of murine interleukin-12. *Protein Engineering, Design and Selection* 2016;29:445–55. <https://doi.org/10.1093/protein/gzw038>.

- [569] Waetzig GH, Chalaris A, Rosenstiel P, Suthaus J, Holland C, Karl N, et al. N-Linked Glycosylation Is Essential for the Stability but Not the Signaling Function of the Interleukin-6 Signal Transducer Glycoprotein 130. *Journal of Biological Chemistry* 2010;285:1781–9. <https://doi.org/10.1074/jbc.M109.075952>.
- [570] Agthe M, Garbers Y, Grötzinger J, Garbers C. Two N-Linked Glycans Differentially Control Maturation, Trafficking and Proteolysis, but not Activity of the IL-11 Receptor. *Cell Physiol Biochem* 2018;45:2071–85. <https://doi.org/10.1159/000488044>.
- [571] Mancilla J, Ikejima T, Dinarello CA. Glycosylation of the interleukin-1 receptor type I is required for optimal binding of interleukin-1. *Lymphokine Cytokine Res* 1992;11:197–205.
- [572] Günther T, Theiss JM, Fischer N, Grundhoff A. Investigation of Viral and Host Chromatin by ChIP-PCR or ChIP-Seq Analysis. *Current Protocols in Microbiology* 2016;40. <https://doi.org/10.1002/9780471729259.mc01e10s40>.
- [573] Hewitson JP, Harcus Y, Murray J, van Agtmaal M, Filbey KJ, Grainger JR, et al. Proteomic analysis of secretory products from the model gastrointestinal nematode *Heligmosomoides polygyrus* reveals dominance of Venom Allergen-Like (VAL) proteins. *Journal of Proteomics* 2011;74:1573–94. <https://doi.org/10.1016/j.jprot.2011.06.002>.
- [574] Skuce PJ, Stewart EM, Smith WD, Knox DP. Cloning and characterization of glutamate dehydrogenase (GDH) from the gut of *Haemonchus contortus*. *Parasitology* 1999;118:297–304. <https://doi.org/10.1017/S0031182098003850>.
- [575] Murray PJ. Amino acid auxotrophy as a system of immunological control nodes. *Nat Immunol* 2016;17:132–9. <https://doi.org/10.1038/ni.3323>.
- [576] Montes CL, Acosta-Rodríguez EV, Mucci J, Zuniga EI, Campetella O, Gruppi A. A *Trypanosoma cruzi* antigen signals CD11b+ cells to secrete cytokines that promote polyclonal B cell proliferation and differentiation into antibody-secreting cells. *Eur J Immunol* 2006;36:1474–85. <https://doi.org/10.1002/eji.200535537>.
- [577] Gause WC, Wynn TA, Allen JE. Type 2 immunity and wound healing: evolutionary refinement of adaptive immunity by helminths. *Nat Rev Immunol* 2013;13:607–14. <https://doi.org/10.1038/nri3476>.
- [578] Guasconi L, Burstein VL, Beccacece I, Mena C, Chiapello LS, Masih DT. Dectin-1 on macrophages modulates the immune response to *Fasciola hepatica* products through the ERK signaling pathway. *Immunobiology* 2018;223:834–8. <https://doi.org/10.1016/j.imbio.2018.08.004>.
- [579] Chen F, El-Naccache DW, Ponessa JJ, Lemenze A, Espinosa V, Wu W, et al. Helminth resistance is mediated by differential activation of recruited monocyte-derived alveolar macrophages and arginine depletion. *Cell Reports* 2022;38:110215. <https://doi.org/10.1016/j.celrep.2021.110215>.
- [580] Kiyoshi M, Caaveiro JMM, Kawai T, Tashiro S, Ide T, Asaoka Y, et al. Structural basis for binding of human IgG1 to its high-affinity human receptor FcγRI. *Nat Commun* 2015;6:6866. <https://doi.org/10.1038/ncomms7866>.

- [581] Cortes-Selva D, Gibbs L, Maschek JA, Nascimento M, Van Ry T, Cox JE, et al. Metabolic reprogramming of the myeloid lineage by *Schistosoma mansoni* infection persists independently of antigen exposure. *PLoS Pathog* 2021;17:e1009198. <https://doi.org/10.1371/journal.ppat.1009198>.
- [582] Jenkins SJ, Ruckerl D, Cook PC, Jones LH, Finkelman FD, van Rooijen N, et al. Local Macrophage Proliferation, Rather than Recruitment from the Blood, Is a Signature of TH2 Inflammation. *Science* 2011;332:1284–8. <https://doi.org/10.1126/science.1204351>.
- [583] Raisner R, Kharbanda S, Jin L, Jeng E, Chan E, Merchant M, et al. Enhancer Activity Requires CBP/P300 Bromodomain-Dependent Histone H3K27 Acetylation. *Cell Reports* 2018;24:1722–9. <https://doi.org/10.1016/j.celrep.2018.07.041>.
- [584] Fork C, Vasconez AE, Janetzko P, Angioni C, Schreiber Y, Ferreirós N, et al. Epigenetic control of microsomal prostaglandin E synthase-1 by HDAC-mediated recruitment of p300. *J Lipid Res* 2017;58:386–92. <https://doi.org/10.1194/jlr.M072280>.
- [585] Liu F, Romantseva T, Park Y-J, Golding H, Zaitseva M. Production of fever mediator PGE2 in human monocytes activated with MDP adjuvant is controlled by signaling from MAPK and p300 HAT: Key role of T cell derived factor. *Mol Immunol* 2020;128:139–49. <https://doi.org/10.1016/j.molimm.2020.10.008>.
- [586] Lu J, Sun H, Wang X, Liu C, Xu X, Li F, et al. Interleukin-12 p40 promoter activity is regulated by the reversible acetylation mediated by HDAC1 and p300. *Cytokine* 2005;31:46–51. <https://doi.org/10.1016/j.cyto.2005.03.001>.
- [587] Chen J, Gu Z, Wu M, Yang Y, Zhang J, Ou J, et al. C-reactive protein can upregulate VEGF expression to promote ADSC-induced angiogenesis by activating HIF-1 α via CD64/PI3k/Akt and MAPK/ERK signaling pathways. *Stem Cell Res Ther* 2016;7:114. <https://doi.org/10.1186/s13287-016-0377-1>.
- [588] Ruckerl D, Campbell SM, Duncan S, Sutherland TE, Jenkins SJ, Hewitson JP, et al. Macrophage origin limits functional plasticity in helminth-bacterial co-infection. *PLoS Pathog* 2017;13:e1006233. <https://doi.org/10.1371/journal.ppat.1006233>.
- [589] Passos LSA, Gazzinelli-Guimarães PH, Oliveira Mendes TA de, Guimarães ACG, Silveira Lemos D da, Ricci ND, et al. Regulatory monocytes in helminth infections: insights from the modulation during human hookworm infection. *BMC Infect Dis* 2017;17:253. <https://doi.org/10.1186/s12879-017-2366-0>.
- [590] Osbourn M, Soares DC, Vacca F, Cohen ES, Scott IC, Gregory WF, et al. HpARI Protein Secreted by a Helminth Parasite Suppresses Interleukin-33. *Immunity* 2017;47:739–751.e5. <https://doi.org/10.1016/j.immuni.2017.09.015>.
- [591] Draijer C, Boersma CE, Reker-Smit C, Post E, Poelstra K, Melgert BN. PGE2-treated macrophages inhibit development of allergic lung inflammation in mice. *Journal of Leukocyte Biology* 2016;100:95–102. <https://doi.org/10.1189/jlb.3MAB1115-505R>.
- [592] Liu M, Saeki K, Matsunobu T, Okuno T, Koga T, Sugimoto Y, et al. 12-hydroxyheptadecatrienoic acid promotes epidermal wound healing by accelerating keratinocyte migration via the BLT2 receptor. *Journal of Experimental Medicine* 2014;211:1063–78. <https://doi.org/10.1084/jem.20132063>.

- [593] Paul BZS, Jin J, Kunapuli SP. Molecular Mechanism of Thromboxane A₂-induced Platelet Aggregation. *Journal of Biological Chemistry* 1999;274:29108–14. <https://doi.org/10.1074/jbc.274.41.29108>.
- [594] Miyahara N, Ohnishi H, Matsuda H, Miyahara S, Takeda K, Koya T, et al. Leukotriene B₄ Receptor 1 Expression on Dendritic Cells Is Required for the Development of Th₂ Responses and Allergen-Induced Airway Hyperresponsiveness. *The Journal of Immunology* 2008;181:1170–8. <https://doi.org/10.4049/jimmunol.181.2.1170>.
- [595] Hodge SH, McSorley HJ. A Good Day for Helminths: how parasite-derived GDH suppresses inflammatory responses. *EMBO Reports* 2022. <https://doi.org/10.15252/embr.202255054>.
- [596] Kalim KW, Groettrup M. Prostaglandin E₂ inhibits IL-23 and IL-12 production by human monocytes through down-regulation of their common p40 subunit. *Mol Immunol* 2013;53:274–82. <https://doi.org/10.1016/j.molimm.2012.08.014>.
- [597] Trinath J, Hegde P, Sharma M, Maddur MS, Rabin M, Vallat J-M, et al. Intravenous immunoglobulin expands regulatory T cells via induction of cyclooxygenase-2-dependent prostaglandin E₂ in human dendritic cells. *Blood* 2013;122:1419–27. <https://doi.org/10.1182/blood-2012-11-468264>.
- [598] Tomić S, Joksimović B, Bekić M, Vasiljević M, Milanović M, Čolić M, et al. Prostaglandin-E₂ Potentiates the Suppressive Functions of Human Mononuclear Myeloid-Derived Suppressor Cells and Increases Their Capacity to Expand IL-10-Producing Regulatory T Cell Subsets. *Front Immunol* 2019;10:475. <https://doi.org/10.3389/fimmu.2019.00475>.
- [599] Baban B, Chandler PR, Sharma MD, Pihkala J, Koni PA, Munn DH, et al. IDO Activates Regulatory T Cells and Blocks Their Conversion into Th₁₇-Like T Cells. *The Journal of Immunology* 2009;183:2475–83. <https://doi.org/10.4049/jimmunol.0900986>.
- [600] Donovan MJ, Tripathi V, Favila MA, Geraci NS, Lange MC, Ballhorn W, et al. Indoleamine 2,3-dioxygenase (IDO) induced by *Leishmania* infection of human dendritic cells: *Leishmania-induced IDO*. *Parasite Immunology* 2012;34:464–72. <https://doi.org/10.1111/j.1365-3024.2012.01380.x>.
- [601] Grohmann U, Volpi C, Fallarino F, Bozza S, Bianchi R, Vacca C, et al. Reverse signaling through GITR ligand enables dexamethasone to activate IDO in allergy. *Nat Med* 2007;13:579–86. <https://doi.org/10.1038/nm1563>.
- [602] Bouchery T, Kyle R, Camberis M, Shepherd A, Filbey K, Smith A, et al. ILC2s and T cells cooperate to ensure maintenance of M2 macrophages for lung immunity against hookworms. *Nat Commun* 2015;6:6970. <https://doi.org/10.1038/ncomms7970>.
- [603] Obata-Ninomiya K, Ishiwata K, Tsutsui H, Nei Y, Yoshikawa S, Kawano Y, et al. The skin is an important bulwark of acquired immunity against intestinal helminths. *Journal of Experimental Medicine* 2013;210:2583–95. <https://doi.org/10.1084/jem.20130761>.
- [604] Robb CT, Zhou Y, Felton JM, Zhang B, Goepf M, Jheeta P, et al. Metabolic regulation by prostaglandin E₂ impairs lung group 2 innate lymphoid cell responses. *Allergy* 2023;78:714–30. <https://doi.org/10.1111/all.15541>.

- [605] Serra-Pages M, Torres R, Plaza J, Herrerias A, Costa-Farré C, Marco A, et al. Activation of the Prostaglandin E₂ receptor EP2 prevents house dust mite-induced airway hyperresponsiveness and inflammation by restraining mast cells' activity. *Clin Exp Allergy* 2015;45:1590–600. <https://doi.org/10.1111/cea.12542>.
- [606] Teloni R, Giannoni F, Rossi P, Nisini R, Gagliardi MC. Interleukin-4 inhibits cyclooxygenase-2 expression and prostaglandin E₂ production by human mature dendritic cells. *Immunology* 2007;120. <https://doi.org/10.1111/j.1365-2567.2006.02482.x>.
- [607] Miyoshi H, VanDussen KL, Malvin NP, Ryu SH, Wang Y, Sonnek NM, et al. Prostaglandin E₂ promotes intestinal repair through an adaptive cellular response of the epithelium. *EMBO J* 2017;36:5–24. <https://doi.org/10.15252/embj.201694660>.
- [608] Zhao J, Shu B, Chen L, Tang J, Zhang L, Xie J, et al. Prostaglandin E₂ inhibits collagen synthesis in dermal fibroblasts and prevents hypertrophic scar formation *in vivo*. *Exp Dermatol* 2016;25:604–10. <https://doi.org/10.1111/exd.13014>.
- [609] Fairweather M, Heit YI, Buie J, Rosenberg LM, Briggs A, Orgill DP, et al. Celecoxib inhibits early cutaneous wound healing. *Journal of Surgical Research* 2015;194:717–24. <https://doi.org/10.1016/j.jss.2014.12.026>.
- [610] Iwanaga K, Okada M, Murata T, Hori M, Ozaki H. Prostaglandin E₂ Promotes Wound-Induced Migration of Intestinal Subepithelial Myofibroblasts via EP2, EP3, and EP4 Prostanoid Receptor Activation. *J Pharmacol Exp Ther* 2012;340:604–11. <https://doi.org/10.1124/jpet.111.189845>.
- [611] Ganesh K, Das A, Dickerson R, Khanna S, Parinandi NL, Gordillo GM, et al. Prostaglandin E₂ Induces Oncostatin M Expression in Human Chronic Wound Macrophages through Axl Receptor Tyrosine Kinase Pathway. *The Journal of Immunology* 2012;189:2563–73. <https://doi.org/10.4049/jimmunol.1102762>.
- [612] Garantziotis S, Brass DM, Savov J, Hollingsworth JW, McElvania-TeKippe E, Berman K, et al. Leukocyte-Derived IL-10 Reduces Subepithelial Fibrosis Associated with Chronically Inhaled Endotoxin. *Am J Respir Cell Mol Biol* 2006;35:662–7. <https://doi.org/10.1165/rcmb.2006-0055OC>.
- [613] Pesce JT, Ramalingam TR, Mentink-Kane MM, Wilson MS, El Kasmi KC, Smith AM, et al. Arginase-1-Expressing Macrophages Suppress Th2 Cytokine-Driven Inflammation and Fibrosis. *PLoS Pathog* 2009;5:e1000371. <https://doi.org/10.1371/journal.ppat.1000371>.
- [614] Moore BB, Ballinger MN, White ES, Green ME, Herrygers AB, Wilke CA, et al. Bleomycin-Induced E Prostanoid Receptor Changes Alter Fibroblast Responses to Prostaglandin E₂. *The Journal of Immunology* 2005;174:5644–9. <https://doi.org/10.4049/jimmunol.174.9.5644>.
- [615] Stumm CL, Wettlaufer SH, Jancar S, Peters-Golden M. Airway remodeling in murine asthma correlates with a defect in PGE₂ synthesis by lung fibroblasts. *American Journal of Physiology-Lung Cellular and Molecular Physiology* 2011;301:L636–44. <https://doi.org/10.1152/ajplung.00158.2011>.
- [616] Marsland BJ, Kurrer M, Reissmann R, Harris NL, Kopf M. *Nippostrongylus brasiliensis* infection leads to the development of emphysema associated with the

- induction of alternatively activated macrophages. *Eur J Immunol* 2008;38:479–88. <https://doi.org/10.1002/eji.200737827>.
- [617] Xu W, Yang H, Liu Y, Yang Y, Wang P, Kim S-H, et al. Oncometabolite 2-Hydroxyglutarate Is a Competitive Inhibitor of α -Ketoglutarate-Dependent Dioxygenases. *Cancer Cell* 2011;19:17–30. <https://doi.org/10.1016/j.ccr.2010.12.014>.
- [618] Intlekofer AM, Dematteo RG, Venneti S, Finley LWS, Lu C, Judkins AR, et al. Hypoxia Induces Production of L-2-Hydroxyglutarate. *Cell Metabolism* 2015;22:304–11. <https://doi.org/10.1016/j.cmet.2015.06.023>.
- [619] Williams NC, Ryan DG, Costa ASH, Mills EL, Jedrychowski MP, Cloonan SM, et al. Signaling metabolite L-2-hydroxyglutarate activates the transcription factor HIF-1 α in lipopolysaccharide-activated macrophages. *Journal of Biological Chemistry* 2022;298:101501. <https://doi.org/10.1016/j.jbc.2021.101501>.
- [620] Li F-L, Liu J-P, Bao R-X, Yan G, Feng X, Xu Y-P, et al. Acetylation accumulates PFKFB3 in cytoplasm to promote glycolysis and protects cells from cisplatin-induced apoptosis. *Nat Commun* 2018;9:508. <https://doi.org/10.1038/s41467-018-02950-5>.
- [621] Infantino V, Iacobazzi V, Menga A, Avantaggiati ML, Palmieri F. A key role of the mitochondrial citrate carrier (SLC25A1) in TNF α - and IFN γ -triggered inflammation. *Biochimica et Biophysica Acta (BBA) - Gene Regulatory Mechanisms* 2014;1839:1217–25. <https://doi.org/10.1016/j.bbagrm.2014.07.013>.
- [622] Selak MA, Armour SM, MacKenzie ED, Boulahbel H, Watson DG, Mansfield KD, et al. Succinate links TCA cycle dysfunction to oncogenesis by inhibiting HIF- α prolyl hydroxylase. *Cancer Cell* 2005;7:77–85. <https://doi.org/10.1016/j.ccr.2004.11.022>.
- [623] Mills EL, Kelly B, Logan A, Costa ASH, Varma M, Bryant CE, et al. Succinate Dehydrogenase Supports Metabolic Repurposing of Mitochondria to Drive Inflammatory Macrophages. *Cell* 2016;167:457-470.e13. <https://doi.org/10.1016/j.cell.2016.08.064>.
- [624] Tang X, Rönnberg E, Säfholm J, Thulasingam M, Trauelsen M, Schwartz TW, et al. Activation of succinate receptor 1 boosts human mast cell reactivity and allergic bronchoconstriction. *Allergy* 2022;all.15245. <https://doi.org/10.1111/all.15245>.
- [625] Bohnacker S, Hartung F, Henkel F, Quaranta A, Kolmert J, Priller A, et al. Mild COVID-19 imprints a long-term inflammatory eicosanoid- and chemokine memory in monocyte-derived macrophages. *Mucosal Immunol* 2022;15:515–24. <https://doi.org/10.1038/s41385-021-00482-8>.
- [626] Zalinger ZB, Elliott R, Weiss SR. Role of the inflammasome-related cytokines Il-1 and Il-18 during infection with murine coronavirus. *J Neurovirol* 2017;23:845–54. <https://doi.org/10.1007/s13365-017-0574-4>.
- [627] Schulte-Schrepping J, Reusch N, Paclik D, Baßler K, Schlickeiser S, Zhang B, et al. Severe COVID-19 Is Marked by a Dysregulated Myeloid Cell Compartment. *Cell* 2020;182:1419-1440.e23. <https://doi.org/10.1016/j.cell.2020.08.001>.

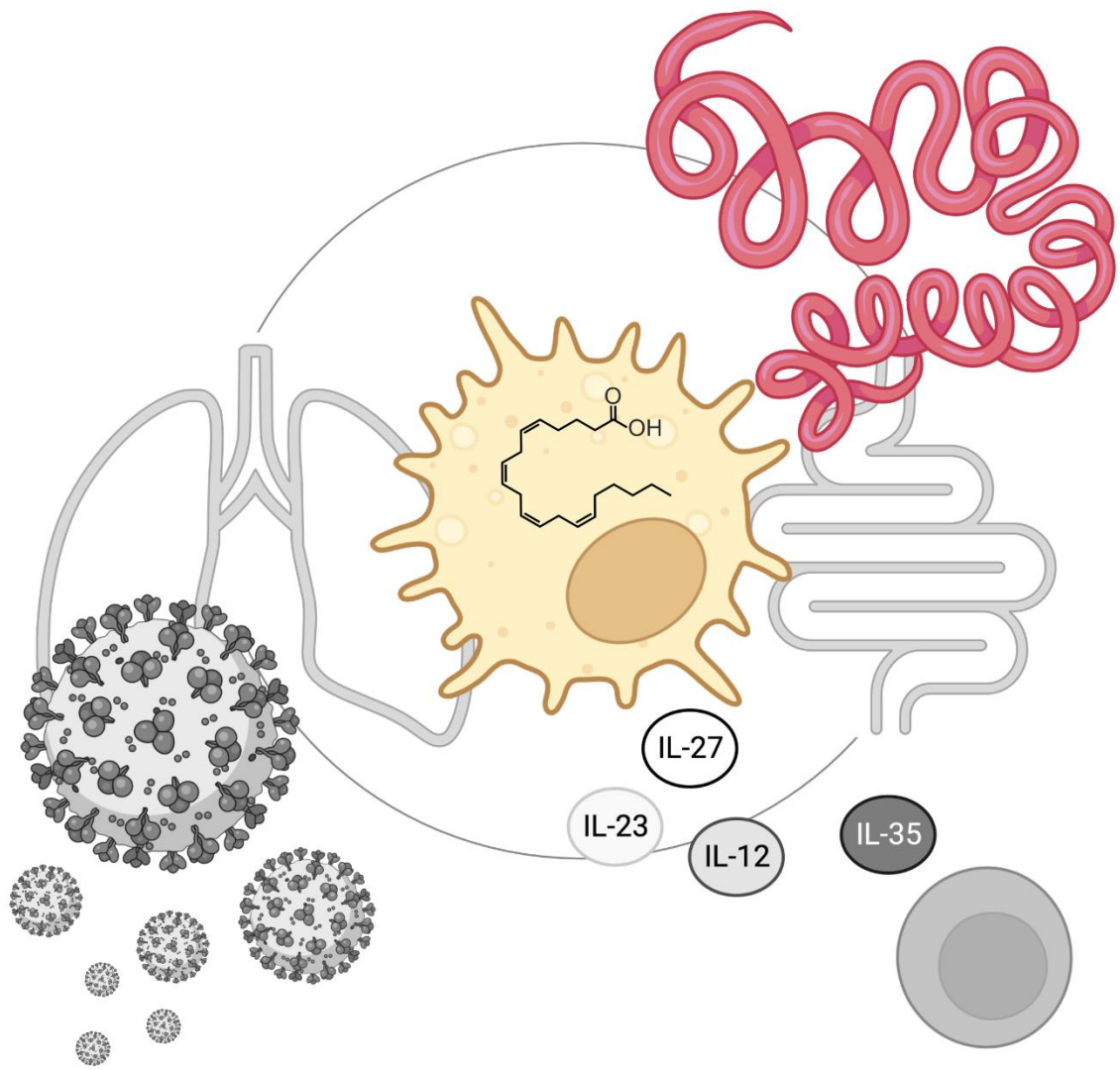
- [628] Shirey KA, Perkins DJ, Lai W, Zhang W, Fernando LR, Gusovsky F, et al. Influenza “Trains” the Host for Enhanced Susceptibility to Secondary Bacterial Infection. *MBio* 2019;10:e00810-19. <https://doi.org/10.1128/mBio.00810-19>.
- [629] Roquilly A, Jacqueline C, Davieau M, Mollé A, Sadek A, Fourgeux C, et al. Alveolar macrophages are epigenetically altered after inflammation, leading to long-term lung immunoparalysis. *Nat Immunol* 2020;21:636–48. <https://doi.org/10.1038/s41590-020-0673-x>.
- [630] Kazani S, Planaguma A, Ono E, Bonini M, Zahid M, Marigowda G, et al. Exhaled breath condensate eicosanoid levels associate with asthma and its severity. *Journal of Allergy and Clinical Immunology* 2013;132:547–53. <https://doi.org/10.1016/j.jaci.2013.01.058>.
- [631] Aegerter H, Kulikauskaite J, Crotta S, Patel H, Kelly G, Hessel EM, et al. Influenza-induced monocyte-derived alveolar macrophages confer prolonged antibacterial protection. *Nat Immunol* 2020;21:145–57. <https://doi.org/10.1038/s41590-019-0568-x>.
- [632] Szabo PA, Dogra P, Gray JI, Wells SB, Connors TJ, Weisberg SP, et al. Longitudinal profiling of respiratory and systemic immune responses reveals myeloid cell-driven lung inflammation in severe COVID-19. *Immunity* 2021;54:797-814.e6. <https://doi.org/10.1016/j.immuni.2021.03.005>.
- [633] You M, Chen L, Zhang D, Zhao P, Chen Z, Qin E-Q, et al. Single-cell epigenomic landscape of peripheral immune cells reveals establishment of trained immunity in individuals convalescing from COVID-19. *Nat Cell Biol* 2021;23:620–30. <https://doi.org/10.1038/s41556-021-00690-1>.
- [634] Gottlieb RL, Vaca CE, Paredes R, Mera J, Webb BJ, Perez G, et al. Early Remdesivir to Prevent Progression to Severe Covid-19 in Outpatients. *N Engl J Med* 2022;386:305–15. <https://doi.org/10.1056/NEJMoa2116846>.
- [635] Ayodele O, Ren K, Zhao J, Signorovitch J, Jonsson Funk M, Zhu J, et al. Real-world treatment patterns and clinical outcomes for inpatients with COVID-19 in the US from September 2020 to February 2021. *PLoS ONE* 2021;16:e0261707. <https://doi.org/10.1371/journal.pone.0261707>.
- [636] WHO Solidarity Trial Consortium. Repurposed Antiviral Drugs for Covid-19 — Interim WHO Solidarity Trial Results. *N Engl J Med* 2021;384:497–511. <https://doi.org/10.1056/NEJMoa2023184>.
- [637] The RECOVERY Collaborative Group. Dexamethasone in Hospitalized Patients with Covid-19. *N Engl J Med* 2021;384:693–704. <https://doi.org/10.1056/NEJMoa2021436>.
- [638] Shacham EC, Ishay A. New Insights on Effects of Glucocorticoids in Patients With SARS-CoV-2 Infection. *Endocrine Practice* 2022;28:1100–6. <https://doi.org/10.1016/j.eprac.2022.07.006>.
- [639] Noreen S, Maqbool I, Madni A. Dexamethasone: Therapeutic potential, risks, and future projection during COVID-19 pandemic. *European Journal of Pharmacology* 2021;894:173854. <https://doi.org/10.1016/j.ejphar.2021.173854>.

- [640] Aigner L, Pietrantonio F, Bessa de Sousa DM, Michael J, Schuster D, Reitsamer HA, et al. The Leukotriene Receptor Antagonist Montelukast as a Potential COVID-19 Therapeutic. *Front Mol Biosci* 2020;7:610132. <https://doi.org/10.3389/fmolb.2020.610132>.
- [641] Dey M, Singh RK. Possible Therapeutic Potential of Cysteinyl Leukotriene Receptor Antagonist Montelukast in Treatment of SARS-CoV-2-Induced COVID-19. *Pharmacology* 2021;106:469–76. <https://doi.org/10.1159/000518359>.
- [642] Koenis DS, Beegun I, Jouvencé CC, Aguirre GA, Souza PR, Gonzalez-Nunez M, et al. Disrupted Resolution Mechanisms Favor Altered Phagocyte Responses in COVID-19. *Circ Res* 2021;129. <https://doi.org/10.1161/CIRCRESAHA.121.319142>.
- [643] Turnbull J, Jha RR, Ortori CA, Lunt E, Tighe PJ, Irving WL, et al. Serum Levels of Proinflammatory Lipid Mediators and Specialized Proresolving Molecules Are Increased in Patients With Severe Acute Respiratory Syndrome Coronavirus 2 and Correlate With Markers of the Adaptive Immune Response. *The Journal of Infectious Diseases* 2022;225:2142–54. <https://doi.org/10.1093/infdis/jiab632>.
- [644] Cherpokova D, Jouvencé CC, Libreros S, DeRoo EP, Chu L, de la Rosa X, et al. Resolvin D4 attenuates the severity of pathological thrombosis in mice. *Blood* 2019;134:1458–68. <https://doi.org/10.1182/blood.2018886317>.
- [645] Pal A, Gowdy KM, Oestreich KJ, Beck M, Shaikh SR. Obesity-Driven Deficiencies of Specialized Pro-resolving Mediators May Drive Adverse Outcomes During SARS-CoV-2 Infection. *Front Immunol* 2020;11:1997. <https://doi.org/10.3389/fimmu.2020.01997>.
- [646] Souza PR, Marques RM, Gomez EA, Colas RA, De Matteis R, Zak A, et al. Enriched Marine Oil Supplements Increase Peripheral Blood Specialized Pro-Resolving Mediators Concentrations and Reprogram Host Immune Responses: A Randomized Double-Blind Placebo-Controlled Study. *Circ Res* 2020;126:75–90. <https://doi.org/10.1161/CIRCRESAHA.119.315506>.
- [647] Braakman I, Bulleid NJ. Protein Folding and Modification in the Mammalian Endoplasmic Reticulum. *Annu Rev Biochem* 2011;80:71–99. <https://doi.org/10.1146/annurev-biochem-062209-093836>.
- [648] Carra G, Gerosa F, Trinchieri G. Biosynthesis and Posttranslational Regulation of Human IL-12. *The Journal of Immunology* 2000;164:4752–61. <https://doi.org/10.4049/jimmunol.164.9.4752>.
- [649] Podlaski FJ, Nanduri VB, Hulmes JD, Pan Y-CE, Levin W, Danho W, et al. Molecular characterization of interleukin 12. *Archives of Biochemistry and Biophysics* 1992;294:230–7. [https://doi.org/10.1016/0003-9861\(92\)90162-P](https://doi.org/10.1016/0003-9861(92)90162-P).
- [650] Ha SJ, Chang J, Song MK, Suh YS, Jin HT, Lee CH, et al. Engineering N-glycosylation mutations in IL-12 enhances sustained cytotoxic T lymphocyte responses for DNA immunization. *Nat Biotechnol* 2002;20:381–6. <https://doi.org/10.1038/nbt0402-381>.
- [651] Aparicio-Siegmund S, Moll JM, Lokau J, Grusdat M, Schröder J, Plöhn S, et al. Recombinant p35 from Bacteria Can Form Interleukin (IL-)12, but Not IL-35. *PLoS ONE* 2014;9:e107990. <https://doi.org/10.1371/journal.pone.0107990>.

- [652] Müller SI, Aschenbrenner I, Zacharias M, Feige MJ. An Interspecies Analysis Reveals Molecular Construction Principles of Interleukin 27. *Journal of Molecular Biology* 2019;431:2383–93. <https://doi.org/10.1016/j.jmb.2019.04.032>.
- [653] Lupardus PJ, Garcia KC. The Structure of Interleukin-23 Reveals the Molecular Basis of p40 Subunit Sharing with Interleukin-12. *Journal of Molecular Biology* 2008;382:931–41. <https://doi.org/10.1016/j.jmb.2008.07.051>.
- [654] Caveney NA, Glassman CR, Jude KM, Tsutsumi N, Garcia KC. Structure of the IL-27 quaternary receptor signaling complex. *ELife* 2022;11:e78463. <https://doi.org/10.7554/eLife.78463>.
- [655] Lee C-C, Lin J-C, Hwang W-L, Kuo Y-J, Chen H-K, Tai S-K, et al. Macrophage-secreted interleukin-35 regulates cancer cell plasticity to facilitate metastatic colonization. *Nat Commun* 2018;9:3763. <https://doi.org/10.1038/s41467-018-06268-0>.
- [656] Sawant DV, Yano H, Chikina M, Zhang Q, Liao M, Liu C, et al. Adaptive plasticity of IL-10+ and IL-35+ Treg cells cooperatively promotes tumor T cell exhaustion. *Nat Immunol* 2019;20:724–35. <https://doi.org/10.1038/s41590-019-0346-9>.
- [657] Mirlekar B, Pylayeva-Gupta Y. IL-12 Family Cytokines in Cancer and Immunotherapy. *Cancers* 2021;13:167. <https://doi.org/10.3390/cancers13020167>.
- [658] Cilenti F, Barbiera G, Caronni N, Iodice D, Montaldo E, Barresi S, et al. A PGE2-MEF2A axis enables context-dependent control of inflammatory gene expression. *Immunity* 2021;54:1665-1682.e14. <https://doi.org/10.1016/j.immuni.2021.05.016>.
- [659] Yen J-H, Kong W, Hooper KM, Emig F, Rahbari KM, Kuo P-C, et al. Differential effects of IFN- β on IL-12, IL-23, and IL-10 expression in TLR-stimulated dendritic cells. *J Leukoc Biol* 2015;98:689–702. <https://doi.org/10.1189/jlb.3HI0914-453R>.
- [660] Desai P, Janova H, White JP, Reynoso GV, Hickman HD, Baldrige MT, et al. Enteric helminth coinfection enhances host susceptibility to neurotropic flaviviruses via a tuft cell-IL-4 receptor signaling axis. *Cell* 2021;184:1214-1231.e16. <https://doi.org/10.1016/j.cell.2021.01.051>.
- [661] Gavett SH, O’Hearn DJ, Li X, Huang SK, Finkelman FD, Wills-Karp M. Interleukin 12 inhibits antigen-induced airway hyperresponsiveness, inflammation, and Th2 cytokine expression in mice. *Journal of Experimental Medicine* 1995;182:1527–36. <https://doi.org/10.1084/jem.182.5.1527>.
- [662] Schwarze J, Hamelmann E, Cieslewicz G, Tomkinson A, Joetham A, Bradley K, et al. Local treatment with IL-12 is an effective inhibitor of airway hyperresponsiveness and lung eosinophilia after airway challenge in sensitized mice. *Journal of Allergy and Clinical Immunology* 1998;102:86–93. [https://doi.org/10.1016/S0091-6749\(98\)70058-2](https://doi.org/10.1016/S0091-6749(98)70058-2).
- [663] Everts B, Tussiwand R, Dreesen L, Fairfax KC, Huang SC-C, Smith AM, et al. Migratory CD103+ dendritic cells suppress helminth-driven type 2 immunity through constitutive expression of IL-12. *Journal of Experimental Medicine* 2016;213:35–51. <https://doi.org/10.1084/jem.20150235>.

- [664] Stobie L, Gurunathan S, Prussin C, Sacks DL, Glaichenhaus N, Wu C-Y, et al. The role of antigen and IL-12 in sustaining Th1 memory cells *in vivo*: IL-12 is required to maintain memory/effector Th1 cells sufficient to mediate protection to an infectious parasite challenge. *Proc Natl Acad Sci USA* 2000;97:8427–32. <https://doi.org/10.1073/pnas.160197797>.
- [665] Jankovic D, Kullberg MC, Hieny S, Caspar P, Collazo CM, Sher A. In the Absence of IL-12, CD4+ T Cell Responses to Intracellular Pathogens Fail to Default to a Th2 Pattern and Are Host Protective in an IL-10^{-/-} Setting. *Immunity* 2002;16:429–39. [https://doi.org/10.1016/S1074-7613\(02\)00278-9](https://doi.org/10.1016/S1074-7613(02)00278-9).
- [666] Dokmeci E, Xu L, Robinson E, Golubets K, Bottomly K, Herrick CA. EBI3 deficiency leads to diminished T helper type 1 and increased T helper type 2 mediated airway inflammation: EBI3 deficiency leads to diminished Th1, increased Th2. *Immunology* 2011;132:559–66. <https://doi.org/10.1111/j.1365-2567.2010.03401.x>.
- [667] Moro K, Kabata H, Tanabe M, Koga S, Takeno N, Mochizuki M, et al. Interferon and IL-27 antagonize the function of group 2 innate lymphoid cells and type 2 innate immune responses. *Nat Immunol* 2016;17:76–86. <https://doi.org/10.1038/ni.3309>.
- [668] Vandersluijs K, Vanelden L, Xiao Y, Arens R, Nijhuis M, Schuurman R, et al. IL-12 deficiency transiently improves viral clearance during the late phase of respiratory tract infection with influenza A virus in mice. *Antiviral Research* 2006;70:75–84. <https://doi.org/10.1016/j.antiviral.2006.01.007>.
- [669] Gounder AP, Yokoyama CC, Jarjour NN, Bricker TL, Edelson BT, Boon ACM. Interferon induced protein 35 exacerbates H5N1 influenza disease through the expression of IL-12p40 homodimer. *PLoS Pathog* 2018;14:e1007001. <https://doi.org/10.1371/journal.ppat.1007001>.

Publications



PUBLICATION I

A helminth enzyme instigates a macrophage-mediated immune evasion via a p300-prostaglandin axis

Sina Bohnacker¹, Arie Geerlof², Fiona Henkel¹, Sandra Riemer¹, Franziska Hartung¹, André Mourão², Stefan Bohn³, Ulrich F. Prodjinotho^{4,5}, Tarvi Teder⁶, Jesper Z. Haeggström⁶, Yannick Schreiber⁷, Robert Gurke⁷, Minhaz Ud-Dean⁸, Francesca Alessandrini¹, Antonie Lechner¹, Agnieszka M. Kabat⁹, Edward Pearce⁹, Per-Johan Jakobsson¹⁰, David Vöhringer¹¹, Matthias J Feige¹², Carsten B Schmidt-Weber^{1,13}, Clarissa Prazeres da Costa^{4,5}, Julia Esser-von Bieren^{1,14*}

Affiliations:

¹Center of Allergy and Environment (ZAUM), Technical University of Munich and Helmholtz Center Munich, 80802 Munich, Germany

²Protein Expression and Purification Facility (PEPF), Institute of Structural Biology, Helmholtz Center Munich, 85764 Neuherberg, Germany

³Department of Molecular Structural Biology, Max-Planck-Institute of Biochemistry, 82152 Martinsried, Germany

⁴Institute for Microbiology, Immunology and Hygiene, Technical University of Munich, 81675 Munich, Germany

⁵Center for Global Health, Technical University of Munich, 81675 Munich, Germany

⁶Department of Medical Biochemistry and Biophysics, Division of Chemistry II, Karolinska Institutet, 171 65 Stockholm, Sweden

⁷Institute of Clinical Pharmacology, Goethe-University Frankfurt, 60590 Frankfurt am Main, Germany

⁸Institute of Computational Biology, Helmholtz Center Munich, 85764 Neuherberg, Germany

⁹Max Planck Institute for Immunobiology and Epigenetics, 79108 Freiburg, Germany

¹⁰Biochemical Toxicology Unit, Institute of Environmental Medicine, Karolinska Institutet, SE-171 77, Stockholm, Sweden

¹¹Infektionsbiologische Abteilung, Universitätsklinikum Erlangen, Friedrich-Alexander-Universität, 91054 Erlangen-Nürnberg, Germany

¹²Department of Chemistry, Technical University of Munich, 85748 Garching, Germany

¹³Member of the German Center of Lung Research (DZL)

¹⁴Department of Immunobiology, Université de Lausanne, 1066 Epalinges, Switzerland

* Corresponding author: Julia Esser-von Bieren

Department of Immunobiology, Université de Lausanne

Chemin des Boveresses 155

1066 Epalinges

Switzerland

Tel: +41 78 246 77 30

Email: julia.esser-vonbieren@unil.ch

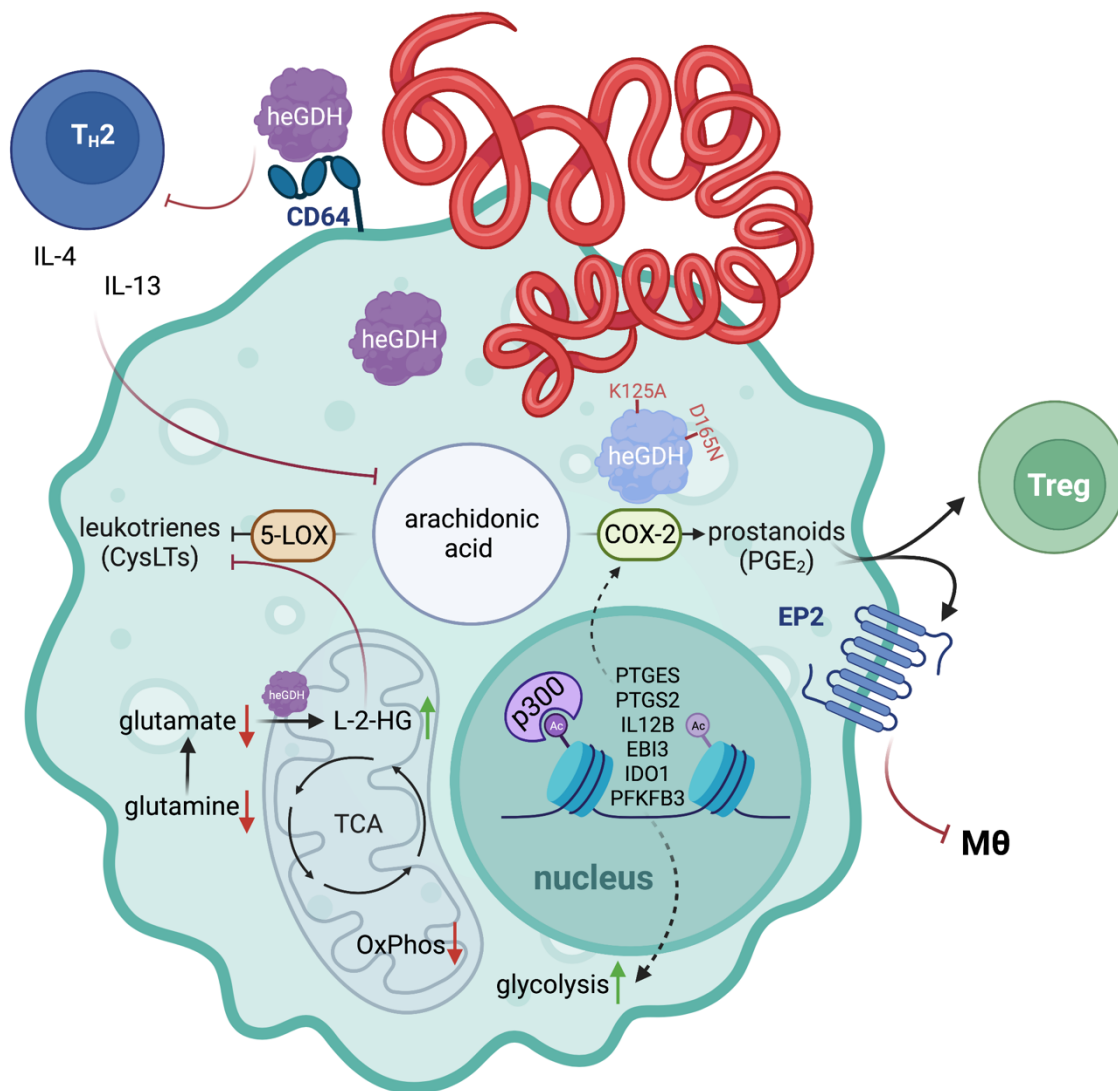
HIGHLIGHTS

- Helminthic glutamate dehydrogenase enables chronic infection by suppressing the host type 2 immune response
- Helminthic glutamate dehydrogenase induces p300 dependent metabolic, epigenetic, and transcriptional reprogramming in macrophages
- Upregulation of myeloid/ hematopoietic prostaglandin E₂ synthesis mediates helminthic immune evasion

SUMMARY

The molecular mechanisms by which worm parasites evade host immunity are incompletely understood. In a mouse model of chronic intestinal helminth infection, we identify helminthic glutamate dehydrogenase (heGDH) as an essential factor for parasite chronicity by using antibody mediated neutralization or treatment with exogenous recombinant heGDH. Macrophages efficiently internalize heGDH and represent a major target of the enzyme *in vivo*. Combining RNA-seq, ChIP, targeted lipidomics and inhibitor studies, we identify prostaglandin E₂ (PGE₂) as a major immune regulatory mechanism of heGDH. The induction of PGE₂ and further immune regulatory factors (IL-12 family cytokines, IDO1) by heGDH depended on the p300-mediated acetylation of histones. While the enzyme's catalytic activity was dispensable for key immune regulatory functions, an N-terminal handle-like structure distinct from mammalian GDHs may confer interaction of heGDH with its targets (e.g. CD64). Thus, helminths employ a ubiquitous metabolic enzyme to epigenetically target macrophages and establish chronicity.

GRAPHICAL ABSTRACT



KEY WORDS

Eicosanoids; glutamate dehydrogenase; *Heligmosomoides polygyrus bakeri*; helminth; host immune response; macrophages; p300; prostaglandins; type 2 immunity

INTRODUCTION

Over 1,000 different parasites can infest humans and around one-third of the human population worldwide are infected by worm parasites (helminths). During evolution, helminths have developed survival strategies to suppress host defense and establish chronic infections. Mechanisms or molecules associated with the evasion of the immune response by parasitic helminths may be exploited for the treatment of type 2 inflammatory disorders. However, the mechanisms and molecules by which helminths control antiparasitic immune responses to persist in the host have remained elusive.

Protective immunity against helminth parasites often relies on the induction of a type 2 immune response characterized by the production of type 2 cytokines that activate host effector cells such as macrophages, granulocytes and T helper 2 (T_H2) cells¹⁻⁶. Helminths can efficiently suppress this type 2 immune response by targeting cytokines (e.g. IL-33) important for its induction⁷ or by inducing regulatory T-cells and macrophages⁸.

We previously showed that larval products containing the glutamate dehydrogenase (GDH) of *Heligmosomoides polygyrus bakeri* (*Hpb*) suppress allergic inflammation in a mouse model of asthma by inducing a shift in the arachidonic acid (AA) metabolic pathway⁹. GDH are widely conserved among free-living parasitic helminths, including the human cestode parasite *Taenia solium*, in which GDH was shown to induce regulatory T cells by inducing the immunoregulatory AA metabolite prostaglandin E₂ (PGE₂)¹⁰. However, it remained unclear how helminth derived GDHs can affect the arachidonic acid (AA) metabolism in innate immune cells and whether this would lead to immune evasion *in vivo*. AA metabolites are important bioactive derivatives of polyunsaturated fatty acids (PUFAs) with key roles in infection and inflammation¹¹. Leukotrienes synthesized by 5-lipoxygenase (5-LOX) promote type 2 inflammation and enable helminth expulsion¹². In contrast, prostaglandins synthesized by the cyclooxygenase (COX) pathway show both type-2 inducing¹³ as well as suppressive capacities^{10,14} during infections with helminth parasites.

Here, we uncover the mechanism of how heGDH affect macrophage metabolism to evade host immunity. We demonstrate that catalytically active heGDH regulates macrophage TCA and amino acid metabolism driving the suppression of cysteinyl leukotrienes, whereas its structure activates the p300 histonacetyltransferase to induce the

expression of multiple type 2 suppressive genes, including prostaglandin E₂ synthetic enzymes. The heGDH-mediated induction of myeloid PGE₂ synthesis suppressed host defense *in vivo*, thus identifying GDH as a key factor of helminthic immune evasion.

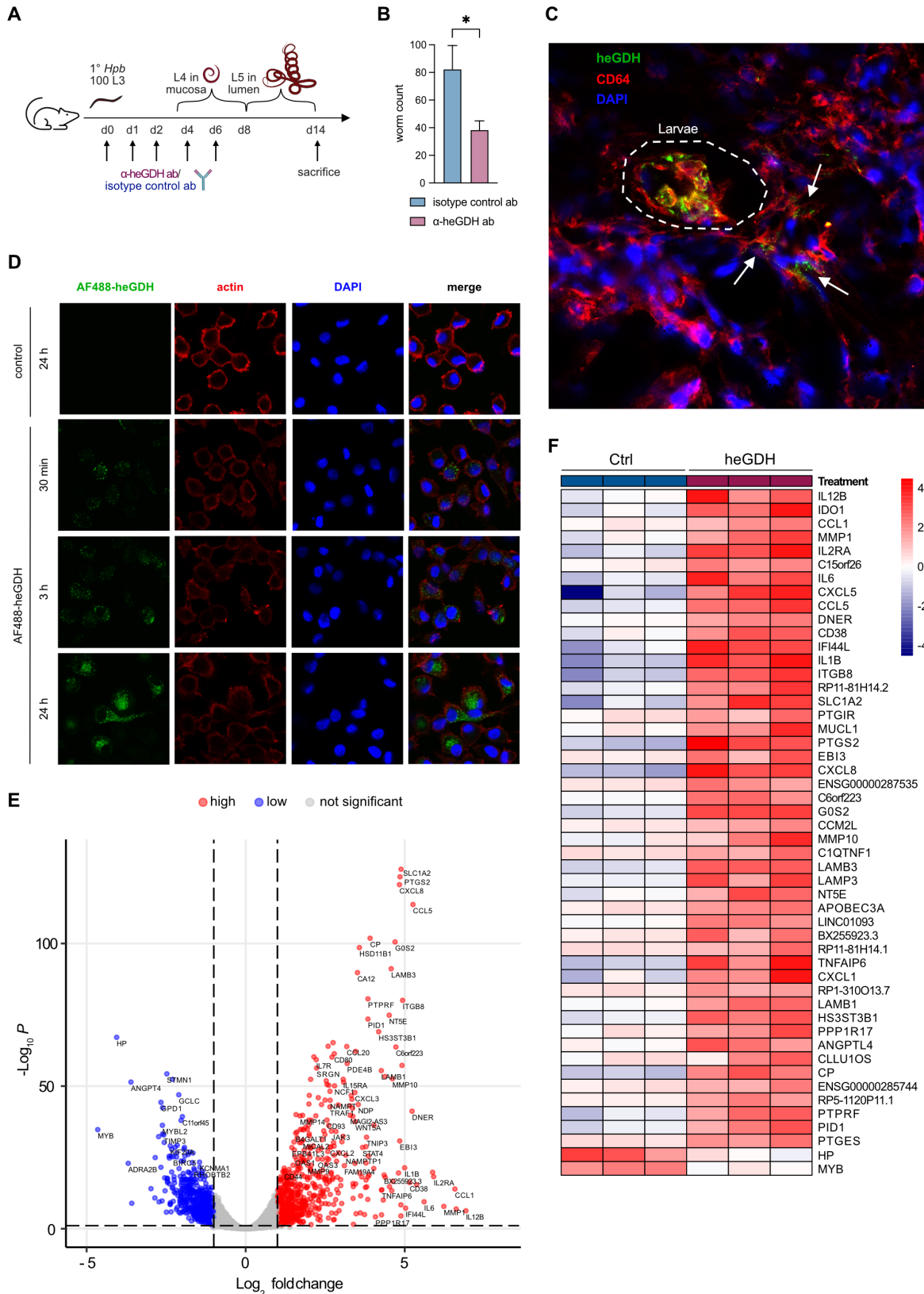
RESULTS

GDH enables helminth immune evasion by inducing type 2 suppressive macrophages

We previously identified GDH as a helminth-derived factor that is able to suppress type 2 inflammation in a mouse model of allergic asthma⁹. However, the evolutionary role of GDH during helminth infection remained unknown. To investigate, if GDH is essential for parasite immune evasion, we neutralized helminthic GDH (heGDH) by using a specific monoclonal antibody (mAb) (clone 4F8)⁹ during infection of mice with the nematode parasite *H. polygyrus bakeri* (*Hpb*) (Figure 1A). During a primary infestation, *Hpb* causes chronic infection with worm counts peaking around two weeks post infection (p.i.). Ab-mediated neutralization of heGDH resulted in lower worm counts 14 days p.i., suggesting that heGDH is a key factor in the *Hpb*-mediated suppression of type 2 immunity (Figure 1B).

Macrophages are essential players in host defense against parasite infections¹⁵ and recruited bone marrow-/ monocyte-derived macrophages are particularly important for anti-helminth immunity⁵. Immunofluorescence (IF) stainings using the heGDH specific (4F8) antibody revealed the colocalization of heGDH with CD64 positive macrophages, near *Hpb* larvae in the small intestinal submucosa (Figure 1C). In keeping, stimulation of human monocyte-derived macrophages (MDM) or murine bone-marrow derived macrophages (BMDM) with recombinant heGDH resulted in binding and uptake of the protein, which was detectable for at least 24h (Figures 1D and S1A-B).

To define the mechanisms underlying the type 2 suppressive function of heGDH, MDM treated with heGDH were subjected to RNA sequencing (RNAseq), which revealed broadly changed transcriptional profiles of heGDH treated compared to control macrophages. MDM treated with heGDH showed increased expression of immunoregulatory and type 2 suppressive genes including *IDO1*, *PTGES* (*mPTGES-1*), *PTGS2* (*COX2*), *PTGIR*, *IL12B* and *EBI3* (Figures 1E and 1F)¹⁶⁻²⁰. To exclude that the heGDH-triggered induction of regulatory mediators was due to endotoxin contamination, we additionally compared the transcriptional profiles of MDM stimulated with



heGDH to MDM stimulated with LPS at the concentration present in the preparation of heGDH (0.5 – 1 ng/mL) (Figures S1C and S1D). Compared to LPS, MDM stimulated with heGDH still showed an induction of the same top DEGs, confirming that heGDH imprints a

type-2 suppressive macrophage phenotype independent of the low amounts of contaminating LPS. Taken together, these data suggest that heGDH suppresses anti-helminth host defense by broadly modulating macrophage effector functions.

Figure 1: GDH serves as a key protein of *H. polygyrus* against the host immunity by shaping a type 2 suppressive gene expression profile in macrophages

(A) Experimental model of infection with *Heligmosomoides polygyrus bakeri* (*Hpb*) and intraperitoneal (i.p.) treatment with α -heGDH monoclonal antibody or respective isotype control antibody.
(B) *Hpb* worm burden 14 days post infection in mice treated with α -heGDH monoclonal antibody or in mice treated with isotype control antibody (n=10 per group).
(C) Representative immunofluorescence staining for heGDH, DAPI (cell nuclei) and CD64 in tissues from mice infected with *Hpb* (4 days). White arrows indicate colocalization of heGDH and macrophages in the surrounding of the larvae.
(D) Representative immunofluorescence staining of actin and DAPI (cell nuclei) in MDM \pm treatment with AF488-labeled heGDH for different time points (30 min, 3h, 24h).
(E) Volcano plot showing DEGs of MDM stimulated \pm heGDH (n=3). Significant DEGs are for all genes with base mean>50, padj<0.1 and log2FC>1. Labeled DEGs are for genes with either padj<1e-20 or with log2FC>4.
(F) Heatmap of top 50 DEGs between MDM treated \pm heGDH (n=3), padj<0.1, log2 FC>1 and base mean>50.

p300 histone acetyltransferase (HAT) activation by heGDH mediates the induction of immune-regulatory genes

The induction of multiple regulatory genes by heGDH and its partial nuclear localization (Figures 1D and S1B) suggested a potential epigenetic mechanism of action. Indeed, PGE₂ synthetic enzymes (COX-2 and mPGES-1) as well as IL-12 β are epigenetically controlled by HDAC-mediated recruitment of the p300 HAT²¹⁻²³. Addition of a p300 HAT inhibitor during treatment with heGDH resulted in the downregulation of top DEGs identified by RNA seq (*PTGES*, *PTGS2*, *IL12B*, *IDO1* and *EBI3*) (Figures 2A and S2A). Decreased gene expression correlated with a strongly diminished secretion of PGE₂ and IL-12 β (p40) in GDH-stimulated macrophages treated with the p300 HAT inhibitor (Figure 2B), which was not due to cellular toxicity (Figure S2B). siRNA knock down of p300 during heGDH stimulation confirmed the downregulation of target proteins, including COX-2 and mPGES1 in MDM and BMDM (Figures 2C and S2C). In line with the heGDH mediated activation of p300 we observed increased p300 dependent H3K27 acetylation in MDM and BMDM after stimulation with heGDH (Figures 2D and S2D). H3K27 enrichment in MDM treated with heGDH was further confirmed by ChIP-qPCR analysis of H3K27ac for *IDO1*, *PTGS2* and *IL6* (Figure 2E), suggesting that heGDH is activating p300 to acetylate H3K27, which results in the induction of immune-regulatory genes.

heGDH induces a broad type 2 suppressive mediator switch

In line with the increased expression of genes involved in prostanoid synthesis and signaling, identified by ChIP-qPCR and RNAseq (Figures 1E-F and S1C-D), LC-MS/MS analysis revealed a shift from type-2-inducing metabolites (cysLTs) to prostanoids involved in tissue repair and the regulation of type 2 immunity (PGD₂, PGE₂, PGF_{2 α} , TXB₂)^{24,25} in heGDH-treated MDM (Figure 3A). HeGDH further increased the anti-inflammatory

cytokine IL-10 (Figure 3B) and neutralization with clone 4F8 partially abrogated the heGDH-mediated regulation of IL-10 and COX-, but not of 5-LOX metabolites (Figures S3A-C). These suggested distinct mechanisms underlying the modulation of anti-inflammatory, reparative mediators on the one and type-2 promoting mediators (LTs) on the other hand.

Low doses of LPS (0.5-1 ng/mL) failed to induce PGE₂ and IL-10 (Figure S3D), supporting a unique property of heGDH to induce a regulatory mediator shift. To elucidate a potential upstream role of IL-12 β in the induction of regulatory mediators, MDM were stimulated with human IL-12 β . However, despite the capacity of IL-12 β to induce PGE₂ and IL-10 (Figure S3E), neutralizing antibodies against IL-12 β did not affect the induction of regulatory mediators in MDM (Figure S3F) or BMDM (Figure S3G), suggesting that IL-12 β does not act as a major upstream inducer of GDH-driven immune regulation. Taken together, these data suggest that heGDH evokes a unique immunoregulatory, type 2 suppressive lipid mediator and cytokine profile in macrophages.

heGDH-induced PGE₂ suppresses type 2 effector functions of macrophages and T-cells

To investigate effects of heGDH on anti-helminth host defense *in vivo* we treated mice with recombinant heGDH at day 4, 8 and 12 during infection with *H. polygyrus* (Figure 3C). Intraperitoneal (i.p.) treatment with heGDH during helminth infection led to a significant increase in worm burdens at 14 days p.i. (Figure 3D). HeGDH treated mice showed reduced expression of the M2 polarization marker RELM α in the small intestine while COX-2 was upregulated in granulomas of heGDH treated mice (Figure 3E). In line with our *in vitro* data (Figure 2), peritoneal macrophages from heGDH-treated mice showed increased H3K27 acetylation (Figure 3F) which correlated with an upregulation in PGE₂ production (Figure 3G). To study the role

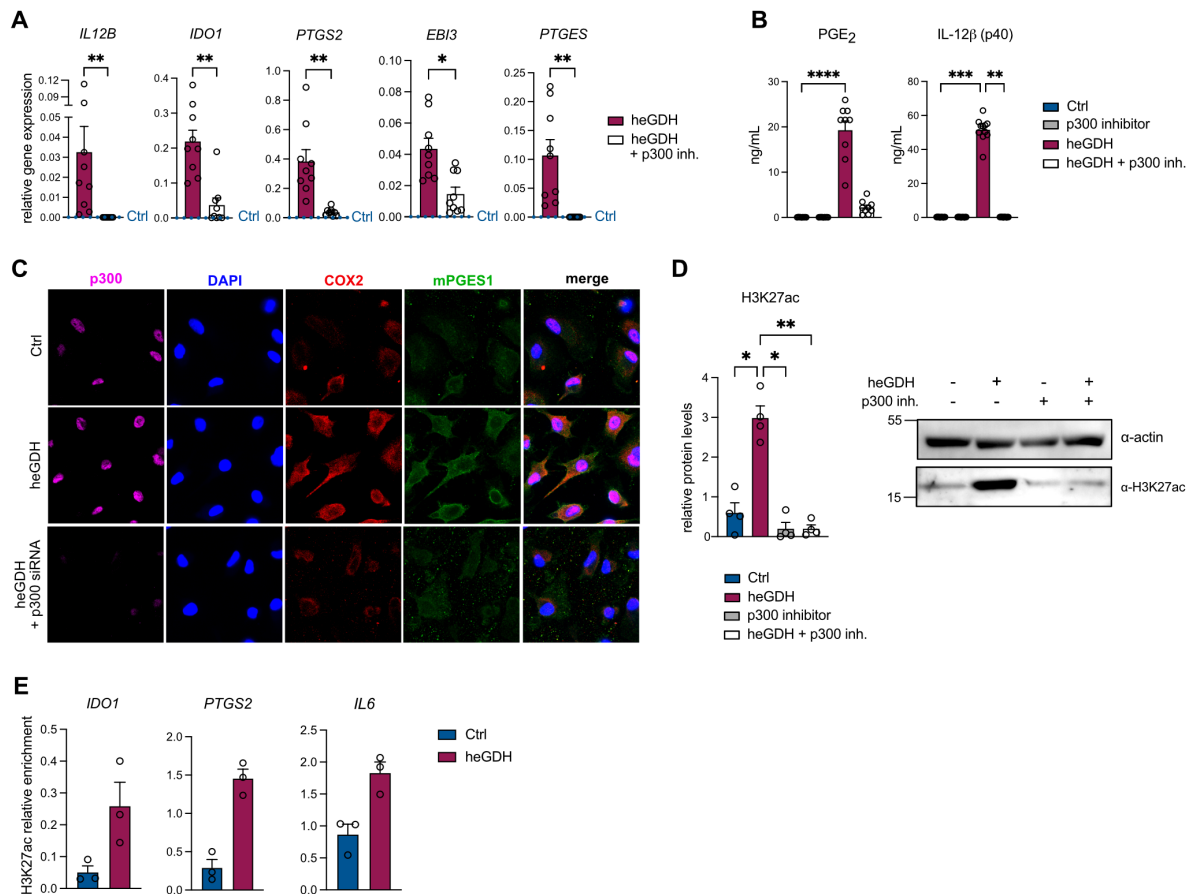


Figure 2: p300 HAT activation by heGDH is responsible for the induction of immune-regulatory genes

(A) Gene expression analysis of top DEGs (qPCR) in MDM ± treatment with heGDH ± inhibitor of p300 HAT (A485) (n=9). Dotted lines indicate expression in control (ctrl) treated cells.

(B) Secretion of PGE₂ or IL-12β (EIA, ELISA) of MDM ± treatment with heGDH ± inhibitor of p300 HAT (A485) (n=9).

(C) Representative immunofluorescence staining of p300, DAPI (cell nuclei), COX2 and mPGES1 in MDM ± treatment with heGDH and heGDH treated cells after p300 siRNA knock down.

(D) Protein amounts of H3K27ac or actin (western blot) in MDM ± treatment with heGDH ± inhibitor of p300 HAT (A485). Left, quantification for n=4 donors; right, representative blots for one blood donor.

(E) H3K27ac ChIP-qPCR signals at indicated genes in MDM ± treatment with heGDH. The ChIP-qPCR signal is shown as relative enrichment vs positive loci (n=3).

Data are pooled from at least two independent experiments and presented as means + SEM. Statistical significance was determined by Wilcoxon test (A,E), Friedman test (B) or RM one-way ANOVA (D). *P < 0.05; **P < 0.01; ***P < 0.001, ****P < 0.0001

of PGE₂ in the suppression of M2 activation, we analyzed M2 marker expression in BMDM from mice lacking the PGE₂ receptor EP2. Interestingly, heGDH downregulated the M2 marker CD206 in an EP2 dependent manner (Figure 3H), suggesting a key role for PGE₂ in the heGDH-mediated suppression of macrophage M2 activation.

To further assess the effect of heGDH on helminth chronicity, worm burdens were quantified at 28 days p.i. (Figure 3I). Indeed, heGDH administration (i.p.) led to an even stronger increase in worm burdens on day 28 as compared to day 14 (Figures 3D and 3J), suggesting that heGDH efficiently promotes helminth chronicity *in vivo*.

While treatment with heGDH did not induce PGE₂ in peritoneal macrophages (Figure 3K) at this later time point, other prostanoids (TXB₂ and 6-keto-PGF_{1α}), which are associated with tissue repair²⁴, were increased in the small intestine of mice treated with heGDH (Figure 3L). While at 14 days p.i., no significant regulation of the Treg and T_H2 immune response was observed (Figure S3H), heGDH treatment reduced the percentage of Gata3⁺ T_H2 cells in the mesenteric lymph nodes at 28 days post *H. polygyrus* infection (Figure 3M). This suggested that the induction of regulatory macrophages by heGDH is particularly important at the beginning of the infection, whereas heGDH modulates the adaptive

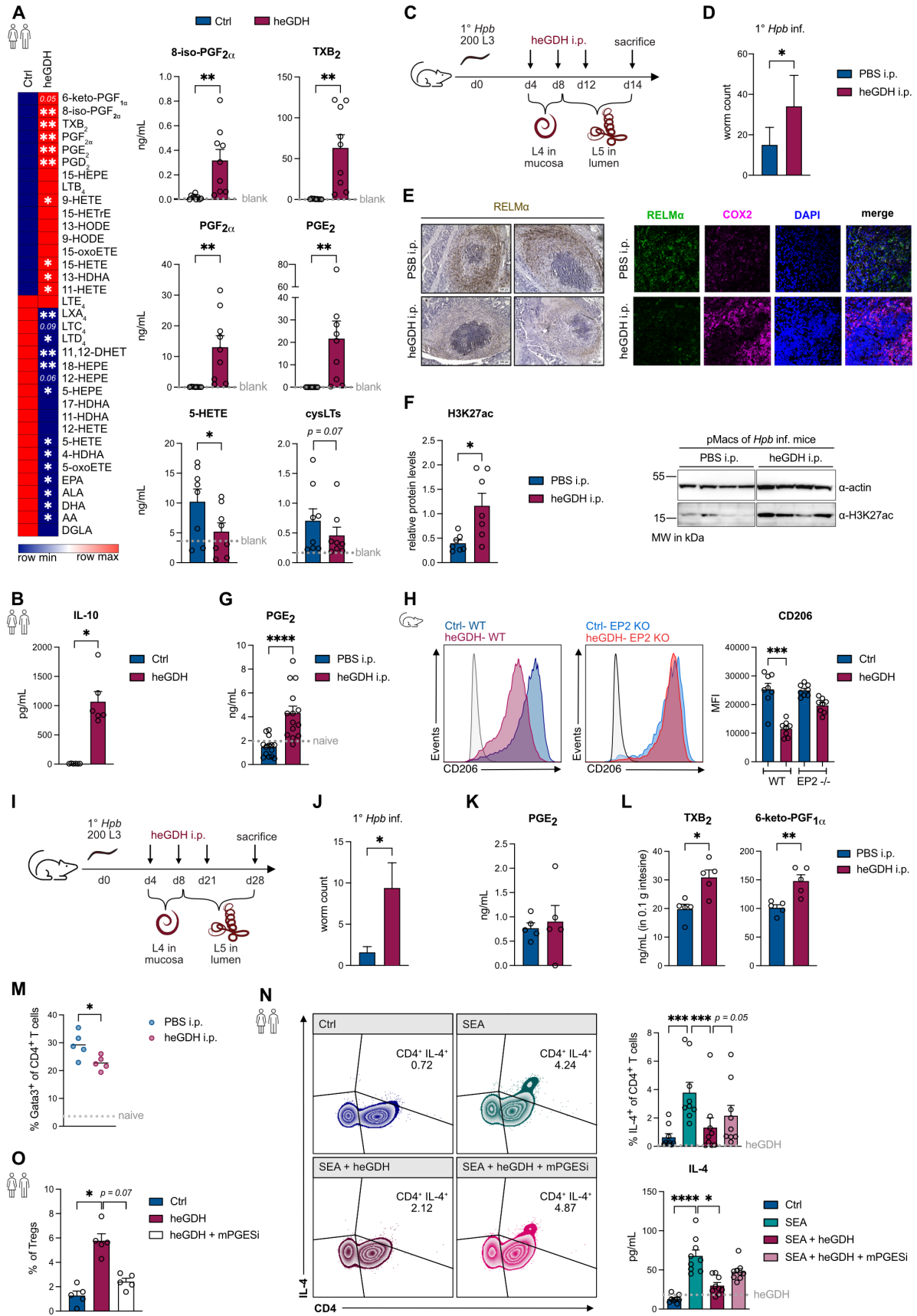


Figure 3: heGDH induces an anti-inflammatory modulation of the arachidonic acid (AA) metabolism in macrophages which promotes helminth chronicity in dependency of PGE₂

(A) Left, heatmap of lipid mediators produced by human MDM ± treatment with heGDH (LC-MS/MS). Data is shown as mean of 9 donors. Right, levels of major COX and 5-LOX metabolites produced by MDM ± treatment with heGDH (n=9).

(B) Secretion of IL-10 (ELISA) of MDM ± treatment with heGDH (n=6).

(C) Experimental model of infection with *Hpb* and intraperitoneal (i.p.) treatment with heGDH. Analysis of mice 14 days post infection (p.i.)

(D) *Hpb* worm burden 14 days p.i. in mice treated with PBS or heGDH (n=14 per group).

(E) Left, representative images of IHC staining for RELM α in largest cross sections of granulomas in tissues from mice infected with *Hpb* and treated with PBS or heGDH. Right, representative images of IF staining for RELM α , COX2 and DAPI (cell nuclei) in granulomas of tissues from mice infected with *Hpb* and treated with PBS or heGDH.

(F) Protein amounts of H3K27ac or actin (western blot) in peritoneal macrophages (pMacs) ± i.p. treatment with heGDH. Left, quantification for n=7 mice per group; right, representative blots for four mice per group.

(G) Secretion of PGE₂ (EIA) of isolated peritoneal macrophages of mice which received i.p. treatment with PBS or heGDH 14 days p.i. (n=14 per group). Dotted line indicates mean secretion of PGE₂ from pMacs of naïve mice.

(H) Surface expression of M2 polarization marker CD206 (flow cytometry) in wildtype (WT) or EP2 knock out murine bone-marrow derived macrophages ± treatment with heGDH.

(I) Experimental model of infection with *Hpb* and i.p. treatment with heGDH. Analysis of mice 28 days p.i.

(J) *Hpb* worm burden 28 days p.i. in mice treated with heGDH (n=5 per group)

(K) Secretion of PGE₂ (EIA) of isolated peritoneal macrophages from mice which received i.p. treatment with PBS or heGDH (n=5 per group) 28 days p.i.

(L) Amounts of TXB₂ and 6-keto-PGF_{1 α} (measured via LC-MS/MS) from isolated intestinal tissue culture supernatants of mice which received i.p. treatment with PBS or heGDH (n=5 per group).

(M) Percentage of Gata3⁺ T_H2 cells (flow cytometry) in mesenteric lymph nodes of mice which received i.p. treatment with PBS or heGDH after 28 days of infection with *Hpb* (n=5 per group). Dotted line indicates mean percentage of Gata3⁺ T_H2 cells from naïve mice.

(N) Percentage of IL-4⁺ T_H2 cells (flow cytometry) and secretion of IL-4 (ELISA) in human PBMC cultures ± treatment with *Schistosoma mansoni* soluble egg antigen (SEA) ± heGDH ± mPGES1 inhibitor (934) (n=9).

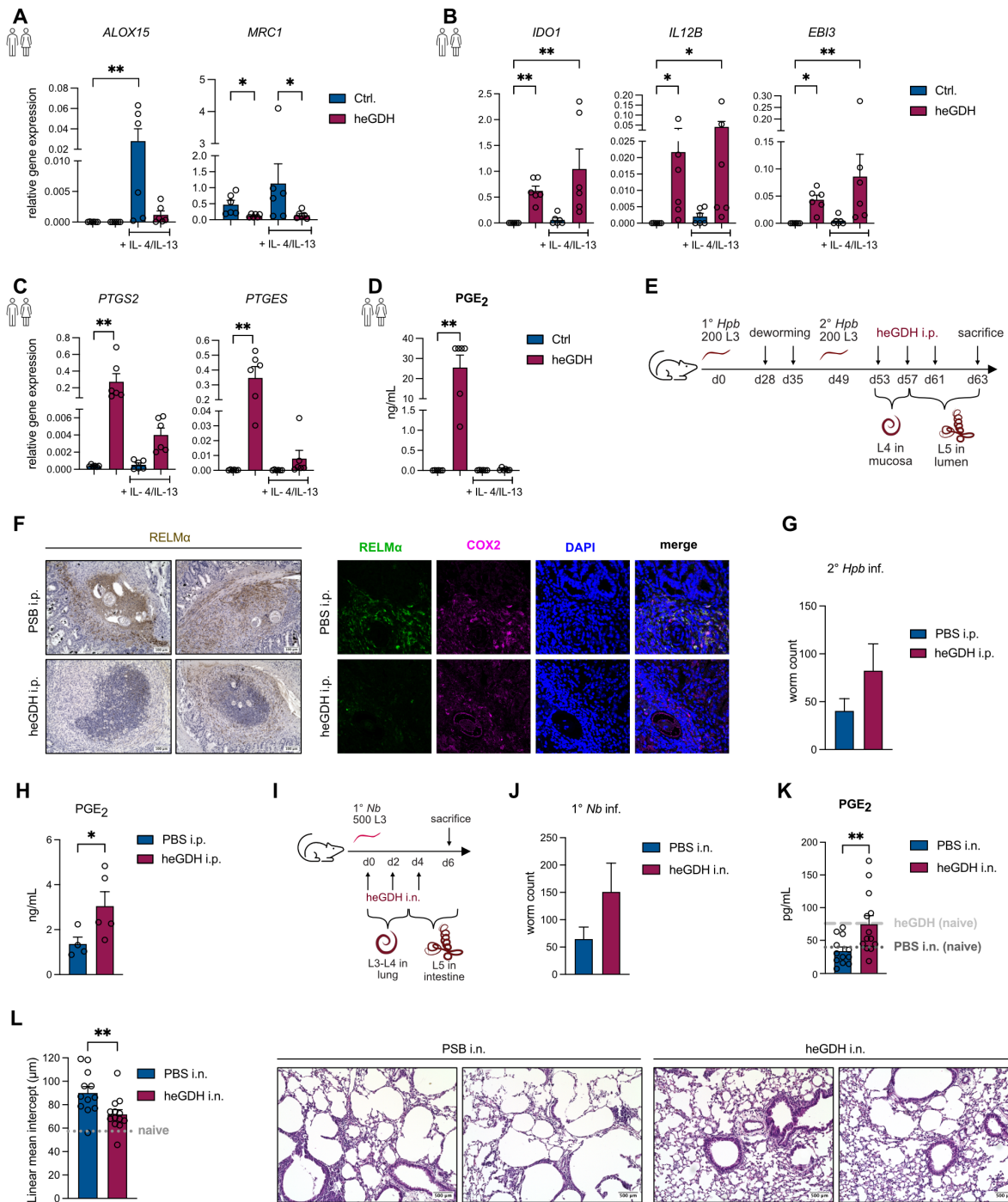
(O) Percentage of CD4⁺CD127⁻CD25^{hi}FoxP3⁺ (flow cytometry) in human PBMC cultures ± heGDH ± mPGES1 inhibitor (934) (n=5). Data are presented as means + SEM. Statistical significance was determined by Wilcoxon test (A, B), Mann-Whitney (D, F, G, J-M), Kruskal-Wallis test (H) or Friedman test (N, O). *P < 0.05; **P < 0.01; ***P < 0.001, ****P < 0.0001.

immune response at later time points. To further investigate the importance of heGDH-triggered PGE₂ in the regulation of the T_H2 response we analyzed the capacity of heGDH to reduce type 2 cytokine production in human PBMCs following stimulation with *Schistosoma mansoni* soluble egg antigen (SEA), a strong parasitic T_H2 trigger. The percentage of SEA-induced IL-4⁺CD4⁺ T_H2 cells was significantly reduced and SEA-induced IL-4 production was diminished after heGDH treatment (Figure 3N), while heGDH induced CD4⁺CD127⁻CD25^{hi}FoxP3⁺ regulatory T cells in human PBMCs (Figure 3O). These T-cell modulatory functions of heGDH at least partially depended on PGE₂ production by mPGES-1 (Figures 3N and 3O). Thus, PGE₂ acts as a key modulator of macrophage and T-cell function by helminthic GDH.

Type 2 immune response counteracts PGE₂-mediated immune evasion

To assess how host type 2 immunity may affect heGDH-driven immune regulation, we mimicked a type 2 milieu *in vitro* by culturing MDM in the presence of IL-4 and IL-13 prior to treatment with heGDH. The IL-4/IL-13-induced genes *ALOX15* and *MRC1* were downregulated by heGDH, confirming the prevention of M2 polarization in a type 2 cytokine milieu (Figure 4A). While some heGDH-induced genes, including *IDO1*, *IL12B*

and *EBI3* were unaffected by additional treatment with IL-4 and IL-13 (Figure 4B), IL-4 and IL-13 suppressed the induction of *PTGS2* and *PTGES* as well as PGE₂ (Figures 4C and 4D). In line with these counter-regulatory effects of type 2 cytokines, the capacity of heGDH to trigger immune evasion was reduced during strong type 2 immune responses, i.e. during challenge infection with *H. polygyrus* or infection with *Nippostrongylus brasiliensis* (Figures 4E-J). While treatment (i.p.) with heGDH resulted in a tendency towards increased worm counts (Figure 4G), suppression of the AAM marker RELM α and PGE₂ secretion by peritoneal macrophages at day 14 post challenge, the upregulation of COX-2 by heGDH was attenuated in the granuloma of challenged infected mice (Figures 4F and 4H). In keeping with the results during the memory T_H2 response against *H. polygyrus*, intranasal treatment with heGDH during infection with the lung-dwelling parasite *N. brasiliensis* resulted in a tendency of increased worm counts in the intestine (Figure 4J). However, intranasal administration of heGDH significantly reduced helminth-induced tissue damage (Figure 4L), despite an increase in the number of neutrophils in heGDH-treated and *N. brasiliensis*-infected mice (Figure S4A). The decreased type 2 immune response and improved tissue repair in mice treated with heGDH during *N. brasiliensis* infection



correlated with an increased production of PGE₂ by BAL macrophages (Figure 4K). This suggested that heGDH-driven immune evasion can be overcome by fully type 2 activated immune cells and that helminthic GDH can support repair of helminth-induced tissue damage.

Induction of prostanoids is structure-dependent, while suppression of leukotrienes is mediated by catalytic activity of heGDH

Glutamate dehydrogenase is a hexameric enzyme that catalyzes the reversible conversion of glutamate to α -ketoglutarate and ammonia while reducing NAD(P)⁺ to NAD(P)H. As there is increasing evidence that GDHs act as epigenetic modulators^{26,27} we wanted to discern if the catalytic activity or the structure of heGDH is necessary to activate p300 and induce regulatory macrophages. To solve the structure of heGDH we performed cryo EM and X-ray crystallography, which yielded similar structures particularly in the enzyme's core (Figure 5A). More significant differences

Figure 4: Full blown type 2 immune response prevent PGE₂-mediated survival strategy

(A-C) Gene expression analysis of M2 polarization markers (A), top DEGs (B) or prostaglandin E₂ synthesis genes (C) (qPCR) in human MDM ± heGDH under baseline conditions or after IL-4, IL-13 pre-treatment (n=6).

(D) Secretion of PGE₂ (EIA) of MDM treated with ± heGDH under baseline conditions or after IL-4, IL-13 pre-treatment (n=6).

(E) Experimental model of secondary infection with *Hpb* and intraperitoneal (i.p.) treatment with heGDH. Analysis of mice 14 days post challenge infection.

(F) Left, representative images of IHC staining for RELM α in largest cross sections of granulomas in tissues from mice secondarily infected with *Hpb* and treated with PBS or heGDH. Right, representative images of IF staining for RELM α , COX2 and DAPI (cell nuclei) in granulomas of tissues from mice infected with *Hpb* and treated with PBS or heGDH.

(G) *Hpb* worm burden after secondary infection with *Hpb* and further i.p. treatment with heGDH (n=8 in PBS i.p. group and n=10 in heGDH i.p. group).

(H) Secretion of PGE₂ (EIA) of isolated peritoneal macrophages of mice which received i.p. treatment with PBS or heGDH (n=5 per group).

(I) Experimental model of infection with *Nippostrongylus brasiliensis* (*Nb*) and intranasal (i.n.) treatment with heGDH. Analysis of mice 6 days post infection.

(J) *Nb* worm burden 6 days post infection in mice treated with PBS or heGDH (n=12 in PBS i.n. group and n=13 in heGDH i.n. group).

(K) Secretion of PGE₂ (EIA) of isolated BAL macrophages of mice which received i.n. treatment with PBS or heGDH (n=12 in PBS i.n. group and n=13 in heGDH i.n. group). Dotted line indicates mean secretion of PGE₂ from pMacs of naïve mice with PBS treatment and dashed line indicates mean secretion of PGE₂ from pMacs of naïve mice with heGDH treatment.

(L) Left, quantification of lung damage as linear means intercept (Lmi) (n=12 in PBS i.n. group and n=13 in heGDH i.n. group). Right, representative H&E staining's of lung sections from *Nb* infected mice treated intranasally with PBS or heGDH. Dotted line indicates mean Lmi of naïve mice.

Data are pooled from at least two independent experiments and presented as means + SEM. Statistical significance was determined by Friedman test (A-D) or Mann-Whitney (G, H, J-L). *P < 0.05; **P < 0.01.

became apparent in the outer domain containing residues 250-400. The EM density is also less well resolved in this area indicative of more flexibility (Figure S5A) However, a more striking difference is a “handle”-like density in the central plane, in the size and shape of a single alpha helix or small unstructured region (Figures 5A-B and S5A). The “handle”-like density connects to two Cys136 of neighboring subunits and likely binds both cysteines. The local resolution of the cryoEM map does not allow direct identification of the nature of the handle-density. However, in close proximity are the two N-termini of the respective subunits (Figure 5A). In our XRAY structure, residues 1-27 are not resolved and residues 28-43 show a disordered conformation (Figure 5A). With residue 43 being only about X Angstrom away from the handle-density, it is likely that a subset of residues from the N-termini form a tight contact.

An enzymatic assay revealed α -ketoglutarate, glutamate and ammonium as sole substrates and an optimum pH at 8.5 (glutamate utilization) and 7.5 (glutamate formation) as well as specificity for NAD⁺/NADH as cofactors (Figures S5B-D). By using the allosteric inhibitor GTP and a glutamate dehydrogenase inhibitor (bithionol), which is also used as an anti-helminthic, we could observe a reduction in heGDH activity (Figure S5E). In contrast, clone 4F8 failed to reduce heGDH catalytic activity (Figure S5F) as well as LT suppression (Figure S3C), while attenuating the heGDH mediated induction of the COX pathway (Figure S3A). This suggested that structural features of heGDH are responsible for the induction of

immune regulatory and tissue reparative prostanoids.

To untangle the role of catalytic activity versus structure we designed a catalytically inactive mutant of heGDH (heGDH^{K126A, D204N})²⁸ (Figure 5C). However, the catalytically inactive mutant heGDH^{K126A, D204N} still induced COX-metabolite and IL-10 production by macrophages to a similar extent as the wildtype protein (Figures 5D and 5F). Gene expression data confirmed a similar or even stronger response of the top DEGs upon stimulation with mutant heGDH^{K126A, D204N} (Figure 5E). Interestingly, heGDH as well as the catalytic inactive mutant reduced the type 2 inducing metabolite PGD₂ in murine BMDM (Figure 5F), but not in human MDM (Figure 3A). In contrast to its intact effects on prostanoids, heGDH^{K126A, D204N} failed to suppress cysLTs (Figure 5G). This supported the hypothesis that the heGDH-driven induction of the cyclooxygenase pathway via p300 is structure dependent, whereas the catalytic function is necessary for the reduction of LT production.

heGDH induces a metabolic shift in macrophages which leads to the reduction of pro-inflammatory cysLTs

In mammalian tissues, oxidative deamination of glutamate via GDH generates α -ketoglutarate, which is metabolized by the TCA cycle, leading to the synthesis of ATP. To assess whether heGDH impacts the macrophage metabolism we performed metabolic flux analysis. In line with the suppressive capacity of heGDH on AAM activation the metabolism of human as well as murine macrophages shifted towards increased basal glycolysis, which is typical for

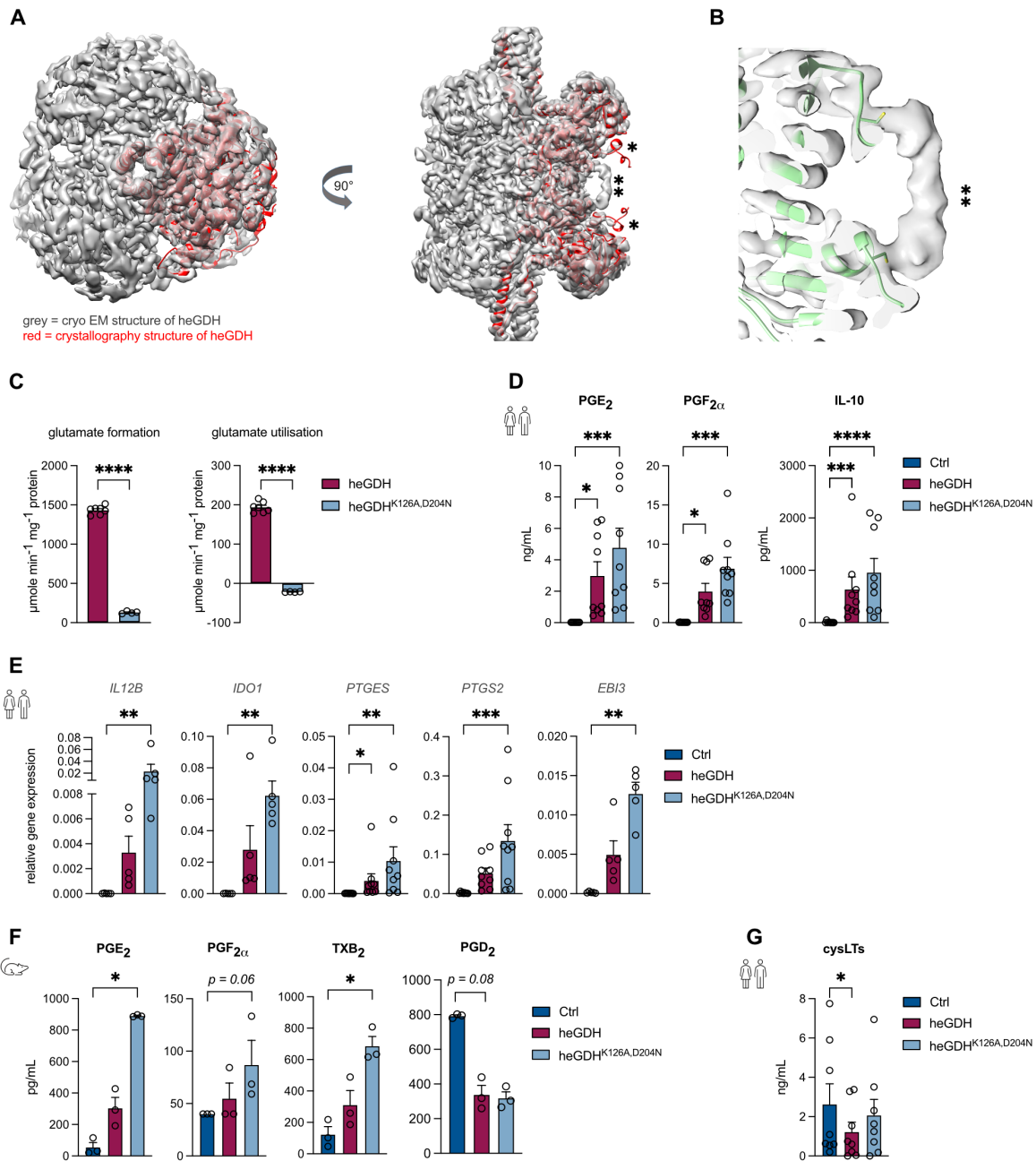


Figure 5: Induction of prostanoids is structure-dependent, while suppression of leukotrienes is mediated by catalytic activity of heGDH

(A) Model of the heGDH crystal structure fitted in the CryoEM reconstruction of the heGDH oligomer. N-termini of two neighboring subunits (*) are not resolved in the X-ray structure while they form a bar-like connection (**) in the cryoEM model.

(B) Close up of local resolution of handle-like structure from the model of the heGDH crystal structure fitted in the CryoEM reconstruction.

(C) Glutamate dehydrogenase activities of heGDH and catalytically inactive heGDH^{K126A, D204N} in the direction of glutamate utilization and formation (n=4-7)

(D) Levels of PGE₂, PGF_{2α} (LC-MS/MS) and IL-10 (ELISA) produced by MDM ± treatment with heGDH or heGDH^{K126A, D204N} (n=9).

(E) Gene expression analysis of top DEGs (qPCR) in MDM ± heGDH or heGDH^{K126A, D204N} (n=5).

(F) Levels of major COX metabolites (LC-MS/MS) produced by BMDM ± treatment with heGDH or heGDH^{K126A, D204N} (n=3).

(G) Secretion of cysLTs (EIA) by MDM ± treatment with heGDH or heGDH^{K126A, D204N} (n=8).

Data are pooled from at least two independent experiments and presented as means ± SEM. Statistical significance was determined by RM one-way ANOVA (C) or Friedman test (D-G). *P < 0.05; **P < 0.01; ***P < 0.001, ****P < 0.0001.

M1 activated macrophages²⁹ (Figures 6A and S6A). In contrast, AAM have been shown to rely primarily on oxidative phosphorylation

(OxPhos), which tended to be downregulated by heGDH (Figures 6A and S6A). The significant p300-dependent upregulation of the

gene *PFKFB3*, a positive regulator of glycolysis, after heGDH stimulation suggested a potential link between glycolysis and heGDH-induced epigenetic reprogramming (Figures 6B and S6B). Indeed, inhibition of p300 activity in MDM during treatment with heGDH blocked the decrease of basal respiration and ATP production as well as the increase of basal glycolysis (Figure 6C), suggesting that the metabolic shift triggered by heGDH is p300 dependent. In inflammatory macrophages a break in the TCA cycle with accumulation of citrate and succinate has been reported²⁹, which might account for the pro-inflammatory phenotype characterized by increased reactive oxygen species (ROS), nitric oxide (NO) and prostaglandin production. Using LC-MS/MS analysis to detect TCA metabolites in heGDH-treated MDM we observed higher levels of 2-hydroxyglutarate (2-HG), while the levels of glutamine and glutamate were reduced as compared to untreated MDM (Figures 6D and 6E). Furthermore, the aconitate decarboxylase 1 (IRG1) product itaconate, an immune-regulatory byproduct of the TCA cycle was increased in response to heGDH (Figure 6D). To determine whether the downstream metabolites of heGDH (itaconate, α -ketoglutarate and 2-HG) could affect immune regulatory AA metabolites, we assessed eicosanoid production by MDM following treatment with these metabolites (Figure S6C). Indeed, we observed that L-2-HG, but not D-2-HG, reduced the production of cysLTs (Figures 6F and S6D). To investigate, if L-2-HG directly affects the activity of LTC4S, we performed an LTC4S activity assay. While LTC4S activity was partially inhibited by addition of L-2-HG (Figure 6G), gene expression of *ALOX5* and *LTC4S* were not affected (Figure S6E). Interestingly, also heGDH directly affected LTC4S activity (Figure 6H) *in vitro* and in a human macrophage cell line (Figure S6F). Thus, effects of heGDH on the synthesis of key mediators of type 2 immunity are - at least in part - mediated via its downstream metabolites.

DISCUSSION

In the present study, we identify a potential evolutionary mechanism by which helminth-derived glutamate dehydrogenases (heGDH) may facilitate immune evasion and promote helminth chronicity. HeGDH are internalized by host macrophages, resulting in profound metabolic, epigenetic and transcriptional changes, which together suppress anti-helminth effector functions. Macrophages play crucial roles in anti-helminth immunity by trapping worms, regulating T-cell responses,

and repairing tissue damage via the production of cytokines and bioactive lipid mediators^{2,9,10,24,30,31}. Thus, helminth parasites have evolved molecular strategies to subvert macrophage functions¹⁵.

Early during infection, we identified a colocalization of CD64 positive macrophages with heGDH-producing larvae. Monocyte-derived macrophages activated during helminth infection highly express CD64 and play an important role in helminth trapping^{5,32}, suggesting that CD64 is targeted by heGDH to reprogram macrophages in the surrounding of the larvae. Although we do not provide experimental evidence that directly links CD64 to p300 activation, a previous study demonstrated that C-reactive protein binds to CD64, resulting in the activation of ERK1/2 and Akt, subsequent HIF-1 α translocation and binding to p300 in the promoter region, thereby activating gene expression³³. In line, we found that heGDH is able to activate p300 and thus to drive acetylation of H3K27 and transcriptional activation.

As a consequence of chronic helminth infections, epigenetic reprogramming of bone marrow-derived, recruited, and resident proliferating macrophages may lead to diverse and persistent alterations in macrophage effector functions. Indeed, human studies have shown that helminths may use myeloid reprogramming as an immune evasion strategy³⁴. In our study, the heGDH-induced, p300-mediated upregulation of PGE₂ in peritoneal macrophages was however transient suggesting that an acute macrophage reprogramming may be sufficient to modulate host immunity. However, it is unclear whether heGDH treatment induces long-lasting epigenetic modifications in BM-derived monocytes/ macrophages or their progenitors *in vivo*.

While heGDH triggered a broad epigenetic and transcriptional reprogramming, the induction of the immune regulatory AA metabolite PGE₂ likely represents a central mechanism of GDH-driven helminth chronicity. Indeed, heGDH-induced PGE₂ suppresses M2 polarization in an EP2-dependent manner and modulates human T cell function *in vitro*. Similar to a GDH of the human and pig parasite *Taeni solium*¹⁰, heGDH efficiently induces Tregs and inhibits helminth-induced T_H2 cell differentiation via enhancing myeloid PGE₂ production. The suppressive effects of heGDH on T_H2 cells are evident after 28 days of *Hpb* infection, indicating that the induction of regulatory macrophages is particularly important in the early stages of infection, while reprogrammed macrophages

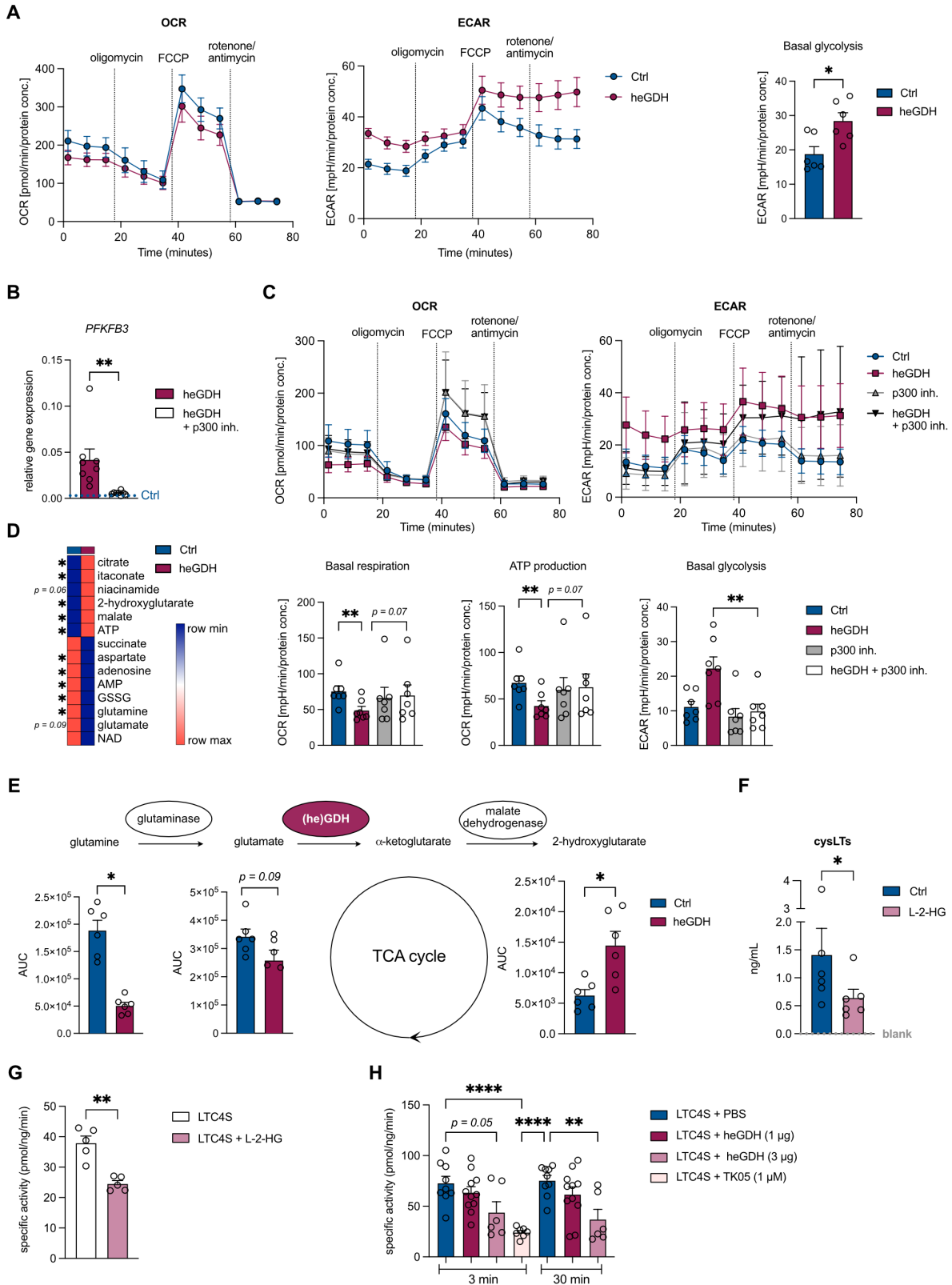


Figure 6: heGDH induces a metabolic shift in macrophages which leads to the reduction of pro-inflammatory cysLTs

(A) Oxygen consumption rate (OCR, left) and extracellular acidification rate (ECAR, middle) of MDM treated \pm heGDH. Right, basal glycolysis of MDM treated \pm heGDH (n=6).
(B) Gene expression analysis of *PFKFB3* (qPCR) in MDM treated with heGDH alone or after inhibition of p300 HAT (A485) (n=8). Dotted line indicates expression in control (Ctrl) treated cells.
(C) Upper panel, Oxygen consumption rate (OCR) and extracellular acidification rate (ECAR) of MDM \pm treatment with heGDH \pm inhibitor of p300 HAT (A485). Lower panel, basal respiration, ATP production and basal glycolysis of MDM \pm treatment with heGDH \pm inhibitor of p300 HAT (A485) (n=7).
(D) Heatmap of targeted metabolomics (LC-MS/MS) in MDM treated \pm heGDH. Data is shown as mean of 6 donors.
(E) Targeted metabolomics for glutamine, glutamate and 2-hydroxyglutarate of MDM treated \pm heGDH (n=6).
(F) Secretion of cysLTs (EIA) by MDM \pm treatment with L-2-hydroxyglutarate (n=6).
(G) Leukotriene C4 synthase activity measured after 30 min during incubation with L-2-hydroxyglutarate (n=5).
(H) Leukotriene C4 synthase activity measured after addition of heGDH in different concentrations (1 μ g and 3 μ g) and for different incubation times (3 min, 30 min) or after addition of a specific LTC4S inhibitor (TK05) (n=9).
Data are pooled from at least two independent experiments and presented as means \pm SEM. Statistical significance was determined by Wilcoxon test (A, B, D-G), Friedman test (C) or ordinary one-way ANOVA (H). *P < 0.05; **P < 0.01; ****P < 0.0001.

then modulate T cell responses at later stages of infection. PGE₂ has been shown to limit ILC2 and mast cell function through an EP2-dependent mechanism^{35,36}, although its direct effects on IL-4/IL-13 production are not yet fully understood. Consistent with the weakened effects of heGDH in the presence of a type 2 cytokine environment, IL-4 has been reported to inhibit COX-2 expression and consequently prevent PGE₂ secretion in DCs³⁷. The timing of PGE₂ upregulation during helminth infection could also be a critical factor: If upregulated before IL-4 and IL-13, PGE₂ may be sufficient to maintain immune evasion, while if IL-4 and IL-13 secretion occurs simultaneously to PGE₂ synthesis, PGE₂ production may be limited, thus hampering heGDH-mediated immune evasion. Thus, our findings suggest that the host type 2 immune response has evolved to counteract helminth driven lipid mediator modulation and immune suppression. Moreover, the induction of PGE₂ during *N.brasiliensis* infection as well as of further COX metabolites (6-keto-PGF_{1 α} and TXB₂) during later stages of *Hpb* infection may promote tissue repair and blood clotting²⁴. In the initial inflammatory stage of tissue repair, myofibroblasts can be activated by PGE₂ producing macrophages and stromal cells, which results in wound contraction and closure in the skin and intestine³⁸⁻⁴¹. These beneficial effects of PGE₂ on tissue repair largely depend on the activation of the EP2 and EP4 receptors. As the proliferative phase begins, myofibroblasts generate PGE₂, thus inducing the expression of high levels of IL-10 and Arg1 in regulatory macrophages. These molecules help in preventing tissue damage and regulating pathological tissue remodeling in type 2 immunity^{2,42,43}. It would thus be interesting to determine whether the capacity of heGDH to repair *N. brasiliensis*-induced lung damage depends on a PGE₂/ EP2/4 signaling axis in macrophages and stromal cells.

In addition to the COX-2/PGE₂ pathway, heGDH upregulates IDO1, which is known to promote the differentiation of regulatory T cells and block their conversion into T effector cells, including during parasite infections^{44,45}. However, it is unclear whether heGDH-induced IDO1 expression in macrophages may contribute to Treg cell induction and T_H2 cell suppression. As another group of potent modulators of T_H2 immunity, heGDH triggers the expression of IL-12 family cytokine subunits (IL-12 β and Ebi3). IL-12 negatively regulates type 2 immune responses in helminth infection²⁰, while promoting T_H1 immunity and IFN γ production during chronic infection with intracellular pathogens^{46,47}. Similarly, IL-35 and IL-27 antagonize type 2 immune responses, and EBI3^{-/-} mice develop enhanced allergic airway inflammation^{19,48}. Thus, IL-12 β and EBI3 may contribute to the heGDH-triggered shift from type 2 to type 1 immunity and thus helminth chronicity.

Glutamate dehydrogenase (GDH) catalyzes the conversion of glutamate to α -ketoglutarate (α -KG) and vice versa, thus influencing the metabolic environment of macrophages by altering their internal metabolite balance or the tissue microenvironment. Analysis of heGDH-treated macrophages revealed decreased glutamine/glutamate consumption and an increased production of the tricarboxylic acid (TCA) intermediate 2-HG. The chiral molecule 2-HG exists in either the D-enantiomer or L-enantiomer, and L-2-HG functions as a potent inhibitor of α -KG-dependent enzymes, including histone demethylase Jmjd3, which promotes macrophage M2 activation⁴⁹. Our data suggest that helminthic GDH contributes to the conversion of α -KG to 2-HG by increasing basal glycolysis and reducing OxPhos in a p300-dependent manner. In contrast, another helminth-derived product, FhHDM-1, switches macrophage metabolism to OxPhos fueled by fatty acids and supported by the induction of

glutaminolysis⁵⁰, suggesting that different helminth molecules modulate specific metabolites to regulate macrophage activation and type 2 immunity. In heGDH-treated macrophages, no upregulation of succinate or α -KG was observed, indicating a specific immune-regulatory macrophage population, rather than a strict M1 or M2-associated macrophage phenotype. Although α -KG and L-2-HG are implicated in epigenetic regulation, such as promoting DNA and histone methylation^{49,51}, metabolic reprogramming does not primarily rely on heGDH's catalytic activity. Instead, our data suggest that p300-dependent epigenetic regulation induces *PFKFB3*, a positive regulator of glycolysis⁵², thus driving macrophage metabolic reprogramming.

The present study further identifies L-2-HG as a direct negative regulator of LTC₄ synthase, resulting in the reduced synthesis of type 2 promoting eicosanoids (cysLTs). However, the precise mechanism by which L-2-HG limits LTC₄ synthase activity remains to be determined.

Indeed, eicosanoid production can be influenced by various factors, including the availability of TCA cycle intermediates. The export of citrate by the mitochondrial citrate carrier, SLC25A1, is necessary for the regulation of prostaglandins through the production of acetyl-CoA and subsequent production of TNF α and INF- γ ⁵³. Although our RNA sequencing data indicates that the expression of the citrate carrier is not altered in macrophages treated with heGDH, further investigation is required to determine if the significant increase in citrate levels in heGDH-treated macrophages plays a role in the regulation of AA-metabolites.

In the context of allergic asthma, GDH has been identified as the major immune regulatory component responsible for anti-inflammatory effects of a homogenate prepared from L3 stage larvae of *H. polygyrus*⁹. GDH activity was found predominantly in L3 extract compared to excretory/secretory products (HES) from adult stages of *Hpb* or homogenates of L4 or L5, indicating a variation in protein profiles depending on the stage of the parasite lifecycle^{9,54}. However, the secretion profiles of L3 and L4 compared to L5 (HES) have not been determined, and further proteomic analysis is needed to determine if GDH can be exclusively secreted by L3. GDH from *H. contortus* is localized to the cytoplasm of the parasite's gut and expressed almost exclusively during the blood-feeding stage, supporting developmental regulation of parasitic GDHs⁵⁵. However, several studies suggest that GDH is an

evolutionarily conserved enzyme involved in regulating host immunity. In vaccination studies, a parasitic GDH was identified as the dominant protein in the soluble extract against which anti-helminth immunity was developed⁵⁵. GDH derived from the protozoan parasite *T. cruzi* was found to be the immunomodulatory compound responsible for the production of IL-10 and IL-6 in CD11b⁺ cells⁵⁶. In a more recent study, a GDH was found in viable cysts of the parasitic cestode *T. solium* that instructs tolerogenic monocytes to release IL-10 and PGE₂, leading to the induction of regulatory T cell responses in mice and humans¹⁰. Similarly, macrophages treated with heGDH released high amounts of IL-10, IL-6, and PGE₂, highlighting GDH as an evolutionarily conserved immune regulatory enzyme shared between different parasites. However, further research is necessary to determine if GDHs from different parasites share structural similarities and whether they use the same mechanisms to drive host immune evasion. The potent immune regulatory functions of parasitic GDHs suggest a potential therapeutic or preventive use, e.g. in inflammatory or fibrotic diseases or as a vaccine antigen for inducing immunity against a wide range of parasitic infections.

AUTHOR CONTRIBUTIONS

Conceptualization, J.E.v.B. and S.B.; Methodology, S.B., A.G., F.D.H., A.M., S.B., U.F.P., T.T., Y.S., R.G., M.U.D. and A.M.K.; Investigation, S.B., A.G., F.D.H., S.R., F.H., A.M., S.B., U.F.P., T.T., Y.S., R.G., F.A., A.L. and A.M.K.; Visualization, S.B., M.U.D.; Writing – Original Draft, J.E.v.B. and S.B.; Funding Acquisition, J.E.v.B.; Resources, A.G., P.-J.J. and D.V.; Supervision, J.E.v.B., C.P.d.C., E.P., M.F., J.Z.H. and C.B.S.W.

ACKNOWLEDGMENTS

We thank our technicians Sonja Schindela, Johanna Grosch and Benjamin Schnautz for technical support and help with animal experimentation. Our thank goes as well to our interns Lara Paulini and Emily Hensch for technical assistance and to all blood donors for participation in this study. The authors would like to thank staff of the histology laboratory of the Dermatology Department, Klinikum rechts der Isar and the Helmholtz Center Munich Genomics platform for technical support. We also would like to thank Prof. Dr. Jan Böttcher for the supply of the EP2^{-/-} KO bones. We particularly would like to thank the animal caretakers of the Helmholtz Center Munich for animal husbandry. This study was supported by grants of the German Research Foundation

(DFG) (ES 471/2-3, FOR2599, ES 471/3-2, 471/7-1), the Swiss National Science Foundation (310030_212312) and a Helmholtz Young Investigator grant (VH-NG-1331) to J.E.v.B.

DECLARATION OF INTERESTS

J.E.v.B. and C.B.S.W. have submitted a patent application (WO2019193140A1) related to the immune regulatory effects of the *H. polygyrus* L3 larval homogenate and its components, including *H. polygyrus* glutamate dehydrogenase.

METHODS

Study design

The aim of this study was to investigate how GDH derived from *H. polygyrus* could modulate eicosanoid pathways to regulate host type-2 inflammation. For the human part of our study, healthy volunteers (total n = 35) (Caucasian men and women) were recruited. Sample sizes, replicates, and statistical methods are specified in the figure legends. All blood donors participated in the study after informed written consent. All procedures were approved by the local ethics committee at the University clinic of the Technical University of Munich (internal references: 802/20S) and in accordance with the declaration of Helsinki.

Mice

C57BL/6J mice were obtained from Charles River Laboratories (Sulzfeld) maintained under specific pathogenfree conditions at the Helmholtz Center Munich. 6- to 8-week-old mice were used. All animal experiments were approved by the local authorities (Regierung von Oberbayern).

Helminth infection and treatment with heGDH or mAb against heGDH

Female mice were infected with *Hpb* by oral gavage with 100 or 200 L3 stage larvae diluted in 200 μ l sterile PBS. Control animals received the same amount of PBS. Mice were sacrificed at the indicated time points (14 days post primary and secondary infection or 28 days post primary infection). heGDH treatment (5 μ g of heGDH in 100 μ l of PBS) was performed intraperitoneally at day 4, 8 and 12 for the 14-days primary infection experiment. When mice were sacrificed at 28 days post primary infection, mice were treated at days 4, 8 and 21. For secondary infection experiment, mice were infected with 200 *Hpb* larvae and two courses of antihelminthic pyrantel (250 μ g in 200 μ l, i.g.) were administered at days 28 and 35 p.i. Mice were re-infected with 200 larvae at day 49 and

heGDH injection was performed at day 53, 57 and 61. In the absence of heGDH treatment, mice received 100 μ l of PBS.

For blocking experiments, 10 μ g of α -heGDH mAb or isotype control antibody (BioCell) in 100 μ l PBS was intraperitoneally given on day 0-2, 4 and 6.

For *Nb* infection, mice were infected s.c. with 500 infectious third-stage larvae (L3). Intranasal treatment with heGDH was performed at day 0, 2 and 4. 6 days post infection, the airways of the mice were lavaged five times with 0.8 ml of PBS. Aliquots of cell-free BALF were frozen immediately with or without equal volumes of methanol. Viability, yield, and differential cell count of BAL cells were performed as described before⁵⁷. Small intestine (SI) of *Hpb* or *Nb* infected mice was removed and opened to count adult worms at the luminal surface using a light microscope.

Alveolar and peritoneal macrophage culture

Peritoneal cells were obtained by peritoneal wash with 2 mL RPMI, whereas alveolar macrophages within the procedure of BALF. Total murine peritoneal cells as well as BAL macrophages were incubated in complete medium containing RPMI-1640 with 10% fetal bovine serum, 2 mmol/L L-glutamine, 100 U/mL penicillin/streptomycin and 10 ng/mL Gentamicin (all Thermo Fisher Scientific) at 37°C and 5% CO₂ for 4-5 hours, before rigorous washing with warm PBS and medium replenishment was performed. Adherent macrophages were stimulated for 10 min with calcium ionophore A23187 (5 μ mol/L, Merck Chemicals) at 37°C and centrifuged at 4°C for harvest of supernatants for EIA and ELISA. Cells pellets were collected, lysed, and stored as described for MDM and BMDM.

Intestinal tissue culture

1-2 cm of the washed duodenal part of the SI was placed in 24-well plates with 1 mL/well RPMI supplemented with 200 Units/mL antibiotics. Tissue was incubated overnight (*Hpb*) or 6 hours (*Nb*) at 37°C before supernatants were harvested and analyzed by LC-MS/MS. Eicosanoid concentrations were normalized against tissue weight and are presented as ng/mL in 0.1 g tissue.

Peripheral blood mononuclear cells (PBMC) culture

2-2.5 x 10⁵ PBMCs per well were resuspended in RPMI-1640 medium (Thermo Fisher Scientific) supplemented with 10% heat-inactivated and filtered FCS (Sigma-Aldrich) and 1% penicillin/streptomycin (Thermo Fisher Scientific) and left untreated as control or

stimulated with 5 µg/mL heGDH alone or in combination with 10 µM mPGES1 inhibitor (934) for 72 h at 37°C in a 5% CO₂ atmosphere to assess Treg induction. For SEA stimulation, 2-2.5 x 10⁵ PBMCs were left untreated (control) or cultured with 50 µg/mL of SEA, prepared from *S. mansoni* eggs as previously detailed⁵⁸, alone or in combination with either 5 µg/mL heGDH and/or 10 µM mPGES1 inhibitor (934) for 5 days. On day 3, 50% of culture medium were exchanged with fresh medium containing respective stimuli or culture medium as control. Culture supernatants were collected, and IL-4 concentrations were determined by ELISA.

Monocyte-derived (MDM) or bone-marrow derived (BMDM) macrophage culture

As previously reported^{2,59}, CD14⁺ PBMCs were used to generate monocyte-derived macrophages (MDM). Macrophages were cultured in complete medium (described above) in the presence of 10 ng/mL human GM-CSF (Miltenyi Biotec) and 2 ng/mL human TGF-β (Peprotech). Bone marrow derived macrophages (BMDM) from bone marrow of wildtype C57BL/6 or EP2^{-/-} mice were isolated and cultured for 6 days in the presence of murine recombinant M-CSF (20 ng/mL) (Miltenyi Biotec). For both MDM and BMDM, exchange of medium and replenishment of cytokines on the third day was performed. After 6 days incubation, cells were harvested and stimulated. When indicated, cells were treated for 24 hours with 5 µg/mL heGDH, catalytically inactive heGDH^{K126A, D204N} or for 30 min, 3 hours, or 24 hours with AF488-fluorochrome labeled heGDH. To compare endotoxin dependent effects, MDM were stimulated with 0.5 or 1 ng/mL LPS (Invivogen). For p300 inhibitor studies 6.6 µM of A485 (Tocris) was added 1 hour prior to heGDH stimulation. MDM were harvested after 24 hours and BMDM after 6 hours stimulation with p300 inhibitor. For experiments with neutralizing antibodies, MDM were incubated with 10 µg/mL anti-human IL-12/IL-23 (p40) antibody (Mabtech) or 10 µg/mL isotype control antibody (Invivogen) or anti-heGDH mAb (clone 4F8) (1:100) before heGDH stimulation. Stimulation of M2 polarized MDM with heGDH were done after 48 hours pre-incubation with 20 ng/mL human IL-4 and IL-13 (both from Miltenyi Biotec). Wildtype BMDM were incubated with 10 µg/mL anti-mouse IL-12 p40 or 10 µg/mL isotype control antibody (both from BioCell). To test effects of p40, MDM were treated with 10 or 100 ng/mL recombinantly produced human IL-12β for 24 hours. TCA-metabolite effects were assessed by stimulation of MDM with 1mM D-2-hydroxyglutarate, L-2-hydroxy-

glutarate, 1 mM itaconate or 1 mM α-ketoglutarate (all from Sigma Aldrich, Merck) for 24 hours. PUFA production was elicited by stimulating cells with 5 µM ionophore A23187 for 10 min at 37°C during harvesting. Cells were not treated with ionophore when they were used for FACS analysis. Supernatants of cells were stored at -70°C in 50% MeOH for LC-MS/MS analysis or undiluted for cytokine analysis. Cell pellets were lysed in RLT buffer with 1% β-mercaptoethanol (Merck Millipore) and stored at -70°C for RNA extraction. For western blot analysis, cell pellets were lysed with RIPA buffer supplemented with complete protease inhibitor cocktail (Roche Applied Science) and stored at -70°C.

siRNA knock down of p300 HAT in MDM and BMDM

4 x 10⁵ cells were seeded in a 12-well plate and MDM were transfected with 100 nM and BMDM with 25 nM siRNA. The transfection approach contained serum-free medium, p300 siRNA (Horizon Discovery) and 3% HiPerFect Transfection Reagent (Qiagen). After 6h incubation, MDM were supplemented with medium containing GM-CSF, TGF-β and heGDH. Immunofluorescence staining was performed 48 hours after transfection. For BMDM, medium was discarded and replaced after 6 hours incubation. heGDH stimulation was done on the next day. After treatment for 24 hours with heGDH immunofluorescence staining was performed.

Histology and immunofluorescence staining

For histology, the proximal 5 cm of the small intestine of *Nb* or *Hpb* infected mice was freed from mucus, extensively washed with cold PBS supplemented with 200 Units/mL penicillin and streptomycin, then rolled into "Swiss rolls". Lung of *Nb* experiments and Swiss rolls of *Hpb*-an *Nb*-infected mice were placed in a tissue cassette and fixed in 3.7% formaldehyde before standard formalin-fixed, paraffin-embedded (FFPE) processing. Swiss rolls of *Hpb*-infected mice which were scarified 4 days post infection were placed in cryo molds and embedded in Tissue-Tek optimum cutting temperature compound (OCT) (Science Services) and then frozen on dry ice.

Sections of all tissues were cut and stained with hematoxylin and eosin. Images were recorded with the EVOS system. Linear means intercept (Lmi) was quantified as a score of *N. brasiliensis*-driven lung damage, as described previously³. Briefly, sections of lung were viewed by microscopy with an original magnification of ×200; 15 random non-

overlapping fields per sample were assessed. Six horizontal lines were drawn across each image and the total number of times the alveolar wall intercepted per line was counted. Line length was then divided by the number of intercepts to calculate Lmi.

FFPE-tissues for immunofluorescence and immunohistochemistry staining of *Hpb*-infected intestine, were first deparaffinized and rehydrated after heating at 65°C for 10 min twice with Roticlear and isopropanol and once with 90% and 70% ethanol. To reduce the autofluorescence background MaxBlock™ Autofluorescence Reducing Reagent (MaxVision Bioscience) on FFPE and rehydrated cryosections was used. Before both stainings, antigen retrieval by repeated boiling in sodium-citrate buffer + 0.05% Tween-20 was performed. Subsequent, tissue was permeabilized and blocked with 3% BSA and 10% donkey serum at room temperature. Tissues for immunohistochemistry staining were further blocked with the Avidin/Biotin Blocking Kit (Thermo Fisher Scientific).

For immunofluorescence staining of MDM or BMDM, cells were seeded on a 12-well glass-chamber slides (IBIDI) and fixed for 15 minutes with 4% paraformaldehyde (Sigma Aldrich, Merck), followed by permeabilization with acetone (10 minutes at -20°C). After the same blocking procedure, cells or tissue were incubated with primary antibodies against goat anti-actin (Santa Cruz Biotechnology), rabbit anti-p300 (Cell Signaling), goat anti-cyclooxygenase-2 (Cayman Chemical), mouse anti-mPGES1 (Cayman Chemical) or rabbit anti-RELM α (Peprotech). For staining of heGDH, α -heGDH mAb (clone 4F8) (1:2) was used. Where indicated, blocking of α -heGDH mAb with its antigen peptide was performed in ratio of 1:1 overnight at 4°C while rotating. Fluorescence conjugated secondary antibodies were used for detection of immunofluorescence staining. Before images were recorded on a Leica SP5 confocal microscope (Leica Microsystems) cells were mounted and stained with Fluoroshield containing DAPI (Genetex). For immunohistochemistry staining the RELM α , biotinylated anti-murine antibody (Peprotech) was used. Detection and development were performed by applying ABC Peroxidase Standard Staining (Thermo Fisher Scientific) and DAB Enhanced Liquid Substrate System (Sigma Aldrich, Merck). Before recording with the EVOS system, nuclear counterstain and mounting was done. Files were adjusted equally for brightness and contrast using ImageJ.

Chromatin immunoprecipitation (ChIP)

For the ChIP with formaldehyde crosslinking, macrophages ($3\text{--}5 \times 10^6$ cells per condition) were washed once with warm PBS and incubated for 30 min at 37°C and 5% CO₂ with accutase (Sigma Aldrich, Merck) to detach the cells. ChIP protocol steps were performed as previously described⁶⁰, except fragmentation of the chromatin, which was carried out by using a focused-ultrasonicator (Covaris) for 15 min at 6°C with 140W peak power, 5% duty factor and 200 cycles/burst. Instead of agarose beads, ChIP grade protein A/G magnetic beads (Thermo Fisher Scientific) were added to the chromatin, antibody mixture and incubation was done for 2 hours at 4°C while rotating. Samples were incubated for ~3 min with a magnetic stand to ensure attachment of beads to the magnet and mixed by pipetting during the wash steps. DNA purification was performed with MinElute PCR Purification Kit (Qiagen). Eluted DNA was either subjected to ChIP-seq or used for ChIP-qPCR experiments. Input chromatin DNA was prepared from 1/4 of chromatin amount used for ChIP. Antibodies used for ChIP were anti-H3K27ac (abcam, ab4729, 4 μ g per ChIP) and isotype control antibody (abcam, ab171870, 4 μ g per ChIP).

ChIP qPCR

ChIP-qPCR was performed with PowerUp (Thermo Fisher Scientific) SYBR Green master mix following manufacturer's instructions. For all primer pairs input chromatin DNA was used to generate standard curves and verify amplification efficiency between 90–100%. qPCR was performed on a ViiA7 Real-Time PCR System (Applied Biosystems, Thermo Fisher Scientific). Changes in enrichment at specific regions were normalized to 3 different positive control regions (GAPDH, NSA2 and TBP) which did not show change in histone modifications during stimulation with heGDH.

RNA isolation

RNA was extracted using a spin-column kit according to the manufacturer's instructions (Zymo Research) and transcribed into DNA using the HighCapacity cDNA Reverse Transcription kit according to the manufacturer's instructions (Thermo Fisher Scientific) or submitted for total RNA sequencing. For genes where expression could not be quantified, CT values were set to 40.

Quantitative RT-PCR

FastStart Universal (Roche, Mannheim) or PowerUp (Thermo Fisher Scientific) SYBR Green master mixes were used for 10 ng cDNA template and qPCR was performed on a ViiA7

Real-Time PCR or QuantStudio 5 System (Applied Biosystems; Thermo Fisher Scientific). The expression levels were normalized to *GAPDH* as house-keeping gene and relative gene expression was represented as $2^{-\Delta CT}$ ($\Delta CT = \Delta CT_{(gene)} - CT_{(housekeeper)}$). A list of primers (4 μ M, Metabion) is shown in Table S1.

RNA sequencing

Sequencing was performed at the Helmholtz Zentrum München (HMGU) by the Genomics Core Facility. The preparation of samples, library preparation and sequencing were done as previously described^{61,62}. Library preparation was performed using the TruSeq Stranded mRNA Library Prep Kit (Illumina). Quality and quantity of RNA was assessed by Qubit 4 Fluorometer (Invitrogen) and RNA integrity number (RIN) was determined with the Agilent 2100 BioAnalyzer (RNA 6000 Nano Kit, Agilent). For library preparation, 1 μ g of RNA was poly(A) selected, fragmented, and reverse transcribed with the Elute, Prime, Fragment Mix (Illumina). A-tailing, adaptor ligation, and library enrichment were performed as described in the TruSeq Stranded mRNA Sample Prep Guide (Illumina). RNA libraries were assessed for quality and quantity with the Agilent 2100 BioAnalyzer and the Quant-iT PicoGreen dsDNA Assay Kit (Life Technologies, Thermo Fisher Scientific). RNA libraries were sequenced as 150 bp paired-end runs on an Illumina NovaSeq 6000 platform.

Flow-cytometry (FACS) analysis

Mesenteric lymph nodes (MLN) of *Hpb*-infected mice were removed and transferred in RPMI-1640 medium on ice until further processing for FACS analysis. Cells of MLN were forced through a 70 μ m cell strainer using cold PBS to prepare a single cell suspension. T cell population were stained extracellularly with CD3 (AF700, Biolegend) and CD4 (FITC, Biolegend). After 30 min fixation and permeabilization using a Fixation/Permeabilization kit (Thermo Fisher Scientific), intracellular staining of Foxp3 (Percp Cy5.5, ebioscience), Gata3 (EF660, ebioscience) and Helios (PB, Biolegend) was performed. EP2^{-/-} BMDM were stained against CD206 (PE-Cy7, Biolegend). Live/dead aqua (Life Technologies) was used for all cells to exclude dead cells from the analysis. Samples were acquired in a BD LSRFortessa (BD Biosciences) and analyzed by using FlowJo v10 software (FlowJo LLC). Treg induction was characterized as CD3⁺CD4⁺CD127⁻CD25^{hi}FoxP3⁺ cells as previously described¹⁰ with the following anti-human antibodies: CD3 (BV510, BioLegend), CD4 (BV421, BioLegend), CD127 (BV605,

BioLegend), CD25 (PE-Dazzle 594, BioLegend) and Foxp3 (APC, Invitrogen).

Metabolic Flux Analysis (Seahorse assay)

MDM and BMDM were cultured on Seahorse Miniplates (Agilent). On the day of assay, medium was exchanged to the Seahorse XF RPMI medium, pH 7.4 (Agilent) containing 10 mmol/L glucose (Sigma Aldrich, Merck), 1 mmol/L pyruvate and 2 mmol/L L-glutamine (both Thermo Fisher Scientific). The Mito Stress Test (Agilent) was performed according to the manufacturer's instructions with subsequent injections of oligomycin (1 μ mol/L, Agilent), FCCP (MDM: 1 μ M, BMDM: 5 μ M, Agilent) and rotenone and antimycin A (both 0.5 μ M, Sigma Aldrich, Merck). After the assay was performed, cells were lysed in 40 μ L RIPA buffer (Thermo Fisher Scientific) and protein concentration was determined for normalization (Pierce BCA protein assay kit, Thermo Fisher Scientific).

Targeted metabolite quantification

Metabolites were extracted from cell pellets using ice-cold 80:20 methanol:water solution followed by LC separation (Agilent 1290 Infinity II UHPLC inline using a Phenomenex Luna propylamine column (50 \times 2 mm, 3 μ m particles) with a solvent gradient of 100% buffer B (5 mM ammonium carbonate in 90% acetonitrile) to 90% buffer A (10 mM NH₄ in water) and a flow rate from 1000 to 750 μ L/min. Autosampler temperature was 5°C and injection volume was 2 μ L. Mass spectrometry was performed using an Agilent 6495 QQQ-MS operating in MRM mode and MRM setting were optimized separately for all compounds using pure standards. Data was processed using an in-house R script.

LDH cytotoxicity assay

Cellular cytotoxicity of stimulation with the A485 p300 inhibitor in MDM and BMDM was quantified using the LDH cytotoxicity assay kit (Thermo Fisher Scientific), according to the manufacturer's instructions.

Enzyme immunoassays (EIA)

The concentration of cysLTs and PGE₂ in culture supernatants was determined by using commercially available enzyme immunoassay (EIA) kits (Cayman Chemical), according to the manufacturer's instructions.

ELISA

MDM supernatants were analyzed for IL-10 or IL-12 β secretion using the human IL-10 ELISA Set (BD Biosciences) or the human IL-12/IL-23 p40 DuoSet ELISA (R&D Systems). PBMC

supernatants were analyzed for IL-4 using the IL-4 human ELISA kit (Thermo Fisher Scientific). All ELISAs were used according to the manufacturer's instructions.

Western Blot

The protein concentration was determined by the BCA method (Thermo Fisher Scientific) and lysates were diluted to equal concentrations between 12-20 μ g. NuPAGE LDS Sample buffer and NuPAGE Sample Reducing Agent (Thermo Fisher Scientific) was added to total lysates and heated at 95 °C for 5 minutes. Samples were loaded on Bolt 4-12% Bis-Tris Plus gels (Thermo Fisher Scientific) and separated by electrophoresis. Gels were transferred to a PVDF membrane (Merck Chemical) and blocked in 5% nonfat dry milk in 1x TBS containing 0.05% Tween for several hours to prevent nonspecific binding. Membranes were incubated overnight with primary antibodies against H3K27ac (Diagenode, dilution 1:1000) or β -actin (Sigma Aldrich, Merck; dilution 1:10000), washed and incubated with the corresponding secondary horseradish peroxidase-conjugated antibody. Detection was performed using enhanced chemiluminescence (SuperSignal West Femto Maximum Sensitivity Substrate, Pierce, Thermo Fisher Scientific) and recorded with the ECL Chemocam Imager (Intas Science Imaging Instruments). ImageJ software was used to quantify the protein concentrations by means of normalization and correction for β -actin in the samples.

LC-MS/MS quantification of lipid mediators of intestinal culture supernatants

The liquid chromatography-tandem mass spectrometry (LC-MS/MS) analysis of prostanoids in intestinal culture supernatant samples was performed as described in the following. Briefly, 200 μ L of the sample were mixed with 20 μ L of an internal standard solution (PGE₂-d₄, PGD₂-d₄, TXB₂-d₄, PGF_{2 α} -d₄, 6-keto PGF_{1 α} d₄, all purchased from Cayman Chemicals), with 100 μ L ice cold methanol containing 0.1% BHT, 400 μ L ice cold methanol and 400 μ L of a disodium hydrogen phosphate buffer solution with pH 6. The samples were extracted using EXPRESS ABN columns (Biotage): First, conditioning with methanol was performed, followed by the equilibration with water and loading of the sample. Next, 2 washing steps with methanol/water (50:50, v/v) and 2 % formic acid as well as water were carried out. The sample was eluted by using methanol/ammoniumhydroxid-solution (98:2, v/v). The samples were evaporated at 45 °C under a

gentle stream of nitrogen and reconstituted with 50 μ L MeOH/water (70:30, v/v) containing 0.0001% BHT. As several analytes resulted in values above the ULOQ, the sample preparation was repeated using a simpler approach and a smaller sample volume. Briefly, 10 μ L of sample were combined with 190 μ L of PBS and extracted using liquid-liquid-extraction with ethyl acetate after adding internal standard solutions containing PGE₂-d₄, PGD₂-d₄, TXB₂-d₄, PGF_{2 α} -d₄, 6-keto PGF_{1 α} d₄, each 40 μ L and 100 μ L 0.15M EDTA solution. The extraction step was repeated, organic layers of both extractions were combined, evaporated at 45 °C under a gentle stream of nitrogen, and reconstituted with 50 μ L MeOH/water (70:30, v/v) containing 0.0001% BHT.

Ten microliters either of the SPE- or the LLE-extracted samples were injected into the LC-MS/MS-system. For liquid chromatography-tandem mass spectrometry analysis, an Agilent 1290 LC system (Agilent) coupled to a hybrid 6500+ QTrap mass spectrometer (Sciex) equipped with a Turbo-V-source operating in negative electrospray ionization mode was used. The chromatographic separation was performed using an Acquity UPLC BEH C18 2.1 \times 100 mm column and VanGuard Pre-Column 2.1 \times 5 mm (both with a particle size of 1.7 μ m, from Waters). Mobile phases consisted of 0.0025% formic acid and acetonitrile with 0.0025% formic acid. Chromatographic separation was achieved under gradient conditions with a total run time of 12 minutes. For analysis, Analyst Software 1.7.1 and MultiQuant Software 3.0.3 (both Sciex, Darmstadt, Germany) were used, employing the internal standard method (isotope-dilution mass spectrometry). The precursor-to-product ion transitions used for quantification were m/z 351.2 \rightarrow m/z 315.0 for PGE₂, m/z 351.2 \rightarrow m/z 189.0 for PGD₂, m/z 353.1 \rightarrow m/z 193.0 for PGF_{2 α} , m/z 369.2 \rightarrow m/z 163.0 for 6-keto PGF_{1 α} , m/z 369.2 \rightarrow m/z 169.1 for TXB₂. The calibration curves were constructed using linear regression with 1/x² weighting.

Lipid mediator quantification via LC-MS/MS of cellular (MDM and BMDM) supernatants

Lipid mediator analysis was performed as described previously⁶³. Automated solid phase extraction was performed on a Microlab STAR robot (Hamilton). Prior to extraction all samples were diluted with H₂O to a methanol (MeOH) content of 15% and internal standard was added. Samples were extracted using Strata-X 96-well plates (30 mg, Phenomenex). After elution with MeOH, samples were evaporated to dryness under N₂ stream and redissolved in

MeOH/H₂O (1:1). Chromatographic separation of eicosanoids was achieved with a 1260 Series HPLC (Agilent) using a Kinetex C18 reversed phase column (2.6 μm, 100 x 2.1 mm, Phenomenex) with a SecurityGuard Ultra Cartridge C18 (Phenomenex) precolumn. The QTRAP 5500 mass spectrometer (Sciex), equipped with a Turbo-VTM ion source, was operated in negative ionization mode. Samples were injected via an HTC PAL autosampler (CTC Analytics), set to 7.5°C. Identification of metabolites was achieved via retention time and scheduled multiple reaction monitoring as previously specified. Acquisition of LC-MS/MS data was performed using Analyst Software 1.6.3 followed by quantification with MultiQuant Software 3.0.2 (both Sciex).

Cloning, expression, and purification of heGDH and catalytically inactive heGDH

Preparation of the expression constructs

The heGDH gene was amplified by PCR using Pfu polymerase and a pET-21a/heGDH construct (GeneArt, Thermo Fisher Scientific) as the template. The obtained PCR product was cloned into a linearized pET TrxA-1a vector, an expression vector containing N-terminal His₆- and thioredoxin-tags followed by a TEV protease cleavage site using the SLiCe method⁶⁴.

The catalytically inactive double mutant (K126A, D204N) of heGDH was produced by site-directed mutagenesis using a QuikChange mutagenesis kit (Agilent) and the N-terminal His₆-tag heGDH construct as the template. All expression constructs were verified by sequencing.

Protein expression and purification

The heGDH expression constructs were transformed into *E. coli* strain BL21 (DE3) CC4 (overexpressing the (co-)chaperones GroEL, GroES, DnaK, DnaJ, GrpE and ClpB)⁶⁵ and cultured overnight at 20°C in 2-L flasks containing 500 ml ZYM 5052 auto-induction medium⁶⁶ and 100 μg/mL kanamycin, 50 μg/mL spectinomycin and 10 μg/mL chloramphenicol. Cells from 2 L of culture were harvested by centrifugation after reaching saturation, resuspended in 120 ml lysis buffer (50 mM Tris-HCl, 300 mM NaCl, 20 mM imidazole, 10 mM MgCl₂, 10 μg/mL DNaseI, 1 mM AEBsf.HCl, 0,2% (v/v) NP-40, 1 mg/mL lysozyme, 0.01% (v/v) 1-thioglycerol, pH 8.0), and lysed by sonication. The lysate was clarified by centrifugation (40,000 x g) and filtration (0.2 μm). The supernatant was applied to a 5-ml HiTrap Chelating HP column (Cytiva), equilibrated in buffer A (50 mM Tris-HCl,

300 mM NaCl, 20 mM imidazole, 0.01% (v/v) 1-thioglycerol, pH 8.0) using an Äkta Purifier (Cytiva). The column was washed with buffer A and buffer A containing 50 mM imidazole until a stable baseline was reached (monitored at 280nm). Bound proteins were eluted with a linear gradient from 50 to 300 mM imidazole in buffer A. Fractions containing heGDH were pooled and dialyzed overnight at 4°C against 1L buffer B (50 mM Tris-HCl, 300 mM NaCl, 0.01% (v/v) 1-thioglycerol, pH 8.0). Next, 5 mM ATP (from a 100 mM stock solution at pH 7) and 1 mM MgCl₂ were added, and the solution was incubated overnight at 4°C to detach bound chaperones. The solution was applied to a 5-ml HiTrap Chelating HP column and the protein purified as described above. Fractions containing heGDH were pooled and dialyzed overnight at 4°C against 1 L buffer B in the presence of His-tagged TEV protease in a 1:25 molar ratio (TEV:protein). The cleaved off heGDH was further purified by affinity chromatography as described above and the flow-through and protein containing wash fractions were pooled and concentrated to less than 5 ml. This was subsequently subjected to size exclusion chromatography using a HiLoad 16/600 Superdex 200 column (Cytiva), equilibrated in buffer B. The fractions containing heGDH were pooled and dialyzed overnight against 1 L PBS pH 7.4 at 4°C. Finally, the solution was concentrated to approx. 2 mg/mL and stored at 4°C.

The catalytically inactive double mutant of heGDH was purified using the same protocol without the ATP-MgCl₂ incubation and the second affinity chromatography step.

Protein concentrations were determined by measuring the absorbance at 280nm using the specific absorbances for heGDH of 1.057 and 1.108 ml/mg*cm, respectively.

Fluorochrome labeling of heGDH

heGDH was labeled with the Atto 488 Protein Labeling Kit (Sigma Aldrich, Merck). 2 mg/mL heGDH was mixed with 10 mg/mL of the reactive dye. The reaction mixture was incubated for 1 hour at room temperature while shaking. Subsequently, the fluorochrome conjugated protein was purified with a PD-10 desalting column.

Cryo-electron microscopy

For cryo-EM sample preparation, 4.5 μl of the protein sample were applied to glow discharged Quantifoil 2/1 grids, blotted for 4 s with force 4 in a Vitrobot Mark III (Thermo Fisher) at 100% humidity and 4 °C, and plunge frozen in liquid ethane, cooled by liquid nitrogen. Cryo-EM data was acquired with a FEI Titan Krios

transmission electron microscope using SerialEM software (PMID: 16182563). Movie frames were recorded at a nominal magnification of 29,000X using a K3 direct electron detector (Gatan). The total electron dose of ~60 electrons per Å² was distributed over 30 frames at a pixel size of 0.84 Å. Micrographs were recorded in a defocus range from -0.5 to -3.0 μm.

Image processing, classification and refinement

Cryo-EM micrographs were processed on the fly using the Focus software package (PMID: 28344036) if they passed the selection criteria (iciness < 1.05, drift 0.4 Å < x < 70 Å, defocus 0.5 μm < x < 5.5 μm, estimated CTF resolution < 6 Å). Micrograph frames were aligned using MotionCor2 (PMID: 28250466) and the contrast transfer function (CTF) for aligned frames was determined using GCTF (PMID: 2659270). From 2,565 acquired micrographs 1,803,297 particles were picked using the Phosaurus neural network architecture from crYOLO (PMID: 31240256). Particles were extracted with a pixel box size of 192 scaled down to 64 using RELION 3.1 (PMID: 22100448) and underwent several rounds of reference-free 2D classification. 1,686,235 selected particles were re-extracted with a box size of 256 and imported into Cryosparc 2.3 (PMID: 28165473). Three *Ab initio* models with C3-symmetry were generated and passed through one round of heterogeneous classification. The best performing calls, containing 932,895 particles, was selected and particles were re-imported to RELION and underwent several rounds of refinement, CTF-refinement (estimation of anisotropic magnification, fit of per-micrograph defocus and astigmatism and beamtilt estimation) and Bayesian polishing (PMID: 25122622). Final refinements yielded models with an estimated resolution of 2.62 Å and 2.7 Å for C3- and C1-symmetry, respectively (gold standard FSC analysis of two independent half-sets at the 0.143 cutoff). Local-resolution and 3D-FSC plots (Figure S7) were calculated using RELION and the "Remote 3DFSC Processing Server" web interface (PMID: 28671674), respectively.

GDH activity assay

GDH activity of purified recombinant heGDH or heGDH^{K126A, D204N} was determined both in the direction of glutamate formation and utilization. Assays were carried out at 37 °C in 250 μl assay mixture containing 100 mM phosphate buffer and 5 μg protein. The enzyme activity of heGDH was determined in the direction of

glutamate utilization by the rate of production of NADH/NADPH or by the rate of utilization of NADH/NADPH in the direction of glutamate formation, measured spectrophotometrically at 340 nm. The optimum pH was determined in both directions with substrate concentrations of 0.5 mM α-ketoglutarate (Sigma Aldrich, Merck) and 40 mM ammonia (Honeywell) or 5 mM glutamate (Sigma Aldrich, Merck) with the pH range 5.5-9.5. The optimum concentration of co-factors was determined by using NAD(P)⁺ concentrations (Sigma Aldrich, Merck) from 0 to 3 mM with 4 mM glutamate or 0 to 0.8 mM NAD(P)H with 0.5 mM α-ketoglutarate and 10 mM ammonia. The Km for glutamate was determined in reaction mixtures containing 0-15 mM glutamate and 3 mM NAD⁺ and the Km for α-ketoglutarate with 0-1 mM α-ketoglutarate, 10 mM ammonia and 0.4 mM NADH. The Km for ammonia was determined with 0-100 mM ammonia, 0.5 mM α-ketoglutarate and 0.4 mM NADH. The inhibitory/stimulatory effects of GTP (Sigma Aldrich, Merck), bithionol (20 μM, Focus Biomolecules) and α-heGDH mAb (1:100) on GDH activity were determined in the direction of both glutamate utilization and formation reaction. For this testing assays the following concentrations were used: 3 mM NAD⁺, 0.4 mM NADH, 4 mM glutamate, 0.5 mM α-ketoglutarate and 10 mM ammonia.

Activity assay of human recombinant leukotriene C4 synthase (LTC4S)

Assay was done as previously described⁶⁷. Incubations were carried out with 100 ng of recombinant human leukotriene C4 synthase (LTC₄S) and 26 μM of leukotriene A4 (LTA₄) in 100 μL of 25 mM Tris-HCl (pH 7.8) containing 0.03% of n-dodecyl-β-D-maltoside (DDM) and 5 mM of glutathione for 15 seconds at room temperature. To determine the effect of heGDH or L-2-hydroxyglutarate (L-2-HG) on the activity of LTC₄S, pre-incubations with 1 μg or 3 μg of heGDH or 1mM L-2-HG were performed for 3 or 30 minutes on ice, followed by the incubation with LTA₄. Pre-incubations with 1 μM of TK05, as a potent inhibitor of LTC₄S, for 3 min on ice were performed in parallel.

Reactions were stopped by addition of 2 vol of MeOH containing 300 pmol of PGB₂ as an internal standard followed by 1 vol of water. Produced LTC₄ was quantified using the reverse-phase HPLC approach. Samples were analyzed on a 3.9 × 150-mm column (C18; Nova-Pak Waters) by eluting products at a flow rate of 1 mL/min with acetonitrile/methanol/water/acetic acid at a ratio of 30:30:40:0.1 (vol/vol) at pH 5.6. Absorbance was monitored at 280 nm. Based on the

produced LTC₄, the specific activity of LTC₄S was determined as picomoles of LTC₄ produced by 1 nanogram of LTC₄S in 1 minute.

LTC₄S activity in differentiated MonoMac6 (MM6) homogenates

MonoMac6 cells (0.3-0.4x10⁶ cells/mL) were differentiated with 50 nM 1 α ,25-dihydroxyvitamin D3 and 5 ng/mL TGF- β 1 in the medium for MM6 cells (RPMI-1640 with 10% FBS, 100 U/mL PEST, 1% OPI-media supplement, 1X MEM-Non-essential amino acid solution, 2 mM L-Glutamine) for 96 hours at 37 °C and 5% CO₂.

To check the effect of 5 μ g/mL heGDH on the LTC₄S activity in cell homogenates, 3x10⁶ differentiated MM6 cells were resuspended in 0.5 mL 1X PBS and incubated for 24 hours at 37°C and 5% CO₂. Controls with 1X PBS were prepared in parallel. Cell suspensions were collected and sonicated 3 times for 5 seconds on ice in the presence of 1 mM EDTA using the VCX 130 Vibra-Cell™ Ultrasonic Liquid Processor. Next, cell sonicates were pre-incubated for 30 seconds at 37°C followed by the incubation with 5 μ M LTA₄ for 10 minutes at 37 °C. Incubations were quenched with 0.5 mL of methanol containing 300 pmol of PGB₂ as the internal standard and acidified to pH 3-4 with 10 μ L of 3 N HCl. Cell debris were removed by centrifugation at 10 000 x g for 10 minutes at 4 °C. Supernatants were carried to new vials and diluted with 2 volumes of pure water prior to the solid phase extraction with Oasis HLB 3 cc (Waters) cartridges. Samples were eluted with methanol and taken to dryness under controlled nitrogen flow with TurboVap LV system (Biotage). Lipids were redissolved in 400 μ L of methanol:water (1:1) mixture prior to the reverse-phase high-performance liquid chromatography.

The formation of LTC₄ was analyzed as described for the activity assay of human LTC₄S.

DATA ANALYSIS AND STATISTICS

Data were analyzed by GraphPad Prism 9 software. For LC-MS/MS (lipid mediator) and ELISA (cytokines/ chemokines) data, missing values below the lower limit of detection were interpolated using ¼ of the minimum value for each metabolite. Statistical analysis of two group comparisons was performed using Mann-Whitney (unpaired), Wilcoxon test (paired) or t test depending on normal distribution. For comparison of more groups, RM one-way ANOVA, Friedmann test (paired) or Kruskal-Wallis test (unpaired) with Dunn correction was used with correction for multiple comparisons. P<0.05 was considered

statistically significant. Details of statistical tests and sample size are provided in the figure legends. Heat maps were generated by the Broad Institute's Morpheus software.

RNAseq data was analyzed with R. Genes with fewer than 100 counts in the RNAseq data were filtered out. Only the genes with more than 10 counts in at least one sample were kept. The vst⁶⁸ normalization implemented in the DESeq2⁶⁹ package was used to normalize the filtered RNA-seq counts. Based on the DESeq2 package calculation of the fold change, base mean and adjusted p-values of the differentially genes for the following contrasts were calculated: heGDH treated vs LPS treated; heGDH treated vs PBS treated; LPS treated vs PBS treated. Subsequently, the pheatmap package (<https://CRAN.R-project.org/package=pheatmap> (2015)) was used to plot heatmaps of the top 50 genes with the largest log2 fold change with at least 50 base counts in the above-mentioned contrasts. Additionally, usage of the EnhancedVolcano package (<https://github.com/kevinblighe/EnhancedVolcano>) created volcano plots of the differentially expressed genes with at least 50 base counts.

REFERENCES

1. Anthony, R.M., Urban, J.F., Jr, Alem, F., Hamed, H.A., Rozo, C.T., Boucher, J.-L., Van Rooijen, N., and Gause, W.C. (2006). Memory T(H)2 cells induce alternatively activated macrophages to mediate protection against nematode parasites. *Nat. Med* **12**, 955–960. 10.1038/nm1451.
2. Esser-von Bieren, J., Mosconi, I., Guet, R., Piersgilli, A., Volpe, B., Chen, F., Gause, W.C., Seitz, A., Verbeek, J.S., and Harris, N.L. (2013). Antibodies Trap Tissue Migrating Helminth Larvae and Prevent Tissue Damage by Driving IL-4R α -Independent Alternative Differentiation of Macrophages. *PLoS Pathog.* **9**, e1003771. 10.1371/journal.ppat.1003771.
3. Sutherland, T.E., Logan, N., Ruckerl, D., Humbles, A.A., Allan, S.M., Papayannopoulos, V., Stockinger, B., Maizels, R.M., and Allen, J.E. (2014). Chitinase-like proteins promote IL-17-mediated neutrophilia in a tradeoff between nematode killing and host damage. *Nat Immunol* **15**, 1116–1125. 10.1038/ni.3023.
4. Chen, F., Wu, W., Millman, A., Craft, J.F., Chen, E., Patel, N., Boucher, J.L., Urban, J.F., Kim,

- C.C., and Gause, W.C. (2014). Neutrophils prime a long-lived effector macrophage phenotype that mediates accelerated helminth expulsion. *Nat. Immunol.* *15*, 938–946. 10.1038/ni.2984.
5. Chen, F., El-Naccache, D.W., Ponessa, J.J., Lemenze, A., Espinosa, V., Wu, W., Lothstein, K., Jin, L., Antao, O., Weinstein, J.S., et al. (2022). Helminth resistance is mediated by differential activation of recruited monocyte-derived alveolar macrophages and arginine depletion. *Cell Rep* *38*, 110215. 10.1016/j.celrep.2021.110215.
 6. Turner, J.D., Pionnier, N., Furlong-Silva, J., Sjöberg, H., Cross, S., Halliday, A., Guimaraes, A.F., Cook, D.A.N., Steven, A., Van Rooijen, N., et al. (2018). Interleukin-4 activated macrophages mediate immunity to filarial helminth infection by sustaining CCR3-dependent eosinophilia. *PLoS Pathog* *14*, e1006949. 10.1371/journal.ppat.1006949.
 7. Osbourn, M., Soares, D.C., Vacca, F., Cohen, E.S., Scott, I.C., Gregory, W.F., Smyth, D.J., Toivakka, M., Kemter, A.M., le Bihan, T., et al. (2017). HpARI Protein Secreted by a Helminth Parasite Suppresses Interleukin-33. *Immunity* *47*, 739-751.e5. 10.1016/j.immuni.2017.09.015.
 8. Sharma, A., Sharma, P., Ganga, L., Satoeya, N., Mishra, S., Vishwakarma, A.L., and Srivastava, M. (2018). Infective Larvae of *Brugia malayi* Induce Polarization of Host Macrophages that Helps in Immune Evasion. *Front Immunol* *9*, 194. 10.3389/fimmu.2018.00194.
 9. de los Reyes Jiménez, M., Lechner, A., Alessandrini, F., Bohnacker, S., Schindela, S., Trompette, A., Haimerl, P., Thomas, D., Henkel, F., Mourão, A., et al. (2020). An anti-inflammatory eicosanoid switch mediates the suppression of type-2 inflammation by helminth larval products. *Sci. Transl. Med.* *12*, eaay0605. 10.1126/scitranslmed.aay0605.
 10. Prodjinotho, U.F., Gres, V., Henkel, F., Lacorcchia, M., Dandl, R., Haslbeck, M., Schmidt, V., Winkler, A.S., Sikasunge, C., Jakobsson, P., et al. (2022). Helminthic dehydrogenase drives PGE₂ and IL-10 production in monocytes to potentiate Treg induction. *EMBO Reports* *23*. 10.15252/embr.202154096.
 11. Esser-von Bieren, J. (2017). Immune-regulation and -functions of eicosanoid lipid mediators. *Biological Chemistry* *398*, 1177–1191. 10.1515/hsz-2017-0146.
 12. McGinty, J.W., Ting, H.-A., Billipp, T.E., Nadsombati, M.S., Khan, D.M., Barrett, N.A., Liang, H.-E., Matsumoto, I., and von Moltke, J. (2020). Tuft-Cell-Derived Leukotrienes Drive Rapid Anti-helminth Immunity in the Small Intestine but Are Dispensable for Anti-protist Immunity. *Immunity* *52*, 528-541.e7. 10.1016/j.immuni.2020.02.005.
 13. Kaiser, M.M.M., Ritter, M., del Fresno, C., Jónasdóttir, H.S., van der Ham, A.J., Pelgrom, L.R., Schramm, G., Layland, L.E., Sancho, D., Prazeres da Costa, C., et al. (2018). Dectin-1/2-induced autocrine PGE₂ signaling licenses dendritic cells to prime Th2 responses. *PLoS Biol* *16*, e2005504. 10.1371/journal.pbio.2005504.
 14. Brattig, N.W., Schwohl, A., Hoerauf, A., and Büttner, D.W. (2009). Identification of the lipid mediator prostaglandin E₂ in tissue immune cells of humans infected with the filaria *Onchocerca volvulus*. *Acta Tropica* *112*, 231–235. 10.1016/j.actatropica.2009.07.018.
 15. Lechner, A., Bohnacker, S., and Esser-von Bieren, J. (2021). Macrophage regulation & function in helminth infection. *Seminars in Immunology* *53*, 101526. 10.1016/j.smim.2021.101526.
 16. Wang, X.-F., Wang, H.-S., Wang, H., Zhang, F., Wang, K.-F., Guo, Q., Zhang, G., Cai, S.-H., and Du, J. (2014). The role of indoleamine 2,3-dioxygenase (IDO) in immune tolerance: Focus on macrophage polarization of THP-1 cells. *Cellular Immunology* *289*, 42–48. 10.1016/j.cellimm.2014.02.005.
 17. Liu, X., Shin, N., Koblisch, H.K., Yang, G., Wang, Q., Wang, K., Leffet, L., Hansbury, M.J., Thomas, B., Rugar, M., et al. (2010). Selective inhibition of IDO1 effectively regulates mediators of antitumor immunity. *Blood* *115*, 3520–3530. 10.1182/blood-2009-09-246124.
 18. Fallarino, F., Grohmann, U., Vacca, C., Bianchi, R., Orabona, C., Spreca, A., Fioretti, M.C., and Puccetti, P. (2002). T cell apoptosis by tryptophan catabolism. *Cell Death Differ* *9*, 1069–1077. 10.1038/sj.cdd.4401073.

19. Dokmeci, E., Xu, L., Robinson, E., Golubets, K., Bottomly, K., and Herrick, C.A. (2011). EBI3 deficiency leads to diminished T helper type 1 and increased T helper type 2 mediated airway inflammation: EBI3 deficiency leads to diminished Th1, increased Th2. *Immunology* 132, 559–566. 10.1111/j.1365-2567.2010.03401.x.
20. Everts, B., Tussiwand, R., Dreesen, L., Fairfax, K.C., Huang, S.C.-C., Smith, A.M., O'Neill, C.M., Lam, W.Y., Edelson, B.T., Urban, J.F., et al. (2016). Migratory CD103+ dendritic cells suppress helminth-driven type 2 immunity through constitutive expression of IL-12. *Journal of Experimental Medicine* 213, 35–51. 10.1084/jem.20150235.
21. Fork, C., Vasconez, A.E., Janetzko, P., Angioni, C., Schreiber, Y., Ferreirós, N., Geisslinger, G., Leisegang, M.S., Steinhilber, D., and Brandes, R.P. (2017). Epigenetic control of microsomal prostaglandin E synthase-1 by HDAC-mediated recruitment of p300. *J. Lipid Res.* 58, 386–392. 10.1194/jlr.M072280.
22. Liu, F., Romantseva, T., Park, Y.-J., Golding, H., and Zaitseva, M. (2020). Production of fever mediator PGE2 in human monocytes activated with MDP adjuvant is controlled by signaling from MAPK and p300 HAT: Key role of T cell derived factor. *Mol Immunol* 128, 139–149. 10.1016/j.molimm.2020.10.008.
23. H, S., J, L., L, W., X, W., X, X., M, D., and B, H. (2004). Histone acetyltransferase activity of p300 enhances the activation of IL-12 p40 promoter. *Molecular immunology* 41. 10.1016/j.molimm.2004.05.013.
24. Esser-von Bieren, J. (2019). Eicosanoids in tissue repair. *Immunol Cell Biol* 97, 279–288. 10.1111/imcb.12226.
25. Oyesola, O.O., Shanahan, M.T., Kanke, M., Mooney, B.M., Webb, L.M., Smita, S., Matheson, M.K., Campioli, P., Pham, D., Früh, S.P., et al. (2021). PGD2 and CRTH2 counteract Type 2 cytokine-elicited intestinal epithelial responses during helminth infection. *Journal of Experimental Medicine* 218, e20202178. 10.1084/jem.20202178.
26. Mandal, P., Verma, N., Chauhan, S., and Tomar, R.S. (2013). Unexpected Histone H3 Tail-clipping Activity of Glutamate Dehydrogenase. *Journal of Biological Chemistry* 288, 18743–18757. 10.1074/jbc.M113.462531.
27. Traube, F.R., Özdemir, D., Sahin, H., Scheel, C., Glück, A.F., Geserich, A.S., Oganessian, S., Kostidis, S., Iwan, K., Rahimoff, R., et al. (2021). Redirected nuclear glutamate dehydrogenase supplies Tet3 with α -ketoglutarate in neurons. *Nat Commun* 12, 4100. 10.1038/s41467-021-24353-9.
28. Paradisi, F., Woolfson, R., Geoghegan, K.F., and Engel, P.C. (2005). Identification of the residue responsible for catalysing regeneration of activity in the inactive glutamate dehydrogenase mutant D165N. *FEBS Letters* 579, 2830–2832. 10.1016/j.febslet.2005.03.098.
29. Jha, A.K., Huang, S.C.-C., Sergushichev, A., Lampropoulou, V., Ivanova, Y., Loginicheva, E., Chmielewski, K., Stewart, K.M., Ashall, J., Everts, B., et al. (2015). Network Integration of Parallel Metabolic and Transcriptional Data Reveals Metabolic Modules that Regulate Macrophage Polarization. *Immunity* 42, 419–430. 10.1016/j.immuni.2015.02.005.
30. Chen, F., Wu, W., Millman, A., Craft, J.F., Chen, E., Patel, N., Boucher, J.L., Urban, J.F., Kim, C.C., and Gause, W.C. (2014). Neutrophils prime a long-lived effector macrophage phenotype that mediates accelerated helminth expulsion. *Nat Immunol* 15, 938–946. 10.1038/ni.2984.
31. Chen, F., El-Naccache, D.W., Ponessa, J.J., Lemenze, A., Espinosa, V., Wu, W., Lothstein, K., Jin, L., Antao, O., Weinstein, J.S., et al. (2022). Helminth resistance is mediated by differential activation of recruited monocyte-derived alveolar macrophages and arginine depletion. *Cell Rep* 38, 110215. 10.1016/j.celrep.2021.110215.
32. Esser-von Bieren, J., Volpe, B., Kulagin, M., Sutherland, D.B., Guiet, R., Seitz, A., Marsland, B.J., Verbeek, J.S., and Harris, N.L. (2015). Antibody-mediated trapping of helminth larvae requires CD11b and Fc γ receptor I. *J Immunol* 194, 1154–1163. 10.4049/jimmunol.1401645.
33. Chen, J., Gu, Z., Wu, M., Yang, Y., Zhang, J., Ou, J., Zuo, Z., Wang, J., and Chen, Y. (2016). C-reactive protein can upregulate VEGF expression to promote ADSC-induced

- angiogenesis by activating HIF-1 α via CD64/PI3k/Akt and MAPK/ERK signaling pathways. *Stem Cell Res Ther* 7, 114. 10.1186/s13287-016-0377-1.
34. Passos, L.S.A., Gazzinelli-Guimarães, P.H., Oliveira Mendes, T.A. de, Guimarães, A.C.G., Silveira Lemos, D. da, Ricci, N.D., Gonçalves, R., Bartholomeu, D.C., Fujiwara, R.T., and Bueno, L.L. (2017). Regulatory monocytes in helminth infections: insights from the modulation during human hookworm infection. *BMC Infect Dis* 17, 253. 10.1186/s12879-017-2366-0.
 35. Robb, C.T., Zhou, Y., Felton, J.M., Zhang, B., Goepf, M., Jheeta, P., Smyth, D.J., Duffin, R., Vermeren, S., Breyer, R.M., et al. (2023). Metabolic regulation by prostaglandin E₂ impairs lung group 2 innate lymphoid cell responses. *Allergy* 78, 714–730. 10.1111/all.15541.
 36. Serra-Pages, M., Torres, R., Plaza, J., Herrerias, A., Costa-Farré, C., Marco, A., Jiménez, M., Maurer, M., Picado, C., and de Mora, F. (2015). Activation of the Prostaglandin E₂ receptor EP2 prevents house dust mite-induced airway hyperresponsiveness and inflammation by restraining mast cells' activity. *Clin Exp Allergy* 45, 1590–1600. 10.1111/cea.12542.
 37. Teloni, R., Giannoni, F., Rossi, P., Nisini, R., and Gagliardi, M.C. (2007). Interleukin-4 inhibits cyclo-oxygenase-2 expression and prostaglandin E₂ production by human mature dendritic cells. *Immunology* 120. 10.1111/j.1365-2567.2006.02482.x.
 38. Miyoshi, H., VanDussen, K.L., Malvin, N.P., Ryu, S.H., Wang, Y., Sonnek, N.M., Lai, C., and Stappenbeck, T.S. (2017). Prostaglandin E₂ promotes intestinal repair through an adaptive cellular response of the epithelium. *EMBO J* 36, 5–24. 10.15252/embj.201694660.
 39. Fairweather, M., Heit, Y.I., Buie, J., Rosenberg, L.M., Briggs, A., Orgill, D.P., and Bertagnolli, M.M. (2015). Celecoxib inhibits early cutaneous wound healing. *Journal of Surgical Research* 194, 717–724. 10.1016/j.jss.2014.12.026.
 40. Iwanaga, K., Okada, M., Murata, T., Hori, M., and Ozaki, H. (2012). Prostaglandin E₂ Promotes Wound-Induced Migration of Intestinal Subepithelial Myofibroblasts via EP2, EP3, and EP4 Prostanoid Receptor Activation. *J Pharmacol Exp Ther* 340, 604–611. 10.1124/jpet.111.189845.
 41. Ganesh, K., Das, A., Dickerson, R., Khanna, S., Parinandi, N.L., Gordillo, G.M., Sen, C.K., and Roy, S. (2012). Prostaglandin E₂ Induces Oncostatin M Expression in Human Chronic Wound Macrophages through Axl Receptor Tyrosine Kinase Pathway. *The Journal of Immunology* 189, 2563–2573. 10.4049/jimmunol.1102762.
 42. Garantziotis, S., Brass, D.M., Savov, J., Hollingsworth, J.W., McElvania-TeKippe, E., Berman, K., Walker, J.K.L., and Schwartz, D.A. (2006). Leukocyte-Derived IL-10 Reduces Subepithelial Fibrosis Associated with Chronically Inhaled Endotoxin. *Am J Respir Cell Mol Biol* 35, 662–667. 10.1165/rcmb.2006-0055OC.
 43. Pesce, J.T., Ramalingam, T.R., Mentink-Kane, M.M., Wilson, M.S., El Kasmi, K.C., Smith, A.M., Thompson, R.W., Cheever, A.W., Murray, P.J., and Wynn, T.A. (2009). Arginase-1–Expressing Macrophages Suppress Th2 Cytokine–Driven Inflammation and Fibrosis. *PLoS Pathog* 5, e1000371. 10.1371/journal.ppat.1000371.
 44. Baban, B., Chandler, P.R., Sharma, M.D., Pihkala, J., Koni, P.A., Munn, D.H., and Mellor, A.L. (2009). IDO activates regulatory T cells and blocks their conversion into TH17-like T cells. *J Immunol* 183, 2475–2483. 10.4049/jimmunol.0900986.
 45. Donovan, M.J., Tripathi, V., Favila, M.A., Geraci, N.S., Lange, M.C., Ballhorn, W., and McDOWELL, M.A. (2012). Indoleamine 2,3-dioxygenase (IDO) induced by *Leishmania* infection of human dendritic cells: *Leishmania-induced IDO*. *Parasite Immunology* 34, 464–472. 10.1111/j.1365-3024.2012.01380.x.
 46. Stobie, L., Gurunathan, S., Prussin, C., Sacks, D.L., Glaichenhaus, N., Wu, C.-Y., and Seder, R.A. (2000). The role of antigen and IL-12 in sustaining Th1 memory cells *in vivo*: IL-12 is required to maintain memory/effector Th1 cells sufficient to mediate protection to an infectious parasite challenge. *Proc. Natl. Acad. Sci. U.S.A.* 97, 8427–8432. 10.1073/pnas.160197797.
 47. Jankovic, D., Kullberg, M.C., Hieny, S., Caspar, P., Collazo, C.M., and Sher, A. (2002). In the

- Absence of IL-12, CD4⁺ T Cell Responses to Intracellular Pathogens Fail to Default to a Th2 Pattern and Are Host Protective in an IL-10^{-/-} Setting. *Immunity* **16**, 429–439. 10.1016/S1074-7613(02)00278-9.
48. Moro, K., Kabata, H., Tanabe, M., Koga, S., Takeno, N., Mochizuki, M., Fukunaga, K., Asano, K., Betsuyaku, T., and Koyasu, S. (2016). Interferon and IL-27 antagonize the function of group 2 innate lymphoid cells and type 2 innate immune responses. *Nat Immunol* **17**, 76–86. 10.1038/ni.3309.
 49. Liu, P.-S., Wang, H., Li, X., Chao, T., Teav, T., Christen, S., Di Conza, G., Cheng, W.-C., Chou, C.-H., Vavakova, M., et al. (2017). α -ketoglutarate orchestrates macrophage activation through metabolic and epigenetic reprogramming. *Nat Immunol* **18**, 985–994. 10.1038/ni.3796.
 50. Quinteros, S.L., von Krusenstiern, E., Snyder, N.W., Tanaka, A., O'Brien, B., and Donnelly, S. (2023). The helminth derived peptide FhHDM-1 redirects macrophage metabolism towards glutaminolysis to regulate the pro-inflammatory response. *Front. Immunol.* **14**, 1018076. 10.3389/fimmu.2023.1018076.
 51. Chowdhury, R., Yeoh, K.K., Tian, Y., Hillringhaus, L., Bagg, E.A., Rose, N.R., Leung, I.K.H., Li, X.S., Woon, E.C.Y., Yang, M., et al. (2011). The oncometabolite 2-hydroxyglutarate inhibits histone lysine demethylases. *EMBO Rep* **12**, 463–469. 10.1038/embor.2011.43.
 52. Li, F.-L., Liu, J.-P., Bao, R.-X., Yan, G., Feng, X., Xu, Y.-P., Sun, Y.-P., Yan, W., Ling, Z.-Q., Xiong, Y., et al. (2018). Acetylation accumulates PFKFB3 in cytoplasm to promote glycolysis and protects cells from cisplatin-induced apoptosis. *Nat Commun* **9**, 508. 10.1038/s41467-018-02950-5.
 53. Infantino, V., Iacobazzi, V., Menga, A., Avantaggiati, M.L., and Palmieri, F. (2014). A key role of the mitochondrial citrate carrier (SLC25A1) in TNF α - and IFN γ -triggered inflammation. *Biochimica et Biophysica Acta (BBA) - Gene Regulatory Mechanisms* **1839**, 1217–1225. 10.1016/j.bbagr.2014.07.013.
 54. Hewitson, J.P., Marcus, Y., Murray, J., van Agtmaal, M., Filbey, K.J., Grainger, J.R., Bridgett, S., Blaxter, M.L., Ashton, P.D., Ashford, D.A., et al. (2011). Proteomic analysis of secretory products from the model gastrointestinal nematode *Heligmosomoides polygyrus* reveals dominance of Venom Allergen-Like (VAL) proteins. *Journal of Proteomics* **74**, 1573–1594. 10.1016/j.jprot.2011.06.002.
 55. Skuce, P.J., Stewart, E.M., Smith, W.D., and Knox, D.P. (1999). Cloning and characterization of glutamate dehydrogenase (GDH) from the gut of *Haemonchus contortus*. *Parasitology* **118**, 297–304. 10.1017/S0031182098003850.
 56. Montes, C.L., Acosta-Rodríguez, E.V., Mucci, J., Zuniga, E.I., Campetella, O., and Gruppi, A. (2006). A *Trypanosoma cruzi* antigen signals CD11b⁺ cells to secrete cytokines that promote polyclonal B cell proliferation and differentiation into antibody-secreting cells. *Eur. J. Immunol.* **36**, 1474–1485. 10.1002/eji.200535537.
 57. Alessandrini, F., Schulz, H., Takenaka, S., Lentner, B., Karg, E., Behrendt, H., and Jakob, T. (2006). Effects of ultrafine carbon particle inhalation on allergic inflammation of the lung. *Journal of Allergy and Clinical Immunology* **117**, 824–830. 10.1016/j.jaci.2005.11.046.
 58. Layland, L.E., Mages, J., Loddenkemper, C., Hoerauf, A., Wagner, H., Lang, R., and Prazeres da Costa, C.U. (2010). Pronounced Phenotype in Activated Regulatory T Cells during a Chronic Helminth Infection. *The Journal of Immunology* **184**, 713–724. 10.4049/jimmunol.0901435.
 59. Dietz, K., de Los Reyes Jiménez, M., Gollwitzer, E.S., Chaker, A.M., Zissler, U.M., Rådmark, O.P., Baarsma, H.A., Königshoff, M., Schmidt-Weber, C.B., Marsland, B.J., et al. (2017). Age dictates a steroid-resistant cascade of Wnt5a, transglutaminase 2, and leukotrienes in inflamed airways. *J. Allergy Clin. Immunol.* **139**, 1343–1354.e6. 10.1016/j.jaci.2016.07.014.
 60. Günther, T., Theiss, J.M., Fischer, N., and Grundhoff, A. (2016). Investigation of Viral and Host Chromatin by ChIP-PCR or ChIP-Seq Analysis. *Current Protocols in Microbiology* **40**. 10.1002/9780471729259.mc01e10s40.
 61. Lechner, A., Henkel, F.D.R., Hartung, F., Bohnacker, S., Alessandrini, F., Gubernatorova, E.O., Drutskaya, M.S., Angioni, C., Schreiber, Y., Haimel, P., et al. (2021). Macrophages acquire

- a TNF-dependent inflammatory memory in allergic asthma. *Journal of Allergy and Clinical Immunology*, S009167492102741X. 10.1016/j.jaci.2021.11.026.
62. Bohnacker, S., Hartung, F., Henkel, F., Quaranta, A., Kolmert, J., Priller, A., Ud-Dean, M., Giglberger, J., Kugler, L.M., Pechtold, L., et al. (2022). Mild COVID-19 imprints a long-term inflammatory eicosanoid- and chemokine memory in monocyte-derived macrophages. *Mucosal Immunol* 15, 515–524. 10.1038/s41385-021-00482-8.
 63. Henkel, F.D.R., Friedl, A., Haid, M., Thomas, D., Bouchery, T., Haimerl, P., de los Reyes Jiménez, M., Alessandrini, F., Schmidt-Weber, C.B., Harris, N.L., et al. (2018). House dust mite drives pro-inflammatory eicosanoid reprogramming and macrophage effector functions. *Allergy*, all.13700. 10.1111/all.13700.
 64. Zhang, Y., Werling, U., and Edlmann, W. (2014). Seamless Ligation Cloning Extract (SLiCE) Cloning Method. In *DNA Cloning and Assembly Methods Methods in Molecular Biology.*, S. Valla and R. Lale, eds. (Humana Press), pp. 235–244. 10.1007/978-1-62703-764-8_16.
 65. de Marco, A., Deuerling, E., Mogk, A., Tomoyasu, T., and Bukau, B. (2007). Chaperone-based procedure to increase yields of soluble recombinant proteins produced in *E. coli*. *BMC Biotechnol* 7, 32. 10.1186/1472-6750-7-32.
 66. Studier, F.W. (2005). Protein production by auto-induction in high-density shaking cultures. *Protein Expression and Purification* 41, 207–234. 10.1016/j.pep.2005.01.016.
 67. Molina, D.M., Wetterholm, A., Kohl, A., McCarthy, A.A., Niegowski, D., Ohlson, E., Hammarberg, T., Eshaghi, S., Haeggström, J.Z., and Nordlund, P. (2007). Structural basis for synthesis of inflammatory mediators by human leukotriene C4 synthase. *Nature* 448, 613–616. 10.1038/nature06009.
 68. Anders, S., and Huber, W. (2010). Differential expression analysis for sequence count data. *Genome Biol* 11, R106. 10.1186/gb-2010-11-10-r106.
 69. Love, M.I., Huber, W., and Anders, S. (2014). Moderated estimation of fold change and dispersion for RNA-seq data with DESeq2. *Genome Biol* 15, 550. 10.1186/s13059-014-0550-8.

KEY RESOURCES TABLE

REAGENT or RESOURCE	SOURCE	IDENTIFIER
Antibodies		
Biotinylated Rabbit anti-murine RELM α polyclonal antibody	PeprTech	Cat#500-P214BT
Donkey anti-goat IgG (H+L) cross-adsorbed secondary antibody, Alexa Fluor® 568	Thermo Fisher Scientific	Cat#A-11057
Donkey anti-Goat IgG-HRP (H+L), secondary Antibody	Novus Biologicals	Cat# NB7357
Donkey anti-Mouse IgG (H+L), cross-adsorbed secondary antibody, Alexa Fluor® 647	Thermo Fisher Scientific	Cat#A-31571
Donkey anti-rabbit IgG (H+L) highly cross-adsorbed secondary antibody, Alexa Fluor® 647	Thermo Fisher Scientific	Cat#A-31573
Donkey anti-rat IgG (H+L) highly cross-adsorbed secondary antibody, Alexa Fluor® 488	Thermo Fisher Scientific	Cat#A-21208
Gata-3 monoclonal Antibody, eFluor™ 660 (clone:TWAJ), eBioscience™	Thermo Fisher Scientific	Cat#50-9966-42
Goat anti-human COX-2 polyclonal antibody	Cayman Chemical	Cat#100034
Goat anti-human β -actin polyclonal antibody	Santa Cruz Biotechnology Inc.	Cat#sc-1616
Hamster anti-mouse Helios monoclonal antibody, PB (clone: 22F6)	Biolegend	Cat#137221
Mouse anti-human CD3 Antibody, Brilliant Violet 510 (clone UCHT1)	BioLegend	Cat#300448
Mouse anti-human CD4 Antibody, Brilliant Violet 421 (clone: RPA-T4)	BioLegend	Cat#300532
Mouse anti-human CD25 Antibody, PE-Dazzle 594 (clone: BC96)	BioLegend	Cat#302646
Mouse anti-human CD127 (IL-7R α) Antibody, Brilliant Violet 605 (clone: A019D5)	BioLegend	Cat#351334
Mouse anti-human IL-12/-23 (p40) monoclonal antibody	Mabtech	Cat#3450-0N-500
Mouse anti-human Prostaglandin E Synthase-1 (microsomal) monoclonal antibody	Cayman Chemical	Cat#10004350
Mouse anti-rabbit IgG-HRP, secondary antibody	Santa Cruz Biotechnology	Cat#sc-2357
Mouse IgG1 monoclonal isotype control antibody	Invivogen	Cat#mabg1-ctrlm
Mouse IgG2a monoclonal isotype control antibody	Invivogen	Cat#mabg2a-ctrlm
Mouse IgG2b monoclonal isotype control antibody	R&D Systems	Cat# MAB0042
Rabbit anti-H3K27ac polyclonal antibody – ChIP grade	Diagenode	Cat#C15410196
Rabbit anti-Histone H3 (acetyl K27) polyclonal antibody - ChIP grade	abcam	Cat#ab4729
Rabbit anti-human p300 monoclonal antibody	Cell Signaling	Cat#86377
Rabbit anti-mouse CD64 monoclonal antibody	Thermo Scientific	Cat# MA5-29705
Rabbit IgG, polyclonal - Isotype Control antibody - ChIP grade	abcam	Cat#ab171870
Rat anti-heGDH (4F8) monoclonal antibody	Core Facility „Monoclonal Antibody“, Helmholtz Zentrum München	N/A
Rat anti-human FOXP3 Monoclonal Antibody, APC (clone: PCH101)	ThermoFisher Scientific	Cat#17-4776-42
Rat anti-mouse CD206 (MMR) monoclonal antibody, PE/Cyanine7 (clone: C068C2)	Biolegend	Cat#141719
Rat anti-mouse CD3, Alexa Fluor® 700 (clone: 17A2)	Biolegend	Cat#100216
Rat anti-mouse CD4, FITC (clone: GK1.5 Ruo)	BD Bioscience	Cat#553729
Rat anti-mouse FOXP3 monoclonal antibody, PerCP-Cyanine5.5 (clone: FJK-16s), eBioscience™	Thermo Fisher Scientific	Cat#45-5773-82
Rat anti-mouse IL-12 p40 monoclonal antibody	BioCell	Cat#BE0051
Rat IgG2a monoclonal isotype control antibody	BioCell	Cat#BE0089

Bacterial and virus strains		
E. coli strain BL21 (DE3) CC4	Core Facility "Protein Expression and Purification Facility", Helmholtz Zentrum München, Germany	N/A
Biological samples		
Human blood cells	Center of Allergy & Environment, Technical University of Munich, Germany Klinikum rechts der Isar, Technical University of Munich, Germany	N/A
Chemicals, peptides, and recombinant proteins		
934	Prof. Dr. Per Johan Jakobsson, Karolinska Institut Stockholm, Sweden	N/A
β -Nicotinamide adenine dinucleotide 2'-phosphate reduced tetrasodium salt hydrate	Sigma-Aldrich, Merck	Cat#N1630
β -Nicotinamide adenine dinucleotide hydrate	Sigma-Aldrich, Merck	Cat#N7004
β -Nicotinamide adenine dinucleotide phosphate sodium salt hydrate	Sigma-Aldrich, Merck	Cat#N0505
β -Nicotinamide adenine dinucleotide, reduced disodium salt hydrate	Sigma-Aldrich, Merck	Cat#N8129
3,3'-Diaminobenzidine (DAB) Enhanced Liquid Substrate System tetrahydrochloride	Sigma-Aldrich, Merck	Cat#D3939
A 485	Tocris	Cat#6387
Ammonium bicarbonate	Honeywell	Cat#A6141
Anitgen peptide for Rat anti-heGDH (4F8) monoclonal antibody: CAQHSEHRTPTKGG	Core Facility „Monoclonal Antibody“, Helmholtz Zentrum München	N/A
Atto 488 Protein Labeling Kit	Sigma-Aldrich, Merck	Cat#38371
Bithionol	Focus Biomolecules	Cat#10-4567
Calcium Ionophore A23187	Sigma-Aldrich, Merck	Cat#C7522
D- α -Hydroxyglutaric acid disodium salt	Sigma-Aldrich, Merck	Cat#16859
Fluoroshield™ with DAPI	GeneTex	Cat#GTX30920
Guanosine 5'-triphosphate sodium salt hydrate	Sigma-Aldrich, Merck	Cat#G8877
HiPerFect Transfection Reagent	Qiagen	Cat#301705
Human GM-CSF	Miltenyi Biotec	Cat#130-093-867
Human IL-12 β	Prof. Matthias Feige, Technische Universität München, Germany	N/A
Human IL-13	Miltenyi Biotec	Cat#130-112-408
Human IL-4	Miltenyi Biotec	Cat#130-093-921
Human TGF- β 1	Miltenyi Biotec	Cat#130-095-066
Itaconic acid	Sigma-Aldrich, Merck	Cat#I29204
Ketoglutar Säure-alpha	Sigma-Aldrich, Merck	Cat#75890
L-Glutamic Acid	Sigma-Aldrich, Merck	Cat#G1251
L- α -Hydroxyglutaric acid disodium salt	Sigma-Aldrich, Merck	Cat#90790
LPS-SM Ultrapure	Invivogen	Cat#lrl-smlps
Mouse M-CSF	Miltenyi Biotec	Cat#130-101-700
Pierce™ ChIP-grade Protein A/G Magnetic Beads	Thermo Fisher Scientific	Cat#26162
PowerUp SYBR Green Master Mix	Thermo Fisher Scientific	Cat#A25778

TK05	Prof. Jesper Z. Haeggström, Karolinska Institut Stockholm, Sweden	N/A
Zombie NIR Fixable Viable Kit	BioLegend	Cat#423105
Critical commercial assays		
ABC Peroxidase Staining Kit	Cayman Chemical	Cat#515211
Avidin/Biotin Blocking Kit	Thermo Fisher Scientific	Cat#004303
Bioanalyzer High Sensitivity DNA Analysis	Agilent	Cat#5067-4627
Bioanalyzer High Sensitivity RNA Analysis	Agilent	Cat#5067-1511
CyQUANT™ LDH Cytotoxicity Assay	Thermo Fisher Scientific	Cat#C20300
Cysteinyl Leukotriene ELISA Kit	Cayman Chemical	Cat#500390
eBioscience™ Intracellular Fixation & Permeabilization Buffer Set	Thermo Fisher Scientific	Cat#88-8824-00
FastStart Universal SYBR Green Master (Rox)	Roche Applied Science	Cat#4913914001
High-Capacity cDNA Reverse Transcription	Thermo Fisher Scientific	Cat#4368814
Human IL-10 ELISA Set	BD Biosciences	Cat#555157
Human IL-12/IL-23 p40 DuoSet ELISA	R&D Systems	Cat#DY1240-05
Human IL-4 ELISA kit	Thermo Fisher Scientific	Cat# KHC0041
LIVE/DEAD™ Fixable Aqua Dead Cell Stain Kit	Thermo Fisher Scientific	Cat#L34965
MaxBlock Autofluorescence Reducing Reagent Kit	MaxVision Biosciences	Cat#MB-M
MinElute PCR Purification Kit	Qiagen	Cat#28004
NEBNext® Ultra™ II DNA Library Prep Kit	New England Biolabs	Cat#E7645
Pierce™ BCA Protein Assay Kit	Thermo Fisher Scientific	Cat#23227
Prostaglandin E2 ELISA Kit	Cayman Chemical	Cat#514010
Quant-iT™ PicoGreen™ dsDNA Assay Kits and dsDNA Reagents	Thermo Fisher Scientific	Cat#P7589
Qubit DNA High Sensitivity Assay	Thermo Fisher Scientific	Cat#Q32851
Quick-RNA Microprep Kit	Zymoresearch	Cat#R1051
QuikChange mutagenesis kit	Agilent	Cat# 200523
Seahorse XF Cell Mito Stress Test Kit	Agilent	Cat#103010-100
TruSeq® Stranded mRNA Library Prep	Illumina	Cat#2002059
Deposited data		
RNA sequencing data	This paper	Will be available upon publication
Experimental models: Cell lines		
Monocyte-derived macrophages	Human blood, Center of Allergy & Environment, Klinikum rechts der Isar Technical University of Munich, Germany	N/A
Peripheral blood mononuclear cells	Herzzentrum, Klinikum rechts der Isar, Technical University of Munich	N/A
Primary bone marrow-derived macrophages	WT C57BL/6 and EP2 ^{-/-}	N/A
Experimental models: Organisms/strains		
<i>Heligmosomoides polygyrus bakeri</i>	Prof. David Vöhringer, Friedrich-Alexander-Universität, Erlangen-Nürnberg, Germany	N/A
Mouse: C57BL/6J	Charles River Laboratories	N/A
Mouse: EP2 ^{-/-} (C57BL/6J background)	Prof. Jan Böttcher, Technische Universität München, Germany	N/A

<i>Nippostrongylus brasiliensis</i>	Prof. David Vöhringer, Friedrich-Alexander- Universität, Erlangen- Nürnberg, Germany	N/A
<i>Schistosoma mansoni</i>	Prof. Clarissa Prazeres da Costa, Technical University of Munich, Germany	N/A
Oligonucleotides		
Human EP300 siRNA	Horizon Discovery	Cat#M-003486- 04-0005
Mouse EP300 siRNA	Horizon Discovery	Cat#M-065607- 01-0005
Primers for quantitative real-time PCR experiments	This paper	See Table S1
Recombinant DNA		
pET TrxA-1a vector	Core Facility "Protein Expression and Purification Facility", Helmholtz Zentrum München, Germany	N/A
Software and algorithms		
Aperio eSlide Manager	Leica Microsystems	www.leicabiosystems.com
Broad Institute's Morpheus software	Broadinstitute	https://software.broadinstitute.org/morpheus/
Cryosparc	Structura Biotechnology Inc.	https://cryosparc.com/
Fiji	ImageJ	https://imagej.nih.gov/ij/
FlowJo v10 software	FlowJo LLC	www.flowjo.com
GCTF	Zhang 2016	
GraphPad Prism version 9	GraphPad Software	www.graphpad.com
MotionCor2	UCSF	https://emcore.ucsf.edu/ucsf-software
RELION	Sjors Scheres at the MRC Laboratory of Molecular Biology	https://github.com/3dem/relion
Seahorse Wave Desktop Software	Agilent	www.agilent.com
SerialEM	David Mastronarde at University of Colorado	https://bio3d.colorado.edu/SerialEM/
Other		
2100 BioAnalyzer	Agilent	N/A
BD LSRII Fortessa™	BD Biosciences	N/A
ECL Chemocam Imager	Intas Science Imaging Instruments	N/A
Epoch ELISA Reader	BioTek	N/A
EVOS™ FL Auto Imaging System	Thermo Fisher Scientific	N/A
Leica SP5 confocal microscope	Leica Microsystems	N/A
Low-throughput Focused-ultrasonicators S220	Covaris	N/A
QuantStudio™ 5 Real-Time PCR System	Thermo Fisher Scientific	N/A
Qubit 4 Fluorometer	Invitrogen	N/A
Seahorse XF HS Mini Analyzer	Agilent	N/A
Titan Krios transmission electron microscope	FEI	N/A
ViiA7 Real-Time PCR System	Applied Biosystems	N/A

Table S1: Primer sequences for aPCR and PCR

Human Primer	Forward Sequence	Reverse Sequence
<i>ALOX15</i>	GGACACTTGATGGCTGAGGT	GTATCGCAGGTGGGGAATTA
<i>ALOX5</i>	GATTGTCCCCATTGCCATCC	AGAAGGTGGGTGATGGTCTG
<i>EBI3</i>	GGCTCCCTACGTGCTCAATG	AGGTCGGGCTTGATGATGT
<i>GAPDH</i>	GAAGGTGAAGGTCGGAGT	GAAGATGGTGATGGGATTTTC
<i>IDO1</i>	ACAGACCACAAGTCACAGCG	TTGGCAAGACCTTACGGACA
<i>IL12B</i>	TGCCGTTTACAAGCTCAAGT	TGGGTCAGGTTTGATGATGTCC
<i>LTC4S</i>	GACGGTACCATGAAGGACGA	GGAGAAGTAGGCTTGCAGCAG
<i>MRC1</i>	CGATCCGACCCTTCCTTGAC	TGTCTCCGCTTCATGCCATT
<i>PFKFB3</i>	AAGATGCCGTTGGAAGTAC	GGGGAGTTGGTCAGCTTTG
<i>PTGES</i>	TCAAGATGTACGTGGTGGCC	GAAAGGAGTAGACGAAGCCCAG
<i>PTGS2</i>	GCTGGAACATGGAATTACCCA	CTTTCTGTACTGCGGGTGGAA
Human ChIP Primer	Forward Sequence	Reverse Sequence
<i>GAPDH</i>	GCGTCTACGAGCCTTGCG	CTACCCTGCCCCCATACGA
<i>IDO1</i>	GCCAGTATGAGCCTAAGCAGC	AGAGAGGCAGTGTGGAATAATGG
<i>IL6</i>	GACAGCCACTCACCTCTTCAG	AAGCCTACCCACCTCCTTTTC
<i>NSA2</i>	CAGCCTGAAAGGTCAGCGGT	TCGAGACTTGAGGCGGTTGC
<i>PTGS2</i>	TAAGTGTATCCAGCCCCACTCC	ACCCATGTCAAACCGAGGTG
<i>TBP</i>	CTGAGACAGCGGGCACGGTA	GCCTGAACCGAGAGACGGGA
Mouse Primer	Forward Sequence	Reverse Sequence
<i>EBI3</i>	CTGGTTACTGAAACAGCTCTC	GGATACCGAGAAGCATGGCA
<i>GAPDH</i>	GGGTGTGAACCACGAGAAAT	CCTTCCACAATGCCAAAGTT
<i>IL12B</i>	TGGGAGTACCCTGACTCCTG	AGGAACGCACCTTTCTGGTT
<i>PFKFB3</i>	AATGTGGGAGAGTATCGGCG	AAGGCACACTGTTTTCGGAC
<i>PTGES</i>	GAAGAAGGCTTTTGCCAACCC	TCCACATCTGGGTCACCTCT
<i>PTGS2</i>	GGGCCATGGAGTGGACTTAAA	TCCATCCTTGAAAAGGCGCA
Cloning Primer	Forward Sequence	Reverse Sequence
heGDH	GAATCTTTATTTTCAGGGCGCCATGCTG AGCACCTGGCAC	GAGCTCGAATTCGGATCCGGTACCTTATT AGGTAAAGGTAAAACCTGC

CONTACT FOR REAGENT AND RESOURCE SHARING

Further information and request for resources and reagents should be directed to and will be fulfilled by the Lead Contact, Julia Esser-von Bieren (julia.esser-vonbieren@unil.ch).

SUPPLEMENTARY FIGURES

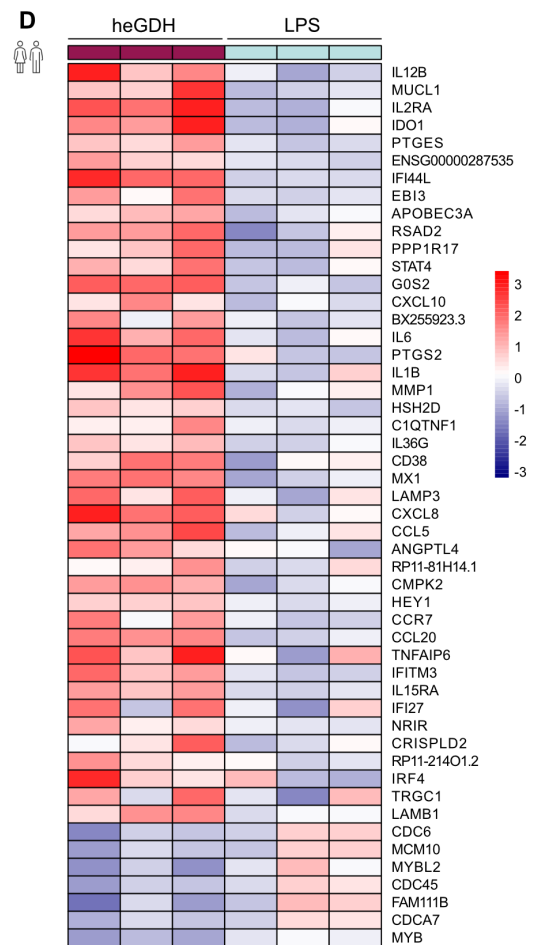
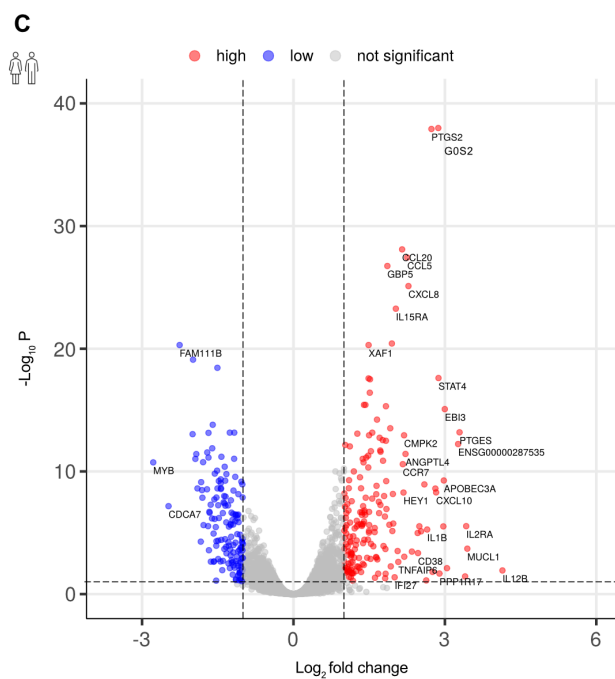
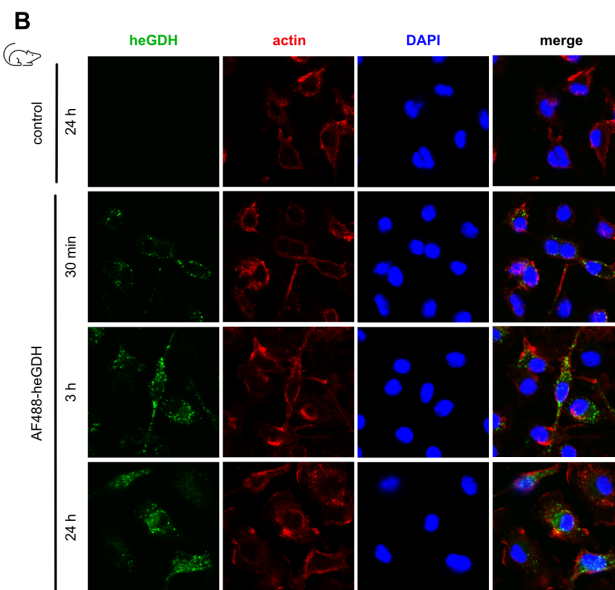
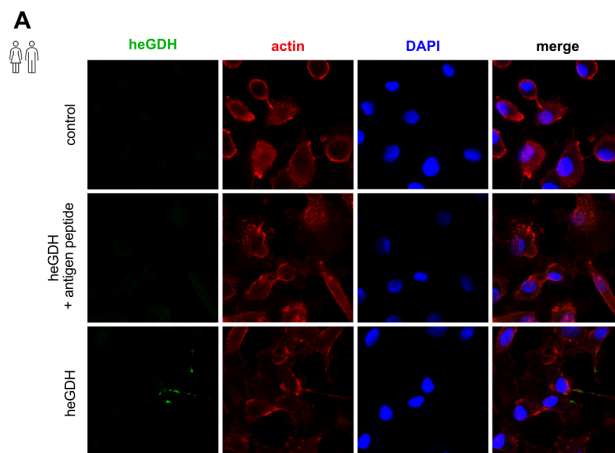


Figure S1: heGDH can be taken up by macrophages and display a different macrophage phenotype compared to low-dose LPS

(A) Representative immunofluorescence staining of heGDH, actin and DAPI (cell nuclei) in MDM \pm treatment with heGDH and heGDH in combination with the antigen peptide for the α -heGDH mAb.

(B) Representative immunofluorescence staining of actin and DAPI (cell nuclei) in BMDM \pm treatment with AF488-labeled heGDH for different time points (30 min, 3h, 24h).

(C) Volcano plot showing DEGs of MDM stimulated with heGDH or 1 ng/mL LPS (n=3) with a $p_{adj} < 0.1$, $\log_2 FC > 1$ and a base mean > 50 . Labeled DEGs are for genes with either $p_{adj} < 1e-20$ or with $\log_2 FC > 2$.

(D) Heatmap of top 50 DEGs between MDM treated with heGDH or 1 ng/mL LPS (n=3), $p_{adj} < 0.1$, $\log_2 FC > 1$; base mean > 50 .

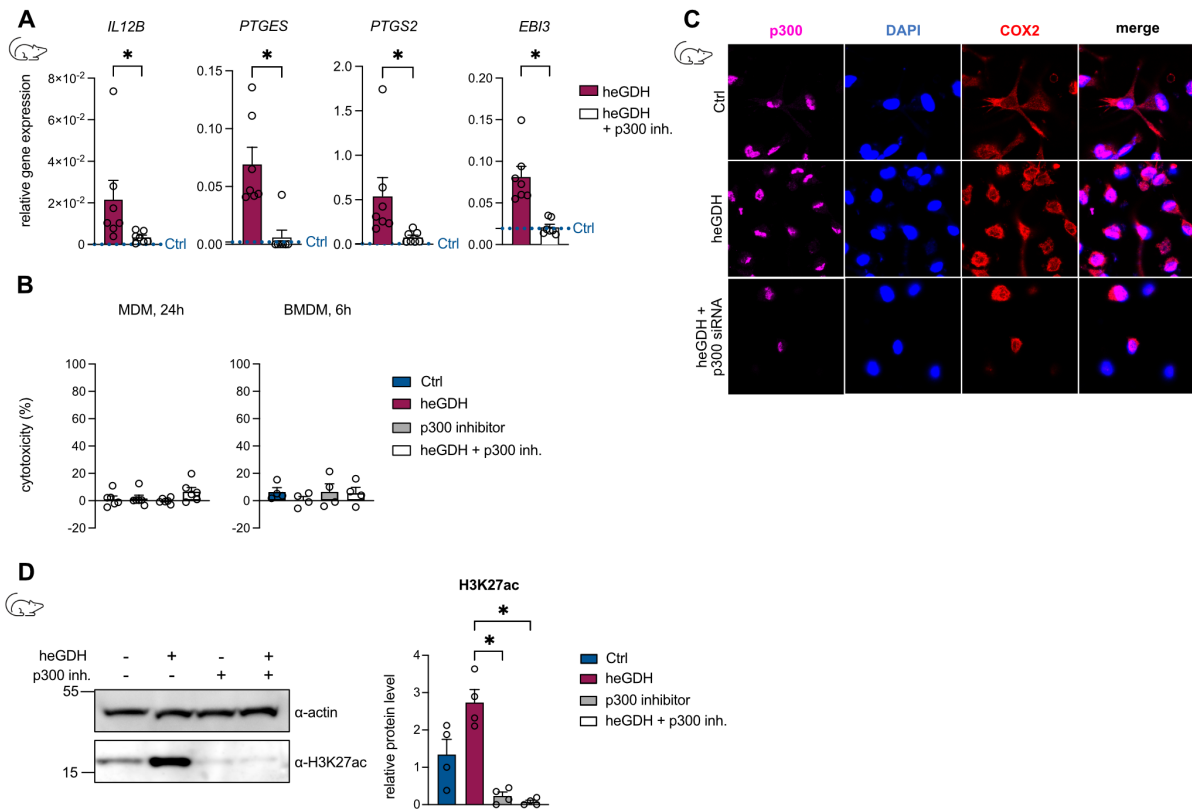


Figure S2: p300 HAT activation by heGDH results in the induction of type-2 suppressive genes in BMDM

(A) Gene expression analysis of top DEGs (qPCR) in BMDM treated with heGDH alone or after inhibition of p300 HAT (A485) (n=6). Dotted lines indicate expression in control treated cells.

(B) Cytotoxicity measurement (LDH assay) of MDM (24h) or BMDM (6h) ± treatment with heGDH ± p300 HAT inhibitor (A485).

(C) Representative immunofluorescence staining of p300, DAPI (cell nuclei) and COX2 in BMDM ± treatment with heGDH and heGDH treated cells after p300 siRNA knock down.

(D) Protein amounts of H3K27ac or actin (western blot) in BMDM ± treatment with heGDH ± inhibitor of p300 HAT (A485). Left, representative blots for one mouse. Right, quantification for n=4 mice.

Data are pooled from at least two independent experiments and presented as means + SEM. Statistical significance was determined by Wilcoxon test (A), Friedman test (B), or RM one-way ANOVA (D). *P < 0.05.

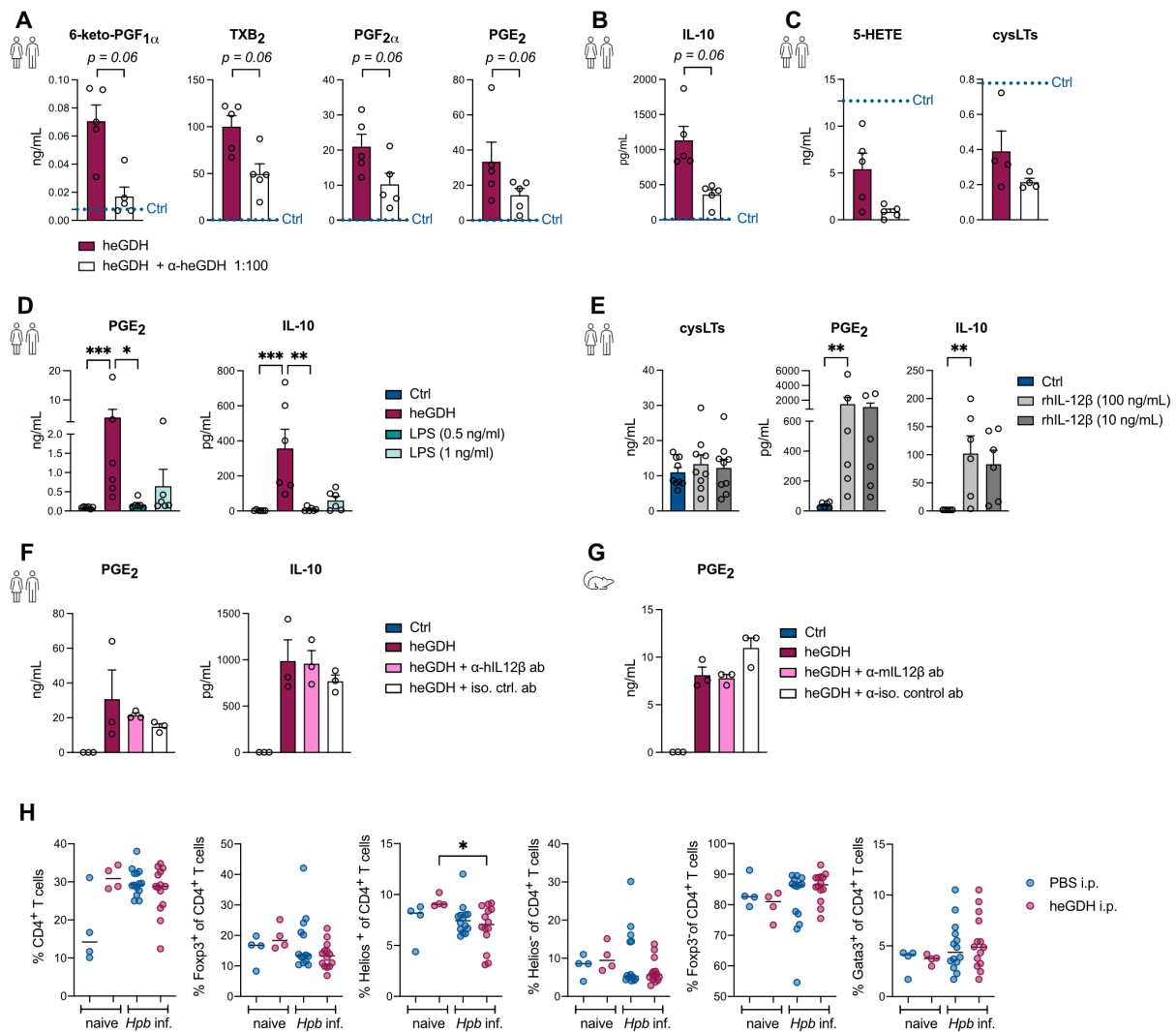


Figure S3: heGDH mediated induction of regulatory prostanoids and cytokines is independent of endotoxins or IL-12β production in macrophages

(A) Prostanoids quantified (LC-MS/MS) in supernatants of MDM treated with heGDH alone or after addition of α-heGDH mAb (n=5). Dotted lines indicate prostanoid levels in control (Ctrl) treated cells.

(B) Secretion of IL-10 (ELISA) in MDM treated with heGDH alone or after addition of α-heGDH mAb (n=5). Dotted line indicates IL-10 level in control (Ctrl) treated cells.

(C) 5-LOX metabolites quantified (LC-MS/MS) in supernatant of MDM treated with heGDH alone or after addition of α-heGDH mAb (n=5). Dotted lines indicate levels in control (Ctrl) treated cells.

(D) Secretion of PGE₂ (EIA) and IL-10 (ELISA) by MDM after treatment ± heGDH, 0.5 ng/mL or 1 ng/mL LPS (n=6).

(E) Secretion of cysLTs, PGE₂ (EIA) and IL-10 (ELISA) by MDM after treatment ± recombinant human IL-12β in different concentrations (10 or 100 ng/mL), (n=6).

(F) Secretion of PGE₂ (EIA) and IL-10 (ELISA) by MDM after treatment ± heGDH ± neutralizing α-hIL-12β ab or isotype control ab.

(G) Secretion of PGE₂ (EIA) by BMDM after treatment ± heGDH ± neutralizing α-mIL-12β ab or isotype control ab.

(H) Analysis of different T-cell populations (flow cytometry) in mesenteric lymph nodes of mice which received intraperitoneal (i.p.) treatment with PBS or heGDH (n=4 per group) or ± i.p. treatment with PBS or heGDH after infection with *Hpb* (n=14).

Data are presented as means + SEM. Statistical significance was determined by Wilcoxon test (A-C), Friedman test (D-G) or Kruskal-Wallis's test (H). *P < 0.05; **P < 0.01; ***P < 0.001.

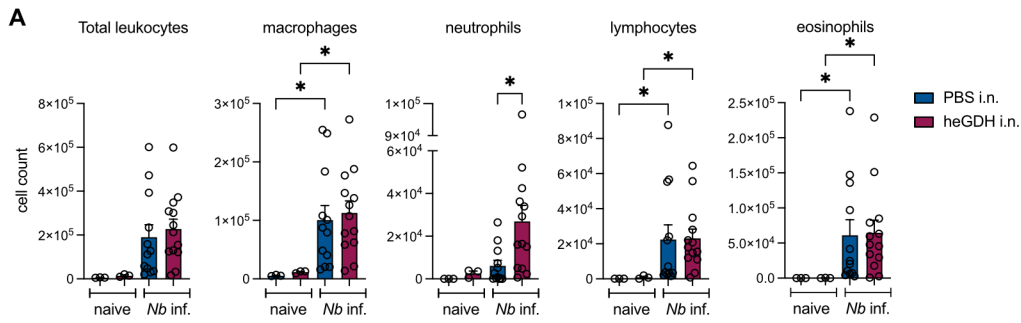


Figure S4: heGDH mediated neutrophil recruitment during infection with *Nippostrongylus brasiliensis*

(A) BALF cell counts in mice after intranasal treatment with PBS or heGDH under naïve conditions (n=3 per group) or after infection with *N. brasiliensis* (n=12 in PBS i.n. group and n=13 in heGDH i.n. group). Data are pooled from four independent experiments and presented as means + SEM. Statistical significance was determined by Kruskal-Wallis's test (A). *P < 0.05.

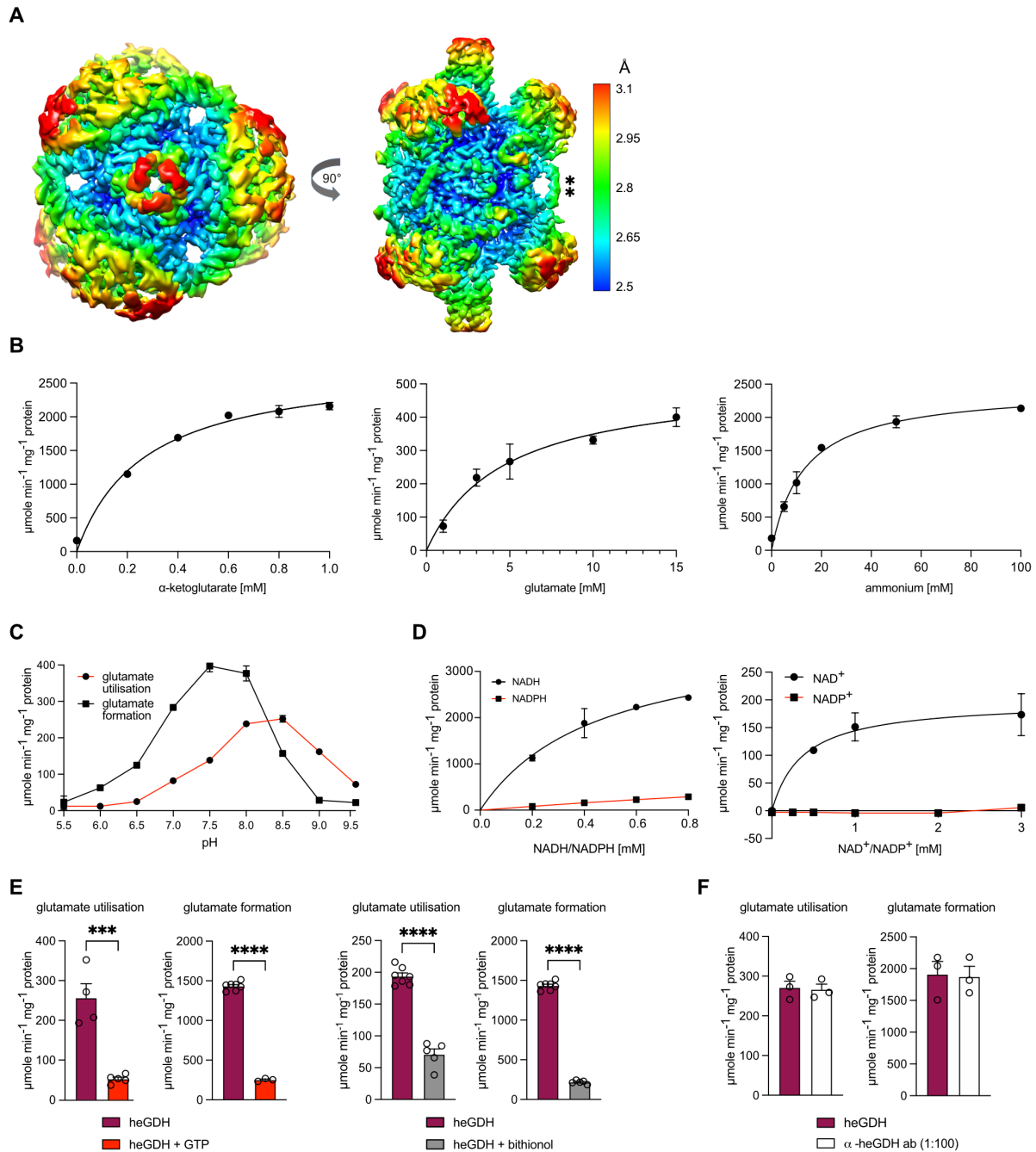


Figure S5: heGDH activity is suppressed by GTP and bithionol, while the addition of mAb did not affect catalytic activity

(A) Local resolution of CryoEM reconstruction of the heGDH oligomer. Bar-like connection of the N-terminus (**) in the cryoEM model.

(B) Activity of recombinant heGDH in the direction of glutamate utilisation and formation with varying concentrations of educts and products (n=4-6).

(C) Effects of pH on the activities of recombinant heGDH in the direction of glutamate utilisation and formation (n=2).

(D) Activity of recombinant heGDH in the direction of glutamate utilisation and formation with varying concentrations of cofactors (n=4-6).

(E) Effect of GTP or GDH inhibitor bithionol on the activity of heGDH in the direction of glutamate utilisation and formation (n=3-7).

(F) Effect of α -heGDH ab on the activity of heGDH in in the direction of glutamate utilisation and formation (n=3).

Data are pooled from at least two independent experiments and presented as means + SEM. Statistical significance was determined by unpaired t test (E-F). ***P < 0.001, ****P < 0.0001.

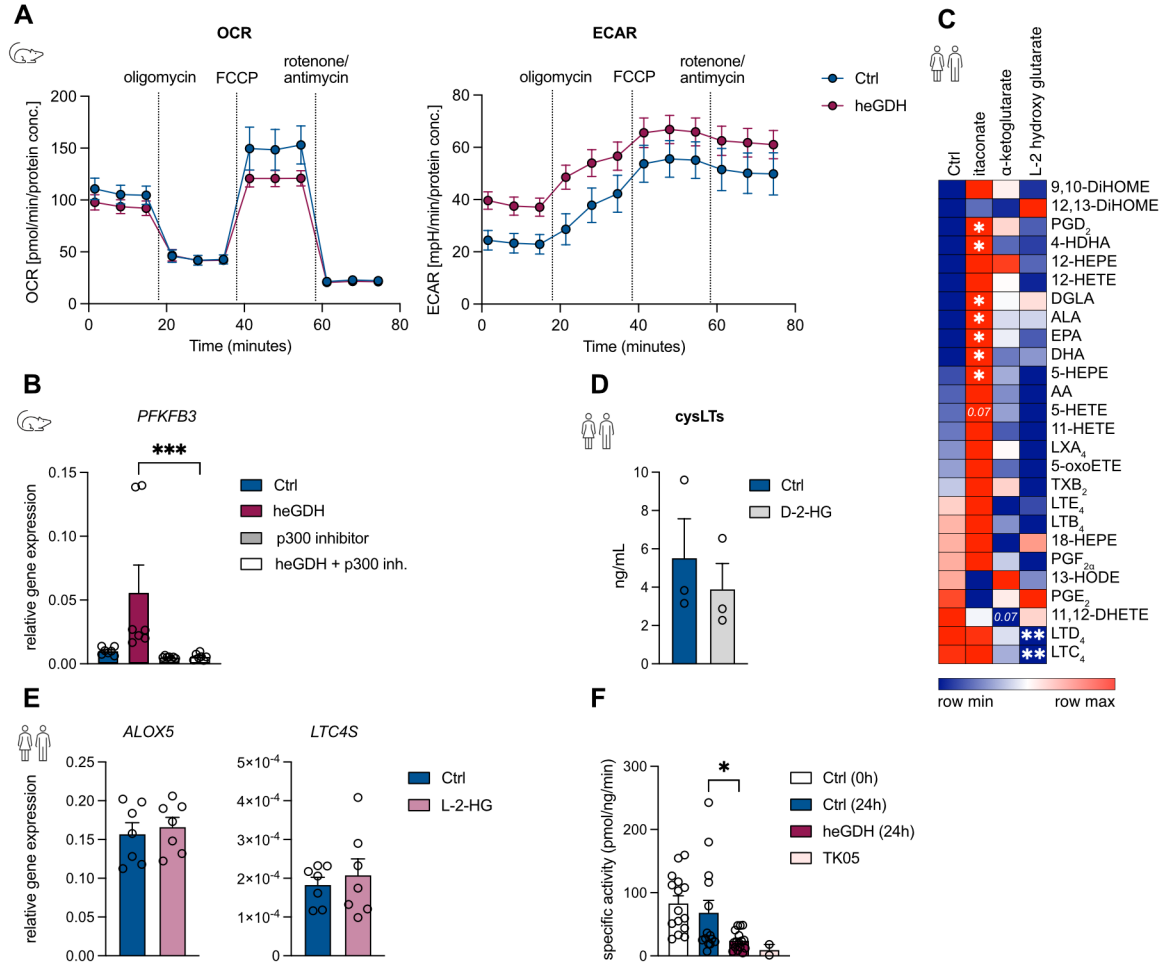


Figure S6: heGDH affect macrophage metabolism in a p300-dependent fashion.

(A) Oxygen consumption rate (OCR, left) and extracellular acidification rate (ECAR, right) of BMDM treated \pm heGDH (n=6).

(B) Gene expression analysis of *PFKFB3* (qPCR) in BMDM after treatment \pm heGDH \pm p300 HAT (A485) inhibitor (n=7).

(C) Heatmap of lipid mediators produced by human MDM \pm treatment with 1mM itaconate, α -ketoglutarate or L-2-hydroxyglutarate (LC-MS/MS). Data is shown as mean of 6 donors.

(D) Secretion of cysLTs (EIA) by MDM after treatment \pm D-2-hydroxyglutarate (n=3).

(E) Gene expression analysis of leukotriene synthesis genes (qPCR) in MDM after treatment \pm L-2-hydroxyglutarate (n=7).

(F) Leukotriene C4 synthase activity of MM6 cells after treatment \pm heGDH or TK05 (n=2-15).

Data are pooled from at least two independent experiments and presented as means + SEM. Statistical significance was determined by Friedmann test (B,C), Wilcoxon test (D-E) or ordinary one-way ANOVA (F). *P < 0.05; **P < 0.01; ***P < 0.001.

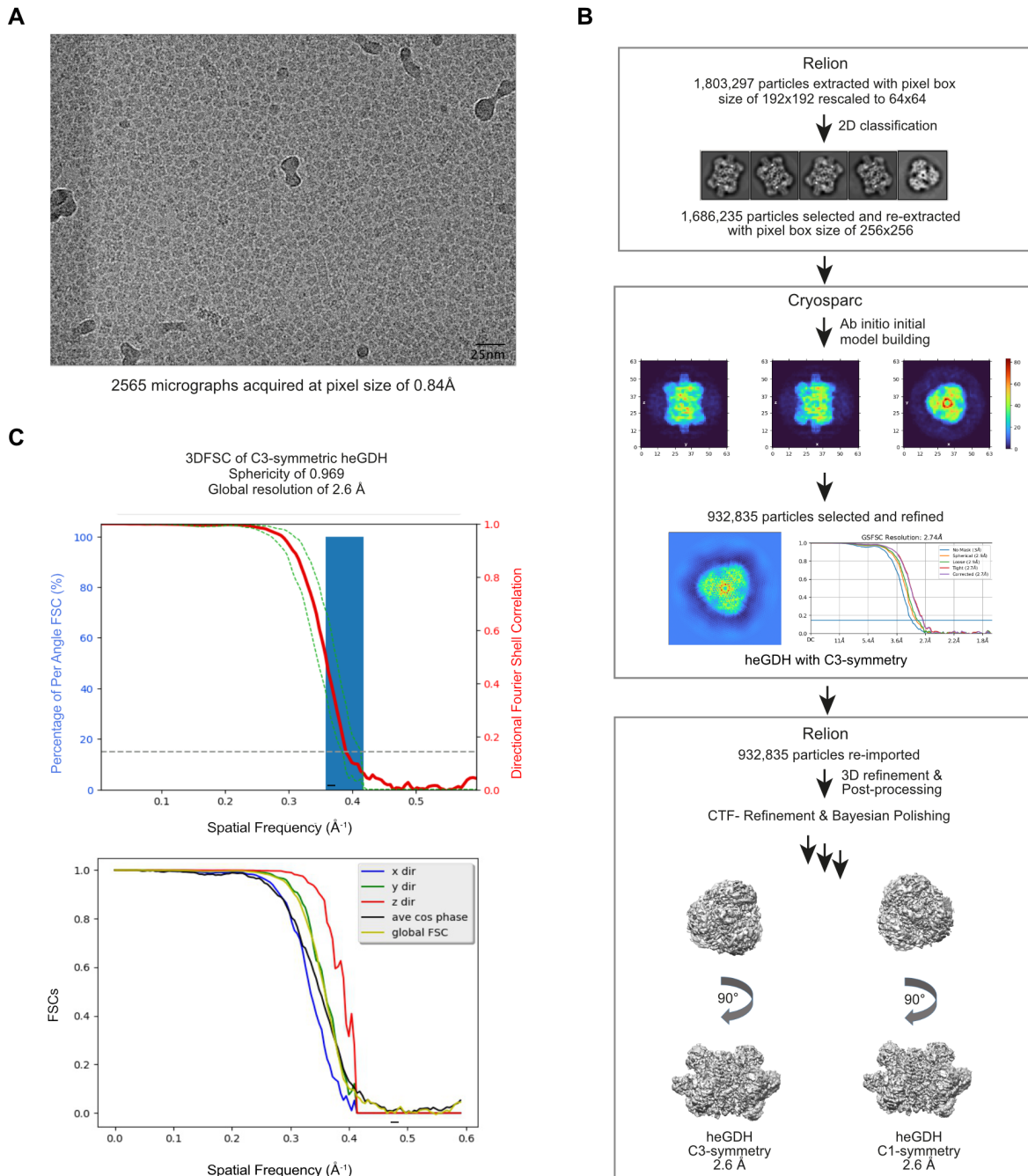
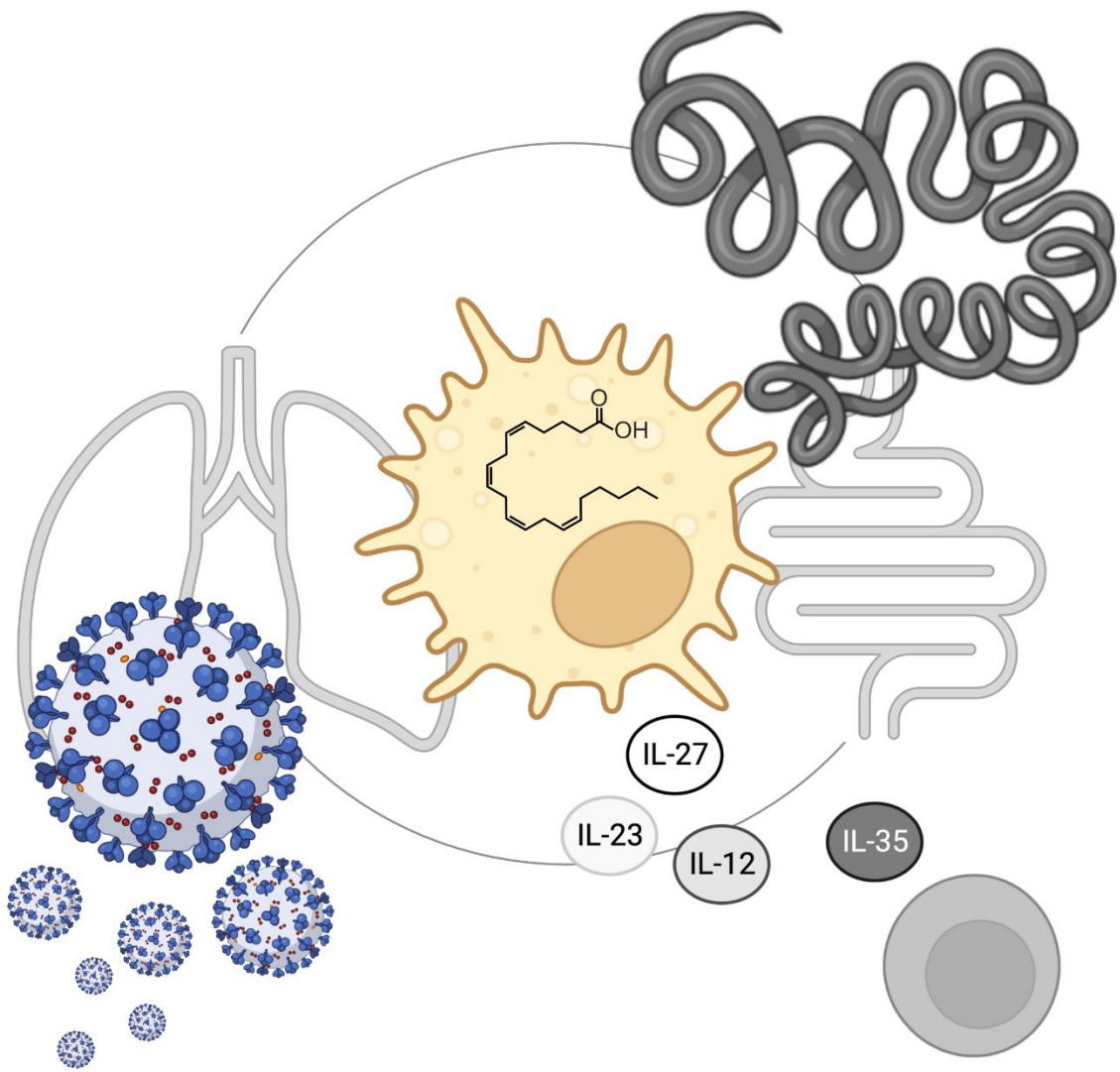


Figure S7: Cryo-EM to determine structure of heGDH

(A) Representantive micrograph of vitrified heGDH (5760x4092 pixel).

(B) cryoEM image processing workflow for heGDH. After 2D-classification in RELION, selected particles were used for ab initio model building, 3D classification and refinement in Cryosparc. Selected particles were re-imported in RELION for CTF-Refinement and Bayesian Polishing for high-resolution refinement.

(C) Plots showing the global (upper) and directional (lower) resolution for heGDH with applied C3 symmetry, calculated using the “Remote 3DFSC Processing Server” web interface (PMID: 28671674).



PUBLICATION II

BRIEF COMMUNICATION OPEN



Mild COVID-19 imprints a long-term inflammatory eicosanoid- and chemokine memory in monocyte-derived macrophages

Sina Bohnacker^{1,14}, Franziska Hartung^{1,14}, Fiona Henkel^{1,14}, Alessandro Quaranta², Johan Kolmert^{2,3}, Alina Priller⁴, Minhaz Ud-Dean⁵, Johanna Giglberger⁶, Luisa M. Kugler⁶, Lisa Pechtold⁶, Sarah Yazici⁴, Antonie Lechner¹, Johanna Erber⁷, Ulrike Protzer^{8,9}, Paul Lingor¹⁰, Percy Knolle^{4,9}, Adam M. Chaker^{1,6}, Carsten B. Schmidt-Weber^{1,11}, Craig E. Wheelock^{2,12,13,15} and Julia Esser-von Bieren^{1,15}

© The Author(s) 2022

Monocyte-derived macrophages (MDM) drive the inflammatory response to severe acute respiratory syndrome coronavirus 2 (SARS-CoV-2) and they are a major source of eicosanoids in airway inflammation. Here we report that MDM from SARS-CoV-2-infected individuals with mild disease show an inflammatory transcriptional and metabolic imprint that lasts for at least 5 months after SARS-CoV-2 infection. MDM from convalescent SARS-CoV-2-infected individuals showed a downregulation of pro-resolving factors and an increased production of pro-inflammatory eicosanoids, particularly 5-lipoxygenase-derived leukotrienes. Leukotriene synthesis was further enhanced by glucocorticoids and remained elevated at 3–5 months, but had returned to baseline at 12 months post SARS-CoV-2 infection. Stimulation with SARS-CoV-2 spike protein or LPS triggered exaggerated prostanoid-, type I IFN-, and chemokine responses in post COVID-19 MDM. Thus, SARS-CoV-2 infection leaves an inflammatory imprint in the monocyte/ macrophage compartment that drives aberrant macrophage effector functions and eicosanoid metabolism, resulting in long-term immune aberrations in patients recovering from mild COVID-19.

Mucosal Immunology; <https://doi.org/10.1038/s41385-021-00482-8>

INTRODUCTION

The Coronavirus disease 2019 (COVID-19) has emerged as a global pandemic caused by severe acute respiratory syndrome coronavirus 2 (SARS-CoV-2) infections¹. Long-term symptoms of COVID-19 are common after severe disease², but may also affect 15–20% of individuals with previous mild disease³. Monocyte-derived macrophages (MDM) drive the inflammatory response to SARS-CoV-2 and contribute to cytokine storms in severe COVID-19^{4,5}. Severe COVID-19 is associated with profound changes in the myeloid compartment, including expansion of dysfunctional, pro-inflammatory monocytes during the first weeks after SARS-CoV-2 infection^{6,7}.

Eicosanoids are bioactive metabolites of polyunsaturated fatty acids (PUFAs) with key roles in infection and inflammation⁸. Eicosanoids are formed from arachidonic acid (AA) through different enzymatic pathways, including the cyclooxygenase (COX) pathway, synthesizing prostanoids and the 5-lipoxygenase (5-LOX) pathway, generating leukotrienes (LTs)⁸. LTs are potent granulocyte-chemotactic metabolites

which cause bronchoconstriction, vascular leakage, and airway remodeling⁹. Resident and recruited macrophages in the lung produce high levels of cysteinyl LTs (cysLTs) and leukotriene B₄ (LTB₄), thereby promoting granulocyte infiltration, airway inflammation and tissue remodeling⁸. Serum and airway prostanoid- and LT levels are increased in severe COVID-19^{10,11}, suggesting a role for eicosanoids in the immune response to SARS-CoV-2 infection.

By studying transcriptome- and lipid mediator profiles in MDM of convalescent SARS-CoV-2-infected individuals with previous mild disease, we show that inflammatory gene expression and eicosanoid profiles as well as altered responsiveness to inflammatory cues are maintained at 3–5 months post infection as well as throughout macrophage differentiation. Pro-inflammatory 5-LOX metabolites were selectively increased in post COVID-19 MDM, suggesting that SARS-CoV-2 infection drives a pro-inflammatory eicosanoid reprogramming that contributes to long-term alterations in innate immune cell function.

¹Center of Allergy and Environment (ZAUM), Technical University of Munich and Helmholtz Center Munich, 80802 Munich, Germany. ²Division of Physiological Chemistry 2, Department of Medical Biochemistry and Biophysics, Karolinska Institute, Stockholm, Sweden. ³The Institute of Environmental Medicine, Karolinska Institute, Stockholm, Sweden. ⁴Institute of Molecular Immunology and Experimental Oncology, University Hospital rechts der Isar, Technical University of Munich (TUM), School of Medicine, 81675 Munich, Germany. ⁵Institute of Computational Biology, Helmholtz Center Munich, 85764 Neuherberg, Germany. ⁶Department of Otorhinolaryngology and Head and Neck Surgery, University Hospital rechts der Isar, Technical University of Munich (TUM), School of Medicine, 81675 Munich, Germany. ⁷Department of Internal Medicine II, University Hospital rechts der Isar, Technical University of Munich (TUM), School of Medicine, 81675 Munich, Germany. ⁸Institute of Virology, Technical University of Munich (TUM), School of Medicine and Helmholtz Zentrum München, 81675 Munich, Germany. ⁹German Center for Infection Research (DZIF), Munich partner site, Munich, Germany. ¹⁰Department of Neurology, University Hospital rechts der Isar, Technical University Munich (TUM), School of Medicine, 81675 Munich, Germany. ¹¹German Center of Lung Research (DZL), Munich partner site, Munich, Germany. ¹²Department of Respiratory Medicine and Allergy, Karolinska University Hospital, 141-86 Stockholm, Sweden. ¹³Gunma Initiative for Advanced Research (GIAR), Gunma University, Maebashi, Japan. ¹⁴These authors contributed equally: Sina Bohnacker, Franziska Hartung, Fiona Henkel. ¹⁵These authors jointly supervised this work: Craig E. Wheelock, Julia Esser-von Bieren. [✉]email: julia.esser@helmholtz-muenchen.de

Received: 13 September 2021 Revised: 18 December 2021 Accepted: 22 December 2021

Published online: 15 March 2022

RESULTS AND DISCUSSION

Recent studies have identified immunological changes in individuals recovering from severe or moderate acute COVID-19 for up to 12 weeks post infection^{6,7,12,13}; however potential immune aberrations in the majority of SARS-CoV-2-infected patients, affected by mild disease, have remained obscure.

Monocyte-derived macrophages of convalescent COVID-19 patients show pro-inflammatory transcriptional reprogramming and enhanced LPS responses

Our recent work had shown that patients suffering from chronic airway inflammation exhibit transcriptional reprogramming of MDM¹⁴, a cell type implicated in COVID-19 pathogenesis⁷. To investigate whether SARS-CoV-2 infection induces persistent changes in MDM gene expression, we studied a sub-cohort from a large SARS-CoV-2 seroprevalence study in healthcare workers¹⁵ (Table S1, Figs. 1a, S1a). To mimic the pulmonary cytokine milieu, in which infiltrating monocytes differentiate into macrophages, MDM were differentiated in the presence of GM-CSF and TGF- β 1^{16,17}, which resulted in a similar MDM population in seronegative and seropositive subjects (Fig. S1b).

At 3–5 months after SARS-CoV-2 infection, antibody levels in the seropositive group had dropped by ~30% and 16.2% (vs. 2.8% in the seronegative group) reported persistent symptoms (Figs. 1a, S1c, Table S1). Differential blood cell counts were similar between seronegative and seropositive individuals (Table S1).

CCL2, which is increased in monocytes during severe, acute disease⁶, was upregulated in post COVID-19 monocytes, suggesting a persistent inflammatory imprint despite mild disease in the investigated cohort (Fig. 1b).

RNA-sequencing (RNAseq) analysis identified 163 differentially expressed genes (DEGs) in MDM differentiated from monocytes of seropositive individuals 3–5 months post infection compared to MDM from seronegative subjects (Fig. 1c, d, Table S1). Post COVID-19 MDM showed higher expression of pro-inflammatory chemokines (*CCL2*, *CCL8*, *CCL7*), driving neutrophil recruitment, including in COVID-19^{18,19} (Fig. 1c, d, Table S1).

FCGBP and endothelin-1 (*EDN1*), implicated in anti-viral defense and pro-fibrotic macrophage activation^{20,21} were also upregulated in post COVID-19 MDM, together with cytochrome B5 reductase 2 (*CYB5R2*), involved in respiratory burst and fatty acid metabolism²² (Fig. 1d). In contrast, Semaphorin-7A (*SEMA7A*), implicated in the synthesis of pro-resolving lipid mediators²³, was downregulated in post COVID-19 MDM (Fig. 1d). Post COVID-19 MDM further showed enhanced inflammatory responses to lipopolysaccharide (LPS), characterized by an exaggerated induction of chemokines involved in neutrophil recruitment^{24,25} (Table S1, Fig. 1e–g). Increased expression of perforin-2 (*MPEG1*) in post COVID-19 MDM at baseline or upon LPS stimulation (Fig. 1d–g) further suggested persistently enhanced interferon (IFN) signaling following SARS-CoV-2 infection²⁶. In contrast, expression of nerve growth factor receptor (*NGFR*), X inactive specific transcript (*XIST*) and *SEMA7A*, mediating anti-inflammatory or pro-resolving effects on macrophages^{23,27,28}, was reduced in LPS-stimulated post COVID-19 MDM (Figs. 1f, g, S1h, Table S1). Thus, despite mild acute disease in the investigated cohort, MDM exhibited a persistent inflammatory imprint, which was associated with increased symptom burdens and aberrant LPS responses at 3–5 months post infection (Figs. S1c, 1e–g).

SARS-CoV-2 S-protein-triggered IFN response is exaggerated in post COVID-19 MDM

To define consequences of SARS-CoV-2-induced macrophage reprogramming for re-infection or vaccination, we investigated the response of post COVID-19 MDM to SARS-CoV-2 spike (S)-protein. Entry of SARS-CoV-2 is mainly mediated via recognition of its transmembrane S-glycoprotein by angiotensin-converting enzyme 2 (*ACE2*) and processing by *TMPRSS2*²⁹. However, *ACE2*

and *TMPRSS2* expression in MDM was 100 times lower compared to airway epithelial cells, the major cellular targets of SARS-CoV-2, regardless of inflammatory stimulation or glucocorticoid treatment (Fig. S1d–f). Yet, macrophages can respond to S-proteins of SARS-CoV-1 or SARS-CoV-2 via innate sensing mechanisms including C-type lectins^{30,31}, which were upregulated in post COVID-19 MDM (Fig. S1g).

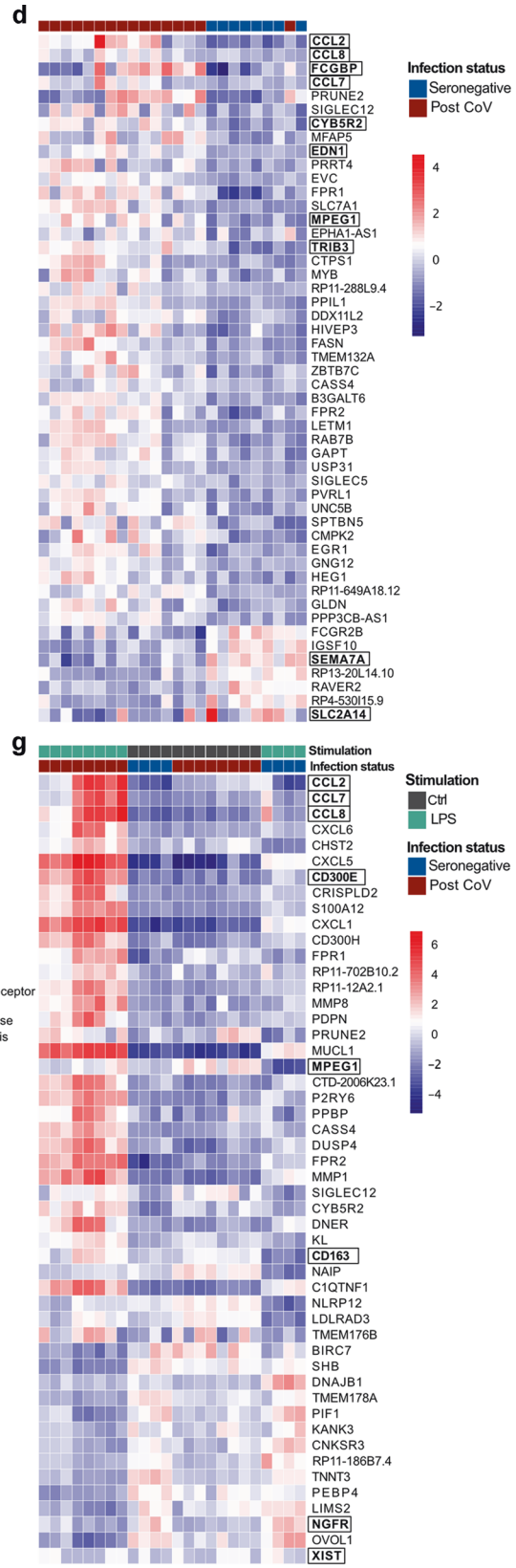
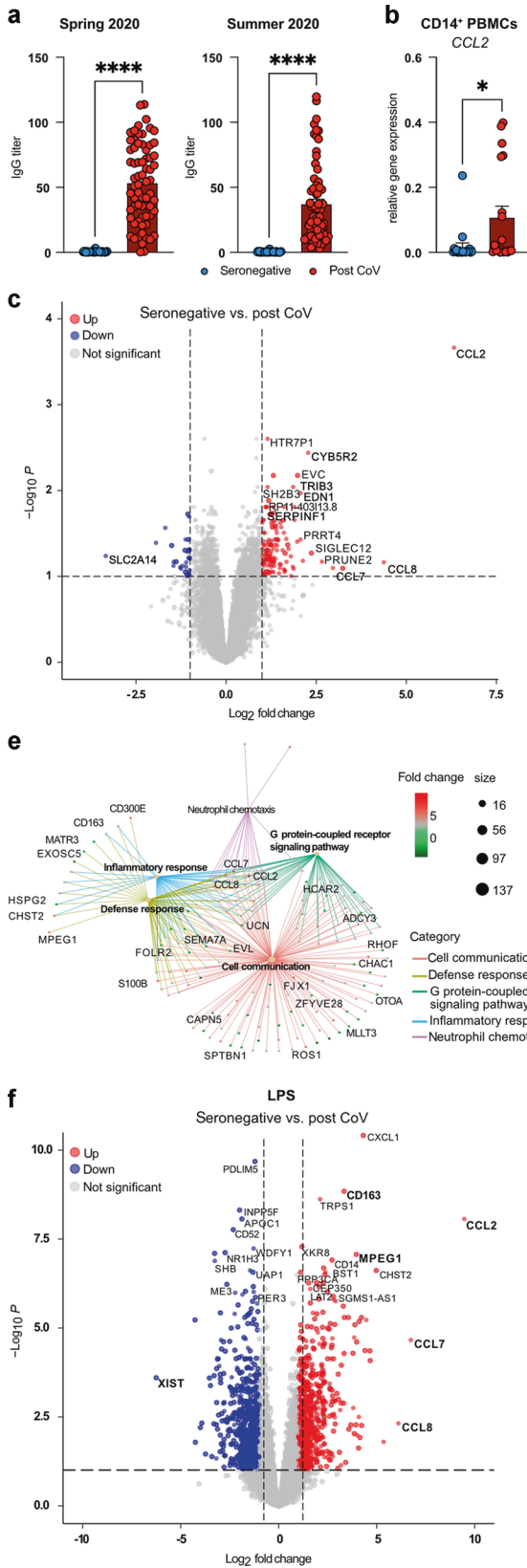
Indeed, MDM readily responded to S-protein and transcriptional differences between seronegative and post COVID-19 MDM were exacerbated by both S-protein and LPS (Fig. 2a). S-protein induced multiple interferon-stimulated genes (ISGs) (e.g. *IFI27*, *IFITM1/3*, *APOBEC3A*, *ISG20*, *MX1/2*, *OAS1/3*) (Fig. 2b, c, Table S1), demonstrating that it induces an antiviral state in MDM. S-protein stimulation of post COVID-19 MDM resulted in a higher number of DEGs compared to seronegative MDM (858 vs. 220), indicative of a persistently enhanced responsiveness to SARS-CoV-2 several months post infection (Table S1).

The induction of IFN-induced genes (e.g. *CXCL10*, *CXCL11*, *MPEG1*) was increased in S-protein-stimulated post COVID-19 MDM (Fig. 2d, e, Table S1), supporting a role for type I IFN signaling in macrophage reprogramming by SARS-CoV-2 infection. MDM from convalescent SARS-CoV-2-infected subjects showed an enhanced LPS- and S-protein-triggered induction of chemokines (*CCL2*, *CCL8*, *CXCL10*, *CXCL11*) and M2-associated genes (*CD226*, *CD163*, *CD209*, *TIMP3*, *MERTK*, *TNIP3*), suggesting a pro-inflammatory, T-cell suppressive^{32,33} MDM phenotype (Figs. 1e–g, 2d, e, Table S1). This was in agreement with the exaggerated S-protein- or LPS-mediated induction of immune regulatory enzymes and receptors, including *ACOD1/IRG1*, *PTGES* and *CD300E* in post COVID-19 MDM (Figs. 1e–g, 2d, e, Table S1)^{32,34,35}.

Thus, previous SARS-CoV-2 infection imprints a pro-inflammatory macrophage phenotype, that mounts exaggerated chemokine- and IFN responses, but likely exhibits impaired T-cell stimulatory and pro-resolving capacities. This was in line with previous studies identifying a dysfunctional, pro-inflammatory monocyte activation for up to 12 weeks after SARS-CoV-2 infection^{7,13} and additionally suggested the long-term persistence of a pro-inflammatory macrophage state following mild disease. Changes in gene expression of post COVID-19 MDM were amplified by inflammatory stimuli, suggesting a “trained” state that lasted for at least 5 months post infection. Mechanistically, this may be driven by IFN-mediated reprogramming as post COVID-19 MDM exhibited an exaggerated upregulation of multiple ISGs, including perforin-2 (*MPEG1*), a driver of type I IFN signaling²⁶.

Post COVID-19 MDM produce increased amounts of inflammatory 5-lipoxygenase metabolites at 3–5 months post SARS-CoV-2 infection

Previous studies had suggested an involvement of pro-inflammatory eicosanoids in severe, acute COVID-19^{10,11,36} and our RNAseq data indicated aberrant expression of genes involved in fatty acid and eicosanoid synthesis in MDM and monocytes of convalescent, SARS-CoV-2 infected individuals (Figs. 1, 2, 3a, b, Table S1). Thus, we performed LC-MS/MS quantification of lipid mediators following stimulation with calcium ionophore to trigger PUFA mobilization and eicosanoid production. Compared to MDM from seronegative individuals, exhibiting considerable production of soluble epoxide hydrolase (sEH) metabolites (11,12-DiHETE, 19,20-DiHDPA, 17,18-DiHETE), post COVID-19 MDM displayed broadly altered eicosanoid profiles that were dominated by pro-inflammatory 5-lipoxygenase (5-LOX) metabolites (Fig. 3c–e). Post COVID-19 MDM synthesized increased amounts of pro-inflammatory 5-LOX metabolites (LTB₄, 5-KETE, 5-HEPE and LTD₄), implicated in granulocyte chemotaxis and airway remodeling (Fig. 3d, e). In addition, the production of pro-inflammatory COX metabolites PGF_{2 α} and 12-HHTrE was increased in post COVID-19 MDM (Fig. 3d, f).



This suggested that the prominent synthesis of inflammatory eicosanoids is not limited to acute and severe COVID-19^{10,11} and that reprogramming of innate immune cells may result in persistently enhanced LT production even following mild disease.

Of note, we did not analyze spontaneous eicosanoid production, but used Ca²⁺ ionophore to elicit maximal eicosanoid responses, which allowed us to quantify lipid mediators in limited numbers of patient cells. Thus, eicosanoid profiles identified in the current

Fig. 1 Pro-inflammatory transcriptional reprogramming and heightened LPS response in post COVID-19 MDM. **a** Serum IgG titers of seronegative ($n = 36$) or SARS-CoV-2 seropositive (post CoV) ($n = 68$) individuals in Spring 2020 or at 3–5 months post infection (p.i.) (Summer 2020). Data are shown as mean + SEM. **b** Expression of *CCL2* in CD14⁺ PBMCs of seronegative ($n = 20$) vs. post CoV ($n = 19$) subjects at 3–5 months p.i. **c** Volcano plot showing DEGs between seronegative ($n = 8$) and post CoV MDM ($n = 16$). Top 10 DEGs (base mean > 50), log₂ FC > 2 or adjusted p value (padj < 0.016 labeled), DEGs with log₂ FC > 1 and padj < 0.1 marked. **d** Heatmap of top 50 DEGs between seronegative ($n = 8$) and post CoV ($n = 16$) MDM, padj < 0.1, log₂ FC > 1; base mean > 50. **e** GSEA between post CoV ($n = 8$) and seronegative ($n = 4$) MDM + LPS, log₂ FC > 2, p value < 0.01. **f** Volcano plot showing DEGs between seronegative ($n = 4$) and post CoV ($n = 8$) MDM + LPS. DEGs with log₂ FC > 3 or padj < 1×10^{-6} labeled, DEGs with log₂ FC > 1 and padj < 0.1 marked. **g** Heatmap of top 50 DEGs between seronegative ($n = 4$) and post CoV ($n = 8$) MDM ± LPS, padj < 0.1, log₂ FC > 1, base mean > 50. Statistical significance was determined by Mann–Whitney test (**a, b**) or DESeq2 (**c–f**). * $p < 0.05$; ** $p < 0.01$; *** $p < 0.001$; **** $p < 0.0001$.

study reflect a setting of acute inflammatory challenge. MDM of convalescent subjects also revealed a marked lower inferred soluble epoxide hydrolase activity. The epoxides of arachidonic acid have been reported to promote the resolution of inflammation, including mitigation of cytokine storms³⁷. Accordingly, inhibition of the sEH has been proposed as a potential therapeutic target for COVID-19³⁸. Our findings suggest that subsequent to mild COVID-19, MDM may exhibit a compensatory sEH activity that is shifted towards a pro-resolution state. In contrast to acute infection, which resulted in increased *ALOX5* expression in neutrophils and monocytes¹⁰, we did not find evidence of increased 5-LOX pathway gene expression in post COVID-19 MDM (Fig. 3g). Instead, genes involved in upstream events of fatty acid and lipid mediator biosynthesis (e.g., *FASN*, *DGAT2*, *PLA2G4C*) were upregulated in post COVID-19 MDM compared to MDM from seronegative subjects, suggesting an MDM phenotype in position for rapid activation of lipid metabolic pathways.

Analysis of MDM eicosanoid profiles from donors of the same cohort at 12 months post infection indicated that LT and prostanoid synthesis of post COVID-19 MDM had largely returned to baseline levels at this time point (Fig. 3h, i). This suggested that pro-inflammatory eicosanoid reprogramming in mild COVID-19 is transient, but that it may contribute to an enhanced inflammatory propensity during the first months post SARS-CoV-2 infection.

When stratified into 5-LOX low- or high producers, post COVID-19 subjects with high MDM LT production exhibited less acute symptoms but a faster decline in SARS-CoV-2 specific IgG titers (Fig. 3j), indicative of an efficient acute anti-viral response³⁹. However, the lack of a defined clinical diagnosis of long COVID and poor reporting of long-term symptoms in the studied post COVID-19 cohort, prevented us from establishing a clear link between high MDM LT production and long-term symptoms of SARS-CoV-2 infection. Thus, future studies should investigate eicosanoid reprogramming in a cohort with clinically defined long COVID. Such studies would be imperative to define a potential pathological relevance of the inflammatory macrophage memory observed in the current study.

As patients in our study were enrolled following seroconversion, we were not able to compare monocyte and macrophage profiles at 3–5 months post infection to those during acute disease. However, we observed a considerable overlap between transcriptional profiles of post COVID-19 MDM and published transcriptomes of macrophages from SARS-CoV-2-infected individuals with mild acute disease⁴⁰. Thus, several of the DEGs identified in our analysis (*MPEG1*, *CD163*, *CXCL9*, *MERTK*, and *MRC1*) were increased and correlated with higher expression of 5-LOX pathway genes in mild vs. severe acute disease⁴⁰. It will be important to compare macrophage reprogramming between convalescent COVID-19 patients with different disease severities as well as following infection with other respiratory viruses (e.g., influenza). While previous studies have suggested an acute and transient increase in eicosanoids during respiratory syncytial virus (RSV) or influenza A virus (IAV) infection^{41–43}, a comprehensive assessment of macrophage eicosanoid profiles in these diseases is currently lacking. PGE₂ production was increased following IAV infection, however we did not observe increased PGE₂ production in post

COVID-19 MDM. Similarly, transcriptional profiles of post COVID-19 MDM showed minimal overlap with post influenza macrophage gene expression profiles^{44,45}, suggesting that infection with different respiratory viruses results in distinct macrophage reprogramming. Increased macrophage LTB₄ production may however contribute to protective immunity during acute infection with multiple respiratory viruses^{41,43}. It will be important to determine, whether the persistent increase of LTB₄ may contribute to a decreased susceptibility to respiratory viral infection during the first months following SARS-CoV-2 infection.

As airway inflammation, including in COVID-19, is commonly treated by glucocorticoids, we investigated potential effects of glucocorticoids on LT synthesis by post COVID-19 MDM. Fluticasone propionate, a commonly used inhaled glucocorticoid, further increased LT synthesis by post COVID-19 at baseline or after stimulation with house dust mite (HDM), used as a ubiquitous trigger of airway inflammation (Fig. S2a–d). This suggested that glucocorticoid treatment may further aggravate the pro-inflammatory eicosanoid reprogramming in post COVID-19 subjects. Given the therapeutic efficacy of glucocorticoids in airway inflammation, the finding that glucocorticoids enhanced LT synthesis may be surprising. However, it is in keeping with studies showing no reduction in LTs following glucocorticoid treatment in humans or enhanced LT production following in vitro treatment with glucocorticoids^{46–48}.

S-protein-triggered prostanoid response is enhanced in post COVID-19 MDM

To assess potential differences in eicosanoid production capacities under inflammatory conditions, we compared Ca²⁺ ionophore-elicited eicosanoid production in post COVID-19 and seronegative MDM stimulated for 24 h with S-protein or LPS. S-protein stimulation profoundly altered eicosanoid profiles (Fig. 4a, b), provoking a prominent induction of prostanoids from the thromboxane pathway (TXB₂ and 12-HHTrE), while 5-LOX metabolites were reduced (Fig. 4b).

Compared to seronegative MDM, post COVID-19 MDM exhibited enhanced S-protein-induced prostanoid production, which was particularly evident for the thromboxane synthesis metabolite 12-HHTrE (Fig. 4b, c). Similarly, the cytochrome P450 metabolite 19-HETE was significantly increased in S-protein-stimulated post COVID-19, indicative of increased S-protein-mediated induction of vasoactive eicosanoids at 3–5 months post infection. In contrast at 12 months post infection, S-protein-triggered eicosanoid responses did not differ between SARS-CoV-2 seronegative and seropositive subjects (Fig. 4d). Compared to S-protein, LPS induced a stronger eicosanoid shift, thus overriding aberrant lipid mediator synthesis of post COVID-19 MDM (Fig. S3a, b). While upregulating prostanoids, LPS reduced the heightened production of LTD₄ in post COVID-19 MDM (Fig. S3c), in line with suppressive effects of 24 h LPS stimulation on LT production by alveolar macrophages⁴⁹. Together, this suggested that eicosanoid responses remain increased for several months following SARS-CoV-2 infection. In addition, during challenge with LPS or S-protein, eicosanoid profiles switch towards prostanoids with tissue reparative, vasoconstrictor and immune regulatory functions,

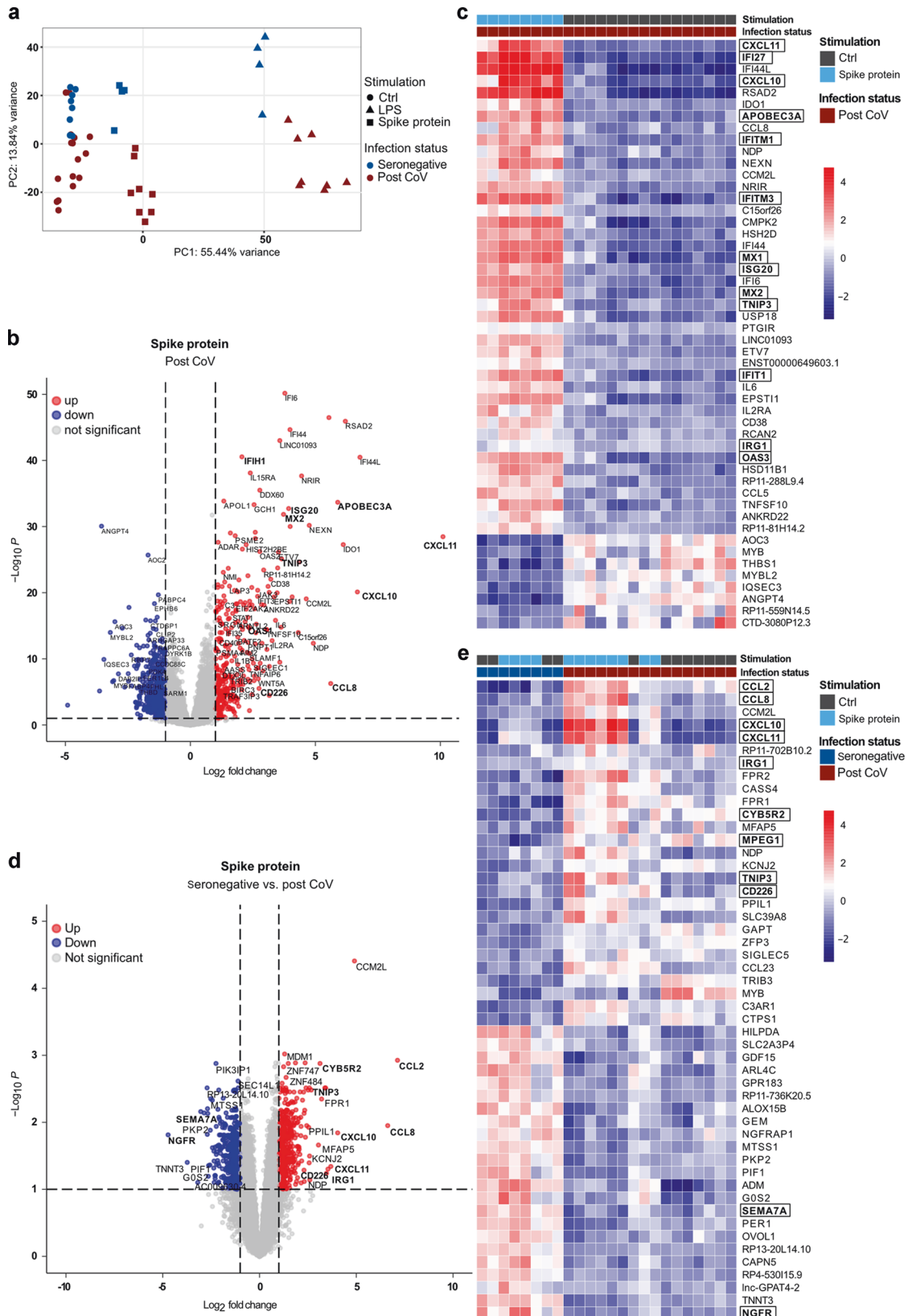
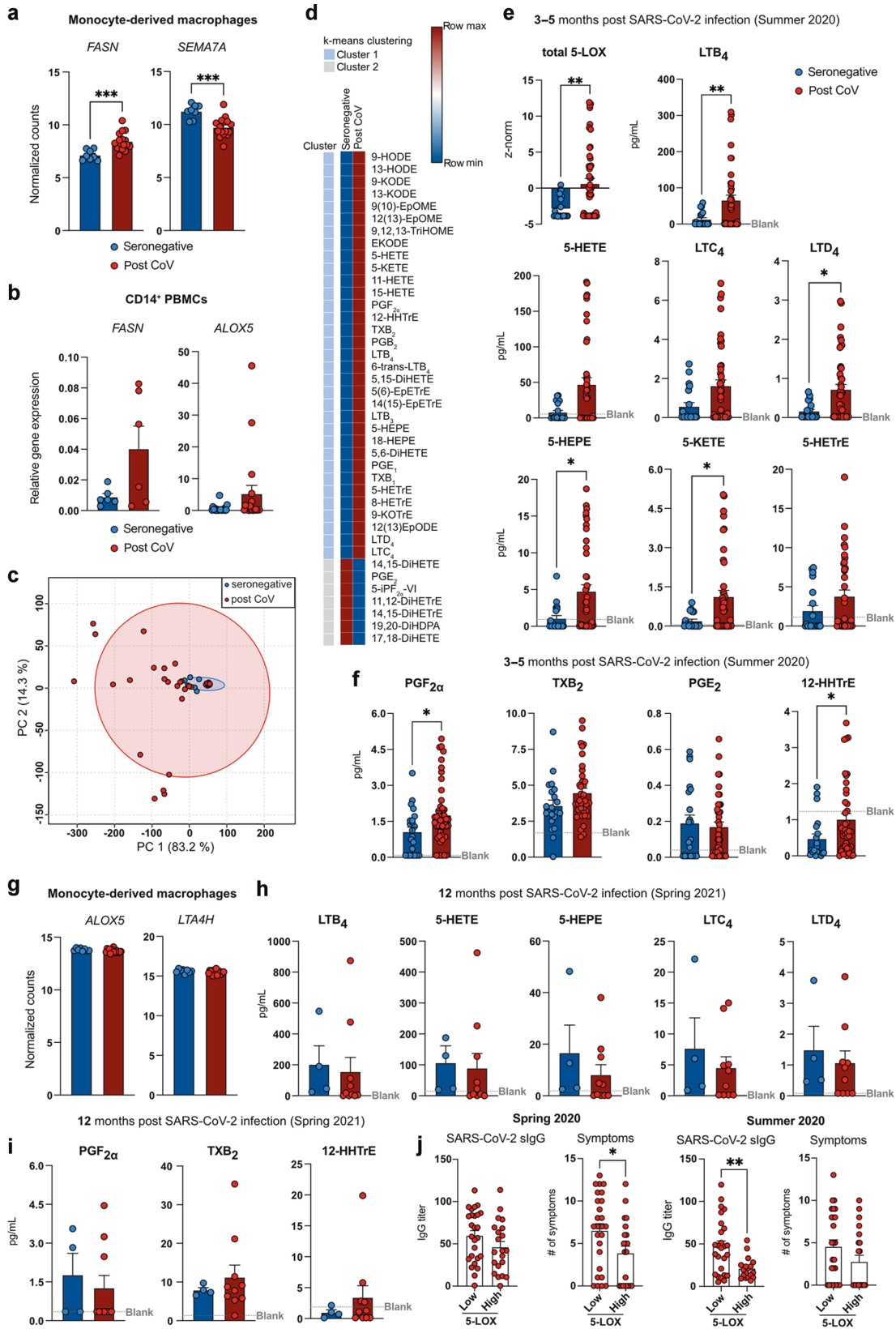


Fig. 2 S-protein-induced type I IFN and chemokine responses are exaggerated in post COVID-19 MDM. **a** PCA of RNAseq datasets (baseline, S-protein, LPS) for seronegative ($n = 4-8$) or post CoV ($n = 8-16$) MDM. **b** Volcano plot of DEGs for post CoV MDM ($n = 8$) \pm S-protein. DEGs with $\log_2 FC > 5$ and $\text{padj} < 0.00001$ (DESeq2) are labeled, DEGs with $\log_2 FC > 1$ and $\text{padj} < 0.1$ are colored. **c** Heatmap of top 50 DEGs in post CoV MDM ($n = 8-16$) \pm S-protein, $\text{padj} < 0.1$, $\log_2 FC > 1$, base mean > 50 . **d** Volcano plot of DEGs of S-protein-stimulated MDM from seronegative ($n = 4$) vs. post-CoV ($n = 8$) donors. DEGs with $\log_2 FC > 2.5$ and $\text{padj} < 0.003$ are labeled, DEGs with $\log_2 FC > 1$ and $\text{padj} < 0.1$ are colored. **e** Heatmap of top 50 DEGs of MDM \pm S-protein from seronegative ($n = 4$) or seropositive ($n = 8$) donors, $\text{padj} < 0.1$, $\log_2 FC > 1$, base mean > 50 .



potentially promoting repair of inflammation-induced tissue damage.

In contrast to eicosanoid profiles, cytokine production at baseline or following stimulation was not significantly different

between post COVID-19 and seronegative MDM (Fig. S2e–h), suggesting that cytokine aberrations may not persist for >12 weeks or during monocyte-macrophage differentiation. However, in contrast to LTs, cytokine and prostanoid production by MDM

Fig. 3 Post COVID-19 MDM produce increased amounts of inflammatory 5-lipoxygenase metabolites. **a** *FASN* and *SEMA7A* expression in seronegative ($n = 8$) and post CoV MDM ($n = 16$). **b** Gene expression of *FASN* and *ALOX5* in seronegative ($n = 6/20$) or post CoV ($n = 6/19$) CD14⁺ PBMCs. **c** PCA of lipid mediator profiles of MDM from seronegative ($n = 22$) or seropositive ($n = 47$) individuals. Red and blue circles: 95% CI. **d** Heatmap of lipid mediators produced by seronegative ($n = 22$) or post CoV ($n = 47$) MDM (LC-MS/MS). Clustering: with k-means using Pearson correlation. Data is shown as mean. **e** Sum of z-scored arachidonic acid derived 5-LOX metabolite concentrations for each donor. Levels of major 5-LOX (**e, h**) and COX (**f, i**) metabolites produced by MDM at 3–5 (**e, f**) or 12 (**h, i**) months p.i. (LC-MS/MS) shown as mean + SEM of $n = 22/n = 4$ seronegative or $n = 47/n = 10$ seropositive individuals. **g** Expression of *ALOX5* and *LTA4H* (RNAseq) in MDM from seronegative ($n = 8$) or post CoV ($n = 16$) individuals. **j** IgG titers in serum or number of symptoms in MDM from post CoV donors stratified into 5-LOX low (z-score < 1) and high producers (z-score > 1). Bar graphs are depicted as mean + SEM. Statistical significance was determined by Mann–Whitney test. * $p < 0.05$; ** $p < 0.01$; *** $p < 0.001$.

was efficiently suppressed by fluticasone propionate (Fig. S2a–d, i). This suggested that cytokines and prostanoids are efficiently targeted, while exaggerated LT responses of post COVID-19 MDM are further exacerbated by glucocorticoids. Indeed, thromboxane is a major eicosanoid produced by inflammatory macrophages and involved in vascular and airway remodeling, thus its inhibition by glucocorticoids may provide a therapeutic benefit. However, glucocorticoids may in turn further enhance the heightened production of pro-inflammatory LTs by post COVID-19 MDM, thus promoting LT-driven airway inflammation and remodeling. Based on the enhanced production of 5-LOX-derived lipid mediators both in acute^{10,11} and post-acute COVID-19 (this study), approved LT pathway inhibitors should be considered as regimens to treat and/ or prevent airway inflammation and remodeling during the first 6 months following SARS-CoV-2 infection.

Future studies should further decipher upstream receptors and epigenetic pathways that drive the persistent pro-inflammatory macrophage and eicosanoid reprogramming during SARS-CoV-2 infection. In addition, a potential heterogeneity in GM-CSF and TGF- β 1-differentiated MDM from seronegative and seropositive individuals should be addressed in single cell analyses. LTs have been reported to induce CCL2 in monocytes^{50,51}, suggesting that enhanced LT synthesis may drive exaggerated pro-inflammatory chemokine responses in post COVID-19 MDM. In turn, increased CCL2 production by post COVID-19 MDM or monocytes may promote LTB₄ production⁵². Thus, our combined RNAseq and LC-MS/MS data suggest a crosstalk between CCL2 and LTs, which perpetuates the persistent pro-inflammatory activation of monocytes and macrophages following SARS-CoV-2 infection. Due to limitations in patient material, we could not perform a comprehensive comparison of MDM and monocytes, however our data suggest that differences in CCL2 and fatty acid synthesis are at least partially present in undifferentiated post COVID-19 monocytes, which differentiate into inflammatory monocyte-derived macrophages when entering the lung⁵. The persistent upregulation of pro-inflammatory eicosanoids in post COVID-19 macrophages may have multiple consequences for subsequent immune responses, e.g. during bacterial or viral infection or in patients suffering from chronic inflammatory diseases such as asthma, thus requiring future investigation.

METHODS

Study design

Symptoms of seronegative (SARS-CoV-2 seronegative) and post COVID-19 (SARS-CoV-2 seropositive) individuals were determined through a questionnaire in Spring 2020 and 3–5 months later, in Summer 2020. Percentage of each symptom was calculated separately for seropositive and -negative individuals (table S1). Sample sizes for each experiment are specified in the corresponding figure legends; an overview is depicted in Fig. S1a. All blood donors participated in the study after informed written consent. All procedures were approved by the local ethics committee at the University clinic of the Technical University of Munich (internal references: 216/20S, 263/21S) and in accordance with the declaration of Helsinki.

Monocyte-derived macrophage culture

Isolated peripheral blood mononuclear cells (PBMCs) of post COVID-19 or seronegative individuals were used to generate monocyte-derived macrophages (MDM), as previously reported^{53,54}. MDM were cultured in the presence of 10 ng/mL human GM-CSF (Miltenyi Biotec, Bergisch-Gladbach, Germany) and 2 ng/mL human TGF- β (Peprotech, Hamburg, Germany). After 7 days incubation, cells were harvested and stimulated for 24 h with 100 ng/mL LPS (Invivogen, San Diego, CA, USA), 20 nM spike protein (antibodies-online GmbH), 10 μ g/mL house dust mite extract (HDM) (Citeq Biologics, Groningen, The Netherlands), 1 μ M fluticasone propionate (FP) (Sigma-Aldrich, St. Louis, MO, USA), 5 μ M or 100 nM dexamethasone (DXM) (Sigma-Aldrich, Merck). After 24 h of stimulation cells were harvested in presence of Ca²⁺-ionophore A23187 (Sigma-Aldrich, Merck).

NHBE and ALI culture

Primary normal human bronchial epithelial cells (NHBEs) (Lonza, Basel, Switzerland) from non-smokers in passage 3 were grown to 80–90% confluency in Bronchial Epithelial Cell Growth Medium (BEGM) (Lonza). Following starvation overnight in bronchial epithelial basal medium (BEBM) (Lonza), NHBEs were stimulated for 24 h with 1 μ g/mL HDM (Citeq) or 1 μ M FP (Sigma-Aldrich, Merck). For air-liquid interface (ALI) cultures, NHBEs were split at 60–80% confluency and 1×10^5 cells were seeded on 12 mm transwells (0.4 μ m pores, Stemcell Technologies, Vancouver, Canada). Cultures were maintained in BEGM (500 μ L apical and 1000 μ L basal) until cells reached full confluency. Subsequently, cells were “airlifted” by removing the apical medium, and basal medium was replaced with PneumaCult-ALI Maintenance Medium (Stemcell Technologies). Medium was replaced every 2 days and excessive mucus washed away with DPBS (Gibco). Cells were cultured at air liquid interface for 3–4 weeks. Before stimulation, cells were starved overnight in PneumaCult-ALI Basal Medium (Stemcell Technologies). ALI cells were stimulated on the apical side with 1 μ g/mL HDM (Citeq), 1 μ M FP (Sigma-Aldrich) or corresponding control for 24 h.

Histology

For histology ALI cells were fixed in 4% formaldehyde and embedded in paraffin. Sections were cut and hematoxylin & eosin (H&E) stained at the Klinikum rechts der Isar, Dermatology Department.

RNA isolation

Cells were lysed in RLT buffer (Qiagen, Hilden, Germany) supplemented with 1% β -mercaptoethanol. RNA was extracted using a spin-column kit according to the manufacturer’s instructions (Zymo Research, Freiburg, Germany) and transcribed into DNA using the HighCapacity cDNA Reverse Transcription kit according to the manufacturer’s instructions (Applied Biosystems) or submitted for total RNA sequencing.

RNA sequencing

Library preparation was performed using the TruSeq Stranded mRNA Library Prep Kit (Illumina, San Diego, CA, USA). Briefly, RNA was isolated from MDM cell lysates according to the

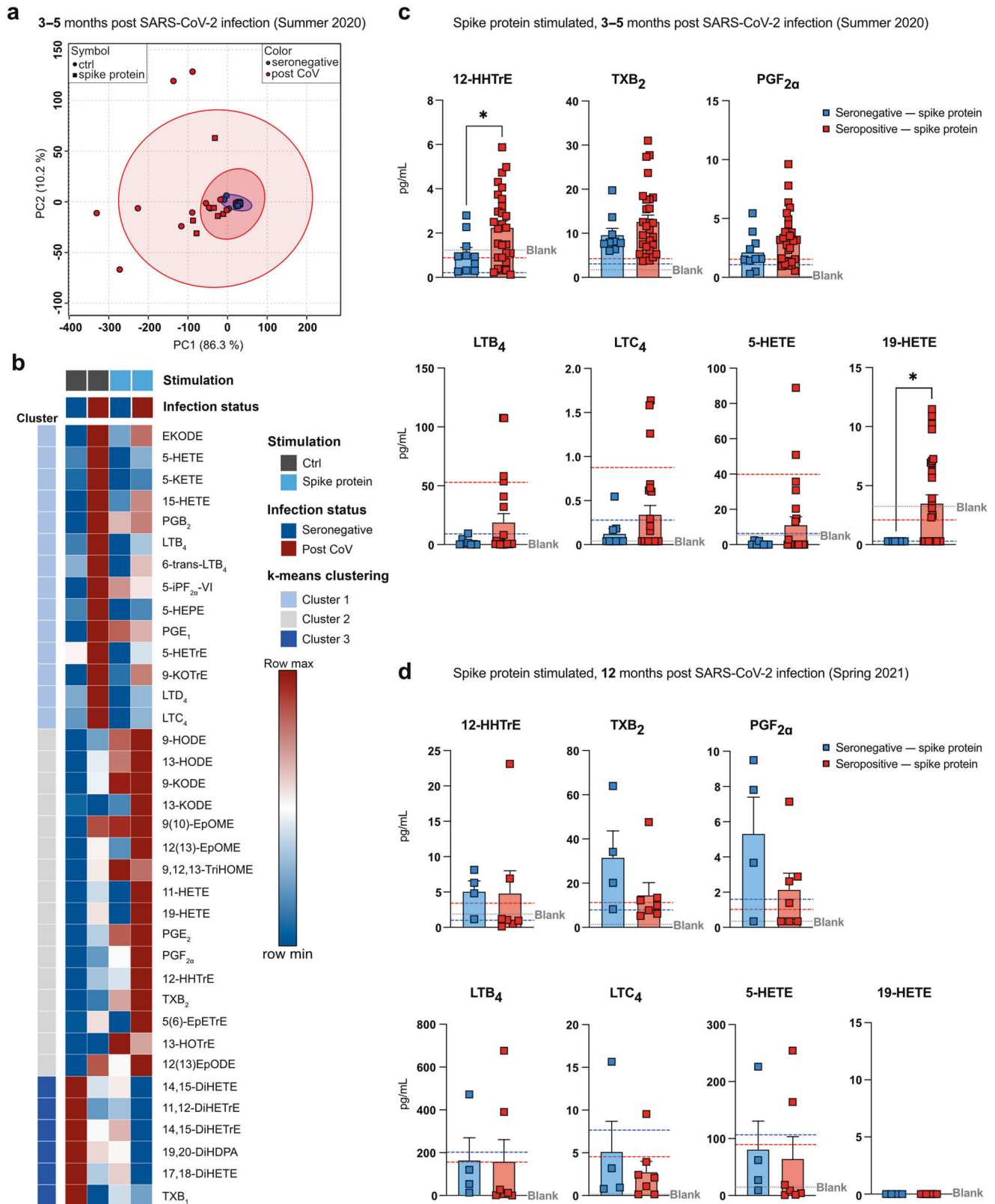


Fig. 4 Increased S-protein-triggered prostanoid response in post COVID-19 MDM. **a** PCA of lipid mediators quantified in seronegative ($n = 10$) or post CoV ($n = 29$) MDM \pm S-protein. Red and blue circles: 95% CI (LC-MS/MS at 3–5 months p.i.). **b** Heatmap of lipid mediators produced by MDM (seronegative/ post CoV) \pm S-protein; clustered with k-means using Pearson correlation. Data are shown as mean of seronegative ($n = 10$) or post CoV ($n = 29$) MDM. Concentrations of 12-HHTrE, TXB₂, PGF_{2 α} and 19-HETE/ 5-HETE produced by MDM + S-protein, at 3–5 months (**c**) or 12 months (**d**) p.i.; **d** $n = 4$ (seronegative); $n = 7$ (post CoV). Dashed lines indicate average ctrl level of either seronegative (blue) or seropositive (red) MDM. Bar graphs are depicted as mean \pm SEM. Statistical significance was determined by Mann–Whitney test. $*p < 0.05$.

manufacturer's instructions (Zymo Research). Total RNA quality and quantity was assessed by Qubit 4 Fluorometer (Invitrogen) and RNA integrity number (RIN) was determined with the Agilent 2100 BioAnalyzer (RNA 6000 Nano Kit, Agilent).

For library preparation, 1 µg of RNA was poly(A) selected, fragmented, and reverse transcribed with the Elute, Prime, Fragment Mix (Illumina). A-tailing, adaptor ligation, and library enrichment were performed as described in the TruSeq Stranded mRNA Sample Prep Guide (Illumina). RNA libraries were assessed for quality and quantity with the Agilent 2100 BioAnalyzer and the Quant-iT PicoGreen dsDNA Assay Kit (Life Technologies, Thermo Fisher Scientific). RNA libraries were sequenced as 150 bp paired-end runs on an Illumina NovaSeq 6000 platform. Sequencing was performed at the Helmholtz Zentrum München (HMGU) by the Genomics Core Facility.

Cytokine analysis (ELISA)

Cell culture supernatants were analyzed for IL-6, IL-1β and IL-8 secretion using the human ELISA Sets (BD Biosciences, Franklin Lakes, NJ, USA) according to the manufacturer's instructions.

Lipid mediator quantification

Briefly, cell supernatants from 200,000 cells, stored in equal volume of methanol, were extracted using solid phase extraction (Evolute Express ABN, Biotage, Uppsala, Sweden) and lipid mediators (see Table S1) were quantified by liquid chromatography coupled to tandem mass spectrometry (LC-MS/MS)⁵⁵. Given that cell culture media has significant background levels of many lipid mediators, compounds whose concentration was below the media level were excluded from data analysis.

Real-time quantitative PCR

10 ng cDNA was used as a template. The list of applied primers (4 µmol/L, Metabion international AG, Planegg, Germany) can be found in the Supplement. FastStart Universal SYBR Green Master Mix (Roche, Basel, Switzerland) was used and fluorescence was measured on a ViiA7™ Real-Time PCR System (Applied Biosystems, Thermo Fisher Scientific). The expression levels were normalized to the house-keeping genes GAPDH (for MDM), ACTB, HPRT1 and TFRC (average for NHBEs and ALI cultured cells). Relative gene expression was calculated as $2^{-\Delta\Delta C_T}$ ($\Delta C_T = C_T(\text{Housekeeper}) - C_T(\text{Gene})$). For genes where expression could not be quantified, CT values were set to 40.

Data analysis and statistics

LC-MS/MS and RNAseq data were analyzed using previously published procedures^{14,48,55,56}. Details can be found in the Supplement.

REFERENCES

- Wang, C., Horby, P. W., Hayden, F. G. & Gao, G. F. A novel coronavirus outbreak of global health concern. *Lancet* **395**, 470–473 (2020).
- Huang, C. et al. 6-month consequences of COVID-19 in patients discharged from hospital: a cohort study. *Lancet* **397**, 220–232 (2021).
- Havervall, S. et al. Symptoms and functional impairment assessed 8 months after mild COVID-19 among Health care workers. *JAMA* <https://doi.org/10.1001/jama.2021.5612> (2021).
- Liao, M. et al. Single-cell landscape of bronchoalveolar immune cells in patients with COVID-19. *Nat. Med.* **26**, 842–844 (2020).
- Merad, M. & Martin, J. C. Pathological inflammation in patients with COVID-19: a key role for monocytes and macrophages. *Nat. Rev. Immunol.* **20**, 355–362 (2020).
- Schulte-Schrepping, J. et al. Severe COVID-19 is marked by a dysregulated myeloid. *Cell Compartment. Cell* **182**, 1419–1440.e23 (2020).
- Szabo, P. A. et al. Longitudinal profiling of respiratory and systemic immune responses reveals myeloid cell-driven lung inflammation in severe COVID-19. *Immunity* **54**, 797–814.e6. (2021).
- Esser-von Bieren, J. Immune-regulation and -functions of eicosanoid lipid mediators. *Biol. Chem.* **398**, 1177–1191 (2017).

- Weiss, J. et al. Bronchoconstrictor effects of leukotriene C in humans. *Science* **216**, 196–198 (1982).
- Schwarz, B. et al. Cutting edge: severe SARS-CoV-2 infection in humans is defined by a shift in the serum lipidome, resulting in dysregulation of eicosanoid immune mediators. *J. Immunol.* **206**, 329–334 (2021).
- Archambault, A.-S. et al. High levels of eicosanoids and docosanoids in the lungs of intubated COVID-19 patients. *FASEB J.* **35**, e21666 (2021).
- Nalbandian, A. et al. Post-acute COVID-19 syndrome. *Nat. Med.* <https://doi.org/10.1038/s41591-021-01283-z> (2021).
- You, M. et al. Single-cell epigenomic landscape of peripheral immune cells reveals establishment of trained immunity in individuals convalescing from COVID-19. *Nat. Cell Biol.* **23**, 620–630 (2021).
- Haimerl, P. et al. Inflammatory macrophage memory in nonsteroidal anti-inflammatory drug-exacerbated respiratory disease. *J. Allergy Clin. Immunol.* **147**, 587–599 (2021).
- Erber, J. et al. *Strategies for infection control and prevalence of anti-SARS-CoV-2 IgG in 4,554 employees of a university hospital in Munich, Germany.* <https://doi.org/10.1101/2020.10.04.20206136> (2020).
- Schneider, C. et al. Induction of the nuclear receptor PPAR-γ by the cytokine GM-CSF is critical for the differentiation of fetal monocytes into alveolar macrophages. *Nat. Immunol.* **15**, 1026–1037 (2014).
- Yu, X. et al. The cytokine TGF-β promotes the development and homeostasis of alveolar macrophages. *Immunity* **47**, 903–912.e4 (2017).
- Chua, R. L. et al. COVID-19 severity correlates with airway epithelium-immune cell interactions identified by single-cell analysis. *Nat. Biotechnol.* **38**, 970–979 (2020).
- Williams, A. E. et al. Evidence for chemokine synergy during neutrophil migration in ARDS. *Thorax* **72**, 66–73 (2017).
- Alvarez, D. et al. A novel role of endothelin-1 in linking Toll-like receptor 7-mediated inflammation to fibrosis in congenital heart block. *J. Biol. Chem.* **286**, 30444–30454 (2011).
- Schwartz, J. L. Fcγbp – A Potential Viral Trap in RV144. *Open AIDS J.* **8**, 21–24 (2014).
- Zhu, H., Qiu, H., Yoon, H.-W. P., Huang, S. & Bunn, H. F. Identification of a cytochrome b-type NAD(P)H oxidoreductase ubiquitously expressed in human cells. *Proc. Natl Acad. Sci.* **96**, 14742–14747 (1999).
- Körner, A. et al. Sema7A is crucial for resolution of severe inflammation. *Proc. Natl. Acad. Sci. USA*, **118**, e2017527118 (2021).
- Talbot, J. et al. CCR2 expression in neutrophils plays a critical role in their migration into the joints in rheumatoid arthritis. *Arthritis Rheumatol.* **67**, 1751–1759 (2015).
- Johnston, B. et al. Chronic inflammation upregulates chemokine receptors and induces neutrophil migration to monocyte chemoattractant protein-1. *J. Clin. Invest* **103**, 1269–1276 (1999).
- McCormack, R., Hunte, R., Podack, E. R., Plano, G. V. & Shembade, N. An essential role for perforin-2 in type I IFN signaling. *J. Immunol.* **204**, 2242–2256 (2020).
- Flügel, A. et al. Anti-inflammatory activity of nerve growth factor in experimental autoimmune encephalomyelitis: inhibition of monocyte transendothelial migration. *Eur. J. Immunol.* **31**, 11–22 (2001).
- Shenoda, B. B. et al. Xist attenuates acute inflammatory response by female cells. *Cell Mol. Life Sci.* **78**, 299–316 (2021).
- Lan, J. et al. Structure of the SARS-CoV-2 spike receptor-binding domain bound to the ACE2 receptor. *Nature* **581**, 215–220 (2020).
- Amraie, R. et al. CD209L/L-SIGN and CD209/DC-SIGN act as receptors for SARS-CoV-2 and are differentially expressed in lung and kidney epithelial and endothelial cells. *bioRxiv* <https://doi.org/10.1101/2020.06.22.165803> (2020).
- Jeffers, S. A. et al. CD209L (L-SIGN) is a receptor for severe acute respiratory syndrome coronavirus. *Proc. Natl Acad. Sci. USA* **101**, 15748–15753 (2004).
- Coletta, S. et al. The immune receptor CD300e negatively regulates T cell activation by impairing the STAT1-dependent antigen presentation. *Sci. Rep.* **10**, 16501 (2020).
- Han, Q., Shi, H. & Liu, F. CD163(+) M2-type tumor-associated macrophage support the suppression of tumor-infiltrating T cells in osteosarcoma. *Int Immunopharmacol.* **34**, 101–106 (2016).
- Jaiswal, A. K. et al. Irg1/itaconate metabolic pathway is a crucial determinant of dendritic cells immune-priming function and contributes to resolute allergen-induced airway inflammation. *Mucosal. Immunol.* <https://doi.org/10.1038/s41385-021-00462-y> (2021).
- Coulombe, F. et al. Targeted prostaglandin E2 inhibition enhances antiviral immunity through induction of type I interferon and apoptosis in macrophages. *Immunity* **40**, 554–568 (2014).
- Zaid, Y. et al. Chemokines and eicosanoids fuel the hyperinflammation within the lungs of patients with severe COVID-19. *J. Allergy Clin. Immunol.* **S0091-6749**, 00893–00899 (2021).
- Panigrahy, D. et al. Inflammation resolution: a dual-pronged approach to averting cytokine storms in COVID-19? *Cancer Metastasis Rev.* **39**, 337–340 (2020).

38. Hammock, B. D., Wang, W., Gilligan, M. M. & Panigrahy, D. Eicosanoids: the overlooked storm in coronavirus disease 2019 (COVID-19)? *Am. J. Pathol.* **190**, 1782–1788 (2020).
39. Long, Q.-X. et al. Clinical and immunological assessment of asymptomatic SARS-CoV-2 infections. *Nat. Med.* **26**, 1200–1204 (2020).
40. Wauters, E. et al. Discriminating mild from critical COVID-19 by innate and adaptive immune single-cell profiling of bronchoalveolar lavages. *Cell Res.* **31**, 272–290 (2021).
41. Shirey, K. A. et al. Role of the lipoxygenase pathway in RSV-induced alternatively activated macrophages leading to resolution of lung pathology. *Mucosal Immunol.* **7**, 549–557 (2014).
42. Bartz, H., Büning-Pfaue, F., Türkler, O. & Schauer, U. Respiratory syncytial virus induces prostaglandin E₂, IL-10 and IL-11 generation in antigen presenting cells. *Clin. Exp. Immunol.* **129**, 438–445 (2002).
43. Pernet, E., Downey, J., Vinh, D. C., Powell, W. S. & Divangahi, M. Leukotriene B₄-type I interferon axis regulates macrophage-mediated disease tolerance to influenza infection. *Nat. Microbiol.* **4**, 1389–1400 (2019).
44. Aegerter, H. et al. Influenza-induced monocyte-derived alveolar macrophages confer prolonged antibacterial protection. *Nat. Immunol.* **21**, 145–157 (2020).
45. Yao, Y. et al. Induction of autonomous memory alveolar macrophages requires T cell help and is critical to trained immunity. *Cell* **175**, 1634–1650.e17 (2018).
46. Riddick, C. A., Ring, W. L., Baker, J. R., Hodulik, C. R. & Bigby, T. D. Dexamethasone increases expression of 5-lipoxygenase and its activating protein in human monocytes and THP-1 cells. *Eur. J. Biochem.* **246**, 112–118 (1997).
47. Manso, G., Baker, A. J., Taylor, I. K. & Fuller, R. W. In vivo and in vitro effects of glucocorticosteroids on arachidonic acid metabolism and monocyte function in nonasthmatic humans. *Eur. Respir. J.* **5**, 712–716 (1992).
48. Kolmert, J. et al. Urinary leukotriene E₄ and prostaglandin D₂ metabolites increase in adult and childhood severe asthma characterized by type 2 inflammation. A clinical observational study. *Am. J. Respir. Crit. Care Med.* **203**, 37–53 (2021).
49. Coffey, M. J., Phare, S. M. & Peters-Golden, M. Prolonged exposure to lipopolysaccharide inhibits macrophage 5-lipoxygenase metabolism via induction of nitric oxide synthesis. *J. Immunol.* **165**, 3592–3598 (2000).
50. Huang, L. et al. Leukotriene B₄ strongly increases monocyte chemoattractant protein-1 in human monocytes. *Arterioscler. Thromb. Vasc. Biol.* **24**, 1783–1788 (2004).
51. Ichiyama, T. et al. Cysteinyl leukotrienes induce monocyte chemoattractant protein 1 in human monocytes/macrophages. *Clin. Exp. Allergy* **35**, 1214–1219 (2005).
52. Pacheco, P. et al. Monocyte chemoattractant protein-1/CC chemokine ligand 2 controls microtubule-driven biogenesis and leukotriene B₄-synthesizing function of macrophage lipid bodies elicited by innate immune response. *J. Immunol.* **179**, 8500–8508 (2007).
53. Dietz, K. et al. Age dictates a steroid-resistant cascade of Wnt5a, transglutaminase 2, and leukotrienes in inflamed airways. *J. Allergy Clin. Immunol.* **139**, 1343–1354.e6 (2017).
54. Esser-von Bieren, J. et al. Antibodies trap tissue migrating helminth larvae and prevent tissue damage by driving IL-4Ra-independent alternative differentiation of macrophages. *PLoS Pathog.* **9**, e1003771 (2013).
55. Kolmert, J. et al. Lipid mediator quantification in isolated human and guinea pig airways: an expanded approach for respiratory research. *Anal. Chem.* **90**, 10239–10248 (2018).
56. Henkel, F. D. R. et al. House dust mite drives proinflammatory eicosanoid reprogramming and macrophage effector functions. *Allergy* **74**, 1090–1101 (2019).

ACKNOWLEDGEMENTS

We would like to thank members of the SeCoMRI study group, Sonja Schindela and staff of the histology laboratory of the Dermatology Department, Klinikum rechts der Isar and of the Helmholtz Center Munich Genomics platform for technical support.

AUTHOR CONTRIBUTIONS

Conceptualization: J.E.v.B., C.E.W., C.B.S.W., A.M.C., P.K., P.L., U.P. Methodology: A.Q., J.K., C.E.W., M.U.D. Investigation: S.B., F.D.H., F.H., A.Q., J.H., A.L., A.P., S.Y., J.E. Visualization: S.B., F.D.H., F.H., M.U.D. Funding acquisition: J.E.v.B., C.E.W. Project administration: J.E.v.B., A.M.C., P.K., U.P., P.L. Supervision: J.E.v.B., A.M.C., P.K. Writing—original draft: J.E.v.B., S.B., F.D.H., F.H. Writing—review & editing: C.E.W., C.B.S.W., A.L., A.M.C., A.P., P.K., P.L.

FUNDING

This study was supported by the German Research Foundation (DFG) (FOR2599, ES 471/3-1; ES 471/2-3), a Helmholtz Young Investigator grant (VH-NG-1331) to J.E.v.B. and grants by the Swedish Heart Lung Foundation HLF 20210519, HLF 20200693 to C.E.W., the German University Medicine network NUM via project B-FAST, the For-COVID consortium funded by the state of Bavaria and the Project “Virological and immunological determinants of COVID-19 pathogenesis – lessons to get prepared for future pandemics (KA1-Co-02 “COVIPA””, a grant from the Helmholtz Association’s Initiative and Networking Fund to UP and PK. C.S.-W. receives grant support by the German Center for Lung Research (DZL; 82DZL00302). Open Access funding enabled and organized by Projekt DEAL.

COMPETING INTERESTS

C. B. S.-W. received grant support from Allergopharma, PLS Design, as well as Zeller AG; and received speaker honoraria from Allergopharma. U. Protzer is co-funder, board member and share holder of SCG Cell Therapy Inc. and serves as ad hoc advisor for Sanofi-Pasteur, BioNTech, Janssen and Swedish Orphan Biovitrum concerning COVID-19. The rest of the authors declare that they have no relevant conflicts of interest related to this work.

ADDITIONAL INFORMATION

Supplementary information The online version contains supplementary material available at <https://doi.org/10.1038/s41385-021-00482-8>.

Correspondence and requests for materials should be addressed to Julia Esser-von Bieren.

Reprints and permission information is available at <http://www.nature.com/reprints>

Publisher’s note Springer Nature remains neutral with regard to jurisdictional claims in published maps and institutional affiliations.



Open Access This article is licensed under a Creative Commons Attribution 4.0 International License, which permits use, sharing, adaptation, distribution and reproduction in any medium or format, as long as you give appropriate credit to the original author(s) and the source, provide a link to the Creative Commons licence, and indicate if changes were made. The images or other third party material in this article are included in the article’s Creative Commons licence, unless indicated otherwise in a credit line to the material. If material is not included in the article’s Creative Commons licence and your intended use is not permitted by statutory regulation or exceeds the permitted use, you will need to obtain permission directly from the copyright holder. To view a copy of this licence, visit <http://creativecommons.org/licenses/by/4.0/>.

© The Author(s) 2022

SPRINGER NATURE

Mild COVID-19 imprints a long-term inflammatory eicosanoid- and chemokine memory in monocyte-derived macrophages

Author: Sina Bohnacker et al

Publication: Mucosal Immunology

Publisher: Springer Nature

Date: Mar 15, 2022

Copyright © 2022, The Author(s)

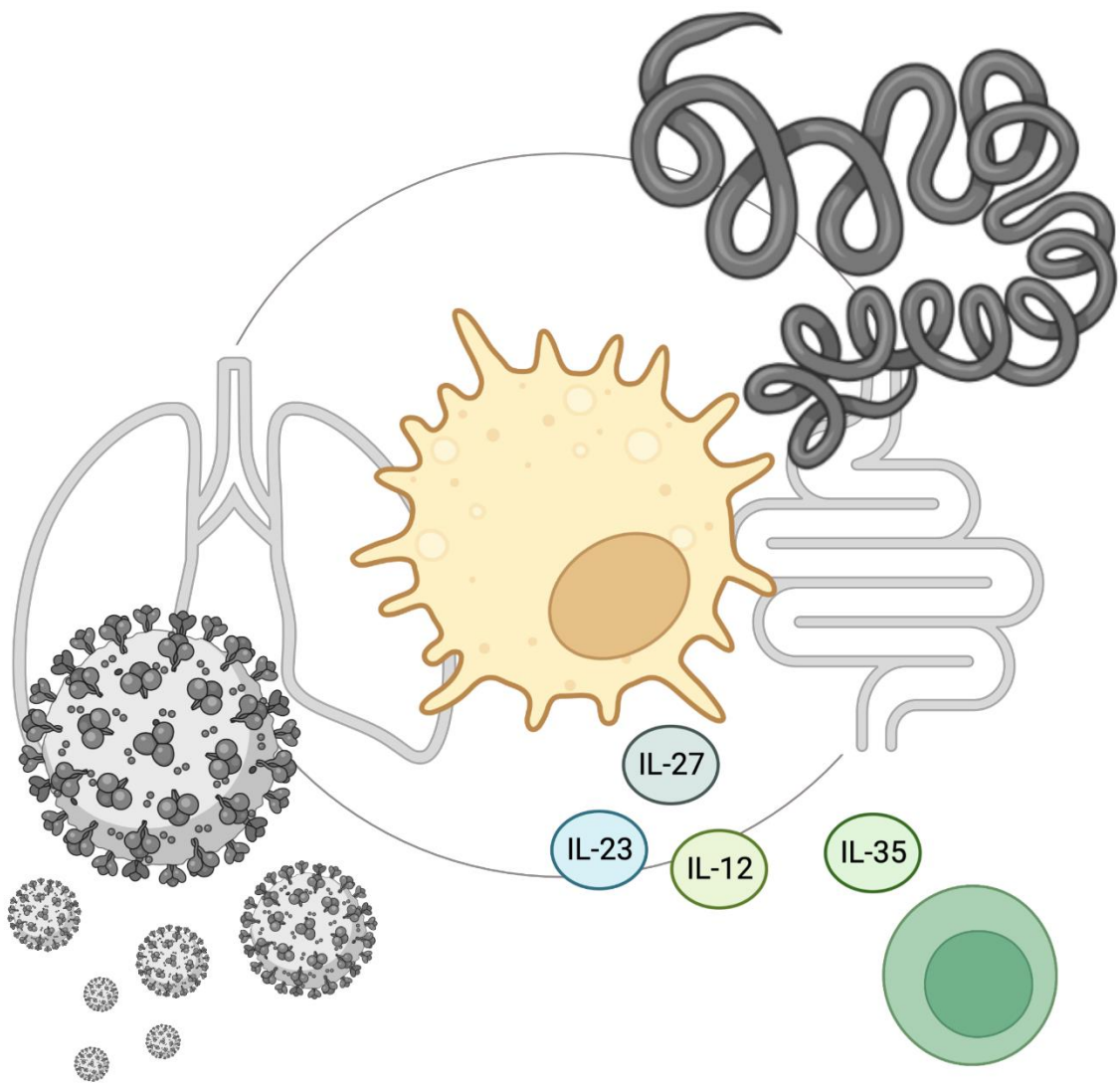
Creative Commons

This is an open access article distributed under the terms of the [Creative Commons CC BY](#) license, which permits unrestricted use, distribution, and reproduction in any medium, provided the original work is properly cited.

You are not required to obtain permission to reuse this article.

To request permission for a type of use not listed, please contact [Springer Nature](#)

<https://www.nature.com/nature-portfolio/reprints-and-permissions/permissions-requests#Author%20reuse>



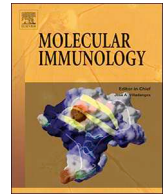
PUBLICATION III



ELSEVIER

Contents lists available at ScienceDirect

Molecular Immunology

journal homepage: www.elsevier.com/locate/molimm

Short communication

Influence of glycosylation on IL-12 family cytokine biogenesis and function

Sina Bohnacker^{a,b,1}, Karen Hildenbrand^{a,1}, Isabel Aschenbrenner^{a,1}, Stephanie I. Müller^a,
Julia Esser-von Bieren^{b,**}, Matthias J. Feige^{a,*}

^a Department of Chemistry and Institute for Advanced Study, Technical University of Munich, 85748, Garching, Germany

^b Center of Allergy & Environment (ZAUM), Technical University of Munich and Helmholtz Zentrum München, 80802, Munich, Germany

ARTICLE INFO

Keywords:

interleukins
protein glycosylation
protein assembly
protein secretion
immune signaling

ABSTRACT

The interleukin 12 (IL-12) family of cytokines regulates T cell functions and is key for the orchestration of immune responses. Each heterodimeric IL-12 family member is a glycoprotein. However, the impact of glycosylation on biogenesis and function of the different family members has remained incompletely defined.

Here, we identify glycosylation sites within human IL-12 family subunits that become modified upon secretion. Building on these insights, we show that glycosylation is dispensable for secretion of human IL-12 family cytokines except for IL-35. Furthermore, our data show that glycosylation differentially influences IL-12 family cytokine functionality, with IL-27 being most strongly affected.

Taken together, our study provides a comprehensive analysis of how glycosylation affects biogenesis and function of a key human cytokine family and provides the basis for selectively modulating their secretion via targeting glycosylation.

1. Introduction

Interleukins (ILs) are secreted proteins that regulate immune cell function. Among the more than 60 ILs known to date (Akdis et al., 2016), the interleukin 12 (IL-12) family is functionally and structurally particularly complex (Tait Wojno et al., 2019; Vignali and Kuchroo, 2012). Each of its family members is a heterodimer composed of an α - and a β -subunit with extensive subunit sharing occurring in the family: IL-12 consists of IL-12 α and IL-12 β (Gubler et al., 1991; Kobayashi et al., 1989; Stern et al., 1990; Wolf et al., 1991), the latter is shared with IL-23 where IL-12 β pairs with IL-23 α (Oppmann et al., 2000). Likewise, EB13 is the β -subunit for IL-27, where it pairs with IL-27 α (Pflanz et al., 2002), but also for IL-35, where it assembles with IL-12 α (Collison et al., 2007; Devergne et al., 1997). This structural complexity goes hand in hand with the broad functional spectrum of the IL-12 family. All family members are produced by antigen presenting cells and regulate T cell functions, thus connecting innate and adaptive immunity, except for IL-35, which is mainly produced by regulatory T and B cells (Tait Wojno et al., 2019; Vignali and Kuchroo, 2012). IL-12 family cytokines span a broad range of pro-inflammatory, immuno-regulatory and anti-inflammatory functions and are involved in diseases

from infection via autoimmunity to cancer (Croxford et al., 2012; Sawant et al., 2015; Teng et al., 2015; Trinchieri et al., 2003; Yoshida and Hunter, 2015). The structural complexity and functional repertoire of the family are extended even further by the fact that also isolated IL-12 family subunits can be secreted and act as regulatory molecules in the immune system (Dambuza et al., 2017; Espigol-Frigole et al., 2016; Garbers et al., 2013; Gately et al., 1996; Lee et al., 2015; Ling et al., 1995; Muller et al., 2019b; Stumhofer et al., 2010).

Like other secreted mammalian proteins, IL-12 family cytokines are produced in the endoplasmic reticulum (ER). There, they also obtain their native structure and assemble into heterodimeric complexes before being transported further along the secretory pathway towards the cell surface for secretion. Most secreted proteins acquire post-translational modifications in the ER, with disulfide bond formation between cysteines and glycosylation of Asn residues being the most prevalent ones (Braakman and Bulleid, 2011). IL-12 family cytokines are no exception to this rule: human IL-12 α , IL-12 β , and EB13 are N-glycosylated and each subunit except IL-27 α contains at least one intramolecular disulfide bond. Additionally, IL-12 and IL-23 are disulfide-linked heterodimers (Carra et al., 2000; Devergne et al., 1996; Lupardus and Garcia, 2008; Oppmann et al., 2000; Pflanz et al., 2002; Podlaski et al.,

* Corresponding author at: Technical University of Munich, Department of Chemistry, Lichtenbergstr. 4, 85748 Garching, Germany.

** Corresponding author at: Center of Allergy & Environment (ZAUM), Technical University of Munich and Helmholtz Zentrum München, Biedersteiner Str. 29, 80802, Munich, Germany.

E-mail addresses: julia.esser@tum.de (J.E.-v. Bieren), matthias.feige@tum.de (M.J. Feige).

¹ These authors contributed equally to this work.

1992; Yoon et al., 2000). For all human IL-12 family α -subunits it was shown that oxidative folding is a key step in their biogenesis and functional roles have been delineated for intra- and intermolecular IL-12 family cytokine disulfide bonds (Jones et al., 2012; Meier et al., 2019; Muller et al., 2019a; Muller et al., 2019b; Reitberger et al., 2017; Yoon et al., 2000). In contrast, the role of glycosylation in IL-12 family biogenesis and function remains incompletely defined. Several studies indicate that glycosylation of IL-12, on its α - and on its β -subunit, is dispensable for IL-12 secretion and function *per se* – but modulates IL-12 activity (Aparicio-Siegmund et al., 2014; Carra et al., 2000; Ha et al., 2002; Podlaski et al., 1992). No comprehensive analyses are available for IL-23, IL-27 or IL-35 yet in this regard. In this study, we thus systematically investigated the effect of *N*- and *O*-glycosylation, the latter occurring in the Golgi, on IL-12 family cytokine biogenesis and function.

2. Materials and Methods

2.1. Constructs

Human interleukin cDNAs (Origene) were cloned into the pSVL vector (Amersham BioSciences) for mammalian expression. Mutants were generated by site-directed mutagenesis. All constructs were sequenced.

2.2. Sequence analysis, structural modeling and structural analyses

N-glycosylation sites were predicted by the NetNGlyc 1.0 Server (<http://www.cbs.dtu.dk/services/NetNGlyc/>) and *O*-glycosylation sites were assessed by the NetOGlyc 4.0 Server (<http://www.cbs.dtu.dk/services/NetOGlyc/>) (Steenfot et al., 2013). Both servers evaluate the potential of glycosylation by using a threshold. Sequence alignments were performed with Clustal Omega (Sievers et al., 2011). Structures were taken from the PDB database (3D87, 3HMX) and missing loops were modeled using Yasara Structure (www.yasara.org) with a subsequent steepest descent energy minimization. The homology-modeled structure of IL-27 was used (Muller et al., 2019a). Structures were depicted with PyMOL (PyMOL Molecular Graphics System, Version 2.0 Schrödinger, LLC).

2.3. Cell culture and transient transfections

Human embryonic kidney (HEK) 293T cells were cultured in Dulbecco's modified Eagle's medium (DMEM) containing L-Ala-L-Gln (AQmedia, Sigma Aldrich), supplemented with 10% (v/v) fetal bovine serum (FBS; Gibco, ThermoFisher) and 1% (v/v) antibiotic-antimycotic solution (25 μ g/ml amphotericin B, 10 mg/ml streptomycin, and 10,000 units of penicillin; Sigma-Aldrich) at 37 °C and 5% CO₂. Transient transfections were carried out in poly D-lysine coated p35 dishes (VWR), or uncoated p60 dishes (VWR) for the functionality assays, using GeneCellin (Eurobio) according to the manufacturer's protocol. A total DNA amount of 2 μ g (p35) or 4 μ g (p60) was used. The α -subunit DNA was co-transfected with the β -subunit DNA or empty pSVL vector in equal amounts (IL-27), in a ratio of 1:2 (IL-23) or 2:1 (IL-12, IL-35) for secretion and de-glycosylation experiments. BL-2 cells were cultured in RPMI-1640 medium with L-Gln and sodium bicarbonate (Sigma-Aldrich), supplemented with 20% (v/v) heat-inactivated FBS (Gibco, ThermoFisher) and 1% (v/v) antibiotic-antimycotic solution (25 μ g/ml amphotericin B, 10 mg/ml streptomycin, and 10,000 units of penicillin; Sigma-Aldrich) at 37 °C and 5% CO₂.

2.4. Immunoblotting experiments

For secretion and de-glycosylation experiments, cells were transfected for 8 h and then supplemented with fresh medium for another 16 h. To analyze secreted proteins, the medium was centrifuged (5 min,

300xg, 4 °C), transferred to a new reaction tube and supplemented with 0.1 volumes 500 mM Tris/HCl, pH 7.5, 1.5 M NaCl, complemented with 10x Roche complete Protease Inhibitor w/o EDTA (Roche Diagnostics). Cells were lysed after washing twice with ice-cold PBS. Cell lysis was carried out in RIPA buffer (50 mM Tris/HCl, pH 7.5, 150 mM NaCl, 1% Nonidet P40 substitute, 0.5% DOC, 0.1% SDS, 1x Roche complete Protease Inhibitor w/o EDTA; Roche Diagnostics) on ice. Both lysate and medium samples were centrifuged (15 min, 15,000xg, 4 °C). Samples were de-glycosylated with PNGase F (SERVA) or a mix of *O*-Glycosidase and α 2-2,6,8 Neuraminidase (New England Biolabs) according to the manufacturer's protocol. For SDS-PAGE, samples were supplemented with 0.2 volumes of 5x Laemmli buffer (0.3125 M Tris/HCl, pH 6.8, 10% SDS, 50% glycerol, bromphenol blue) containing 10% (v/v) β -mercaptoethanol (β -Me). For immunoblots, samples were run on 12% SDS-PAGE gels and transferred to polyvinylidene difluoride (PVDF) membranes by blotting overnight (o/n) at 30 V (4 °C). After blocking the membrane with Tris-buffered saline (25 mM Tris/HCl, pH 7.5, 150 mM NaCl; TBS) containing 5% (w/v) skim milk powder and 0.05% (v/v) Tween-20 (M-TBST), binding of the primary antibody was carried out o/n at 4 °C with anti-Hsc70 (Santa Cruz, sc-7298, 1:1,000), anti-IL-12 β (abcam ab133752, 1:500), anti-IL-12 α (abcam ab133751, 1:500), anti-IL-23 α (BioLegend 511202, 1:500), anti-IL-27 α (R&D Systems, Bio-Techne, 1:200) in M-TBST containing 0.002% Na₃ or anti-EBI3 antiserum (Devergne et al., 2001) (1:20) in PBS. Species-specific HRP-conjugated secondary antibodies (Santa Cruz Biotechnology; 1:10,000 in M-TBST or 1:5,000 for IL-23 α in M-TBST) were used to detect the proteins. Amersham ECL prime (GE Healthcare) and a Fusion Pulse 6 imager (Vilber Lourmat) were used for detection.

2.5. Functionality assays

The **IL-12 activity assay** was performed following a previously published protocol (Reitberger et al., 2017). CD14-negative PMBCs were thawed and resuspended in RPMI-1640 (Thermo Fisher Scientific) supplemented with 10% heat-inactivated FBS (GE Healthcare) and 100 μ g/ml streptomycin, 1 μ g/ml gentamicin, 100 units/ml penicillin, and 2 mM L-glutamine (Thermo Fisher Scientific). Cells were seeded at a density of 5×10^5 cells/ml and stimulated with the supernatants of transfected HEK293T cells expressing the IL-12 constructs for 24 h at 37 °C and 5% CO₂. After harvesting (2 min, 1,000xg, 4 °C), cells were washed once with PBS prior to lysis in RLT buffer (Qiagen) supplemented with 1% β -Me. Total RNA was isolated (QuickRNATM Micro-Prep, Zymo Research) and cDNA (High-Capacity cDNA Reverse Transcription Kit, Thermo Fisher Scientific) was synthesized following the instructions of the manufacturer's protocol. Real-time PCR was performed using a Viia 7 Real-Time PCR System (Applied Biosystems, Thermo Fisher Scientific) and the FastStart Universal SYBR Green Master Mix (Roche). Transcript levels were normalized to actin (ACTB forward, 5'-GGATGCAGAAGGAGATCACT-3'; ACTB reverse, 5'-CGATC CACACGGAGTACTTG-3'; IFN γ forward, 5'-TCAGCCATCACTTGAT GAG-3'; IFN γ reverse, 5'-CGAGATGACTTCGAAAAGCTG-3').

For the **IL-23 activity test**, CD14-negative PMBCs were thawed in RPMI-1640 (Thermo Fisher Scientific) and 300,000 cells were resuspended in 100 μ l RPMI-1640 supplemented with 5% human serum (Sigma Aldrich), 1% non-essential amino acids, 100 μ g/ml streptomycin, 100 units/ml penicillin, 1 mM sodium pyruvate, and 2 mM L-glutamine (Thermo Fisher Scientific). The cells were stimulated with HEK293T supernatants containing 100 ng/ml secreted IL-23 constructs, previously quantified *via* immunoblotting with the help of recombinant IL-23 (R&D), and 10 μ g/ml Phytohemagglutinin-L (Sigma Aldrich) for 72 h at 37 °C and 5% CO₂. After harvesting (2 min, 1,000xg, 4 °C), supernatants were analyzed for IL-17 secretion using human IL-17 DuoSet ELISA (R&D Systems), according to the manufacturer's protocol.

For IL-12 and IL-23, a **receptor activation assay** was performed using IL-12 or IL-23 iLite[®] reporter cells (Svar Life Science AB), respectively, according to the supplier's instructions. The cells were

stimulated with HEK293T supernatants containing 10 ng/ml secreted IL-12 or IL-23 constructs, previously quantified via immunoblotting by comparing immunoblot signals to those of recombinant IL-12 or IL-23 with known concentrations (R&D Systems). The firefly and renilla luminescence signals were detected via the Dual-Glo Luciferase Assay System (Promega) in a multimode microplate reader (CLARIOstar Plus, BMG LABTECH).

To determine IL-27 activity dependent on its glycosylation pattern, BL-2 cells were stimulated with IL-27 protein, derived from transiently transfected HEK293T, secreted into the medium. Protein amounts of the IL-27 variants used in this functionality assay were determined by quantification via immunoblotting with anti-IL-27 α antibody (R&D Systems, Bio-Techne, 1:200) relative to the wild-type protein signal prior to stimulation. BL-2 cells were starved o/n in serum-free RPMI-1640 and seeded into uncoated 48-well plates (Sigma-Aldrich) resuspended in RPMI-1640 supplemented with 0.5% (w/v) bovine serum albumin (BSA; Sigma A3294) at a cell number of 1×10^6 cells/well. Subsequently, cells were stimulated for one hour with IL-27 protein or control supernatant (mock) and the reaction was stopped by adding ice-cold PBS. Cells were transferred to reaction tubes, centrifuged (5 min, 300xg, 4 °C) and lysed with NP-40 lysis buffer (50 mM Tris/HCl, pH 7.5, 150 mM NaCl, 0.5% NP40, 0.5% DOC) supplemented with 1x Roche complete Protease Inhibitor w/o EDTA (Roche Diagnostics) and 1x Phosphatase Inhibitor (SERVA). The supernatant (5 min, 20,000xg, 4 °C centrifugation) was complemented with 0.2 volumes 5x Laemmli buffer containing 10% (v/v) β -Me and loaded on 12% SDS-PAGE gels. After blotting o/n, membranes were washed with TBS, blocked with TBS containing 5% (w/v) skim milk powder and 0.1% (v/v) Tween-20 for one hour, washed again with TBS with 0.1% Tween-20 and incubated in the primary antibody (α -STAT1 or α -STAT1-P, Cell Signaling Technology, 1:1,000 in TBS with 5% (w/v) BSA, 0.1% Tween-20) o/n. Anti-rabbit HRP-conjugated antibody (Santa Cruz Biotechnology; 1:10,000 in 5% (w/v) skim milk powder and 0.1% (v/v) Tween-20 in TBS) was used for subsequent detection.

2.6. Quantification and statistics

Immunoblots were quantified using the Bio-1D software (Vilber Lourmat). Statistical analyses were performed using Prism (GraphPad Software). Differences were considered statistically significant when $p < 0.05$. Where no statistical data are shown, all experiments were performed at least two times, with one representative experiment selected.

3. Results

3.1. Defining IL-12 family subunit glycosylation sites

Glycosylation often is a major determinant of protein biogenesis and function. To develop a comprehensive understanding of the role of glycosylation within the IL-12 family, we first aimed at defining glycosylation sites within each constituent subunit. In this study, all analyses and experiments were performed on the human proteins. Based on a sequence analysis (Fig. S1a), multiple *N*-glycosylation sites are expected to be present within both IL-12 subunits (IL-12 α , IL-12 β) as well as in EBI3, the β -subunit of IL-27 and IL-35 (Fig. 1a). For both β -subunits, the Asn residues predicted to be *N*-glycosylated are located within the two Fibronectin type-III (FnIII) domains, whereas the immunoglobulin (Ig) domain of IL-12 β lacks glycosylation sites. The remaining subunits of the heterodimeric IL-12 family, IL-23 α and IL-27 α , are not predicted to be *N*-glycosylated (Figs. 1a and S1a).

Hence, at least one subunit of every IL-12 family cytokine is predicted to be *N*-glycosylated (Fig. 1a). To assess these predictions, we first investigated the overall glycosylation status of each IL-12 family subunit by enzymatic assays. Subsequently, if glycosylation was detectable, we identified modified residues by mutational analyses

(Fig. 1b). In these experiments, $\alpha\beta$ pairs were always co-expressed and secreted cytokines were analyzed. Using PNGase F, which removes *N*-linked glycans, electrophoretic mobility shifts were observed for IL-12 α , IL-12 β , and EBI3 but not for IL-23 α and IL-27 α (Fig. 1b), verifying overall predictions of *N*-glycosylation (Figs. 1a and S1a). Likewise, *O*-Glycosidase was used to detect *O*-glycosylation of each IL-12 family subunit. Of note, secreted wild-type IL-12 α migrates differently when enzymatically digested with the *O*-Glycosidase mix. However, this mix also contains α 2-2,6,8 Neuraminidase, which cleaves terminal sialic acid residues from glycosylation moieties. IL-12 α has previously been shown to be modified with sialic acid (Carra et al., 2000), which is consistent with this observation. In agreement with this notion, the mutant IL-12 α ^{N93,107Q} lacking *N*-glycosylation sites did not show any different migration upon this enzymatic de-glycosylation treatment any more (Fig. 1b). The shift in molecular weight for wild-type IL-12 α can thus most likely be attributed to the enzymatic removal of terminal sialic acid residues from the complex *N*-linked sugar moiety, which arises from glycoprotein processing along the secretory pathway (Bohm et al., 2015; Zhang et al., 2019). In contrast, IL-27 α was found to be *O*-glycosylated (Fig. 1a and b), in agreement with previous studies (Muller et al., 2019a; Muller et al., 2019b; Pflanz et al., 2002).

Using mutational analyses, we next proceeded to identify individual glycosylation sites within each modified subunit. For IL-12 α , mutation of two Asn residues (N93, N107), both predicted to be *N*-glycosylation sites (Fig. S1a), to Gln resulted in a protein with the same electrophoretic migration behavior as the wild-type counterpart after PNGase F treatment (Fig. 1b). Furthermore, treating this mutant with PNGase F did not lead to any further changes in electrophoretic mobility, verifying that mutation of N93 and N107 was sufficient to abolish IL-12 α *N*-glycosylation (Fig. 1b).

Using mutated variants of IL-12 β (IL-12 β ^{N125,135,222,303Q}) and EBI3 (EBI3^{N55,105Q}) that lacked all possible glycosylation sites, we could verify *N*-glycosylation of these two proteins (Fig. 1a and b). In EBI3^{N55,105Q}, only the two predicted sites were mutated (Fig. S1a), and confirmed by electrophoretic mobility shift assays (Fig. 1b). In case of IL-12 β , two Asn residues were predicted to be *N*-glycosylated (N135 and N222, Fig. S1a) but only N222 could be experimentally validated (Fig. S1b). Since secreted IL-12 β ^{N222Q} still showed glycosylation, we analyzed further possible *N*-glycosylation sites that were below the threshold for glycosylation-prediction (Fig. S1b). This approach revealed that also N125 and N303 were glycosylated to a certain extent in IL-12 β .

To identify *O*-glycosylated Ser/Thr residues within human IL-27 α , we made use of the fact that murine IL-27 α is not *O*-glycosylated (Muller et al., 2019a; Muller et al., 2019b; Pflanz et al., 2002) despite approximately 75% sequence conservation. A sequence alignment of the murine and human IL-27 α -subunits showed only few Ser and Thr residues that were present in the human but not the murine protein (Fig. S2a). Focusing on surface-exposed residues among those (Fig. S2b), mutational analyses of respective residues in a secretion-competent human IL-27 α variant (Muller et al., 2019b) identified two C-terminal *O*-glycosylated residues, T238 and S240 (Fig. S2c). Mutation of these residues to Ala completely abolished *O*-glycosylation in human IL-27 α (Figs. 1b and S2c).

Taken together, we could confirm predicted and identify new glycosylation sites of human IL-12 family cytokine subunits. Although modifications of subunits vary within the IL-12 family, each heterodimer was modified (Fig. 1a and b). Next, we thus aimed at defining how glycosylation affected heterodimerization and secretion of each IL-12 family cytokine.

3.2. Glycosylation is essential for IL-35 secretion, but not for secretion of other IL-12 family members

When expressed in isolation, all human IL-12 family α -subunits are retained in the cell. Only the presence of a corresponding β -subunit

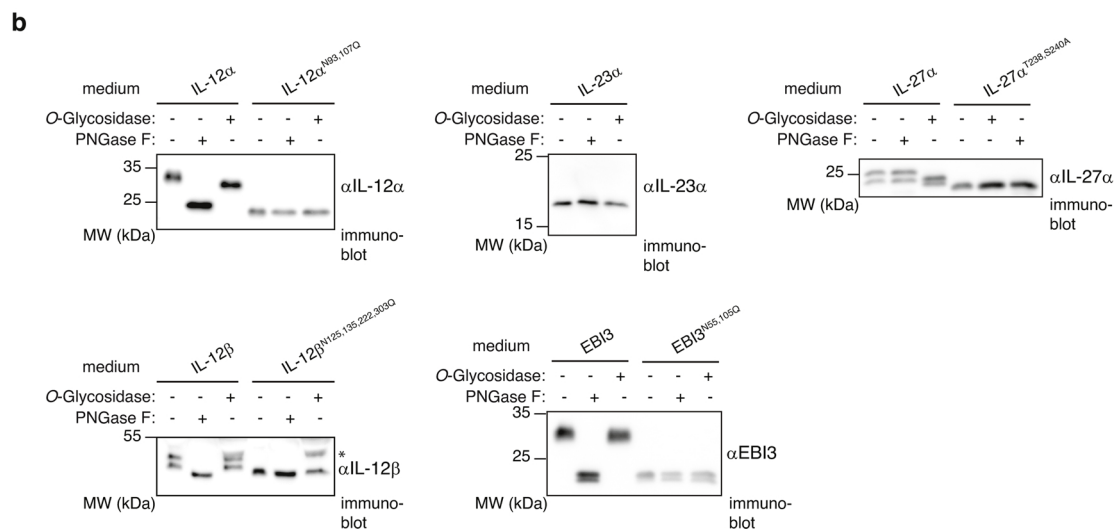
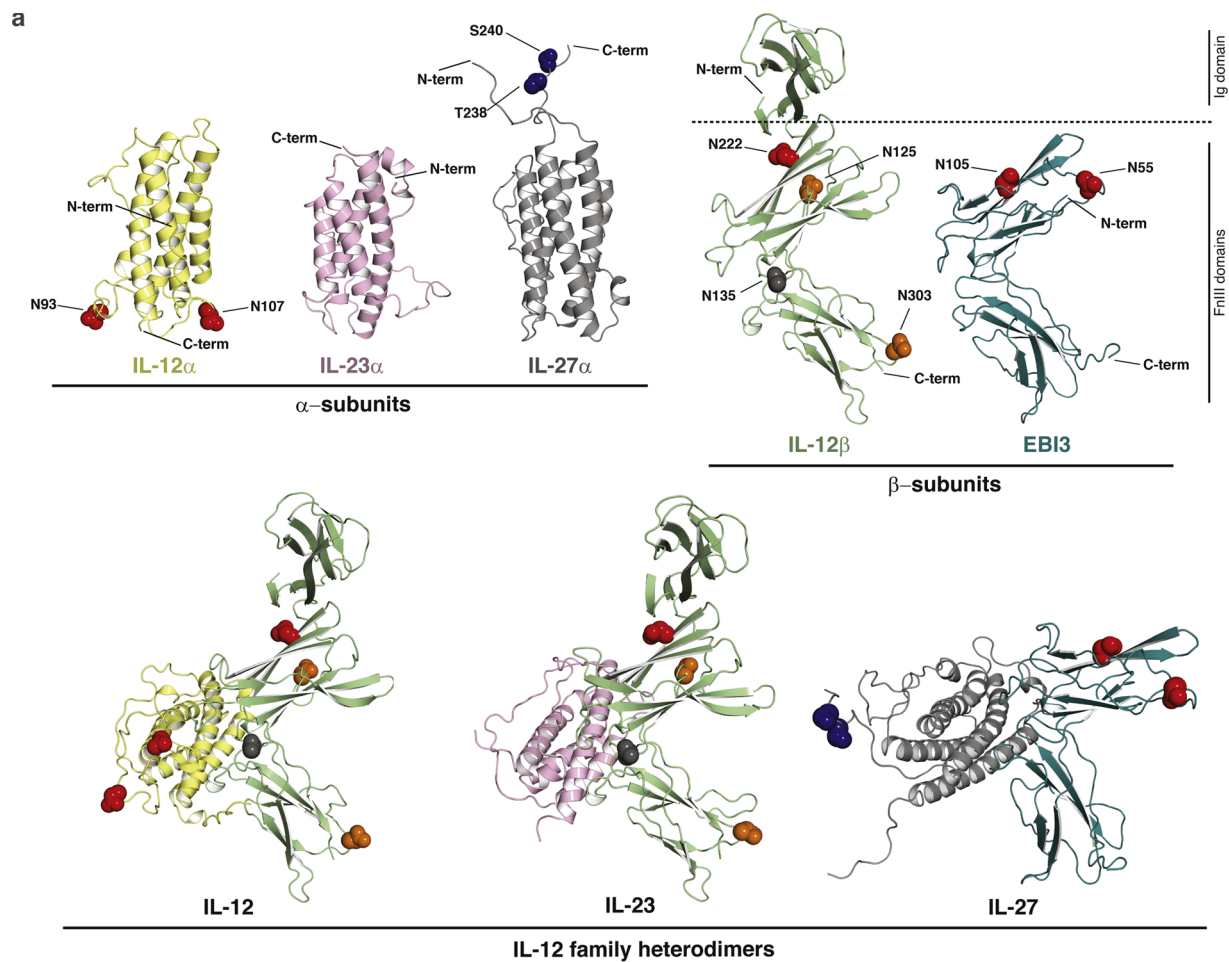


Fig. 1. Interleukin 12 family cytokines differ in their glycosylation patterns. (a) Top: Structural overview and glycosylation sites of the five shared subunits of the heterodimeric IL-12 family. Within the structures of the 4-helix bundle α -subunits IL-12 α (PDB: 3HMX), IL-23 α (PDB: 3D87), and the homology model of IL-27 α (Muller et al., 2019a), glycosylation sites are labeled and shown in a CPK representation. The β -subunits IL-12 β (PDB: 3HMX) and EBI3 (homology model, (Muller et al., 2019a)) possess predicted *N*-glycosylation sites in the Fibronectin III (FnIII) domains, but not in the immunoglobulin (Ig) domain of IL-12 β . Experimentally verified *N*-glycosylation sites are shown in red, *O*-glycosylation sites in blue. For IL-12 β , the residue N135 (gray) was predicted as *N*-glycosylation site but could not be experimentally verified. Instead, two other *N*-glycosylation sites (N125, N303) that were below the threshold for prediction, were experimentally identified as glycosylation-modified and are shown in orange. Bottom: The heterodimers IL-12 (PDB: 3HMX) and IL-23 (PDB: 3D87) share IL-12 β (green), whereas the β -subunit EBI3 (cyan) is part of IL-27 (homology model, (Muller et al., 2019a)) and IL-35 (no structural model available). (b) Verification of the predicted glycosylation sites of IL-12 family subunits by enzymatic treatment (PNGase F or *O*-Glycosidase) and mutagenesis of the respective sites. IL-12 α is *N*-glycosylated at N93 and N107, whereas IL-23 α is not glycosylated. IL-27 α is *O*-glycosylated at two residues (T238, S240). Both β -chains, IL-12 β and EBI3, are *N*-glycosylated at multiple sites (IL-12 β : N125, N222, N303; EBI3: N55, N105). For EBI3, a double band pattern arose only after enzymatic digest and thus seems to be an artefact related to the enzymatic treatment. α - and β -subunits were co-expressed and treated with PNGase F or *O*-Glycosidase/Neuraminidase. 1.8% medium, or 3.6% medium in case of IL-12 β , was applied to the gel and blotted with antibodies against the respective subunits. Electrophoretic mobility shifts indicate de-glycosylation. The asterisk indicates non-specific detection of the Neuraminidase. MW, molecular weight.

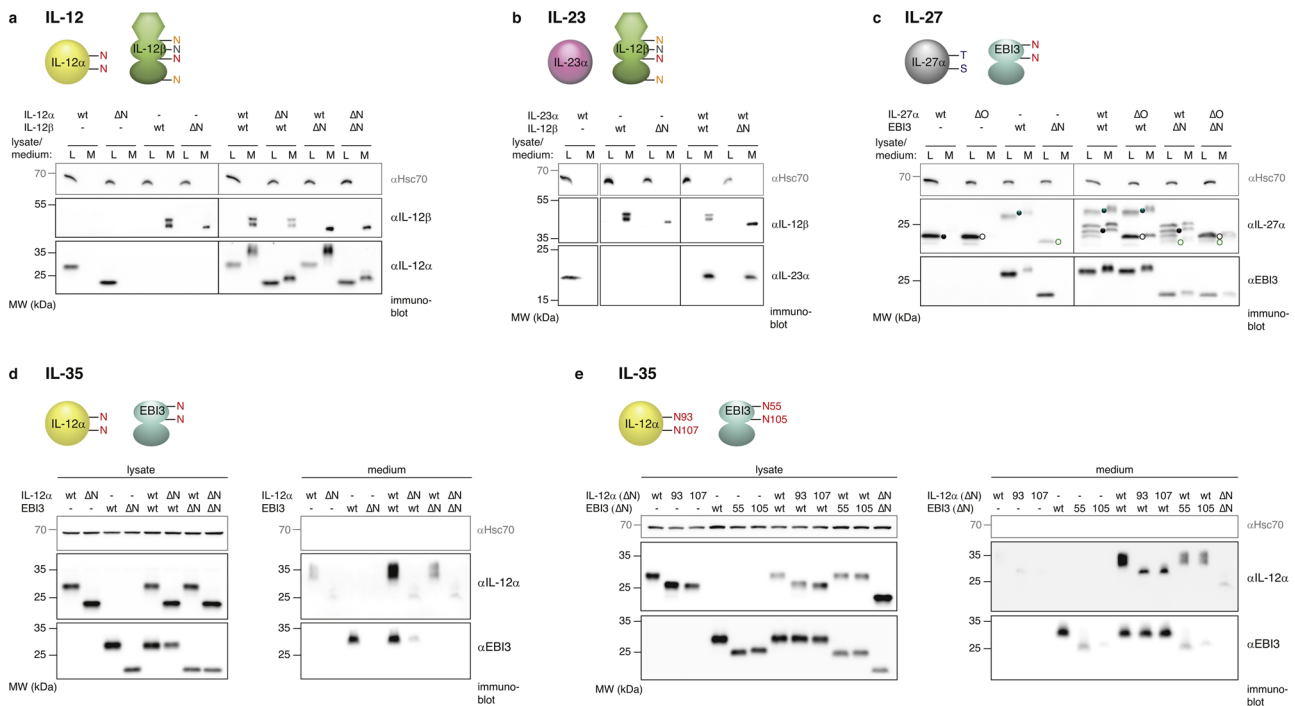


Fig. 2. Impact of glycosylation on IL-12 family cytokine secretion. (a-d) All human wild-type α -subunits are secretion-incompetent in isolation (IL-12 α , IL-23 α , IL-27 α) and retained in cells (L). Their pairing with secretion-competent wild-type β -subunits (IL-12 β , EBI3) to form the heterodimeric ILs induces secretion into cell media (M). (a) For IL-12, glycosylation mutants do neither affect the formation of the heterodimer nor its secretion behavior. (b) IL-23 heterodimer formation is not affected by lacking glycosylation of IL-12 β and is secreted similarly to the wild type. (c) For IL-27, the α -subunit lacking *O*-glycosylation (open gray circle) behaves analogous to the wild type (filled gray circle), whereas the mutant EBI3 without *N*-glycosylation (open cyan circle) is retained in cells in isolation in contrast to wild-type EBI3 (filled cyan circle). Co-transfection of both subunits results in heterodimer formation as both non-glycosylated cytokine subunits become secreted. The used α IL-27 α antibody detects also the EBI3 subunit. (d) For IL-35, both IL-12 $\alpha^{\Delta N}$ and EBI3 ΔN are not secreted in isolation and heterodimer formation is severely impaired. (e) Secretion behavior and heterodimer formation of IL-35 are affected by the individual *N*-glycosylation sites of IL-12 α and EBI3. IL-12 α^{N93Q} and IL-12 α^{N107Q} are only secreted to a much lower extent upon co-expression with EBI3, compared to the wild type. Similarly, the individual EBI3 glycosylation mutants are mostly retained in isolation and only induce reduced secretion levels of IL-12 α . (d-e) To facilitate an analysis regarding low IL-35 secretion levels, lysate and medium samples were analyzed on separate blots. (a-e) ΔN and ΔO indicate subunits where *N*-glycosylation sites are mutated to Gln or *O*-glycosylation sites are mutated to Ala, respectively. In the schematic models, circles represent the 4-helix bundle α -subunits, hexamers stand for the Ig domains and ellipses for the FnIII domains of the β -subunits. L, lysate. M, medium. MW, molecular weight. 2% L/M (in (b): 4% L/M, for IL-23 α transfected alone 6.4% L/M, in (d-e): 6% M) were applied to the gel and blotted with antibodies against the respective subunits. Hsc70 served as a loading control.

leads to assembly-induced secretion of the heterodimeric cytokine (Devergne et al., 1997; Gubler et al., 1991; Oppmann et al., 2000; Pflanz et al., 2002). Conversely, IL-12 β is readily secreted in isolation, whereas EBI3 shows only inefficient secretion (Devergne et al., 1996; Ling et al., 1995). Thus, heterodimerization is a prerequisite for secretion of most of the IL-12 subunits to occur or increase. This suggests that glycosylation, which is often coupled to ER folding and quality control processes, may impact IL-12 family cytokine secretion. To assess the effect of subunit glycosylation on the secretion of single subunits as well as heterodimer formation, we investigated the secretion behavior of each IL-12 family member.

For IL-12 and IL-23, even the complete absence of glycosylation did not result in pronounced effects on secretion and thus heterodimerization (Fig. 2a and b). IL-12 $\beta^{N125,135,222,303Q}$ (IL-12 $\beta^{\Delta N}$) behaved comparable to the wild-type protein with regard to its secretion levels and was still able to induce secretion of IL-12 α , its non-glycosylated variant IL-12 $\alpha^{N93,107Q}$ (IL-12 $\alpha^{\Delta N}$) (Fig. 2a) and the naturally non-glycosylated IL-23 α (Fig. 2b).

In contrast to IL-12 β , glycosylation of EBI3 turned out to be essential for its secretion as EBI3 N55,105Q (EBI3 ΔN) was not secreted in isolation anymore (Fig. 2c and d). Wild-type EBI3 induced the secretion of both IL-27 α and IL-27 $\alpha^{T238,S240A}$ (IL-27 $\alpha^{\Delta O}$), lacking *O*-glycosylation. Interestingly, although retained itself, EBI3 ΔN also induced secretion of both these IL-27 α variants and was co-secreted (Fig. 2c). Thus, IL-27 subunit mutants lacking glycosylation are still able to interact and enhance their mutual secretion despite being secretion-incompetent in

isolation.

Although sharing the same β -subunit as IL-27, secretion of IL-35 was strongly affected by missing glycosylation (Fig. 2d). Mutation of either of its subunits, IL-12 α or EBI3, was sufficient to block or severely reduce secretion of the other subunit in this heterodimeric cytokine. Furthermore, co-expression of non-glycosylated IL-12 $\alpha^{\Delta N}$ and EBI3 ΔN showed no co-secretion into the medium (Fig. 2d). The fact that IL-12 $\alpha^{\Delta N}$ reduced secretion of wild-type EBI3, which is secretion-competent on its own, implies that heterodimerization still occurred for this pair leading to retention of the heterodimeric cytokine by ER quality control. Based on these findings, we examined the effect of the individual glycosylation sites of each IL-35 subunit. IL-12 α single mutants N93Q and N107Q were secreted upon co-expression of EBI3, but to a lesser extent than wild-type IL-12 α (Fig. 2e). The two individual EBI3 mutants N55Q and N105Q were secreted in isolation, but to decreased levels, which was not further enhanced upon IL-12 α co-expression. Especially glycosylation at N105 seemed to be critical for efficient secretion of EBI3 (Fig. 2e).

In summary, the absence of glycosylation affects the secretion of IL-12 family cytokines in a surprisingly different manner. IL-12 and IL-23 seem to be secreted independently of their glycosylation status, whereas deleting glycosylation in IL-27 subunits led to a decreased secretion. Most pronounced effects were observed for IL-35, where absence of glycosylation caused an almost complete and dominant retention in the cell.

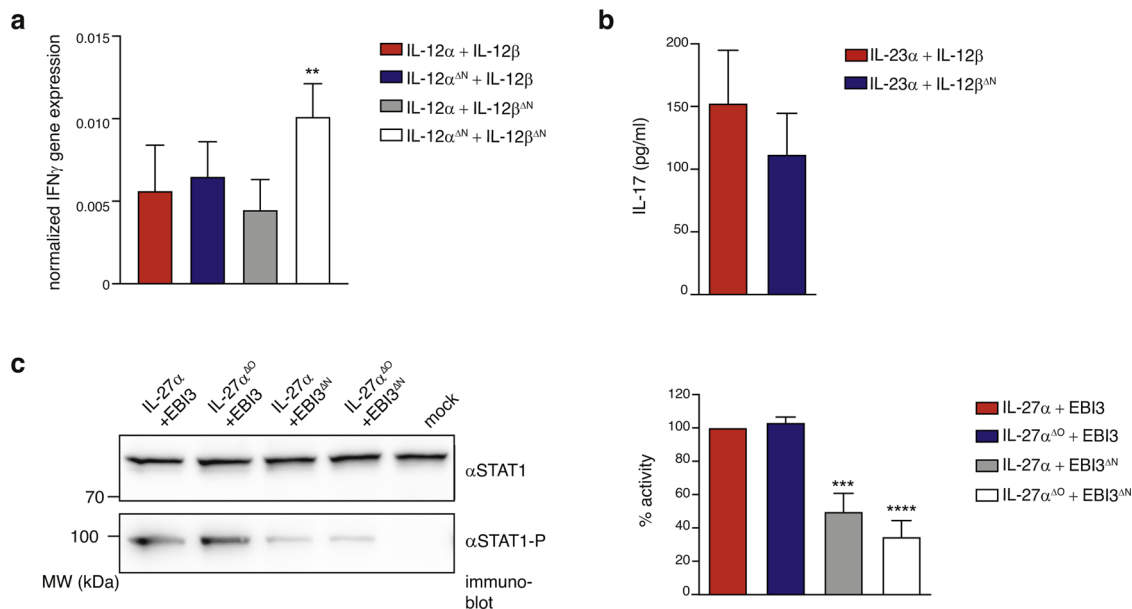


Fig. 3. Glycosylation influences the functionality of IL-12 family cytokines differently. (a) Glycosylation states of IL-12 α and IL-12 β influence biological functionality of heterodimeric IL-12. Stimulation of human peripheral blood mononuclear cells (PBMCs) with the indicated IL-12 glycosylation-variants show IFN γ induction by all analyzed heterodimers measured by qPCR. Data were normalized to secretion levels (Fig. S3a) and transcription levels were normalized to actin. The IL-12 heterodimer lacking glycosylation in both subunits shows significantly enhanced gene expression levels compared to the wild-type proteins. Data are presented as mean \pm SEM, PBMCs were from $n = 9$ donors. Statistical significance was determined by the Friedman test (more than 2 groups). (b) IL-23 function is not significantly affected by lacking glycosylation. PBMCs were stimulated with previously quantified supernatants of HEK293T cells co-transfected with IL-23 α and IL-12 β variants (Fig. S3b). IL-17 production measured in the supernatant *via* ELISA, was not significantly changed for the glycosylation mutant. Data are shown as mean \pm SEM, PBMCs were from $n = 6$ donors. Statistical significance was calculated using a two-tailed paired t-test. (c) Functionality of IL-27 depends on the glycosylation states of EB13. Stimulation of human BL-2 cells with differently glycosylated IL-27, using previously quantified HEK293T supernatants co-transfected with IL-27 α and EB13 (Fig. S3c), shows significantly reduced cytokine signaling for EB13 ΔN in complex with IL-27 α or IL-27 $\alpha^{\Delta O}$. Levels of STAT1 phosphorylation (α -STAT1-P) were quantified and indicate receptor activation by heterodimeric IL-27. α -STAT1-immunoblot signals serve as loading control. Activity levels were determined from at least four independent experiments (shown \pm SEM). Signals were normalized to the wild-type signal which was set to 100% activity. Statistical significance was calculated using a two-way ANOVA. (a-c) ** $p < 0.01$, *** $p < 0.001$, and **** $p < 0.0001$ indicate statistical significance. Mock, empty vector transfection. MW, molecular weight.

3.3. Lack of glycosylation does not compromise IL-12- or IL-23-mediated responses, but reduces IL-27 signaling

Our data indicate that for the IL-12 family members IL-12, IL-23, and IL-27 glycosylation was dispensable for heterodimer formation and secretion (Fig. 2). For these three cytokines, we thus investigated the impact of glycosylation on their biological functions by comparison of the different glycosylation mutants with their wild-type counterparts.

A major physiological activity of IL-12 is the induction of IFN γ expression (Chan et al., 1991). We therefore assessed the IL-12-induced IFN γ production in human peripheral blood mononuclear cells (PBMCs) by qPCR, using wild-type IL-12 and its glycosylation mutants (Figs. 3a and S3a). All IL-12 glycosylation variants induced IFN γ gene expression (Fig. 3a). Mutation of *N*-glycosylation sites in either the α - or β -subunit (IL12 $\alpha^{\Delta N}$ + IL-12 β , IL12 α + IL-12 $\beta^{\Delta N}$) did not significantly change the level in gene expression compared to wild-type IL-12. Surprisingly, non-glycosylated IL-12 (IL12 $\alpha^{\Delta N}$ + IL-12 $\beta^{\Delta N}$) showed a particularly strong increase of IFN γ -induction in PBMCs (Fig. 3a), whereas a slight decrease in receptor activation of IL-12 iLite[®] reporter cells compared to wild-type heterodimer was observed (Fig. S4a).

Next, we examined the dependency of IL-23 signaling on cytokine glycosylation by measuring IL-23-induced IL-17 production in PBMCs (Langrish et al., 2005). Since IL-23 α has no glycosylation sites (Fig. 1), only IL-17 production after stimulation with wild-type IL-23 and the mutant heterodimer consisting of IL-23 α and IL-12 $\beta^{\Delta N}$ were assessed using ELISA (Figs. 3b and S3b). In these experiments, no significant change in IL-17 secretion was observed for wild-type IL-23 α in comparison to the non-glycosylated variant (Fig. 3b). Stimulation of IL-23 iLite[®] reporter cells with the IL-23 glycosylation mutant (IL-23 α + IL-

12 $\beta^{\Delta N}$) showed a slightly reduced receptor activation (Fig. S4b).

Lastly, we assessed the impact of glycosylation on IL-27 activity. Toward this end, we used the lymphoma BL-2 cell line which, in response to IL-27 stimulation, shows induction of STAT1 phosphorylation (Dietrich et al., 2014). Quantification of the phospho-STAT1 signals *via* immunoblotting confirmed signaling-competency for all IL-27 glycosylation variants in BL-2 cells (Figs. 3c and S3c). The heterodimer composed of IL-27 $\alpha^{\Delta O}$ and wild-type EB13 showed no significant change in activity compared to IL-27. In contrast, the activity of the complex of wild-type IL-27 α with EB13 ΔN as well as of the non-glycosylated IL-27 heterodimer (IL-27 $\alpha^{\Delta O}$ + EB13 ΔN) was significantly decreased in comparison to IL-27 wild type (Fig. 3c).

Taken together, glycosylation in the interleukin-12 family does not seem to be essential for cytokine signaling. However, not only the secretion but also the biological functions of IL-12 family cytokines seem to be affected by the absence of glycosylation to a different extent: IL-27 signaling was reduced when EB13 lacked glycosylation, whereas IL-12 and IL-23 function was less dependent of their glycosylation status, which may however modulate responses induced by these cytokines (Ha et al., 2002).

4. Discussion

In this study we provide a comprehensive analysis of how glycosylation influences human IL-12 family cytokine biogenesis and function. This extends previous studies on the impact of disulfide bond formation within IL-12 family cytokines (Jalah et al., 2013; Meier et al., 2019; Muller et al., 2019a; Muller et al., 2019b; Reitberger et al., 2017; Yoon et al., 2000) by insights into the second major post-translational

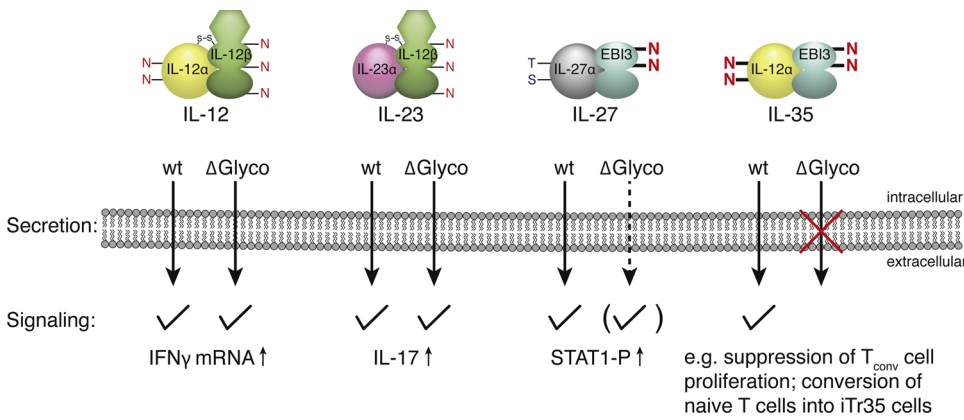


Fig. 4. The impact of glycosylation on human IL-12 family biogenesis and function. All heterodimeric wild-type (wt) IL-12 family cytokines are secreted and show biological function. IL-35 wild-type signaling was previously described (Collison et al., 2012; Collison et al., 2007). Both, IL-12 and IL-23 were secreted irrespective of their glycosylation status and also their biological functions (IFN γ gene expression and IL-17 production, respectively) were not compromised by lacking glycosylation. In contrast, lacking glycosylation of IL-27 led to a decreased secretion and signaling (phosphorylation of STAT1). Non-glycosylated IL-35 was almost completely retained in the cell. Red letters indicate N-glycosylated sites, blue letters O-glycosylated sites. Bold letters indicate glycosylation sites critical for secretion and functionality.

modification occurring in the ER. We could verify that all IL-12 family subunits except IL-23 α are glycosylated and identified new glycosylation sites. Moreover, our study reveals that loss of glycosylation affects secretion, heterodimer formation and biological activity of the IL-12 family members to different extents (Fig. 4).

A general principle for the human IL-12 family is assembly-induced folding of the α -subunit by a suitable β -subunit and subsequent secretion of the heterodimeric cytokine (Devergne et al., 1997; Gubler et al., 1991; Jalah et al., 2013; Meier et al., 2019; Müller et al., 2019b; Oppmann et al., 2000; Pflanz et al., 2002; Reitberger et al., 2017). It can thus be expected that whenever glycosylation is a prerequisite for proper β -subunit folding and assembly with its cognate α -subunit, effects on cytokine secretion should be dominant. In complete agreement with this idea, non-glycosylated and consequently cell-retained EBI3 abrogated secretion of IL-35 and significantly reduced IL-27 secretion. Interestingly, although diminished, mutant IL-27 subunits (IL-27 α and EBI3) lacking glycosylation were still able to interact and induce their mutual secretion despite being secretion-incompetent in isolation. This possibility of pairing of two secretion-incompetent subunits to become secreted together has previously been observed in the context of oxidative subunit folding for IL-27 (Müller et al., 2019a). It suggests that IL-27 subunits are (partially) folded even when lacking glycosylation but still expose features that do not allow them to pass ER quality control. Among the four human IL-12 family cytokines investigated, our study reveals IL-35 formation to be most strongly dependent on glycosylation. This may explain failed attempts of IL-35 reconstitution using a recombinant non-glycosylated IL-12 α subunit purified from bacteria (Aparicio-Siegmund et al., 2014).

In contrast to EBI3, IL-12 β without glycosylation behaved comparable to its wild-type counterpart and still formed IL-12 and IL-23. Thus, heterodimers containing IL-12 β are in general less affected by their extent of glycosylation than those containing EBI3. Of note, IL-12 and IL-23 contain intermolecular disulfide bridges (Lupardus and Garcia, 2008; Yoon et al., 2000), which may facilitate heterodimer secretion even without other stabilizing factors like sugar moieties. In agreement with this notion, IL-12 and IL-23 were still functional with regard to IFN γ or IL-17 induction in human lymphocytes, respectively, and exhibited receptor activation capabilities in reporter cell lines. In contrast, we observed impaired functionality for IL-27, when its β -subunit lacked N-glycosylation.

IL-12 family cytokines are attractive therapeutic targets and potential biopharmaceuticals (Müller et al., 2019b; Tait Wojno et al., 2019; Teng et al., 2015; Vignali and Kuchroo, 2012; Yan et al., 2016; Yeku and Brentjens, 2016). Our study assesses the impact of glycosylation on IL-12 family cytokine secretion and functionality by a limited number of tests and therefore builds the basis for further pharmaceutical investigations. Although we observed functionality for non-

glycosylated IL-12 family cytokines, it should be considered that the biological activity of the tested cytokines may vary dependent on their glycosylation patterns. Furthermore, glycosylation serves not only as a checkpoint for trafficking along the secretory pathway but also influences protein characteristics such as solubility, stability, and biodistribution within the human body, as already investigated for an antibody-p40 fusion protein (Bootz et al., 2016). On the other hand, since our study reveals IL-12, IL-23, and IL-27 to be secreted and functional even when completely lacking glycosylation, modifying glycosylation patterns may also open new doors towards rationally modifying IL-12 family cytokine functionality, as exemplified by G-CSF (Chamorey et al., 2002).

Finally, it is noteworthy that deleting glycosylation sites abolished IL-35 formation yet was compatible with formation of functional IL-12 and IL-27, which each share one subunit with IL-35. In the light of the chain sharing promiscuity within the IL-12 family this is relevant, since a simple knockout of single IL-12 family subunits generally affects more than one of the heterodimeric family members. Mutating glycosylation sites may thus be a viable way to selectively delete individual IL-12 family members from an organism's cytokine repertoire. Our findings concerning glycosylation-dependent secretion of IL-35 could be of particular interest with regard to the immunosuppressive role of this cytokine (Vignali and Kuchroo, 2012; Xue et al., 2019), e.g. in cancer forms that are difficult to treat (Mirlekar et al., 2018; Pylayeva-Gupta et al., 2016). As our study identifies a pivotal role for IL-35 subunit glycosylation in IL-35 formation, its targeting could represent a promising strategy for future immunotherapies.

5. Conclusions

In this study, we characterized the human IL-12 family in regard of their glycosylation profile. We were able to verify that at least one subunit of all IL-12 family members is glycosylated and furthermore identified new glycosylation sites. Our data indicate that loss of glycosylation does not severely affect IL-12 and IL-23 secretion, heterodimer formation, and biological activity. In contrast, non-glycosylated IL-27 shows partially impaired biogenesis and reduced signaling, whereas missing glycosylation of IL-35 led to complete retention in the cell. These findings extend our insights into this key cytokine family and provide a possibility to selectively remove individual IL-12 cytokines from an organism's cytokine repertoire.

Author contributions

MJF conceived the study. Experiments were performed by SB, KH, IA, and SIM. SB, KH, IA, SIM, JEvB, and MJF analyzed data. SB, KH, IA, JEvB, and MJF wrote the paper.

Declaration of Competing Interest

A patent on IL-27 glycosylation mutants has been submitted.

Acknowledgements

We are grateful to Odile Devergne, INSERM/France, for the kind gift of anti-EBI3 antiserum. Furthermore, we thank the group of Dr. Stefanie Eyrych for the kind gift of PHA and T-cell medium. IA gratefully acknowledges a PhD scholarship by the Studienstiftung des Deutschen Volkes and KH by the Cusanuswerk.

This study was supported by a Helmholtz Young Investigator grant (VH-NG-1331) by the Helmholtz Initiative and Networking fund of the Helmholtz Association to JEvB. MJF is a Rudolf Mößbauer Tenure Track Professor and as such gratefully acknowledges funding through the Marie Curie COFUND program and the Technical University of Munich Institute for Advanced Study, funded by the German Excellence Initiative and the European Union Seventh Framework Program under Grant Agreement 291763. This work was performed within the framework of SFB 1035 (German Research Foundation DFG, Sonderforschungsbereich 1035, Projektnummer 201302640, project B11).

Appendix A. Supplementary data

Supplementary material related to this article can be found, in the online version, at doi:<https://doi.org/10.1016/j.molimm.2020.07.015>.

References

- Akdis, M., Aab, A., Altunbulakli, C., Azkur, K., Costa, R.A., Cramer, R., Duan, S., Eiwegger, T., Eljaszewicz, A., Ferstl, R., Frei, R., Garbani, M., Globinska, A., Hess, L., Huitema, C., Kubo, T., Komlosi, Z., Konieczna, P., Kovacs, N., Kucuksezer, U.C., Meyer, N., Morita, H., Olzhausen, J., O'Mahony, L., Pezer, M., Prati, M., Rebane, A., Rhyner, C., Rinaldi, A., Sokolowska, M., Stanic, B., Sugita, K., Treis, A., van de Veen, W., Wanke, K., Wawrzyniak, M., Wawrzyniak, P., Wirz, O.F., Zakzuk, J.S., Akdis, C.A., 2016. Interleukins (from IL-1 to IL-38), interferons, transforming growth factor beta, and TNF-alpha: Receptors, functions, and roles in diseases. *J Allergy Clin Immunol* 138, 984–1010.
- Aparicio-Siegmund, S., Moll, J.M., Lokau, J., Grusdat, M., Schroder, J., Plohn, S., Rose-John, S., Grotzinger, J., Lang, P.A., Scheller, J., Garbers, C., 2014. Recombinant p35 from bacteria can form Interleukin (IL)-12, but Not IL-35. *PLoS One* 9, e107990.
- Bohm, E., Seyfried, B.K., Dockal, M., Graninger, M., Hasslacher, M., Neurath, M., Konetschny, C., Matthiessen, P., Mitterer, A., Scheiflinger, F., 2015. Differences in N-glycosylation of recombinant human coagulation factor VII derived from BHK, CHO, and HEK293 cells. *BMC Biotechnol* 15, 87.
- Booth, F., Venetz, D., Ziffels, B., Neri, D., 2016. Different tissue distribution properties for glycosylation variants of fusion proteins containing the p40 subunit of murine interleukin-12. *Protein Eng Des Sel* 29, 445–455.
- Braakman, I., Bülleid, N.J., 2011. Protein folding and modification in the mammalian endoplasmic reticulum. *Annu Rev Biochem* 80, 71–99.
- Carra, G., Gerosa, F., Trinchieri, G., 2000. Biosynthesis and posttranslational regulation of human IL-12. *Journal of immunology* 164, 4752–4761.
- Chamorey, A.L., Magne, N., Pivrot, X., Milano, G., 2002. Impact of glycosylation on the effect of cytokines. A special focus on oncology. *Eur Cytokine Netw* 13, 154–160.
- Chan, S.H., Perussia, B., Gupta, J.W., Kobayashi, M., Pospisil, M., Young, H.A., Wolf, S.F., Young, D., Clark, S.C., Trinchieri, G., 1991. Induction of interferon gamma production by natural killer cell stimulatory factor: characterization of the responder cells and synergy with other inducers. *J Exp Med* 173, 869–879.
- Collison, L.W., Delgoffe, G.M., Guy, C.S., Vignali, K.M., Chaturvedi, V., Fairweather, D., Satoskar, A.R., Garcia, K.C., Hunter, C.A., Drake, C.G., Murray, P.J., Vignali, D.A., 2012. The composition and signaling of the IL-35 receptor are unconventional. *Nature immunology* 13, 290–299.
- Collison, L.W., Workman, C.J., Kuo, T.T., Boyd, K., Wang, Y., Vignali, K.M., Cross, R., Sehly, D., Blumberg, R.S., Vignali, D.A., 2007. The inhibitory cytokine IL-35 contributes to regulatory T-cell function. *Nature* 450, 566–569.
- Croxford, A.L., Mair, F., Becher, B., 2012. IL-23: one cytokine in control of autoimmunity. *European journal of immunology* 42, 2263–2273.
- Dambuzza, I.M., He, C., Choi, J.K., Yu, C.R., Wang, R., Mattapallil, M.J., Wingfield, P.T., Caspi, R.R., Egwuagu, C.E., 2017. IL-12p35 induces expansion of IL-10 and IL-35-expressing regulatory B cells and ameliorates autoimmune disease. *Nat Commun* 8, 719.
- Devergne, O., Birkenbach, M., Kieff, E., 1997. Epstein-Barr virus-induced gene 3 and the p35 subunit of interleukin 12 form a novel heterodimeric hematopoietin. *Proceedings of the National Academy of Sciences of the United States of America* 94, 12041–12046.
- Devergne, O., Coulomb-L'Hermine, A., Capel, F., Moussa, M., Capron, F., 2001. Expression of Epstein-Barr virus-induced gene 3, an interleukin-12 p40-related molecule, throughout human pregnancy: involvement of syncytiotrophoblasts and extravillous trophoblasts. *Am J Pathol* 159, 1763–1776.
- Devergne, O., Hummel, M., Koeppen, H., Le Beau, M.M., Nathanson, E.C., Kieff, E., Birkenbach, M., 1996. A novel interleukin-12 p40-related protein induced by latent Epstein-Barr virus infection in B lymphocytes. *J Virol* 70, 1143–1153.
- Dietrich, C., Candon, S., Ruummele, F.M., Devergne, O., 2014. A soluble form of IL-27Ralpha is a natural IL-27 antagonist. *Journal of immunology* 192, 5382–5389.
- Espigol-Frigole, G., Planas-Rigol, E., Ohnuki, H., Salvucci, O., Kwak, H., Ravichandran, S., Luke, B., Cid, M.C., Tosato, G., 2016. Identification of IL-23p19 as an endothelial proinflammatory peptide that promotes gp130-STAT3 signaling. *Sci Signal* 9 ra28.
- Garbers, C., Spudy, B., Aparicio-Siegmund, S., Waetzig, G.H., Sommer, J., Holscher, C., Rose-John, S., Grotzinger, J., Lorenzen, I., Scheller, J., 2013. An interleukin-6 receptor-dependent molecular switch mediates signal transduction of the IL-27 cytokine subunit p28 (IL-30) via a gp130 protein receptor homodimer. *J Biol Chem* 288, 4346–4354.
- Gately, M.K., Carvajal, D.M., Connaughton, S.E., Gillessen, S., Warriar, R.R., Kolinsky, K.D., Wilkinson, V.L., Dwyer, C.M., Higgins Jr., G.F., Podlaski, F.J., Faherty, D.A., Familletti, P.C., Stern, A.S., Presky, D.H., 1996. Interleukin-12 antagonist activity of mouse interleukin-12 p40 homodimer in vitro and in vivo. *Ann N Y Acad Sci* 795, 1–12.
- Gubler, U., Chua, A.O., Schoenhaut, D.S., Dwyer, C.M., McComas, W., Motyka, R., Nabavi, N., Wolitzky, A.G., Quinn, P.M., Familletti, P.C., et al., 1991. Coexpression of two distinct genes is required to generate secreted bioactive cytotoxic lymphocyte maturation factor. *Proceedings of the National Academy of Sciences of the United States of America* 88, 4143–4147.
- Ha, S.J., Chang, J., Song, M.K., Suh, Y.S., Jin, H.T., Lee, C.H., Nam, G.H., Choi, G., Choi, K.Y., Lee, S.H., Kim, W.B., Sung, Y.C., 2002. Engineering N-glycosylation mutations in IL-12 enhances sustained cytotoxic T lymphocyte responses for DNA immunization. *Nature biotechnology* 20, 381–386.
- Jalah, R., Rosati, M., Ganneru, B., Pilkington, G.R., Valentin, A., Kulkarni, V., Bergamaschi, C., Chowdhury, B., Zhang, G.M., Beach, R.K., Alicea, C., Broderick, K.E., Sardesai, N.Y., Pavlakis, G.N., Felber, B.K., 2013. The p40 Subunit of Interleukin (IL)-12 Promotes Stabilization and Export of the p35 Subunit: implications for improved IL-12 cytokine production. *J Biol Chem* 288, 6763–6776.
- Jones, L.L., Chaturvedi, V., Uyttenhove, C., Van Snick, J., Vignali, D.A., 2012. Distinct subunit pairing criteria within the heterodimeric IL-12 cytokine family. *Mol Immunol* 51, 234–244.
- Kobayashi, M., Fitz, L., Ryan, M., Hewick, R.M., Clark, S.C., Chan, S., Loudon, R., Sherman, F., Perussia, B., Trinchieri, G., 1989. Identification and purification of natural killer cell stimulatory factor (NKSF), a cytokine with multiple biologic effects on human lymphocytes. *J Exp Med* 170, 827–845.
- Langrish, C.L., Chen, Y., Blumenschein, W.M., Mattson, J., Basham, B., Sedgwick, J.D., McClanahan, T., Kastelein, R.A., Cua, D.J., 2005. IL-23 drives a pathogenic T cell population that induces autoimmune inflammation. *J Exp Med* 201, 233–240.
- Lee, S.Y., Jung, Y.O., Kim, D.J., Kang, C.M., Moon, Y.M., Heo, Y.J., Oh, H.J., Park, S.J., Yang, S.H., Kwok, S.K., Ju, J.H., Park, S.H., Sung, Y.C., Kim, H.Y., Cho, M.L., 2015. IL-12p40 Homodimer Ameliorates Experimental Autoimmune Arthritis. *Journal of immunology* 195, 3001–3010.
- Ling, P., Gately, M.K., Gubler, U., Stern, A.S., Lin, P., Hollfelder, K., Su, C., Pan, Y.C., Hakimi, J., 1995. Human IL-12 p40 homodimer binds to the IL-12 receptor but does not mediate biologic activity. *Journal of immunology* 154, 116–127.
- Lupardus, P.J., Garcia, K.C., 2008. The structure of interleukin-23 reveals the molecular basis of p40 subunit sharing with interleukin-12. *J Mol Biol* 382, 931–941.
- Meier, S., Bohnacker, S., Klose, C.J., Lopez, A., Choe, C.A., Schmid, P.W.N., Bloemke, N., Ruhmoss, F., Haslbeck, M., Bieren, J.E., Sattler, M., Huang, P.S., Feige, M.J., 2019. The molecular basis of chaperone-mediated interleukin 23 assembly control. *Nat Commun* 10, 4121.
- Mirlekar, B., Michaud, D., Searcy, R., Greene, K., Pylayeva-Gupta, Y., 2018. IL35 Hinders Endogenous Antitumor T-cell Immunity and Responsiveness to Immunotherapy in Pancreatic Cancer. *Cancer immunology research* 6, 1014–1024.
- Muller, S.I., Aschenbrenner, I., Zacharias, M., Feige, M.J., 2019a. An Interspecies Analysis Reveals Molecular Construction Principles of Interleukin 27. *J Mol Biol* 431, 2383–2393.
- Muller, S.I., Friedl, A., Aschenbrenner, I., Esser-von Bieren, J., Zacharias, M., Devergne, O., Feige, M.J., 2019b. A folding switch regulates interleukin 27 biogenesis and secretion of its alpha-subunit as a cytokine. *Proceedings of the National Academy of Sciences of the United States of America* 116, 1585–1590.
- Oppman, B., Lesley, R., Blom, B., Timans, J.C., Xu, Y., Hunte, B., Vega, F., Yu, N., Wang, J., Singh, K., Zonin, F., Vaisberg, E., Churakova, T., Liu, M., Gorman, D., Wagner, J., Zurawski, S., Liu, Y., Abrams, J.S., Moore, K.W., Rennick, D., de Waal-Malefyt, R., Hannum, C., Bazan, J.F., Kastelein, R.A., 2000. Novel p19 protein engages IL-12p40 to form a cytokine, IL-23, with biological activities similar as those of distinct from IL-12. *Immunity* 13, 715–725.
- Pflanz, S., Timans, J.C., Cheung, J., Rosales, R., Kanzler, H., Gilbert, J., Hibbert, L., Churakova, T., Travis, M., Vaisberg, E., Blumenschein, W.M., Mattson, J.D., Wagner, J.L., To, W., Zurawski, S., McClanahan, T.K., Gorman, D.M., Bazan, J.F., de Waal-Malefyt, R., Rennick, D., Kastelein, R.A., 2002. IL-27, a heterodimeric cytokine composed of EBI3 and p28 protein, induces proliferation of naive CD4(+) T cells. *Immunity* 16, 779–790.
- Podlaski, F.J., Nanduri, V.B., Hulmes, J.D., Pan, Y.C., Levin, W., Danho, W., Chizzonite, R., Gately, M.K., Stern, A.S., 1992. Molecular characterization of interleukin 12. *Arch Biochem Biophys* 294, 230–237.
- Pylayeva-Gupta, Y., Das, S., Handler, J.S., Hajdu, C.H., Coffre, M., Korolov, S.B., Bar-Sagi, D., 2016. IL35-Producing B Cells Promote the Development of Pancreatic Neoplasia.

- Cancer Discov 6, 247–255.
- Reitberger, S., Haimerl, P., Aschenbrenner, I., Esser-von Bieren, J., Feige, M.J., 2017. Assembly-induced folding regulates interleukin 12 biogenesis and secretion. *J Biol Chem* 292, 8073–8081.
- Sawant, D.V., Hamilton, K., Vignali, D.A., 2015. Interleukin-35: Expanding Its Job Profile. *J Interferon Cytokine Res*.
- Sievers, F., Wilm, A., Dineen, D., Gibson, T.J., Karplus, K., Li, W., Lopez, R., McWilliam, H., Remmert, M., Soding, J., Thompson, J.D., Higgins, D.G., 2011. Fast, scalable generation of high-quality protein multiple sequence alignments using Clustal Omega. *Mol Syst Biol* 7, 539.
- Steentoft, C., Vakhrushev, S.Y., Joshi, H.J., Kong, Y., Vester-Christensen, M.B., Schjoldager, K.T., Lavrsen, K., Dabelsteen, S., Pedersen, N.B., Marcos-Silva, L., Gupta, R., Bennett, E.P., Mandel, U., Brunak, S., Wandall, H.H., Lavery, S.B., Clausen, H., 2013. Precision mapping of the human O-GalNAc glycoproteome through SimpleCell technology. *Embo j* 32, 1478–1488.
- Stern, A.S., Podlaski, F.J., Hulmes, J.D., Pan, Y.C., Quinn, P.M., Wolitzky, A.G., Familletti, P.C., Stremlo, D.L., Truitt, T., Chizzonite, R., et al., 1990. Purification to homogeneity and partial characterization of cytotoxic lymphocyte maturation factor from human B-lymphoblastoid cells. *Proceedings of the National Academy of Sciences of the United States of America* 87, 6808–6812.
- Stumhofer, J.S., Tait, E.D., Quinn 3rd, W.J., Hosken, N., Spudy, B., Goenka, R., Fielding, C.A., O'Hara, A.C., Chen, Y., Jones, M.L., Saris, C.J., Rose-John, S., Cua, D.J., Jones, S.A., Elloso, M.M., Grotzinger, J., Cancro, M.P., Levin, S.D., Hunter, C.A., 2010. A role for IL-27p28 as an antagonist of gp130-mediated signaling. *Nature immunology* 11, 1119–1126.
- Tait Wojno, E.D., Hunter, C.A., Stumhofer, J.S., 2019. The Immunobiology of the Interleukin-12 Family: Room for Discovery. *Immunity* 50, 851–870.
- Teng, M.W., Bowman, E.P., McElwee, J.J., Smyth, M.J., Casanova, J.L., Cooper, A.M., Cua, D.J., 2015. IL-12 and IL-23 cytokines: from discovery to targeted therapies for immune-mediated inflammatory diseases. *Nat Med* 21, 719–729.
- Trinchieri, G., Pflanz, S., Kastelein, R.A., 2003. The IL-12 family of heterodimeric cytokines: new players in the regulation of T cell responses. *Immunity* 19, 641–644.
- Vignali, D.A., Kuchroo, V.K., 2012. IL-12 family cytokines: immunological playmakers. *Nature immunology* 13, 722–728.
- Wolf, S.F., Temple, P.A., Kobayashi, M., Young, D., Dacic, M., Lowe, L., Dzialo, R., Fitz, L., Ferenz, C., Hewick, R.M., et al., 1991. Cloning of cDNA for natural killer cell stimulatory factor, a heterodimeric cytokine with multiple biologic effects on T and natural killer cells. *Journal of immunology* 146, 3074–3081.
- Xue, W., Yan, D., Kan, Q., 2019. Interleukin-35 as an Emerging Player in Tumor Microenvironment. *Journal of Cancer* 10, 2074–2082.
- Yan, J., Mitra, A., Hu, J., Cutrera, J.J., Xia, X., Doetschman, T., Gagea, M., Mishra, L., Li, S., 2016. Interleukin-30 (IL27p28) alleviates experimental sepsis by modulating cytokine profile in NKT cells. *J Hepatol* 64, 1128–1136.
- Yeku, O.O., Brentjens, R.J., 2016. Armored CAR T-cells: utilizing cytokines and pro-inflammatory ligands to enhance CAR T-cell anti-tumour efficacy. *Biochem Soc Trans* 44, 412–418.
- Yoon, C., Johnston, S.C., Tang, J., Stahl, M., Tobin, J.F., Somers, W.S., 2000. Charged residues dominate a unique interlocking topography in the heterodimeric cytokine interleukin-12. *EMBO J* 19, 3530–3541.
- Yoshida, H., Hunter, C.A., 2015. The immunobiology of interleukin-27. *Annu Rev Immunol* 33, 417–443.
- Zhang, Z., Shah, B., Richardson, J., 2019. Impact of Fc N-glycan sialylation on IgG structure. *MAbs* 11, 1381–1390.



Author rights

The below table explains the rights that authors have when they publish with Elsevier, for authors who choose to publish either open access or subscription. These apply to the corresponding author and all co-authors.

Author rights in Elsevier's proprietary journals	Published open access	Published subscription
Retain patent and trademark rights	√	√
Retain the rights to use their research data freely without any restriction	√	√
Receive proper attribution and credit for their published work	√	√
Re-use their own material in new works without permission or payment (with full acknowledgement of the original article): 1. Extend an article to book length 2. Include an article in a subsequent compilation of their own work 3. Re-use portions, excerpts, and their own figures or tables in other works.	√	√
Use and share their works for scholarly purposes (with full acknowledgement of the original article): 1. In their own classroom teaching. Electronic and physical distribution of copies is permitted 2. If an author is speaking at a conference, they can present the article and distribute copies to the attendees 3. Distribute the article, including by email, to their students and to research colleagues who they know for their personal use 4. Share and publicize the article via Share Links, which offers 50 days' free access for anyone, without sign-up or registration 5. Include in a thesis or dissertation (provided this is not published commercially) 6. Share copies of their article privately as part of an invitation-only work group on commercial sites with which the publisher has a hosting agreement	√	√
Publicly share the preprint on any website or repository at any time.	√	√

<https://www.elsevier.com/about/policies/copyright>